Control of iron homeostasis in *Corynebacterium glutamicum* by a hierarchical regulatory network

A dissertation submitted to the

Mathematisch-Naturwissenschaftliche Fakultät

of the Heinrich-Heine-Universität Düsseldorf

presented by

Julia Frunzke

born in Lich

October 2007

The thesis in hand has been performed at the Institute of Biotechnology 1, Research Centre Jülich, from November 2004 until October 2007 under the supervision of Prof. Dr. M. Bott.

Printed with acceptance of the Mathematisch-Naturwissenschaftlichen Fakultät of the Heinrich-Heine-Universität Düsseldorf.

Examiner: Prof. Dr. Michael Bott
Institute of Biotechnology 1
Biochemistry Group
Research Centre Jülich GmbH

Coexaminer: Prof. Dr. Rolf Wagner
Department of Biophysics
Heinrich-Heine-Universität Düsseldorf

Oral examination: November 29, 2007

Results described in this dissertation have been published in the following original publications:

Wennerhold, J.*, Krug, A.* and Bott, M. **(2005)** The AraC-type regulator RipA represses aconitase and other iron proteins from *Corynebacterium* under iron limitation and is itself repressed by DtxR. *J. Biol. Chem*. **280** (49): 40500-40508.

Wennerhold, J. and Bott, M. **(2006)** The DtxR regulon of *Corynebacterium glutamicum.* *J. Bacteriol*. **188** (8): 2907-2918.

Cramer, A., Auchter, M., **Frunzke, J**., Bott, M. and Eikmanns, B. J. **(2006)** RamB, the transcriptional regulator of acetate metabolism in *Corynebacterium glutamicum* is subject to regulation by RamA and RamB. *J Bacteriol* **189** (3):1145-1149.

Frunzke, J. and Bott, M. (2007) Evidence for the involvement of the two-component system CgtSR11 in the regulation of heme homeostasis in *Corynebacterium glutamicum* *FEMS letters* **to be submitted.**

Frunzke, J., Bramkamp, M., Schweitzer, J. and Bott, M. **(2007)** Genome heterogeneity in *Corynebacterium glutamicum* ATCC 13032 caused by the prophage CGP3. *J Bacteriol* **to be submitted.**

Frunzke, J. and Bott, M. (2008) Regulation of iron homeostasis in *Corynebacterium glutamicum.* Book Chapter in "Corynebacteria: Genomics and molecular biology". (Burkovski A., ed.), Horizon Scientific Press, Norwich, UK, **in press**.

Results of further projects not discussed in this thesis have been published in:

Frunzke, J., Engels, V., Hasenbein, S., Gätgens, C. and Bott, M. **(2007)** Coordinated regulation of gluconate catabolism and glucose uptake in *Corynebacterium glutamicum* by two functionally equivalent transcriptional regulators, GntR1 and GntR2. *Mol Microbiol* **in press**.

*These authors contributed equally to this work.

Content

Abbreviations

Amp^R	Ampicillin resistance
ATCC	American Type Culture Collection
BHI(S)	Brain Heart Infusion (+ Sorbitol)
DNase	Desoxyribonuclease
et al.	*et alii*
Gm^R	Gentamycin resistance
IPTG	Isopropyl-thio-β-D-galactopyranosid
Kan^R	Kanamycin resistance
LB	Luria Bertani
OD_{600}	optical density at 600 nm
qRT-PCR	quantitative real-time PCR
RBS	ribosome binding site
$Spec^R$	Spectinomycin resistance
TBE	Tris base - Boric acid - EDTA
TCA	Trichloric acid
TE	Tris base – EDTA
TNI	Tris base – NaCl - Imidazol
UTR	untranslated region
UV	ultraviolet
v/v	volume per volume
WT	wild type
w/v	weight per volume
YFP	Yellow fluorescent protein

Further abbreviations not included in this section are according to international standards, as for example listed in the author guidelines of the *FEBS Journal.*

1 Summary

Iron is an essential trace element for nearly all organisms as it participates in major biological processes, but on the other hand it poses problems of poor solubility and toxicity. Therefore, many organisms have evolved sophisticated mechanisms to ensure sufficient but not excess levels of intracellular iron. In *Corynebacterium diphtheriae* the transcriptional regulator DtxR in complex with Fe^{2+} represses transcription of genes involved in iron acquisition under iron excess. In this work the control of iron homeostasis on the transcriptional level was investigated in the Gram-positive soil bacterium *Corynebacterium glutamicum,* a non-pathogenic relative of *C. diphtheriae*.

In *C. glutamicum* DtxR directly regulates transcription of about 60 genes involved in iron uptake, iron storage and synthesis of iron sulfur clusters in response to iron availability. The majority of these genes are repressed by DtxR and encode high affinity iron uptake systems, such as siderophore ABC transporters, siderophore binding proteins as well as heme transport systems and heme oxygenase. On the other hand, DtxR seems to act as a direct activator of the iron storage proteins ferritin and Dps under conditions of sufficient iron supply. These results clearly emphasize DtxR as the master regulator of iron-dependent gene expression in *C. glutamicum*. In studies with a *dtxR* deletion mutant an increased induction rate of the CGP3 prophage was observed. Subsequently, it was shown that this prophage is induced spontaneously not only in this mutant but also in a small fraction of *C. glutamicum* wild type cells (<5%). Evidence for lysis of cells containing several CGP3 phage DNA molecules was obtained.

Three of the genes repressed by DtxR, *ripA*, *cgtR11* and *cg0527*, encode themselves transcriptional regulators. Under iron limitation the AraC-type regulator RipA acts as a repressor of genes encoding several prominent iron-containing proteins, such as aconitase, succinate dehydrogenase, catalase or nitrate reductase. By the reduced synthesis of these proteins, the cell is probably able to sustain more important iron-requiring processes, like respiration or DNA biosynthesis. CgtR11, the response regulator of the two-component system CgtSR11, directly activates expression of the *hmuO* gene encoding heme oxygenase in a heme-dependent manner. This enzyme is required for the utilization of heme as an iron source by *C. glutamicum*, which occurs under iron deprivation. Moreover, strong evidence could be provided that the CgtSR11 two-component system is also involved in the regulation of heme biosynthesis as well as in the production of heme-containing proteins in response to iron and heme availability. The Cg0527 protein is a member of the ArsR family of transcriptional regulators, which are often involved in the adaptation to high concentrations of heavy metal ions, but its exact function is still unknown. Altogether, the four transcriptional regulators DtxR, RipA, CgtR11 and Cg0527 constitute a hierarchical regulatory network controlling iron homeostasis in *Corynebacterium glutamicum*.

2 Introduction

Gold is for the mistress -- silver for the maid --
Copper for the craftsman cunning at his trade.
"Good!" cried the Baron, sitting in his hall,
"But iron, cold iron, is the master of them all

By Rudyard Kipling

2.1 Iron - essential but dangerous

Iron is an essential element for almost all organisms as constituent of proteins containing heme, iron-sulfur clusters or mono- or binuclear iron species. Such proteins play important roles in many biological processes, such as electron transport, the tricarboxylic acid (TCA) cycle or gene regulation. Although iron is one of the most abundant elements in the earth crust, it is not readily available. Under aerobic conditions the predominant form of iron is the ferric state (Fe^{3+}). Due to the extremely low solubility product of $Fe(OH)_3$ ($[Fe^{3+}][OH^-]^3 = 10^{-39}$), the concentration of ferric iron at pH 7 is 10^{-18} M, in contrast to the relatively soluble ferrous state (0.1 M at pH 7.0) (Chipperfield and Ratledge, 2000). Other ferric minerals occuring in the soil, *e.g.* hematit (α-Fe_2O_3), goethit (α-FeO(OH)), or maghemit (γ-Fe_2O_3), have even lower solubility products (Cornell and Schwertmann, 2003). To cope with this problem, many microbes have evolved complex systems to solubilize iron from their environment.

Besides being essential, iron can also be harmful to cells, mainly due to its reaction with hydrogen peroxide, a by-product of aerobic metabolism. In the Fenton reaction, Fe^{2+} reacts with H_2O_2 to yield Fe^{3+}, OH^- and the highly reactive and strongly damaging hydroxyl radical $\cdot OH$ (Pierre and Fontecave, 1999). Thus, cells have to cope with poor iron solubility on one hand and to avoid high levels of free intracellular Fe^{2+} on the other hand. As pointed out by Andrews *et al.* (Andrews *et al.*, 2003), five major strategies are used by bacteria to deal with these problems: (i) high-affinity iron transport systems for scavenging iron from the environment; (ii) intracellular iron storage proteins providing an iron source when the external ones are transiently unavailable; (iii) redox stress resistance mechanisms such as degradation of reactive oxygen species and repair of damaged molecules; (iv) reduction of the cellular iron demand by partial repression of iron-containing proteins; and (v) a sophisticated regulatory system that controls all of the above-mentioned processes according to iron availability.

2.2 Control of gene expression by iron

2.2.1 Two families of global iron regulators – Fur and DtxR

In bacteria iron-dependent control of gene expression is accomplished by two protein families, Fur and DtxR (Andrews *et al.*, 2003; Hantke, 2001). Proteins of these two families are widely distributed in bacteria, and although they do not exhibit significant sequence similarity to each other they are functional homologs.

In *Escherichia coli* the ferric-uptake regulator (Fur) was shown to directly and indirectly control expression of nearly 100 genes in response to iron availability. Under conditions of sufficient iron supply Fur in complex with its co-repressor Fe^{2+} represses transcription of iron acquisition genes and of genes involved in the biosynthesis of siderophores. The Fur protein exists as a homodimer and contains two metal-binding sites, one structural Zn^{2+} site as well as a regulatory active Fe^{2+} site. In this way DNA-binding by Fur is coupled to the intracellular iron concentration. Another important function of Fur is the down-regulation of several iron-containing proteins under iron limitation, accomplished by repression of a small RNA named RhyB. RhyB, when de-repressed under iron limitation, facilitates degradation of several mRNAs positively regulated by Fur (Masse and Gottesman, 2002; Masse *et al.*, 2007). Targets of RhyB include genes encoding iron proteins such as aconitase (*acnA*), succinate dehydrogenase (*sdhCDAB*), superoxide dismutase (*sodB*), ferritin (*ftn*), and bacterioferritin (*bfr*). Due to the down-regulation of non-essential iron-containing proteins under iron limitation, available iron can more efficiently used for other more important processes (*e.g.* DNA biosynthesis). However, recent studies reveal that some Fur regulators can also funtion as a direct transcriptional activator. For example Fur of *Neisseria meningitidis* was shown to acitvate transcription of *pan1* (encoding nitrite reductase), *norB* (nitrate reductase) and *nuoABCDE* (NADH dehydrogenase) encoding metalloproteins/complexes involved in anaerobic and aerobic respiration, respectively (Delany *et al.*, 2004). In *Helicobacter pylori* expression *nifS* involved in iron-sulfur cluster synthesis is directly activated by Fur (Alamuri *et al.*, 2006). Fur homologs involved in iron-dependent regulation have been found in several Gram-negative bacteria, but also in some Gram-positives with low GC content, such as *Bacillus subtilis* (Escolar *et al.*, 1999; Hantke, 2001; Lee and Helmann, 2007).

In many Gram-positive bacteria with high GC content (*e.g.* corynebacteria, mycobacteria and streptomycetes), members of another family of transcriptional regulators, including DtxR of *Corynebacterium diphtheriae* and IdeR of *Mycobacterium tuberculosis*, function as major

iron-dependent transcriptional regulators (Boyd *et al.*, 1990; Hantke, 2001; Rodriguez, 2006). Similar to Fur, DtxR-like regulators also act as Fe^{2+}-dependent regulators and repress transcription of the high-affinity iron uptake systems under iron sufficiency. Although the functional similarities between DtxR and Fur are striking, no significant similarity exists on the level of amino acid sequence. The following section will focus in more detail on the regulon and the metal ion activation of DtxR-like transcriptional regulators.

2.2.2 DtxR, the diphtheria toxin repressor

In the early 1930s it was demonstrated that high levels of iron in the growth medium repressed the production of diphtheria toxin by *C. diphtheriae* (Pappenheimer and Johnson, 1936). About 60 years later, this effect was shown to be mediated by the transcriptional regulator DtxR (diphtheria toxin regulator) (Boyd *et al.*, 1990; Schmitt and Holmes, 1991a). Under iron excess, DtxR in complex with Fe^{2+} represses transcription of the *tox* gene. When iron becomes limiting, Fe^{2+} dissociates from DtxR and apo-DtxR becomes inactive, causing derepression of the *tox* gene. In contrast to diphtheria toxin, which is encoded in the genome of some corynephages, DtxR is encoded by the *C. diphtheriae* genome (locus tag DIP1414; (Cerdeno-Tarraga *et al.*, 2003)). Homologs of DtxR are widely distributed in bacteria and some have been characterized, *e.g.* the IdeR protein of *Mycobacterium tuberculosis* (Gold *et al.*, 2001).

Meanwhile, it has become clear that DtxR is not a specific regulator of the *tox* gene, but controls many genes associated with iron uptake and siderophore biosynthesis in *C. diphtheriae* (Kunkle and Schmitt, 2005). Additionally, DtxR was shown to act as a repressor of genes encoding an ABC transporter (*hmuTUV*) for heme uptake and a heme oxygenase (*hmuO*) which are involved in the utilization of heme as an iron source under iron limitation (Kunkle and Schmitt, 2003; Schmitt, 1997). In *M. tuberculosis* the gene encoding the iron-dependent regulator IdeR was shown to be essential and deletion of *ideR* was only possible due to the occurrence of a secondary-site suppressor mutation (Rodriguez *et al.*, 2002). Nevertheless, comparative transcriptome analysis of this mutant with the *M. tuberculosis* wild type strain provided important insights into iron- and IdeR-dependent gene expression in this organism. Under conditions of sufficient iron supply, IdeR combines with Fe^{2+} and downregulates iron uptake by repressing transcription of genes involved in siderophore production and transport, similar to DtxR of *C. diphtheriae*. Additionally, IdeR of *M. tuberculosis* was shown to act as a direct activator of *bfrA* and *bfrB* expression. These genes

encode a putative bacterioferritin and ferritin, respectively (Gold *et al.*, 2001; Rodriguez, 2006). This dual function of IdeR as repressor of iron uptake genes and activator of iron storage proteins most probably depends on the location of the IdeR binding site in the corresponding promoter region. In the case of *bfrA* and *bfrB*, IdeR binds to two tandem IdeR boxes located in the –35 to –100 region with respect to the transcriptional start site (TS). Whereas promoters being repressed by IdeR generally contain one single binding site which overlaps with the –10 region. Further studies with DtxR homologs of other species will show whether the action as a dual transcriptional regulator is a common feature of DtxR-like proteins.

The protein structures of DtxR from *C. diphtheriae* and IdeR from *M. tuberculosis* have been intensively investigated and provided important knowledge about the mechanism of metal ion activation of DtxR-like proteins (D'Aquino *et al.*, 2005; Ranjan *et al.*, 2006). The active form of DtxR is a homodimer, with each monomer consisting of two domains connected by a flexible tether of 23 amino acids that contains a proline-rich region (Qiu *et al.*, 1995; Schiering *et al.*, 1995). The N-terminal domain contains the helix-turn-helix motif responsible for DNA binding as well as two metal ion binding sites (Figure 2.1). The ancillary binding site (site 1) binds Fe^{2+} with high affinity (K_d = 2 x 10^{-7} M for Ni^{2+}, (D'Aquino *et al.*, 2005)) and, when occupied, stabilizes the monomeric form of the repressor. When the iron concentration increases, the primary binding site (site 2), a low affinity Fe^{2+} binding site (K_d = 6.3 x 10^{-4} M for Ni^{2+}, (D'Aquino *et al.*, 2005)), is occupied, leading to conformational changes in the N-terminal region and subsequently dimerization of the protein. Besides Fe^{2+}, several other divalent metal ions can activate the binding of DtxR to its target promoters *in vitro*, preferred in the following order Fe^{2+} ~ Ni^{2+} > Co^{2+} >> Mn^{2+} (Spiering *et al.*, 2003; Tao and Murphy, 1992). The C-terminal domain has been shown to be structurally similar to eukaryotic SH3 domains (Qiu *et al.*, 1995).

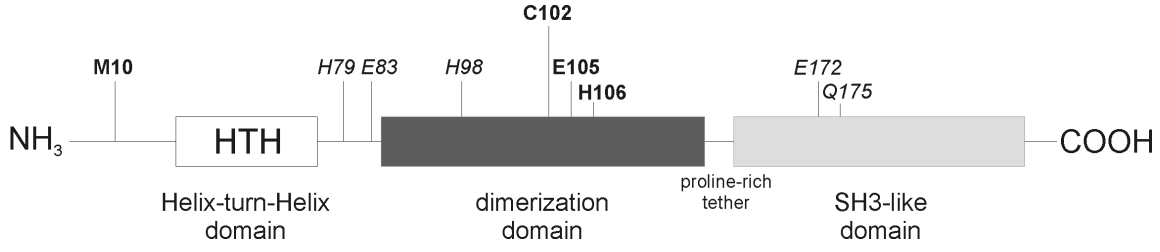

Figure 2.1. Domain structure of DtxR of *C. diphtheriae*. In the structure of DtxR, amino acids printed in *italics* are ligands of the ancillary metal-binding site (site 1) and amino acids printed in **bold** constitute the primary binding site (site 2).

So far, the function of this domain is not completely understood. Although contributing two ligands (Glu170 and Gln173) to the ancillary ion binding site, studies with mutants lacking this domain indicate that it is not essential for DNA binding (Posey *et al.*, 1999). Crystal structures of the complex of metal-ion activated DtxR and a DNA fragment containing the *tox* operator have shown that two DtxR dimers interact with the target DNA at almost opposite sites of the DNA and do not interact with each other (Figure 2.2) (Pohl *et al.*, 1999; White *et al.*, 1998). The minimal essential nucleotide sequence for DtxR binding is a 9-bp inverted repeat with an 1-bp gap (TWAGGTWAGSCTWACCTWA) (Tao and Murphy, 1994).

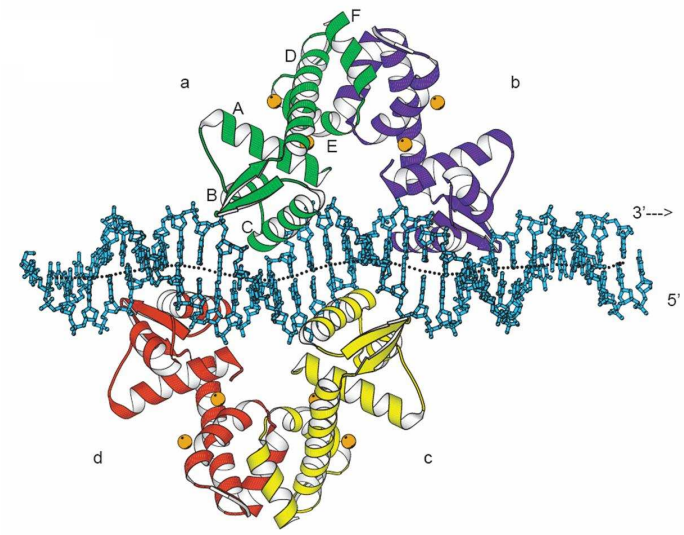

Figure 2.2. X-ray structure of the active Ni(II)-DtxR(C102D)-*tox* operator complex. Subunits of DtxR are labelled a-d. Ribbons and arrows illustrate α-helices (marked A-F) and β-strands, respectively. The orange balls represent nickel atoms bound to metal ion sites one and two in each DtxR monomer. This structure visualizes that the two DtxR dimers bind to nearly opposite sites of the 33-bp DNA fragment including the tox promoter. One dimer (subunits a and b) binds closer to the 3′ end, the other closer to the 5′ end of the coding strand (White *et al.*, 1998).

2.2.3 Heme-dependent two-component systems in *C. diphtheriae*

Besides using siderophores many bacteria can also acquire iron from heme. Following the transport of heme into the cytoplasm *via* specific heme transporters, the iron is extracted by heme oxygenases that degrade the tetrapyrrole ring. Up to now heme uptake in Gram-positive organisms has rarely been studied, however, heme uptake systems have recently been documented in *C. diphtheriae* and *Corynebacterium ulcerans* (Drazek *et al.*, 2000; Schmitt and Drazek, 2001). The heme-dependent ABC transport system consists of the binding protein HmuT, the permease HmuU and the ATPase component HmuV (Drazek *et al.*, 2000). Based on experimental data it has been proposed that HmuT is a heme- and hemoglobin-binding lipoprotein, sharing ~25% sequence identity to the periplasmic heme binding proteins (PBPs) from *Yersinia* species (Hornung *et al.*, 1996; Wandersman and Stojiljkovic, 2000).

In *C. diphtheriae* the genes encoding the heme ABC transporter (*hmuTUV*) and heme oxygenase (*hmuO*) are all under negative control by DtxR under iron-replete conditions. Additionally, expression of *hmuO* was shown to be induced in the presence of heme or hemoglobin (Schmitt, 1997). A few years ago the identification of a two-component signal transduction system, designated ChrS-ChrA was reported, which is involved in the heme-dependent activation of *hmuO* expression (Schmitt, 1999). A mechanism has been suggested where the membrane-bound sensor kinase ChrS is involved in the detection of extracellular heme, which most likely triggers autophosphorylation at the conserved histidine residue (H215) of ChrS. Subsequently, the phosphoryl group is transferred to an aspartate residue (D50) of the response regulator ChrA, which thereby is converted into its active form, binds to the promoter region of the *hmuO* gene and activates transcription. However, *C. diphtheriae* mutants lacking either *chrS* or *chrA* did not loose heme-dependent activation of *hmuO* expression completely, suggesting the participation of an additional regulatory system in this process (Bibb *et al.*, 2005). Recent studies indeed revealed that for full hemoglobin-dependent activation of *hmuO* a second two-component system is required, named HrrS-HrrA, which shares significant sequence similarity to the ChrS-ChrA system (Bibb *et al.*, 2007). Both systems were shown to be involved not only in the activation of *hmuO*, but also in the repression of *hemA* encoding the heme biosynthesis protein glutamyl-tRNA synthetase (Bibb *et al.*, 2007). Thus, these two-component systems are part of a complex regulatory system which controls heme homeostasis in *C. diphtheriae*.

2.3 Iron demand and uptake of *Corynebacterium glutamicum*

A main focus of this PhD thesis was the control of iron homeostasis in the biotechnologically relevant organism *Corynebacterium glutamicum,* a non-phathogenic relative of *C. diphtheriae*. *C. glutamicum* is a predominantly aerobic, biotin-auxotrophic Gram-positive soil bacterium that was isolated in Japan due to its ability to excrete L-glutamate under biotin-limiting growth conditions (Kinoshita *et al.*, 1957). It is used today for the industrial production of more than two million tons of amino acids per year, mainly L-glutamate and L-lysine. Additionally, this species has become a model organism of the *Corynebacterineae*, a suborder of the *Actinomycetales* which also comprises the genus *Mycobacterium*. An overview on the current knowledge on *C. glutamicum* can be found in a recent monograph (Eggeling and Bott, 2005).

Early studies showed that growth of *C. glutamicum* (formerly *Micrococcus glutamicus*) in synthetic medium depends on a sufficient supply of iron, which could be provided *e.g.* in form of ferrichrome (10 mg/l), or by high concentrations of iron salts (0.5-2.0 g/l). Moreover, a synergistic action between iron and several chelating agents on growth was demonstrated (Nakayama *et al.*, 1964a; Nakayama *et al.*, 1964b). Twenty-five years later, two studies addressed once again the problem of iron acquisition by *C. glutamicum* when a defined medium was required for metabolic studies. Von der Osten *et al.* showed that 0.1% (3.9 mM) citrate (provided as sodium salt) in combination with ≥20 mg/l $FeSO_4$ x 7 H_2O (72 µM) allowed good growth (von der Osten *et al.*, 1989). Interestingly, citrate was co-metabolized with glucose, but the depletion of citrate within 10 hours had no negative effect on the growth rate. The authors therefore suggested that iron is accumulated intracellularly in the early stages of cultivation. Liebl *et al.* (1989) confirmed the results of von der Osten *et al.*, but noticed that the high concentrations of citrate required might be undesirable in metabolic studies. They were able to show that low concentrations (10 µM) of protocatechuate (3,4-dihydroxybenzoate) or catechol (2-hydroxyphenol) in combination with 72 µM $FeSO_4$ suffice to achieve the same growth as 0.1% citrate (Liebl *et al.*, 1989b). The standard minimal medium used in our and several other laboratories called CGXII (Keilhauer *et al.*, 1993) contains 30 mg/l (195 µM) protocatechuate. Like in the case of citrate (Polen *et al.*, 2007), protocatechuate is used as a carbon source by *C. glutamicum*, too (Merkens *et al.*, 2005). Again, accumulation of iron in the initial growth phase might be responsible for maintaining a high growth rate when protocatechuate has been consumed. According to the studies described above, *C. glutamicum* is able to take up ferrichrome, ferric citrate and iron complexes of protocatechuate and catechol. The overall iron content of *C. glutamicum* cells has been determined to vary between 0.04 mg iron/g cell dry weight on CGIII complex medium and 0.3-0.5 mg iron/g cell dry weight on BMCG and CGXII minimal medium (Liebl *et al.*, 1989a).

To overcome the poor solubility of ferric iron, many microorganisms synthesize and excrete low molecular mass (<1000 Da) compounds called siderophores that are characterized by their high specificity and affinity ($K_d \sim 10^{-30}$ M^{-1}) towards ferric iron. More than 500 different siderophores are currently known and formation of iron complexes usually involves either hydroxamate groups, catechol rings, or hydroxy acids. Upon import of iron siderophore complexes into the bacterial cytoplasm, the iron is released either by reduction to Fe^{2+} catalyzed by ferri-siderophore reductases (Schröder *et al.*, 2003) or by breaking down the siderophore structure as described for several siderophores, *e.g.*

bacillibactin (Miethke *et al.*, 2006) or enterobactin (Lin *et al.*, 2005). In 1997, Budzikiewicz and co-workers (Budzikiewicz *et al.*, 1997) reported the isolation of a cyclic catecholate siderophore from *C. glutamicum* strain ATCC14067 which they named corynebactin. A siderophore of identical structure was later isolated from *Bacillus subtilis* and designated bacillibactin (May *et al.*, 2001). Moreover, the genes *dhbABCEF* responsible for bacillibactin synthesis were identified (May *et al.*, 2001). Analysis of the genome sequence of *C. glutamicum* strain ATCC13032 revealed a gene homologous to *dhbC* (encoding isochorismate synthetase), but there were no genes present that are homologous to *dhbA*, *dhbB*, *dhbE* or *dhbF*. Moreover, no other genes obviously involved in siderophore biosynthesis were identified, leading to the conclusion that at least the type strain ATCC13032 does not produce siderophores (Wennerhold and Bott, 2006). Recently, Raymond and co-workers reinvestigated corynebactin (*alias* bacillibactin) synthesis by *C. glutamicum* ATCC14067 and failed to detect the production of this siderophore (Dertz *et al.*, 2006). The strain was also negative in the Chrome Azurol S (CAS) assay, which indicates the inability to synthesize siderophores that remove iron from the CAS chromophore. Finally, the strain did not take up ^{55}Fe-labeled bacillibactin, which would be expected for a strain that synthesises and excretes this siderophore. Thus, *C. glutamicum* ATCC14067 like the type strain ATCC13032 does not produce siderophores (Dertz *et al.*, 2006).

Except for the studies described above, no experimental data on iron transport in *C. glutamicum* appear to exist. Therefore, the current knowledge on iron acquisition is primarily based on the annotated genome sequence (Ikeda and Nakagawa, 2003; Kalinowski *et al.*, 2003) and on DNA microarray studies in which global gene expression was analyzed in cells grown with different iron supplies (Krug *et al.*, 2005).

2.4 Iron-dependent changes in gene expression in *C. glutamicum*

First insights into the influence of iron limitation on global gene expression were obtained in DNA microarray experiments where the transcriptomes of *C. glutamicum* wild type cultivated with different iron concentrations (508 µM *versus* 8 µM $FeSO_4$) were compared (Krug *et al.*, 2005). At this time the exact iron concentration leading to a significant iron-starvation response on the transcriptome level was unknown. However, in cells grown in CGXII minimal medium with 8 µM $FeSO_4$ the mRNA concentration of several genes encoding putative siderophore ABC transporters, siderophore-binding lipoproteins and a heme transport system was more than ≥3-fold increased in comparison to cells grown under

iron excess (508 µM $FeSO_4$). In contrast, many genes encoding iron-containing proteins (*e.g.* aconitase, succinate dehydrogenase and nitrate reductase) showed a significantly decreased mRNA level under iron limitation.

In many organisms aconitases, which contain a 4Fe-4S cluster as cofactor, are regulated in response to iron availability or, as iron regulatory proteins (IRPs), are involved in iron-dependent regulation on the post-transcriptional level themselves (Eisenstein, 2000; Rouault, 2006; Wong *et al.*, 1999). As already mentioned above, expression of the aconitase gene *acnA* in *E. coli* is down-regulated by the small RNA RhyB, which is repressed under iron sufficiency by the global iron regulator Fur (Masse *et al.*, 2007). In mammalians the cytoplasmic isoform of aconitase (cAcn) was shown to live a double life. Under iron excess, cAcn with an intact 4Fe-4S cluster catalyzes the conversion of citrate to isocitrate. Under iron limitation cAcn becomes an iron regulatory protein, which does not contain a Fe-S cluster but binds specifically to iron regulatory elements (IREs) on mRNA. This leads for example to the stabilization of the mRNA of the transferrin receptor, which is involved in iron uptake, and on the other hand to the degradation of the mRNA of the iron storage protein ferritin (Eisenstein, 2000).

The DNA microarray experiments with *C. glutamicum* described above were originally designed to test an involvement of AcnR, a repressor of the aconitase gene (*acn*), in iron-dependent regulation of *acn* (Krug *et al.*, 2005). However, comparison of the transcriptomes of *C. glutamicum* strain Δ*acnR* under iron excess (508 µM) and iron limitation (8 µM) argued against this possibility, as the *acn* mRNA level was still decreased under iron limitation. Nevertheless, another candidate for iron-dependent regulation of *acn* was discovered in the course of these studies. Under iron limitation, the mRNA level of the AraC-type regulator Cg1120 was significantly increased, both in the wild type and the Δ*acnR* mutant. Thus, it was speculated whether a direct connection exists between the up-regulation of Cg1120 and the downregulation of several prominent iron-containing proteins under iron depletion. A *C. glutamicum* mutant with an in-frame deletion of the *cg1120* gene showed a significantly reduced final cell density (A_{600} ~20) in comparison to the wild type (A_{600} ~40), when the cells were cultivated in CGXII minimal medium under iron limitation (1 µM $FeSO_4$). In contrast, no differences were observed between wild type and mutant when cultivated under iron excess (100 µM $FeSO_4$) (Krug, 2004). These results supported an involvement of the AraC-type regulator Cg1120 in the adaption of *C. glutamicum* to iron limitation. Based on the

results described in this work, Cg1120 was named RipA, which stands for regulator of iron proteins A.

2.5 Aims of this work

The first aim of this work was to investigate whether in fact a direct connection exists between the downregulation of iron-containing proteins and the upregulation of RipA under iron limitation. For this purpose, the direct target genes of RipA had to be identified, using both biochemical and genome-based approaches. A second topic of this work addressed the question of the mechanism by which *ripA* expression itself is regulated in an iron-dependent manner. A *C. glutamicum* protein (Cg2103) with high sequence identity (72%) to the diphtheria toxin repressor (DtxR) of *C. diphtheriae* was assumed to be a good candidate for regulating the expression of *ripA* in response to the intracellular Fe^{2+} concentration. To follow up this assumption, DNA-binding with purified DtxR had to be performed and the effect of a *dtxR* deletion on *ripA* expression had to be determined using DNA microarray analysis. Comparative transcriptome analysis of a *dtxR* deletion mutant and the wild type would give valuable insights on the influence of DtxR on global gene expression in *C. glutamicum*. Using this approach even additional transcriptional regulators could be identified to be controlled by DtxR in response to iron availability. The investigation of their particular role in *C. glutamicum* will provide a more complete understanding of the control of iron homeostasis by a hierarchical regulatory network in this non-pathogenic soil bacterium.

3 Results

The major topic of this PhD thesis was the control of iron homeostasis in *C. glutamicum*. The results allocated to this research field have been summarized in three publications and two manuscripts which will be submitted in near future.

The first publication "The AraC-type regulator RipA represses aconitase and other iron proteins from *Corynebacterium* under iron limitation and is itself repressed by DtxR" describes the identification of a novel transcriptional "regulator of iron proteins A" which is responsible for the diminished synthesis of several prominent iron proteins under iron limitation, such as aconitase or succinate dehydrogenase. This type of regulation reduces the iron demand of the cell and thus presumably contributes to a prolonged survival. RipA itself was induced under iron limitation, due to the inactivity of the transcriptional regulator DtxR under these conditions.

The definition of "The DtxR regulon of *Corynebacterium glutamicum*", which is described in the second publication, represents a continuation of the previous work on RipA. Two independent approaches were used to identify direct target genes of the transcriptional regulator DtxR. On the one hand the global expression pattern of a *dtxR* deletion mutant was analyzed using DNA microarrays. On the other hand we used a bioinformatics approach to identify putative DtxR binding sites within the *C. glutamicum* genome, which were subsequently tested by gel retardation assays with purified DtxR. By combining the two approaches, more than 50 genes were found to be repressed by DtxR, while about a dozen genes are presumably activated by DtxR, which thus was established as the master regulator of iron homeostasis in *C. glutamicum*.

Interestingly, a functional DtxR binding site was present in the intergenic region of the divergently arranged genes *ramB* and *sdhCAB* which encode a global transcriptional regulator of carbon metabolism and succinate dehydrogenase, respectively. In order to test whether DtxR directly regulates *ramB* expression, a promoter fusion with a reporter gene encoding chloramphenicol acetyltransferase (CAT) was constructed and CAT activities were determined in *C. glutamicum* wild type and a *dtxR* deletion mutant, which indicated that *ramB* expression is not controlled by DtxR. These data and further results on the regulation of *ramB* expression obtained in the group of our collaboration partner Prof. Bernhard Eikmanns (University of Ulm, Germany) were published in "RamB, the transcriptional

regulator of acetate metabolism in *Corynebacterium glutamicum*, is subject to regulation by RamA and RamB".

Amongst others the *cgtR11* gene encoding the response regulator of the CgtSR11 two-component signal transduction system (Kocan *et al.*, 2006b) was shown to be repressed by DtxR under iron excess. A further manuscript with the title "Evidence for the involvement of the two-component system CgtSR11 in the regulation of heme homeostasis in *Corynebacterium glutamicum*" describes the studies on the role of this two-component system. The CgtSR11 system shares high sequence similarity to the two-component sytems HrrAS and ChrAS of *C. diphtheriae*, which are involved in the heme-dependent induction of heme oxygenase (Bibb *et al.*, 2005; Bibb *et al.*, 2007). DNA microarray analysis with a *cgtSR11* deletion mutant, quantitative real-time PCR data as well as biochemical experiments showed that CgtR11 also controls genes involved in heme utilization and heme biosynthesis, but also heme-containing proteins. The CgtSR11 system thus controls a specific part of the overall iron regulatory network.

DNA microarray analysis of the *dtxR* deletion mutant, described in the publication "The DtxR regulon of *Corynebacterium glutamicum*", revealed that more than 50 genes located within the prophage region CGP3 (*cg1890-cg2071*) showed a strongly increased mRNA level in the deletion mutant. This led us to the assumption whether this might be due to an induction of this prophage in the *dtxR* deletion mutant. In the manuscript "Genome heterogeneity in *Corynebacterium glutamicum* ATCC 13032 caused by the prophage CGP3" experiments are described which indicate that the prophage CGP3 can indeed exist as an extrachromosomal element. This is the first report of prophage induction in *C. glutamicum* and a starting point for analyzing genome heterogeneity in this species.

The last part of this section is a book chapter with the title "Regulation of iron homeostasis in *Corynebacterium glutamicum*" which will be published in "Corynebacteria: Genomics and molecular biology" (Burkovski A., ed.). This article summarizes the current knowledge on the regulatory network controlling iron homeostasis, and furthermore, gives an overview on transport systems putatively involved in iron aquistion in *C. glutamicum.*

THE JOURNAL OF BIOLOGICAL CHEMISTRY VOL. 280, NO. 49, pp. 40500–40508, December 9, 2005

The AraC-type Regulator RipA Represses Aconitase and Other Iron Proteins from *Corynebacterium* under Iron Limitation and Is Itself Repressed by DtxR*[S]

Received for publication, August 8, 2005, and in revised form, September 22, 2005 Published, JBC Papers in Press, September 22, 2005, DOI 10.1074/jbc.M508693200

Julia Wennerhold[1], **Andreas Krug**[1], **and Michael Bott**[2]

From the Institut für Biotechnologie 1, Forschungszentrum Jülich, Jülich D-52425, Germany

The mRNA level of the aconitase gene *acn* of *Corynebacterium glutamicum* is reduced under iron limitation. Here we show that an AraC-type regulator, termed RipA for "regulator of iron proteins A," is involved in this type of regulation. A *C. glutamicum* Δ*ripA* mutant has a 2-fold higher aconitase activity than the wild type under iron limitation, but not under iron excess. Comparison of the mRNA profiles of the Δ*ripA* mutant and the wild type revealed that the *acn* mRNA level was increased in the Δ*ripA* mutant under iron limitation, but not under iron excess, indicating a repressor function of RipA. Besides *acn*, some other genes showed increased mRNA levels in the Δ*ripA* mutant under iron starvation (*i.e.* those encoding succinate dehydrogenase (*sdhCAB*), nitrate/nitrite transporter and nitrate reductase (*narKGHJI*), isopropylmalate dehydratase (*leuCD*), catechol 1,2-dioxygenase (*catA*), and phosphotransacetylase (*pta*)). Most of these proteins contain iron. Purified RipA binds to the upstream regions of all operons mentioned above and in addition to that of the catalase gene (*katA*). From 13 identified binding sites, the RipA consensus binding motif RRGCGN$_4$RYGAC was deduced. Expression of *ripA* itself is repressed under iron excess by DtxR, since purified DtxR binds to a well conserved binding site upstream of *ripA*. Thus, repression of *acn* and the other target genes indicated above under iron limitation involves a regulatory cascade of two repressors, DtxR and its target RipA. The modulation of the intracellular iron usage by RipA supplements mechanisms for iron acquisition that are directly regulated by DtxR.

Corynebacterium glutamicum is a nonpathogenic, aerobic Gram-positive soil bacterium that is used for large scale industrial production of amino acids, predominantly L-glutamate (1.5 million tons/year) and L-lysine (0.7 million tons/year). In addition, *C. glutamicum* has gained interest as a suitable model organism for the *Corynebacterineae*, a suborder of the actinomycetes that includes the genus *Mycobacterium*. An overview on *C. glutamicum* biology, genetics, physiology, and biotechnology can be found in a recent monograph (1).

The citric acid cycle is of central importance for metabolism in general and for amino acid production in particular, because it provides the biosynthetic precursors of the aspartate and glutamate family of amino acids. Despite its key role, knowledge about the genetic regulation of this pathway in *C. glutamicum* is scarce. We recently could show that the activity of aconitase (EC 4.2.1.3), which catalyzes the stereospecific and reversible isomerization of citrate to isocitrate via *cis*-aconitate, varies depending on the carbon source and that this is caused by transcriptional regulation (2). A repressor of the TetR family, called AcnR, was identified, which represses aconitase by binding to an imperfect inverted repeat within the *acn* promoter region and interfering with the binding of RNA polymerase (2). The factors that control binding of AcnR to its operator are not yet known. DNA microarray experiments revealed that *acn* expression is not only influenced by the carbon source but also by the iron concentration of the medium (2). Under iron limitation, the *acn* mRNA level in the wild type was 3-fold lower than under iron excess. In the Δ*acnR* mutant, this decrease was even larger (4.8-fold), presumably because the increased expression of aconitase, which contains a 4Fe-4S cluster, leads to an enhanced iron starvation.

We now have identified a new transcriptional regulator, designated RipA, which is responsible for iron-dependent regulation of aconitase and several other iron-containing proteins. Evidence is provided that RipA represses *acn* and six other target operons under iron limitation and is itself repressed under iron excess by the global iron repressor DtxR.

EXPERIMENTAL PROCEDURES

Bacterial Strains, Media, and Growth Conditions—All strains and plasmids used in this work are listed in supplemental Table S1. The *C. glutamicum* type strain ATCC13032 (3) was used as wild type. Strain Δ*ripA* is a derivative containing an in-frame deletion of the *ripA* gene. For growth experiments, 5 ml of brain heart infusion medium (Difco) was inoculated with colonies from a fresh LB agar plate (4) and incubated for 6 h at 30 °C. After washing, the cells of this first preculture were used to inoculate a 500-ml shake flask containing 50 ml of CGXII minimal medium (5) with 4% (w/v) glucose and either 1 μM $FeSO_4$ (iron starvation) or 100 μM $FeSO_4$ (iron excess). This second preculture was cultivated overnight at 30 °C and then used to inoculate the main culture to an A_{600} ~1. The main culture contained the same iron concentration as the second preculture. The trace element solution with iron salts omitted and the $FeSO_4$ solution were always added after autoclaving. For growth of *C. glutamicum* strains carrying plasmid pJC1 or pJC1-*ripA*, the medium was supplemented with 25 μg/ml kanamycin. For all cloning purposes, *Escherichia coli* DH5 (Invitrogen) was used as host, for overproduction of RipA and DtxR *E. coli* BL21(DE3) (6). The *E. coli* strains were cultivated aerobically in LB medium at 37 °C (DH5) or at 30 °C (BL21(DE3)). When appropriate, kanamycin was added to a concentration of 50 μg/ml.

Recombinant DNA Work—The enzymes for recombinant DNA work were obtained from Roche Applied Science or New England Biolabs (Frankfurt, Germany). The oligonucleotides used in this study were obtained from Operon (Cologne, Germany) and are listed in supplemental Table S2. Routine methods like PCR, restriction, or ligation were

* The costs of publication of this article were defrayed in part by the payment of page charges. This article must therefore be hereby marked "*advertisement*" in accordance with 18 U.S.C. Section 1734 solely to indicate this fact.

[S] The on-line version of this article (available at http://www.jbc.org) contains supplemental Tables S1 and S2 and supplemental Figs. S1 and S2.

[1] Both authors contributed equally to this work.

[2] To whom correspondence should be addressed. Tel.: 49-2461-615515; Fax: 49-2461-612710; E-mail: m.bott@fz-juelich.de.

carried out according to standard protocols (4). Chromosomal DNA from *C. glutamicum* was prepared as described (7). Plasmids from *E. coli* were isolated with the QIAprep spin miniprep kit (Qiagen, Hilden, Germany). *E. coli* was transformed by the RbCl method (8), and *C. glutamicum* was transformed by electroporation (9). DNA sequencing was performed with a Genetic Analyzer 3100-Avant (Applied Biosystems, Darmstadt, Germany). Sequencing reactions were carried out with the Thermo Sequenase primer cycle sequencing kit (Amersham Biosciences).

An in-frame *ripA* deletion mutant of *C. glutamicum* was constructed via a two-step homologous recombination procedure as described previously (10). The *ripA* up- and downstream regions (~500 bp each) were amplified using the oligonucleotide pairs orf1558-A-for/orf1558-B-rev and orf1558-C-for/orf1558-D-rev, respectively, and the products served as template for cross-over PCR with oligonucleotides orf1558-A-for and orf1558-D-rev. The resulting PCR product of ~1 kb was digested with EcoRI and HindIII and cloned into pK19*mobsacB* (11). DNA sequence analysis confirmed that the cloned PCR product did not contain spurious mutations. Transfer of the resulting plasmid pK19*mobsacB*-Δ*ripA* into *C. glutamicum* and screening for the first and second recombination event were performed as described previously (10). Kanamycin-sensitive and saccharose-resistant clones were tested by PCR analysis of chromosomal DNA with the primer pair orf1558-amp-for/orf1558-amp-rev (supplemental Table S2). Of 10 clones tested, five showed the wild-type situation (2.0-kb fragment) and five had the desired in-frame deletion of the *ripA* gene (1.1-kb fragment), in which all nucleotides except for the first six codons and the last 12 codons were replaced by a 21-bp tag.

In order to complement the Δ*ripA* mutant, the *ripA* coding region and 250-bp upstream DNA containing the promoter region were amplified using oligonucleotides (ripA+250-for (2) and ripA+250-rev) introducing a SalI and a PstI restriction site, respectively. The resulting 1245-bp PCR product was cloned into the vector pJC1 (12). The resulting plasmid pJC1-ripA and pJC1 were used to transform *C. glutamicum* wild type and the Δ*ripA* strain.

For overproduction and purification of RipA with an N-terminal StrepTag-II (13), the *ripA* coding region was amplified using oligonucleotides that introduce an NdeI restriction site, including the start codon (ripA-2-for) and an XhoI restriction site after the stop codon (ripA-2-rev). The purified PCR product was cloned in the modified expression vector pET28b-Streptag (14), resulting in plasmid pET28b-Streptag-*ripA*. The RipA protein encoded by this plasmid contains 14 additional amino acids (MASWSHPQFEKGAH) at the amino terminus. For overproduction and purification of DtxR, the *dtxR* coding region (equivalent to NCgl1845) was amplified using oligonucleotides that introduced an NdeI restriction site at the translation initiation codon (dtxR-for-1) and four histidine codons plus an XhoI restriction site before the stop codon (dtxR-rev-1). The PCR product was cloned into the pET24b vector, resulting in plasmid pET24b-*dtxR*-C. The DtxR protein encoded by this plasmid contains 12 additional amino acids at the carboxyl terminus (HHHHLEHHHHHH). The PCR-derived portions of pET28b-Streptag-*ripA* and pET24b-*dtxR*-C were analyzed by DNA sequence analysis and found to contain no spurious mutations. For overproduction of RipA and DtxR, the two plasmids were transferred into *E. coli* BL21(DE3).

Preparation of Total RNA—Cultures of the wild type and the Δ*ripA* mutant were grown in CGXII minimal medium containing 4% (w/v) glucose under iron limitation (1 μM $FeSO_4$) or iron excess (100 μM $FeSO_4$). In the exponential growth phase at an A_{600} of 4–6, 25 ml of the cultures were used for the preparation of total RNA as described previously (15). Isolated RNA samples were analyzed for quantity and quality by UV spectrophotometry and denaturing formaldehyde-agarose gel electrophoresis (4), respectively, and stored at −70 °C until use.

DNA Microarray Analyses—The generation of whole-genome DNA microarrays (16), synthesis of fluorescently labeled cDNA from total RNA, microarray hybridization, washing, and data analysis were performed as described previously (2, 17–19). Genes that exhibited significantly changed mRNA levels ($p < 0.05$ in a Student's t test) by at least a factor of 1.7 were determined in two series of DNA microarray experiments: (i) five comparisons of the wild type and the Δ*ripA* mutant cultivated in CGXII minimal medium with 4% (w/v) glucose under iron limitation (1 mM $FeSO_4$); (ii) two comparisons of the wild type and the Δ*ripA* mutant cultivated in CGXII-glucose medium under iron excess (100 μM $FeSO_4$).

Aconitase Assay—Aconitase activity was determined as the rate of *cis*-aconitate formation from isocitrate (20), as described previously (2), except that the assay was performed at 30 °C. Cells of the 20-ml main culture were harvested by centrifugation at 5,000 × *g* for 10 min and 4 °C. The cell pellet was resuspended in 90 mM Tris/HCl, pH 8.0, and used for the preparation of cell extract. The assay mixture contained 950–995 μl of 90 mM Tris/HCl, pH 8.0, and 20 mM DL-trisodium isocitrate. The reaction was started with the addition of 5–50 μl of cell extract, and the formation of *cis*-aconitate was followed by measuring the absorbance increase at 240 nm using a Jasco V560 spectrophotometer. An extinction coefficient for *cis*-aconitate of 3.6 mM^{-1} cm^{-1} at 240 nm was used. One unit of activity corresponds to 1 μmol of isocitrate converted to *cis*-aconitate per min.

Overproduction and Purification of RipA—E. coli BL21(DE3) carrying the plasmid pET28b-*strep-ripA* was grown at 30 °C in 200 ml of LB medium with 50 μg/ml kanamycin to an A_{600} of ~1.2 before adding 1 mM isopropyl β-D-thiogalactoside. After cultivation for another 4 h, cells were harvested by centrifugation, washed once, and stored at −20 °C. For cell extract preparation, thawed cells were resuspended in 10 ml of buffer W (100 mM Tris/HCl, pH 8.0, 150 mM NaCl). After the addition of 1 mM diisopropylfluorophosphate and 1 mM phenylmethylsulfonyl fluoride, the cell suspension was passed three times through a French pressure cell (SLM Aminco, Spectronic Instruments, Rochester, NY) at 207 megapascals. Intact cells and cell debris were removed by centrifugation (15 min, 5,000 × *g*, 4 °C), and the cell-free extract was subjected to ultracentrifugation (1 h, 150,000 × *g*, 4 °C). The supernatant obtained after ultracentrifugation was applied to a StrepTactin-Sepharose column with a bed volume of 1 ml (IBA, Göttingen, Germany). The column was washed with 6 ml of buffer W, and RipA tagged with StrepTag-II was eluted with 8 × 0.5 ml of buffer W containing 7.5 mM desthiobiotin (Sigma). Fractions containing RipA were pooled, and the buffer was exchanged against TG buffer (30 mM Tris/HCl, pH 7.5, 10% (v/v) glycerin) using Vivaspin concentrators with a cut-off of 10 kDa. Protein concentrations were determined with the BCA protein assay kit (Pierce) using bovine serum albumin as a standard. The purity of the protein preparations was assessed by SDS-PAGE and subsequent protein detection with Gel Code blue stain reagent (Pierce). Using this protocol, ~0.2 mg of RipA protein was purified to apparent homogeneity from 200 ml of culture.

Overproduction and Purification of DtxR—E. coli BL21(DE3) carrying the plasmid pET24b-*dtxR* was grown at 30 °C in 100 ml of LB with 50 μg/ml kanamycin. Expression was induced at an A_{600} of ~0.3 with 1 mM isopropyl β-D-thiogalactoside. Four hours after induction, cells were harvested by centrifugation and stored at −20 °C. For cell extract preparation, thawed cells were washed once and resuspended in 10 ml of TNGI5 buffer (20 mM Tris/HCl, pH 7.9, 300 mM NaCl, 5% (v/v) glycerol,

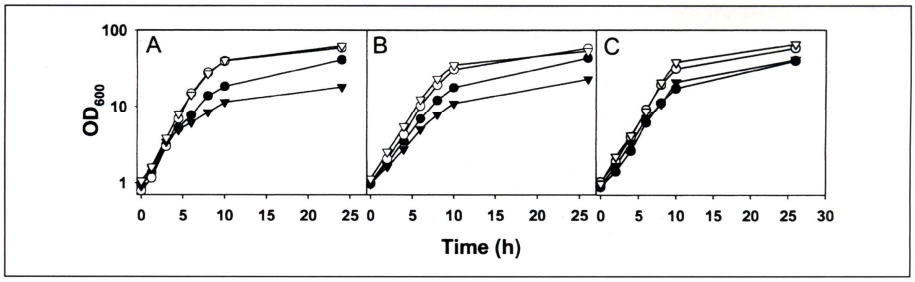

FIGURE 1. **Growth of *C. glutamicum* wild type (*circles*) and the Δ*ripA* mutant (*triangles*) in CGXII minimal medium with 4% (w/v) glucose and either 100 μM $FeSO_4$ (*open symbols*) or 1 μM $FeSO_4$ (*filled symbols*).** In the experiments shown in *A–C*, the strains contained either no plasmid (*A*) or pJC1 (*B*) or pJC1-*ripA* (*C*).

5 mM imidazol) containing 1 mM diisopropylfluorophosphate and 1 mM phenylmethylsulfonyl fluoride. Disruption of the cells and fractionation by centrifugation was performed as described above for RipA purification. DtxR present in the supernatant of the ultracentrifugation step was purified by nickel affinity chromatography using nickel-activated nitrilotriacetic acid-agarose (Novagen). After washing the column with TNGI50 buffer (which contains 50 mM imidazol), DtxR protein was eluted with TNGI100 buffer (which contains 100 mM imidazol). Fractions containing DtxR were pooled, and the elution buffer was exchanged against TG buffer (30 mM Tris/HCl, pH 7.5, 10% (v/v) glycerin). From 100 ml of culture, ~3 mg of DtxR was purified to apparent homogeneity.

Gel Shift Assays—For band shift assays of RipA with putative target promoters, purified RipA protein was mixed with DNA fragments (200–630 bp, final concentration 8–13 nM) in a total volume of 20 μl. The binding buffer contained 20 mM Tris/HCl, pH 7.5, 0.5 mM EDTA, 5% (v/v) glycerol, 1 mM dithiothreitol, 0.005% (v/v) Triton X-100, 50 mM NaCl, 5 mM $MgCl_2$, and 2.5 mM $CaCl_2$. Approximately 20 nM of different nontarget promoter fragments (*clpC*, *clpP*, *ripA*, and *porB*) were added as a negative control. After incubation for 30 min at room temperature, the samples were separated on a 10% native polyacrylamide gel at room temperature and 170 V using 1× TBE (89 mM Tris base, 89 mM boric acid, 2 mM EDTA) as electrophoresis buffer. The gels were subsequently stained with Sybr Green I according to the instructions of the supplier (Sigma) and photographed.

Binding of DtxR to the *ripA* promoter was carried out in a 20-μl reaction mixture containing 100 mM Tris/HCl (pH 7.5), 5 mM $MgCl_2$, 40 mM KCl, 10% (v/v) glycerol, 1 mM dithiothreitol, 150 μM $MnCl_2$, an 18 nM concentration of a 300-bp *ripA* promoter DNA fragment, and DtxR in concentrations ranging from 0 to 3.6 μM. The *ripA* fragment covered the region from position −230 to +70 relative to the translation start and was obtained by PCR with primers ripA-Prom-for and ripA-Prom-rev. As a negative control, a 23 nM concentration of a 200-bp *acn* promoter fragment extending from position +190 to −50 relative to the *acn* transcription start site (2) was added. This fragment was amplified with primers acn-Prom4-for and acn-Prom4-rev. The reaction mixture was incubated at room temperature for 30 min and then loaded onto a 10% native polyacrylamide gel containing 1 mM dithiothreitol and 150 μM $MnCl_2$. Electrophoresis was performed at room temperature and 170 V using 1× TB (89 mM Tris base, 89 mM boric acid) supplemented with 1 mM dithiothreitol and 150 μM $MnCl_2$ as electrophoresis buffer. All PCR products used in the gel shift assays were purified with the PCR purification Kit (Qiagen, Hilden, Germany) and eluted in EB buffer (10 mM Tris/HCl, pH 8.5).

RESULTS

Identification of RipA as a Potential Iron-dependent Regulator of the Aconitase Gene—In a previous study, we showed that expression of the aconitase gene *acn* of *C. glutamicum* is influenced by the iron availability, being reduced under iron limitation (2). This regulation also occurred in a mutant lacking AcnR, a repressor of the *acn* gene, and thus must be mediated by a different regulator or regulatory mechanism. A candidate gene that might be responsible for iron-dependent regulation of *acn* was identified in the DNA microarray experiments used to compare the gene expression profile of *C. glutamicum* under iron excess and iron limitation. Expression of the gene NCgl0943 was strongly influenced by the iron availability (2). Its mRNA level was always found to be increased under iron-limiting conditions, and it thus behaved like typical iron starvation genes. The protein derived from NCgl0943 is composed of 331 amino acid residues (36.044 kDa) and contains a DNA binding domain of the AraC family (PF00165 in the PFAM data base (21), PS01124 in the PROSITE data base (22)) with two helix-turn-helix motifs extending from position 113 to 159 and from position 165 to 208. It is flanked by amino- and carboxyl-terminal domains of 112 and 123 residues, respectively, which show no significant sequence similarity to other proteins. Based on the results described below, the NCgl0943 gene was designated *ripA* (repressor of iron proteins A).

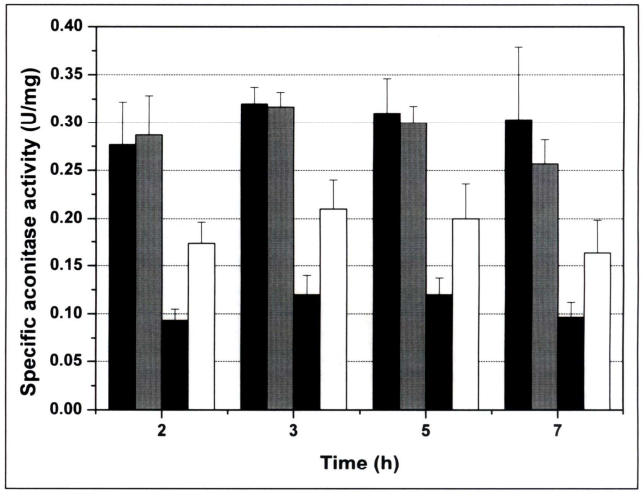

FIGURE 2. **Aconitase activity of *C. glutamicum* wild type and the Δ*ripA* mutant cultivated under iron excess (100 μM $FeSO_4$) and iron limitation (1 μM $FeSO_4$).** Cells were grown in CGXII minimal medium with 4% (w/v) glucose and harvested at four time points within the exponential growth phase (A_{600} between 2 and 9). Aconitase activity was determined in cell-free extracts. *Black* and *dark gray bars*, wild type cultivated with 100 μM iron and 1 μM iron, respectively. *Light gray bars* and *white bars*, Δ*ripA* cultivated with 100 μM iron and 1 μM iron, respectively. The values for the specific activity represent means ± S.D. for at least three independent cultivations and two determinations per experiment.

In order to test an involvement of the RipA protein in *acn* regulation, a *ripA* deletion mutant of *C. glutamicum* was constructed. In a first set of experiments, the growth behavior of the Δ*ripA* mutant was tested. As shown in Fig. 1*A*, no differences were observed between wild type and mutant cultivated in glucose minimal medium containing excess iron

TABLE ONE

Genes showing altered expression in the *C. glutamicum* Δ*ripA* mutant compared with wild type

NCgl number[a]	Gene	Annotation	Ratio, iron limitation[a]	Ratio, iron excitation[b]
NCgl2319	*catA*	Catechol 1,2-dioxygenase	4.41	1.03
NCgl1482	*acn*	Aconitase	2.40	0.88
NCgl1262	*leuC*	3-Isopropylmalate dehydratase, large subunit	1.65	0.90
NCgl1263	*leuD*	3-Isopropylmalate dehydratase, small subunit	2.13	0.91
NCgl0359	*sdhC*	Succinate dehydrogenase, cytochrome *b* subunit	1.90	0.85
NCgl0360	*sdhA*	Succinate dehydrogenase, flavoprotein	1.71	0.81
NCgl0361	*sdhB*	Succinate dehydrogenase, FeS protein	1.64	1.01
NCgl1143	*narK*	Nitrate/nitrite transporter	1.63	1.04
NCgl1142	*narG*	Nitrate reductase, α subunit	1.89	1.00
NCgl1141	*narH*	Nitrate reductase, β subunit	1.67	0.90
NCgl1140	*narJ*	Nitrate reductase, δ subunit	1.75	1.05
NCgl1139	*narI*	Nitrate reductase, γ subunit	1.72	0.99
NCgl2657	*pta*	Phosphotransacetylase	1.82	1.24
NCgl2439	*ftn*	Ferritin	0.55	0.58
NCgl1490		Putative membrane protein	0.52	0.65
NCgl2434		Putative membrane protein	0.46	0.91
NCgl0140		Putative sugar *O*-acetyltransferase	0.44	1.09
NCgl1096		Putative flavin-containing monooxygenase	0.38	0.46
NCgl2001		Conserved hypothetical protein	0.30	0.81
NCgl2897	*dps*	Starvation-induced DNA protection protein	0.29	0.30
NCgl0943	*ripA*	Transcriptional regulator, AraC family	0.11	0.16

[a] This column includes those genes whose average mRNA ratio (Δ*ripA* mutant/wild type) was altered ≥1.7-fold or ≤1.7-fold (p value ≤0.05) in five DNA microarray experiments performed with RNA isolated from five independent cultivations in CGXII minimal medium under iron limitation (1 μM $FeSO_4$). The genes *leuC*, *sdhB*, *narK*, and *narH* show an average mRNA ratio below 1.7 but were included, since they are organized in operons with genes (*leuD*, *sdhCA*, or *narKGJI*) having an mRNA ratio above 1.7.

[b] This column provides the mRNA ratio (Δ*ripA* mutant/wild type) of the genes under iron excess conditions. It represents the average of two DNA microarray experiments performed with RNA isolated from two independent cultivations in CGXII minimal medium under iron excess (100 μM $FeSO_4$).

(100 μM). However, under iron-limiting conditions (1 μM), the *ripA* mutant grew initially like the wild type, but after an A_{600} of about 5, the growth rate of the mutant decreased more strongly than that of the wild type. The final cell density of the mutant (A_{600} of 20) was only half that of the wild type (A_{600} = 40). Thus, the Δ*ripA* mutant has a growth defect under iron limitation but not under iron excess. As shown in Fig. 1*C*, this growth defect could be reversed by transformation with a plasmid carrying the *ripA* gene with its native promoter region (pJC1-*ripA*), but not with pJC1 alone (Fig. 1*B*).

In a second set of experiments, aconitase activity was determined in wild-type and Δ*ripA* cells from cultures grown under iron excess and iron limitation. As shown in Fig. 2, the aconitase activity of the two strains was nearly identical under iron excess, whereas under iron limitation, the Δ*ripA* mutant had a 1.5–2-fold higher activity than the wild type at four different time points. Thus, the absence of *ripA* might result in an increased expression of the *acn* gene under iron limitation, but not under iron excess.

Comparison of the Expression Profiles of Δripa Mutant and Wild Type with DNA Chips—In order to determine the effects of RipA on *acn* expression as well as on global gene expression, whole genome DNA microarrays of *C. glutamicum* (16) were used to compare the mRNA ratios of the Δ*ripA* mutant and the wild type under iron limitation and iron excess. Under iron starvation (1 μM iron), nine genes showed a >1.7-fold higher mRNA level in the Δ*ripA* mutant (TABLE ONE). This group included the aconitase gene *acn*, supporting the above made assumption that increased *acn* expression is responsible for the elevated aconitase activity in the Δ*ripA* mutant under iron limitation. Besides *acn*, *catA* (catechol 1,2-dioxygenase), *leuCD* (isopropylmalate dehydratase), *narKGHJI* (nitrate/nitrite transporter and nitrate reductase), *sdhCAB* (succinate dehydrogenase), and *pta* (phosphotransacetylase) showed higher mRNA levels in the Δ*ripA* mutant compared with the wild type. The mRNA level of the *ackA* gene for acetate kinase, which is co-transcribed with *pta* (23), was slightly increased in the Δ*ripA* mutant but below the cut-off used. Except for the transporter NarK, phosphotransacetylase, and acetate kinase, the enzymes encoded by these genes are known to contain iron, mostly in the form of iron-sulfur clusters (aconitase, isopropylmalate dehydratase, nitrate reductase, succinate dehydrogenase) and/or heme (nitrate reductase, succinate dehydrogenase) (24). Remarkably, the mRNA level of the genes mentioned above was changed only under iron limitation but not under iron excess (TABLE ONE).

Besides *ripA*, seven other genes showed a >1.7-fold decreased mRNA level in the Δ*ripA* mutant under iron limitation (TABLE ONE). There is no obvious common property of these genes; however, *dps* (starvation-induced DNA protection protein) and *ftn* (ferritin) are critically involved in iron homoeostasis (25, 26). In contrast to the genes with an increased mRNA level in the Δ*ripA* mutant, *dps* and *ftn* had decreased mRNA levels not only under iron limitation but also under iron excess.

Binding of Purified RipA Protein to the acn Promoter—In order to test whether the influence of RipA on *acn* expression is direct, binding of RipA to the *acn* promoter was analyzed. For that purpose, the RipA protein containing an amino-terminal StrepTag-II was overproduced in *E. coli* and purified to apparent homogeneity by affinity chromatography (Fig. 3). Gel shift assays showed that the RipA protein bound with high affinity to fragment 1 covering the entire *acn* promoter region, whereas a control fragment covering the promoter of the *porB* gene encoding an anion channel (27) was not shifted (Fig. 4). A RipA-fragment 1 complex was already observed at a 5-fold molar excess of RipA. At a 10-fold excess, two RipA-fragment 1 complexes were observed, and at a 30-fold excess, only the second RipA-DNA complex was observed, suggesting the presence of two binding sites. Gel shift assays with 10 different subfragments (Fig. 4) clearly confirmed the presence of two

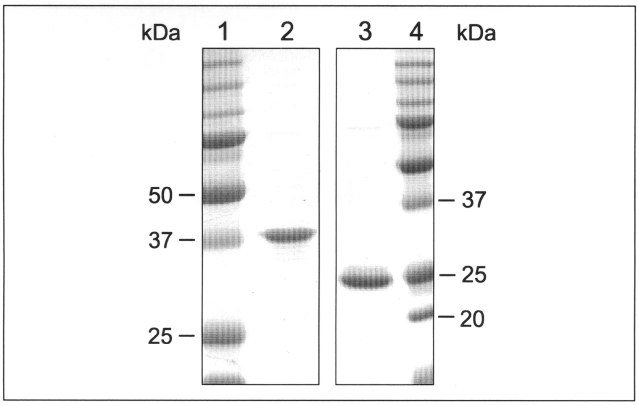

FIGURE 3. **Purification of RipA and DtxR.** *Lane 1*, protein standard; *lane 2*, purified RipA obtained after desthiobiotin elution from a StrepTactin affinity column; *lane 3*, purified DtxR obtained after imidazol elution from a nickel-chelate affinity column; *lane 4*, protein standard. Proteins were separated on a 12% SDS-polyacrylamide gel and stained with Coomassie Blue.

distinct binding sites, extending from position −212 to −194 (binding site A) and from −155 to −137 (binding site B) relative to the transcription start site of *acn* determined previously (2). Fragments lacking these regions (*e.g.* fragment 2) were not shifted, fragments containing one of the two regions formed a single RipA-DNA complex (*e.g.* fragment 7), and fragments containing both regions (*e.g.* fragment 8) formed two RipA-DNA complexes (Fig. 4).

Inspection of the two regions revealed that they contained a similar sequence motif but in opposite orientation (Fig. 5). The relevance of this motif was tested by mutational analysis, in which three or four nucleotides were exchanged simultaneously. As shown in Fig. 5, all mutations within the proposed motif prevented RipA binding, whereas the mutations outside did not inhibit binding. These results confirmed the importance of the sequence G(A/T)GCGN$_6$GAC for RipA binding.

Binding of Purified RipA Protein to Additional Target Promoters—As a result of the DNA microarray experiments, the operons *catA*, *leuCD*, *narKGHJI*, *sdhCAB*, and *pta-ack* were identified as further putative target genes of RipA, since their mRNA level was also increased in the Δ*ripA* mutant. We therefore tested the binding of RipA to the corresponding promoter regions. As shown in Fig. 6, all five promoter fragments were shifted by RipA at a molar excess (protein/DNA) of 5–10, and in all cases, two RipA-DNA complexes were formed. This indicates that there are two RipA binding sites in the corresponding promoter regions, as shown above for the *acn* promoter. Since expression of the *katA* gene encoding the hemoprotein catalase was also altered in some of the DNA microarray experiments, the *katA* promoter region was also tested for RipA binding and shown to contain two RipA binding sites with affinities comparable with those described above. In addition, a third binding site of lower affinity was detected (Fig. 6). Binding of RipA was also tested with the promoter regions of *ripA*, *dps*, and *ftn*. In the case of *ripA* and *dps*, no shift was observed, suggesting that there is no autoregulation of *ripA* and no direct control of *dps* expression by RipA. In the case of *ftn*, a weak binding was observed, with about 30% of the *ftn* fragment shifted at a 100-fold molar excess of RipA (data not shown). For the other RipA targets, a complete shift was observed at a 10–30-fold molar RipA excess. Thus, the affinity of RipA to the *ftn* promoter appears to be much lower. If RipA directly influences *ftn* expression, it should act as an activator, since the *ftn* mRNA level was decreased in the Δ*ripA* mutant. Considering that induction of an iron storage protein under iron limitation appears counterproductive, the role of RipA in *ftn* expression is not yet clear.

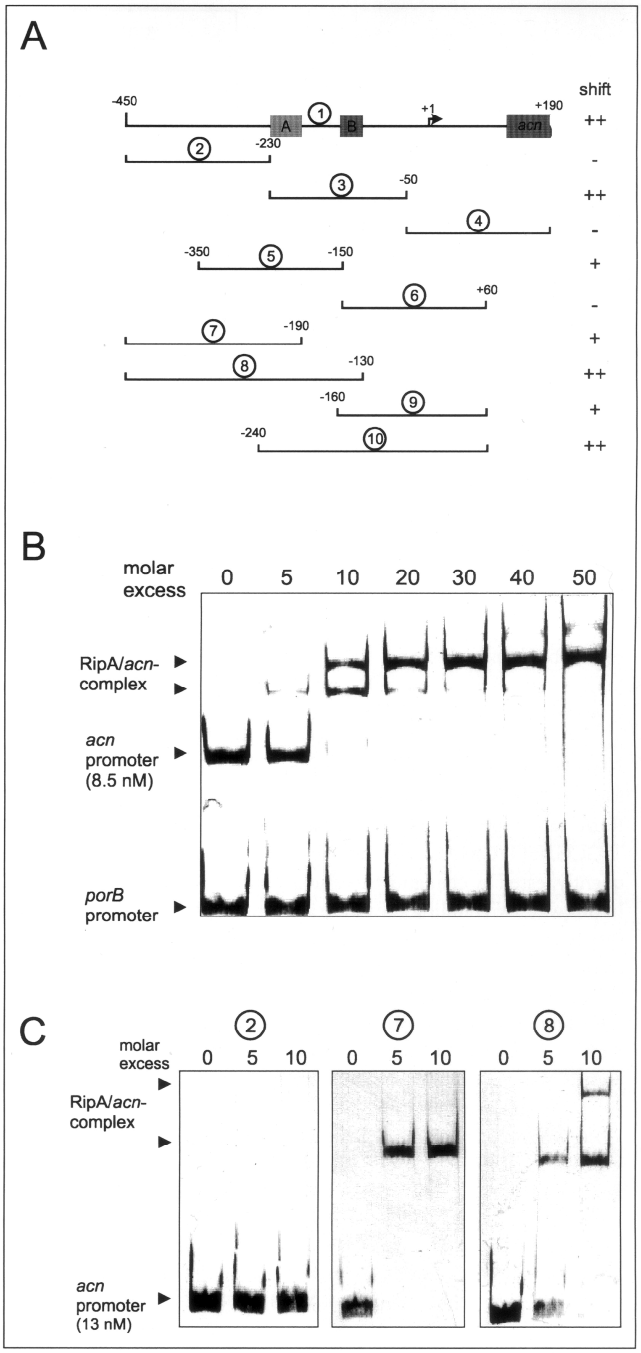

FIGURE 4. **Binding of RipA to the *acn* promoter.** *A*, DNA fragments (*circled 1–10*) used to analyze RipA binding to the *acn* promoter by gel shift assays. The *numbers* indicate the ends of the fragments relative to the *acn* transcription start site (+1). Oligonucleotides used for amplification of the 10 fragments by PCR are listed in supplemental Table S2 (acn-for-3–acn-Prom10-for). At the *right*, it is indicated whether the fragment was shifted once (+), twice (++), or not at all (−). The *boxes labeled A* and *B* indicate the regions that were identified to contain RipA binding sites. *B*, gel showing binding of purified RipA (5–50-fold molar excess) to fragment 1 (8.5 nM 632-bp fragment). A 485-bp *porB* promoter fragment (11 nM) served as negative control. The DNA-protein mixture was incubated for 30 min at room temperature before separation by native polyacrylamide gel electrophoresis (10%) and staining with SybrGreen I. *C*, gel showing binding of RipA (5- and 10-fold molar excess) to fragment 2 (no binding site), fragment 7 (one binding site), and fragment 8 (two binding sites).

As described above for *acn*, the RipA binding sites within the *sdhCAB* promoter were narrowed down with six different subfragments (data not shown). In this way, binding site A was shown to be located in the

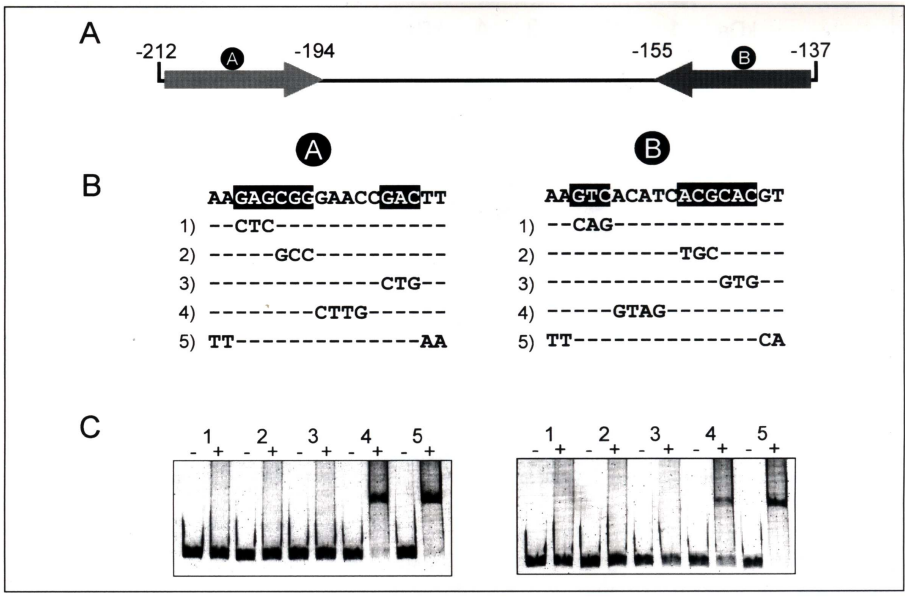

FIGURE 5. **Mutational analysis of the RipA binding sites within the *acn* promoter.** *A*, the *two inverted arrows* denoted *A* and *B* indicate the two RipA binding sites forming an imperfect inverted repeat as deduced from gel shift assays. The *numbers* indicate their positions relative to the *acn* transcription start site. *B*, mutations introduced within (*1*, *2*, and *3*) and outside (*4* and *5*) the proposed RipA binding sites A and B are listed *below* the wild-type sequence. Fragments containing these mutations were obtained with the primer pairs acn-A.1/acn-for-3 to acn-A.5/acn-for-3 and acn-B.1/acn-Prom4-rev to acn-B.5/acn-Prom4-rev (see supplemental Table S2). *C*, gel showing binding of RipA to the mutated DNA fragments. Approximately 30 nM fragments A1–A5 and B1–B5 were incubated for 30 min at room temperature either without RipA (*lanes* labeled with a *minus sign*) or with 1.2 μM of purified RipA protein (*lanes* labeled with a *plus sign*). Subsequently, the samples were separated on a 10% nondenaturating polyacrylamide gel, and the gels were stained with SybrGreen I.

region between −180 and −90 relative to the *sdhC* start codon and binding site B between −90 and +12. Inspection of these regions revealed sequence motifs similar to the ones identified in the *acn* promoter. The relevance of these sites for RipA binding was again confirmed by mutational analysis (supplemental Fig. S1). Based on the four RipA binding sites identified upstream of *acn* and *sdhC*, the other RipA target promoters were searched for motifs similar to G(A/T)GCGN5(T/C)GAC, and the relevance of putative motifs was subsequently tested by changing three adjacent nucleotides within the motif. In this way, two binding sites were identified upstream of *narK* and *pta*, three upstream of *katA*, and one upstream of *leuC* and *catA*. Fig. 7 gives an overview of all identified RipA binding sites, their position relative to the respective start codon, and their orientation. From the alignment of the 13 binding sites, the RipA consensus motif RRGCGN$_4$RYGAC was derived. From the 13 motifs, two were present in inverted orientation (acn-B and pta-A). The distance between neighboring RipA binding sites varied between 57 and 339 bp.

Regulation of ripA Expression by DtxR—As shown previously (2), expression of *ripA* followed the same pattern as that of typical iron acquisition genes (*i.e.* its mRNA level was always increased under iron-limiting conditions). In *Corynebacterium diphtheriae*, DtxR in complex with iron represses expression of the iron starvation proteins under iron excess but is inactivated under iron limitation (28). *C. glutamicum* contains a protein with 72% sequence identity to *C. diphtheriae* DtxR (encoded by NCgl1845), and the *C. glutamicum* homolog was previously shown to repress the *tox* promoter from *C. diphtheriae* in an iron-dependent manner (29). It was therefore tempting to speculate that expression of *ripA* is repressed under iron excess by DtxR and derepressed under iron starvation. A 19-bp consensus operator of DtxR from *C. diphtheriae* has been defined as TWAGGTTAGSCTAACCTWA (30). Inspection of the *C. glutamicum ripA* promoter region revealed a sequence motif (*i.e.* TGAGGTTAGCGTAACCTAC) that differs in only three positions from the consensus binding site and ends 32 bp upstream of the *ripA* start codon. In order to test whether this motif is a DtxR binding site, the DtxR protein from *C. glutamicum* was overproduced in *E. coli* and isolated by means of a carboxyl-terminal histidine tag (Fig. 2). Gel shift analysis revealed that the purified DtxR protein bound to the *ripA* promoter region (Fig. 8). A partial shift was

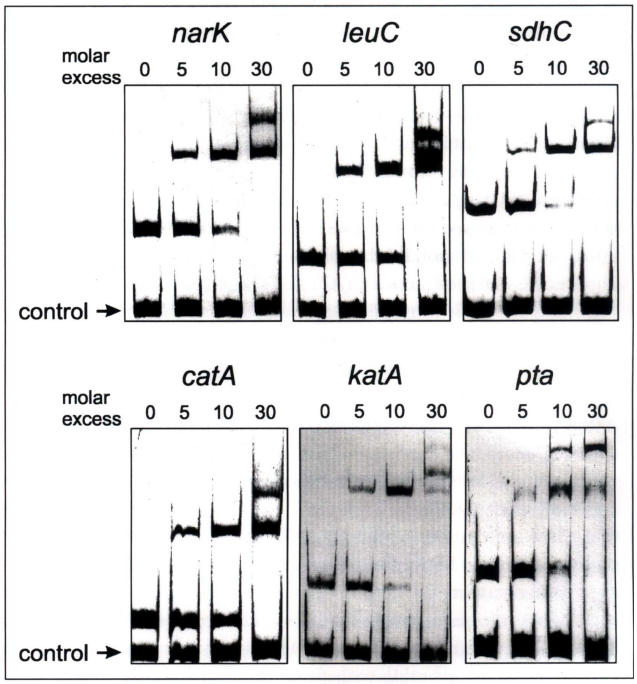

FIGURE 6. **Binding of RipA to the promoter regions of *narK*, *leuC*, *sdhC*, *catA*, *katA*, and *pta*.** DNA fragments (400–600 bp) covering the promoter regions of *narK* (13 nM), *leuC* (13 nM), *sdhC* (10 nM), *catA* (17 nM), *katA* (13 nM), and *pta* (9 nM) were incubated for 30 min at room temperature with a 5-, 10-, or 30-fold excess of purified RipA protein before separation by native polyacrylamide gel electrophoresis (10%) and staining with SybrGreen I. DNA fragments (200–350 bp) covering the promoter regions of *clpC* or *ripA* served as negative controls.

observed at a 20-fold molar excess (protein/DNA), whereas a 100-fold molar excess was required for a complete shift. Binding of DtxR to the *ripA* promoter was strictly dependent on the presence of divalent cations (*e.g.* Mn^{2+}) (data not shown). As a negative control, the promoter region of *acn* was used, which was not shifted. These results clearly support a regulation of *ripA* expression by DtxR.

RipA binding site	Sequence	Position	Orientation
acn-A	AA GAGCGGGAACCGAC TT	-312.5	+
acn-B	AC GTGCGTGATGTGAC TT	-255.5	-
sdhC-A	AT GAGCGTCAAACGAC AA	-138.5	+
sdhC-B	GG GAGCGCCCCGTGAC TG	-57.5	+
narK-A	TA AAGTCAATTACGAC AC	-148.5	+
narK-B	AG AGGCATCACGTGAC AC	-2.5	+
pta-A	AA GCGCGCAGCGTGAC AA	-268.5	-
pta-B	AC AAGCCTGAAGTGTC AT	-2.5	+
katA-A	GG GGGCGTGCCATGTC GT	-485.5	+
katA-B	AG GAGCGCGCTGCGAA GC	-410.5	+
katA-C	GG TGGCGCGAAGTGAC AT	-71.5	+
leuC-A	TT GGGCGGGACGTGAC AT	-98.5	+
catA-A	TG AAGCGGTGTGTGAC AT	-342.5	+
Consensus	dn RRGCGNNNNRYGAC wn		

FIGURE 7. **Overview on RipA binding sites.** The 13 RipA binding sites identified in this work were aligned. The position of the center of the binding sites relative to the translation start site is given by the *numbers* in the *position column*, and the orientation of the binding sites is indicated by *plus* and *minus signs*. The designations *A*, *B*, and *C* of the binding sites were assigned according to the distance to the translation start site, with the A sites located most distantly. In the derived consensus sequence, single residues are indicated when they occur in at least 10 binding sites. The first two and the last two bases shown are probably not essential for binding, since mutation of these sites did not inhibit RipA binding in the case of acn-A, acn-B, sdhC-A and sdh-B. The bases interfering with RipA binding in the case of the *acn* and *sdhC* regions are shown in Figs. 5 and S1, respectively. The relevance of the other binding sites was confirmed by showing that mutation of three consecutive bases inhibited binding of RipA to the fragment containing the proposed binding site. The bases mutated were GAC for narK-A, GGC for narK-B, GCG for pta-A, GTC for pta-B, GCG for katA-A, GAG for katA-B, GCG for katA-C, GCG for leuC-A, and GCG for catA-A.

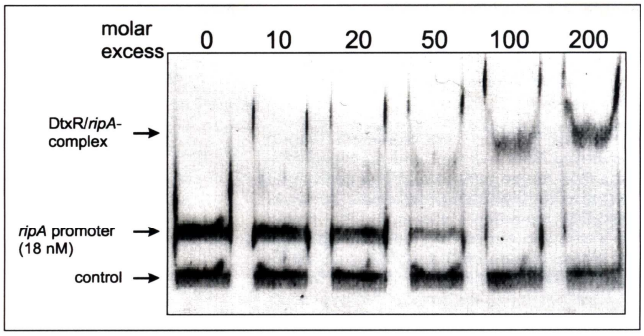

FIGURE 8. **Binding of DtxR to the *ripA* promoter region.** Different concentrations of purified DtxR protein (10–200-fold molar excess) were incubated with 18 nM of a 320-bp DNA fragment covering the *ripA* promoter region (−230 to +70 relative to the translation start site), including a putative DtxR binding site (TGAGGTTAGCGTAACCTAC). A 200-bp fragment covering the promoter region of *acn* served as a negative control. The samples were separated by native polyacrylamide gel electrophoresis, and DNA was stained with SybrGreen I.

DISCUSSION

Iron is a critical element for bacteria, being essential as a co-factor in a multitude of enzymes, poorly soluble and dangerous, by catalyzing the formation of reactive oxygen species (25). Therefore, most cells have sophisticated regulatory systems to ensure a sufficient supply of iron but to avoid high levels of free Fe^{2+}, the form responsible for hydroxyl radical production via the Fenton reaction (31). In many Gram-negative and low GC Gram-positive bacteria, the Fur protein is the central regulator of iron regulation (32, 33), whereas in many high GC Gram-positive genera (*e.g. Corynebacterium*, *Mycobacterium*, *Rhodococcus*, or *Streptomyces*), DtxR and homologous proteins are the key regulators in iron metabolism (28, 34). Under iron excess, DtxR in complex with its co-repressor Fe^{2+} represses its target genes, in particular uptake systems for iron siderophores, heme, or other iron sources. When iron becomes limiting, Fe^{2+} dissociates from DtxR, and apo-DtxR dissociates from its target promoters. The DtxR protein was first identified in *C. diphtheriae*, where it regulates the expression of the diphtheria toxin gene carried by corynebacteriophage β. In this work, we have unraveled a completely new aspect of DtxR (*i.e.* its influence on the expression of several prominent iron-containing proteins via the AraC-type regulator RipA).

The involvement of RipA in iron-dependent regulation was suggested by recent microarray experiments in which the *ripA* mRNA level was always found to be increased under iron limitation, similar to a multitude of iron acquisition genes (2). In our present study, transcriptome comparisons of a Δ*ripA* mutant and the wild type revealed seven operons whose mRNA level was increased in the Δ*ripA* mutant under iron limitation, but not under iron excess (*i.e.* those encoding aconitase (*acn*), isopropylmalate dehydratase (*leuCD*), succinate dehydrogenase (*sdhCAB*), nitrate/nitrite transporter and nitrate reductase (*narKGHJI*), catechol 1,2-dioxygenase (*catA*), phosphotransacetylase (*pta*), and catalase (*katA*)). The hypothesis that RipA functions as a repressor of these operons was supported by gel shift assays showing that purified RipA binds to the seven corresponding promoter upstream regions. In all cases, at least two RipA-DNA complexes of distinct mobility were identified in the gel shift experiments, suggesting the presence of at least two RipA binding sites. Using subfragments and mutational analysis, the binding sites upstream of *acn* and *sdhCAB* were identified and used to search for similar sequences in the other target promoters. Subsequently, mutational analysis led to the identification of three binding sites upstream of *katA* and of two binding sites upstream of *narKGHJI* and *pta*, whereas in the case of *catA* and *leuCD* only one of the binding sites could be identified up to now. Alignment of the corresponding sequences revealed a minimal consensus sequence of the type RRGCGN$_4$RYGAC. AraC-type regulators (35, 36) contain two adjacent helix-turn-helix (HTH)[3] motifs, which in the case of MarA insert in two adjacent segments of the major groove of the *mar* promoter (37). Thus, one might speculate that one HTH motif of RipA interacts with the conserved RRGCG motif and the adjacent HTH with the RYGAC motif.

Whereas the vast majority of AraC-type regulators investigated to date function as transcriptional activators (35, 36), the results presented here indicate that RipA predominantly acts as a transcriptional repressor. Repression is usually accomplished by binding of the regulator between the −35 and −10 regions of the promoter and blocking access of RNA polymerase. From the RipA target operons identified in this work, transcriptional start sites have been determined for *acn* (located 113 bp (TS2) and 110 bp (TS1) upstream of the start codon (2)) and for *pta* (located 158 bp (TS2) and 46 bp (TS1) upstream of the initiation codon (38)). In the case of *acn*, the two identified RipA binding sites are centered at −203.5 and −146.5 with respect to TS2. Since these sites are far upstream of the RNA polymerase binding site, the question arises of how RipA represses *acn* expression. One possibility is the presence of one or more additional binding sites that we have not yet identified. A weak third RipA-*acn* complex that was observed at high RipA concentrations (Fig. 4*B*) supports this suggestion. A promising RipA binding motif is located immediately downstream of the *acn* start codon (GAGCTCACTGTGAC). However, fragment 4 in Fig. 4*A*, which contains this motif, was not shifted by RipA, at least under the conditions used in the experiment. Possibly, this site can only be occupied after previous binding to one of the other sites or under different conditions. Another possibility could be that an additional protein is involved whose binding is influenced by the presence of RipA. In the case of *pta*, the identified RipA binding sites are centered at −111.5 and +156.5 with respect to TS2, with the second binding site overlapping the *pta*

[3] The abbreviation used is: HTH, helix-turn-helix.

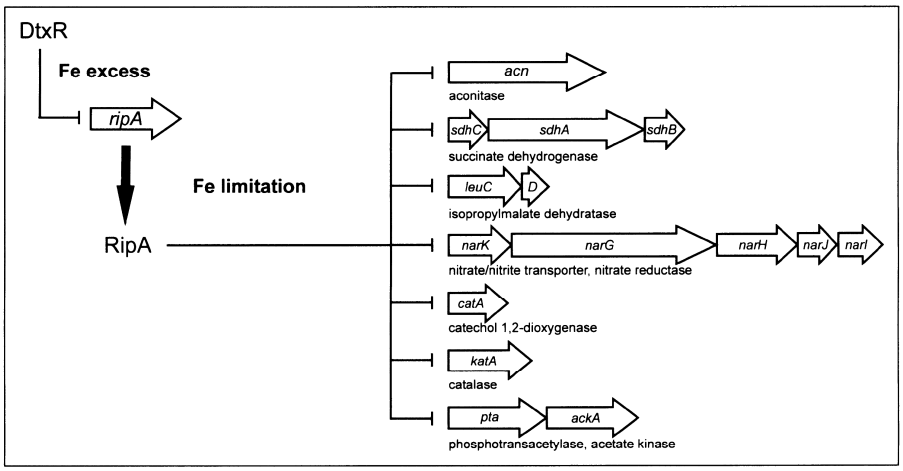

FIGURE 9. **Model of the regulatory cascade involving DtxR and RipA and organization of the RipA target genes.** Under iron excess, DtxR represses the expression of *ripA*. Under iron limitation, DtxR repression is relieved, and RipA protein is synthesized and partially represses expression of its target genes, which encode iron-containing proteins, except for *narK*, *pta*, and *ackA*. In this way, intracellular iron usage is modulated and supplements mechanisms for iron uptake that are directly regulated by DtxR.

start codon. In this case, direct inhibition of transcription by RipA can be envisaged. For *narKGHJI*, the RipA binding sites are centered at −149.5 and −2.5 with respect to the *narK* start codon. As in the case of *pta*, the second site very likely interferes with transcription of the *nar* operon. In the case of *sdhCAB*, *katA*, *catA*, and *leuCD*, no predictions can be made on the mechanism of repression yet. The presence of at least two binding sites in each RipA target promoter and the large and varying distances between these binding sites might suggest that DNA looping is involved in the mechanism of action of RipA, as reported, for example, for the AraC-type regulators AraC (39) and MelR (40).

Except for the nitrate/nitrite transporter NarK and presumably phosphotransacetylase, all of the enzymes repressed by RipA contain iron; aconitase and isopropylmalate dehydratase possess one iron-sulfur cluster, succinate dehydrogenase probably harbors three iron-sulfur clusters and two hemes (24), nitrate reductase presumably contains four iron sulfur-clusters and two hemes (24), catalase contains heme,[4] and catechol 1,2-dioxygenase contains one non-heme iron (41). Therefore, it is obvious to assume that a major function of RipA is to reduce the synthesis of iron proteins under iron-limiting conditions, thus reducing the cell's iron demand and preventing the formation of inactive apoenzymes lacking iron. In agreement with such a function, the mRNA levels of *acn*, *leuCD*, *sdhCAB*, *narKGHJI*, *catA*, *pta*, and *katA* were decreased under iron limitation compared with iron excess, both in the wild type and in the Δ*acnR* mutant (2). Whereas repression of the non-iron protein NarK can be explained by co-transcription with the nitrate reductase structural genes, the inclusion of phosphotransacetylase in the RipA regulon must have other reasons. A dependence on iron has only been described for the enzyme of *Clostridium acidiurici* (42), whereas phosphotransacetylase from other species apparently does not require iron. Phosphotransacetylase catalyzes the reversible conversion of acetylphosphate and acetyl-CoA and, in concert with acetate kinase, is involved in the catabolism of acetate (38) as well as in the formation of acetate from acetyl-CoA. *C. glutamicum*, in contrast to *E. coli*, usually does not form acetate as a product of aerobic overflow metabolism, and therefore the primary function of phosphotransacetylase in this species appears to be in acetate utilization. Since acetate catabolism involves a 2–3-fold higher carbon flux through the citric acid cycle compared with growth on glucose (43), repression of *pta* by RipA may serve to reduce acetate utilization under iron limitation and thus to prevent an increased citric acid cycle flux, which cannot be maintained if aconitase and succinate dehydrogenase are repressed at the same time.

A regulatory cascade with an analogous function to that of DtxR and RipA in *Corynebacterium* is found in *E. coli*. Here the role of DtxR is fulfilled by Fur, whereas the small RNA RyhB plays a function similar to that of RipA (44). Expression of *ryhB* is repressed by Fur under iron excess and increases under iron limitation. RyhB acts as an antisense RNA and inhibits translation of the mRNAs encoding succinate dehydrogenase (*sdhCDAB*), aconitase A (*acnA*), fumarase A (*fumA*), ferritin (*ftnA*), bacterioferritin (*bfr*), and superoxide dismutase B (*sodB*). Although the spectrum of target genes regulated by RipA and RyhB only partially overlaps, it is remarkable that both involve the iron-containing proteins of the citric acid cycle (the only fumarase of *C. glutamicum* belongs to the type II fumarases and does not contain iron).

A search for the distribution of RipA revealed that homologous proteins are only present in *Corynebacterium efficiens* (CE1047; 70.1% sequence identity) and *C. diphtheriae* (DIP0922; 51.5% sequence identity), but not in *Corynebacterium jeikeium* (45) and other high GC gram positives (*e.g.* the genera *Mycobacterium* or *Streptomyces*). The *C. efficiens ripA* gene, as annotated in the genome sequence (46), encodes a protein of 400 amino acids. We prefer an ATG start codon that is located 68 codons downstream of the annotated GTG start codon, because the derived protein has a length comparable with the RipA proteins from *C. glutamicum* and *C. diphtheriae* (supplemental Fig. S2) and because a well conserved DtxR binding site (TGAGGTTAGCGTAACCTAC) deviating in only two positions from the consensus sequence (30) ends 40 bp upstream of the *ripA* ATG start codon proposed here (164 bp downstream of the annotated GTG start codon). In *C. diphtheriae*, the annotated genome sequence from strain NCTC13129 predicts that the *ripA* homologous gene DIP0922 encodes a protein of 335 amino acid residues (47). Inspection of the corresponding upstream sequence revealed a putative DtxR binding site (CGAGCAAGGAGTAACCTTA) ending 87 bp upstream of the proposed start codon, which, however, differed in eight positions from the consensus sequence and thus is quite speculative. Interestingly, Lee *et al.* (48) previously identified a DtxR-regulated gene region designated IRP3 from *C. diphtheriae* strain C7, which is equivalent to the one described above. The DtxR binding site they identified experimentally by DNase I footprinting (TTAGGTGAGACGCACCCAT) is located upstream of an open reading frame encoding a 124-amino acid polypeptide showing high identity to regions of *C. diphtheriae* RipA (data not shown). The IRP3 DtxR binding site starts 267 bp downstream of the proposed start codon of

[4] M. Bott and M. Wingens, unpublished data.

DIP0922. Further studies are required to determine the relevance of the strain differences and the functionality of the putative DtxR binding site upstream of DIP0922.

The discovery of RipA as a repressor of iron proteins and its own repression by DtxR have unraveled a new aspect of the regulatory network controlling iron metabolism in *Corynebacterium* (Fig. 9). Aspects that have to be addressed in future work are the mechanism(s) of repression by RipA and the mechanism of RipA inactivation after a shift from iron limitation to iron excess. This will probably require an understanding of the function of the N- and C-terminal domains that show no homology to other proteins.

Acknowledgments—We thank Hermann Sahm for continuous support and Volker Wendisch for stimulating discussions in the initial phase of this project and for establishing the DNA chip technique in our institute.

REFERENCES

1. Eggeling, L., and Bott, M. (eds) (2005) *Handbook of Corynebacterium glutamicum*, CRC Press, Taylor & Francis Group, Boca Raton, FL
2. Krug, A., Wendisch, V. F., and Bott, M. (2005) *J. Biol. Chem.* **280,** 585–595
3. Kinoshita, S., Udaka, S., and Shimono, M. (1957) *J. Gen. Appl. Microbiol.* **3,** 193–205
4. Sambrook, J., Fritsch, E. F., and Maniatis, T. (1989) *Molecular Cloning: A Laboratory Manual*, Cold Spring Harbor Laboratory, Cold Spring Harbor, NY
5. Keilhauer, C., Eggeling, L., and Sahm, H. (1993) *J. Bacteriol.* **175,** 5595–5603
6. Studier, F. W., and Moffatt, B. A. (1986) *J. Mol. Biol.* **189,** 113–130
7. Eikmanns, B. J., Thum-Schmitz, N., Eggeling, L., Luedtke, K. U., and Sahm, H. (1994) *Microbiology* **140,** 1817–1828
8. Hanahan, D. (1985) in *DNA Cloning* (Glover, D. M., ed) Vol. 1, pp. 109–135, IRL Press, Oxford, UK
9. van der Rest, M. E., Lange, C., and Molenaar, D. (1999) *Appl. Microbiol. Biotechnol.* **52,** 541–545
10. Niebisch, A., and Bott, M. (2001) *Arch. Microbiol.* **175,** 282–294
11. Schäfer, A., Tauch, A., Jäger, W., Kalinowski, J., Thierbach, G., and Pühler, A. (1994) *Gene (Amst.)* **145,** 69–73
12. Cremer, J., Eggeling, L., and Sahm, H. (1990) *Mol. Gen. Genet.* **220,** 478–480
13. Skerra, A., and Schmidt, T. G. (2000) *Methods Enzymol.* **326,** 271–304
14. Engels, S., Schweitzer, J. E., Ludwig, C., Bott, M., and Schaffer, S. (2004) *Mol. Microbiol.* **52,** 285–302
15. Möker, N., Brocker, M., Schaffer, S., Krämer, R., Morbach, S., and Bott, M. (2004) *Mol. Microbiol.* **54,** 420–438
16. Wendisch, V. F. (2003) *J. Biotechnol.* **104,** 273–285
17. Lange, C., Rittmann, D., Wendisch, V. F., Bott, M., and Sahm, H. (2003) *Appl. Environ. Microbiol.* **69,** 2521–2532
18. Polen, T., and Wendisch, V. F. (2004) *Appl. Biochem. Biotech.* **118,** 215–232
19. Ishige, T., Krause, M., Bott, M., Wendisch, V. F., and Sahm, H. (2003) *J. Bacteriol.* **185,** 4519–4529
20. Henson, C. P., and Cleland, W. W. (1967) *J. Biol. Chem.* **242,** 3833-&
21. Bateman, A., Coin, L., Durbin, R., Finn, R. D., Hollich, V., Griffiths-Jones, S., Khanna, A., Marshall, M., Moxon, S., Sonnhammer, E. L. L., Studholme, D. J., Yeats, C., and Eddy, S. R. (2004) *Nucleic Acids Res.* **32,** D138–D141
22. Falquet, L., Pagni, M., Bucher, P., Hulo, N., Sigrist, C. J. A., Hofmann, K., and Bairoch, A. (2002) *Nucleic Acids Res.* **30,** 235–238
23. Reinscheid, D. J., Schnicke, S., Rittmann, D., Zahnow, U., Sahm, H., and Eikmanns, B. J. (1999) *Microbiology* **145,** 503–513
24. Bott, M., and Niebisch, A. (2003) *J. Biotechnol.* **104,** 129–153
25. Andrews, S. C., Robinson, A. K., and Rodriguez-Quinones, F. (2003) *FEMS Microbiol. Rev.* **27,** 215–237
26. Smith, J. L. (2004) *Crit. Rev. Microbiol.* **30,** 173–185
27. Costa-Riu, N., Maier, E., Burkovski, A., Kramer, R., Lottspeich, F., and Benz, R. (2003) *Mol. Microbiol.* **50,** 1295–1308
28. Tao, X., Schiering, N., Zeng, H. Y., Ringe, D., and Murphy, J. R. (1994) *Mol. Microbiol.* **14,** 191–197
29. Oguiza, J. A., Tao, X., Marcos, A. T., Martin, J. F., and Murphy, J. R. (1995) *J. Bacteriol.* **177,** 465–467
30. Tao, X., and Murphy, J. R. (1994) *Proc. Natl. Acad. Sci. U. S. A.* **91,** 9646–9650
31. Pierre, J. L., and Fontecave, M. (1999) *Biometals* **12,** 195–199
32. Hantke, K. (2001) *Curr. Opin. Microbiol.* **4,** 172–177
33. Escolar, L., Perez-Martin, J., and De Lorenzo, V. (1999) *J. Bacteriol.* **181,** 6223–6229
34. Rodriguez, G. M., and Smith, I. (2003) *Mol. Microbiol.* **47,** 1485–1494
35. Gallegos, M. T., Schleif, R., Bairoch, A., Hofmann, K., and Ramos, J. L. (1997) *Microbiol. Mol. Biol. Rev.* **61,** 393-&
36. Martin, R. G., and Rosner, J. L. (2001) *Curr. Opin. Microbiol.* **4,** 132–137
37. Rhee, S., Martin, R. G., Rosner, J. L., and Davies, D. R. (1998) *Proc. Natl. Acad. Sci. U. S. A.* **95,** 10413–10418
38. Gerstmeir, R., Wendisch, V. F., Schnicke, S., Ruan, H., Farwick, M., Reinscheid, D., and Eikmanns, B. J. (2003) *J. Biotechnol.* **104,** 99–122
39. Lobell, R. B., and Schleif, R. F. (1990) *Science* **250,** 528–532
40. Wade, J. T., Belyaeva, T. A., Hyde, E. I., and Busby, S. J. W. (2000) *Mol. Microbiol.* **36,** 223–229
41. Shen, X. H., Liu, Z. P., and Liu, S. J. (2004) *Biotechnol. Lett.* **26,** 575–580
42. Robinson, J. R., and Sagers, R. D. (1972) *J. Bacteriol.* **112,** 465–473
43. Wendisch, V. F., De Graaf, A. A., Sahm, H., and Eikmanns, B. J. (2000) *J. Bacteriol.* **182,** 3088–3096
44. Masse, E., and Gottesman, S. (2002) *Proc. Natl. Acad. Sci. U. S. A.* **99,** 4620–4625
45. Tauch, A., Kaiser, O., Hain, T., Goesmann, A., Weisshaar, B., Albersmeier, A., Bekel, T., Bischoff, N., Brune, I., Chakraborty, T., Kalinowski, J., Meyer, F., Rupp, O., Schneiker, S., Viehoever, P., and Puhler, A. (2005) *J. Bacteriol.* **187,** 4671–4682
46. Nishio, Y., Nakamura, Y., Kawarabayasi, Y., Usuda, Y., Kimura, E., Sugimoto, S., Matsui, K., Yamagishi, A., Kikuchi, H., Ikeo, K., and Gojobori, T. (2003) *Genome Res.* **13,** 1572–1579
47. Cerdeno-Tarraga, A. M., Efstratiou, A., Dover, L. G., Holden, M. T. G., Pallen, M., Bentley, S. D., Besra, G. S., Churcher, C., James, K. D., De Zoysa, A., Chillingworth, T., Cronin, A., Dowd, L., Feltwell, T., Hamlin, N., Holroyd, S., Jagels, K., Moule, S., Quail, M. A., Rabbinowitsch, E., Rutherford, K. M., Thomson, N. R., Unwin, L., Whitehead, S., Barrell, B. G., and Parkhill, J. (2003) *Nucleic Acids Res.* **31,** 6516–6523
48. Lee, J. H., Wang, T., Ault, K., Liu, J., Schmitt, M. P., and Holmes, R. K. (1997) *Infect. Immun.* **65,** 4273–4280

JOURNAL OF BACTERIOLOGY, Apr. 2006, p. 2907–2918 Vol. 188, No. 8
0021-9193/06/$08.00+0 doi:10.1128/JB.188.8.2907–2918.2006

The DtxR Regulon of *Corynebacterium glutamicum*†

Julia Wennerhold and Michael Bott*

Institut für Biotechnologie 1, Forschungszentrum Jülich, D-52425 Jülich, Germany

Received 23 December 2005/Accepted 7 February 2006

Previous studies with *Corynebacterium diphtheriae* and *Mycobacterium* species revealed that the transcriptional regulator DtxR and its ortholog IdeR play a central role in the control of iron metabolism. In the present work, we used genome-based approaches to determine the DtxR regulon of *Corynebacterium glutamicum*, a nonpathogenic relative of *C. diphtheriae*. First, global gene expression of a *dtxR* deletion mutant was compared with that of the wild type using DNA microarrays. Second, we used a computer-based approach to identify 117 putative DtxR binding sites in the *C. glutamicum* genome. In the third step, 74 of the corresponding genome regions were amplified by PCR, 51 of which were shifted by the DtxR protein. Finally, we analyzed which of the genes preceded by a functional DtxR binding site showed altered mRNA levels in the transcriptome comparison. Fifty-one genes organized in 27 putative operons displayed an increased mRNA level in the Δ*dtxR* mutant and thus are presumably repressed by DtxR. The majority of these genes are obviously involved in iron acquisition, three encode transcriptional regulators, e.g., the recently identified repressor of iron proteins RipA, and the others encode proteins of diverse or unknown functions. Thirteen genes showed a decreased mRNA level in the Δ*dtxR* mutant and thus might be activated by DtxR. This group included the *suf* operon, whose products are involved in the formation and repair of iron-sulfur clusters, and several genes for transcriptional regulators. Our results clearly establish DtxR as the master regulator of iron-dependent gene expression in *C. glutamicum*.

Corynebacterium glutamicum is a nonpathogenic, aerobic, gram-positive soil bacterium used for the large-scale biotechnological production of amino acids, mainly L-glutamate (1.5 million tons/year) and L-lysine (0.7 million tons/year). In addition, this species has gained interest as a model organism for the *Corynebacterineae*, a suborder of the *Actinomycetales*, which also includes the genus *Mycobacterium* (34). An overview on the current knowledge on *C. glutamicum* can be found in a recent monograph (9).

Our group has initiated studies on the regulation of *C. glutamicum* genes and enzymes involved in the citric acid cycle, which is of central importance for metabolism in general and for amino acid production in particular because it provides the precursors of the aspartate and glutamate family of amino acids. We identified and characterized AcnR, a member of the TetR family of transcriptional regulators, which functions as a repressor of the aconitase gene *acn* (24). In the course of these studies, it became evident that *acn* expression is controlled by iron in an AcnR-independent manner, being reduced under iron limitation. Subsequently, we were able to show that the iron-dependent transcriptional regulation of aconitase is exerted by the AraC-type regulator RipA, which represses aconitase under iron limitation but not under iron excess (40). RipA stands for "regulator of iron proteins A," and this name was given because RipA represses not only aconitase but also succinate dehydrogenase (*sdhCAB* operon), isopropylmalate dehydratase (*leuCD* operon), nitrate reductase (*narKGHJI* operon), catechol 1,2-dioxygenase (*catA*), catalase (*katA*), and phosphotransacetylase and acetate kinase (*pta-ackA* operon). Except for the latter two enzymes and the nitrate/nitrite transporter NarK, all other enzymes contain iron, and RipA thus functions to reduce the cellular iron demand under iron limitation by reducing the synthesis of prominent iron proteins.

The observation that RipA functions only under iron limitation is due to the fact that expression of *ripA* itself is repressed under iron excess (24). It thus behaves like typical iron starvation genes. In many high-GC gram-positive species, e.g., *Corynebacterium diphtheriae*, *Mycobacterium smegmatis*, *Mycobacterium tuberculosis*, or *Streptomyces coelicolor*, proteins of the DtxR family function as global iron regulators. In complex with iron, these proteins are active as transcriptional regulators, usually as repressors of genes coping with iron starvation, e.g., genes encoding high-affinity iron uptake systems or siderophore biosynthesis enzymes. In some cases, DtxR proteins can also function as transcriptional activators, as shown for the bacterioferritin gene *bfrA* of *M. tuberculosis* (14). When not complexed with iron, the DtxR proteins appear to be inactive. Since the DNA-binding site of DtxR and its homologs is known (14, 36), we were able to identify a well-conserved DtxR operator upstream of the *C. glutamicum ripA* gene and we could show that the DtxR protein from *C. glutamicum* (encoded by NCgl1845) binds in vitro to the *ripA* promoter/operator region (40). Thus, we proposed that *ripA* expression is controlled by DtxR, being repressed under iron excess.

In this work, we performed a genome-wide search for the DtxR target genes in *C. glutamicum*. To this end, we constructed a *dtxR* deletion mutant and compared its global gene expression with that of the parent wild type using DNA microarrays. In parallel, we searched the genome for putative DtxR-binding sites and tested these in vitro using band shift assays with purified DtxR. By combining the results of these

* Corresponding author. Mailing address: Institut für Biotechnologie 1, Forschungszentrum Jülich, D-52425 Jülich, Germany. Phone: 49 2461 61 5515. Fax: 49 2461 61 2710. E-mail: m.bott@fz-juelich.de.

† Supplemental material for this article may be found at http://jb.asm.org/.

TABLE 1. Bacterial strains and plasmids used in this study

Strain or plasmid	Relevant characteristics	Source or reference
Strains		
C. glutamicum		
ATCC 13032	Biotin-auxotrophic wild type	22
13032Δ*dtxR*	In-frame deletion of the *dtxR* gene	This work
E. coli		
DH5α	*supE44 ΔlacU169* (ϕ80*lacZ*ΔM15) *hsdR17 recA1 endA1 gyrA96 thi-1 relA1*	Invitrogen
BL21(DE3)	*ompT hsdS*$_B$($r_B^- m_B^-$) *gal dcm* (DE3)	35
Plasmids		
pK19*mobsacB*	Kan^r; vector for allelic exchange in *C. glutamicum*; (pK18 *oriV*$_{E.c.}$ *sacB lacZ*α)	32
pK19*mobsacB*-Δ*dtxR*	Km^r; pK19*mobsacB* derivative containing a crossover PCR product covering the up- and downstream regions of *dtxR*	This work
pET24b	Kan^r; vector for overexpression of genes in *E. coli*, adding a C-terminal hexahistidine affinity tag to the synthesized protein (pBR322 *oriV*$_{E.c.}$ P_{T7} *lacI*)	Novagen
pET24b-*dtxR*-C	Kan^r; pET24b derivative for overproduction of DtxR with a C-terminal decahistidine tag—the four additional histidines were attached to the *dtxR* fragment	40

two approaches, we were able to identify 27 operons with 51 genes that are presumably repressed by DtxR and 7 operons with 13 genes that might be activated by DtxR.

MATERIALS AND METHODS

Bacterial strains, media, and growth conditions. All strains and plasmids used in this work are listed in Table 1. The *C. glutamicum* type strain ATCC 13032 (22) was used as the wild type. The Δ*dtxR* strain is a derivative containing an in-frame deletion within the *dtxR* gene. For growth experiments, 5 ml of brain heart infusion medium (Difco Laboratories, Detroit, MI) was inoculated with colonies from a fresh LB agar plate (31) and incubated for 6 h at 30°C and at 170 rpm. After washing with 5 ml 0.9% NaCl, the cells of this first preculture were used to inoculate a 500-ml shake flask containing 50 ml CGXII minimal medium (21) with 4% (wt/vol) glucose and either 1 μM $FeSO_4$ (iron starvation) or 100 μM $FeSO_4$ (iron excess). This second preculture was cultivated overnight at 30°C and then used to inoculate the main culture to an optical density at 600 nm of ~1. The main culture contained the same iron concentration as the second preculture. The trace element solution with iron salts omitted and the $FeSO_4$ solution were always added after autoclaving. For all cloning purposes, *Escherichia coli* DH5α (Invitrogen) was used as the host, for overproduction of DtxR *E. coli* BL21(DE3) (35). The *E. coli* strains were cultivated aerobically in LB medium at 37°C (DH5α) or at 30°C [BL21(DE3)]. When appropriate, kanamycin was added to a concentration of 50 μg/ml.

Recombinant DNA work. The enzymes for recombinant DNA work were obtained from Roche Diagnostics (Mannheim, Germany) or New England Biolabs (Frankfurt, Germany). The oligonucleotides used in this study were obtained from Operon (Cologne, Germany) and are listed in Table S1 in the supplemental material. Routine methods like PCR, restriction, or ligation were carried out according to standard protocols (31). Chromosomal DNA from *C. glutamicum* was prepared as described previously (10). Plasmids from *E. coli* were isolated with the QIAprep spin miniprep kit (QIAGEN, Hilden, Germany). *E. coli* was transformed by the RbCl method (15), *C. glutamicum* by electroporation (37). DNA sequencing was performed with a 3100-Avant genetic analyzer (Applied Biosystems, Darmstadt, Germany). Sequencing reactions were carried out with the Thermo Sequenase primer cycle sequencing kit (Amersham Biosciences, Freiburg, Germany).

An in-frame *dtxR* deletion mutant of *C. glutamicum* was constructed via a two-step homologous recombination procedure as described previously (27). The *dtxR* up- and downstream regions (approximately 450 bp each) were amplified using the oligonucleotide pairs Delta-dtxR-1 with Delta-dtxR-2 and Delta-dtxR-3 with Delta-dtxR-4, respectively, and the products served as a template for crossover PCR with oligonucleotides Delta-dtxR-1 and Delta-dtxR-4. The resulting PCR product of ~0.9 kb was digested with EcoRI and HindIII and cloned into pK19*mobsacB* (32). DNA sequence analysis confirmed that the cloned PCR product did not contain spurious mutations. Transfer of the resulting plasmid, pK19*mobsacB*-Δ*dtxR*, into *C. glutamicum* and selection for the first and second recombination event were performed as described previously (27). Kanamycin-sensitive and saccharose-resistant clones were tested by PCR analysis of chromosomal DNA with the primer pair Delta-dtxR-for and Delta-dtxR-rev (see Table S1 in the supplemental material). Of 20 clones tested, 11 showed the wild-type situation (1.6-kb fragment) and 9 had the desired in-frame deletion of the *dtxR* gene (0.9-kb fragment), in which all nucleotides except for the first 6 codons and the last 12 codons were replaced by a 21-bp tag.

Preparation of total RNA. Cultures of the wild type and the Δ*dtxR* mutant were grown in CGXII minimal medium containing 4% (wt/vol) glucose under iron limitation (1 μM $FeSO_4$) or iron excess (100 μM $FeSO_4$). In the exponential growth phase at an optical density at 600 nm of 4 to 6, 25 ml of the cultures was used for the preparation of total RNA as described previously (26). Isolated RNA samples were analyzed for quantity and quality by UV spectrophotometry and denaturing formaldehyde agarose gel electrophoresis (31), respectively, and stored at −70°C until use.

DNA microarray analyses. The generation of whole-genome DNA microarrays (39), synthesis of fluorescently labeled cDNA from total RNA, microarray hybridization, washing, and data analysis were performed as described previously (18, 25, 29). Genes that exhibited significantly changed mRNA levels ($P < 0.05$ in Student's t test) by at least a factor of 2 were determined in two series of DNA microarray experiments: (i) four comparisons of the wild type and the Δ*dtxR* mutant cultivated in CGXII minimal medium with 4% (wt/vol) glucose under iron excess (100 μM $FeSO_4$); (ii) three comparisons of the wild type and the Δ*dtxR* mutant cultivated in CGXII-glucose medium under iron limitation (1 μM $FeSO_4$).

Overproduction and purification of DtxR. The *C. glutamicum* DtxR protein containing 12 additional amino acid at the carboxyl terminus (HHHHLEHHH HHH) was overproduced in *E. coli* BL21(DE3) using the expression plasmid pET24b-*dtxR* and purified by Ni^{2+}-chelate affinity chromatography as described previously (40).

Gel shift assays. For testing the binding of DtxR to putative target promoters, purified DtxR protein (0 to 4 μM dimeric form) was mixed with DNA fragments (200 to 450 bp; final concentration, 8 to 20 nM) in a total volume of 20 μl. The binding buffer contained 50 mM Tris-HCl (pH 7.5), 5 mM $MgCl_2$, 40 mM KCl, 5% (vol/vol) glycerol, 1 mM dithiothreitol (DTT), 150 μM $MnCl_2$. Approximately 20 nM of a promoter fragment lacking a DtxR binding site (*acn*, *pta*, *katA*, or *porB*) was used as negative control. The reaction mixture was incubated at room temperature for 30 min and then loaded onto a 15% native polyacrylamide gel containing 1 mM DTT and 150 μM $MnCl_2$. Electrophoresis was performed at room temperature and 170 V using 1× TB (89 mM Tris base, 89 mM boric acid) supplemented with 1 mM DTT and 150 μM $MnCl_2$ as an electrophoresis buffer. The gels were subsequently stained with Sybr Green I according to the instructions of the supplier (Sigma-Aldrich, Taufkirchen, Germany) and photographed. All PCR products used in the gel shift assays were purified with the PCR purification kit (QIAGEN, Hilden, Germany) and eluted in EB buffer (10 mM Tris-HCl, pH 8.5).

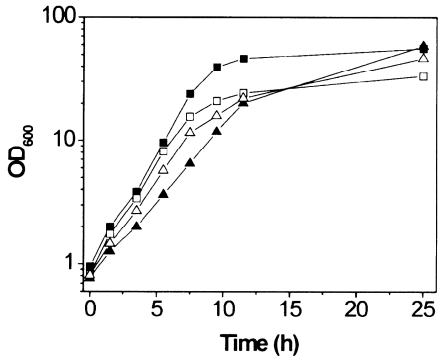

FIG. 1. Growth of *C. glutamicum* wild type (squares) and the Δ*dtxR* mutant (triangles). The cells were cultivated in CGXII minimal medium with 4% (wt/vol) glucose and either 100 μM $FeSO_4$ (filled symbols) or 1 μM $FeSO_4$ (unfilled symbols).

RESULTS

Construction and growth properties of a *C. glutamicum dtxR* deletion mutant. The genome of the *C. glutamicum* type strain ATCC 13032 (20) contains a gene (NCgl1845) encoding a protein of 228 amino acid residues (25.484 kDa) with 72% sequence identity to *C. diphtheriae* DtxR. The corresponding protein from *C. glutamicum* strain ATCC 13869 (previously designated "*Brevibacterium lactofermentum*"), which differs in only two positions from the ATCC 13032 homolog, was shown to repress the *tox* promoter from *C. diphtheriae* in an iron-dependent manner (28). Therefore, the DtxR protein from *C. glutamicum* might have the same regulatory function as its ortholog from *C. diphtheriae*, i.e., mainly transcriptional control of genes involved in iron metabolism.

In order to identify the target genes of DtxR in *C. glutamicum*, an in-frame *dtxR* deletion mutant was constructed by two-step homologous recombination and verified by PCR analysis (see Materials and Methods). In order to exclude the possibility that large genomic alterations (duplication or deletion) had occurred in the course of the deletion of the *dtxR* gene, the chromosomal DNA of the wild type and the Δ*dtxR* mutant was compared with DNA microarrays. The only significant difference observed was the loss of the *dtxR* gene in the mutant DNA.

In a first set of experiments, the growth behavior of the mutant was compared with that of the wild type (Fig. 1). Under iron limitation (1 μM $FeSO_4$), the Δ*dtxR* mutant showed a slightly decreased growth rate ($\mu = 0.32 \pm 0.02\ h^{-1}$) compared to the wild type ($\mu = 0.35 \pm 0.03\ h^{-1}$) but reached a higher final cell density (10.6 ± 1.4 g dry weight/liter versus 8.1 ± 0.2 g dry weight/liter). Under iron excess (100 μM $FeSO_4$), the Δ*dtxR* mutant grew significantly slower ($\mu = 0.27 \pm 0.03\ h^{-1}$) than the wild type ($\mu = 0.41 \pm 0.01\ h^{-1}$) and reached a final cell density (14.6 ± 0.8 g dry weight/liter) similar to that of the wild type (15.6 ± 2.0 g dry weight/liter). Thus, deletion of the *dtxR* gene in *C. glutamicum* has a negative influence on the growth rate under iron excess and a positive influence on the growth yield under iron limitation.

Comparison of the expression profiles of Δ*dtxR* mutant and wild type with DNA microarrays. To investigate the effect of the *dtxR* deletion on global gene expression and to identify target genes of DtxR, the transcriptomes of the Δ*dtxR* mutant and the *C. glutamicum* wild type were compared using DNA microarray analysis (39). Two series of experiments were performed: (i) four comparisons of the wild type and the Δ*dtxR* mutant cultivated in glucose minimal medium under iron excess (100 μM $FeSO_4$); (ii) three comparisons of the wild type and the Δ*dtxR* mutant cultivated in glucose minimal medium under iron limitation (1 μM $FeSO_4$). RNA was always isolated from cells in the exponential growth phase. Table S2 in the supplemental material shows all genes whose mRNA level was changed ≥2-fold under iron excess or under iron limitation in at least two independent experiments. Under the chosen conditions, 164 genes fell under these criteria, of which 118 showed a higher mRNA level and 46 a lower mRNA level in the Δ*dtxR* mutant. Seventy-three of the genes encode hypothetical proteins.

Remarkably, more than 50 genes within the NCgl numbers 1611 and 1816 showed more than twofold-increased mRNA levels in the Δ*dtxR* mutant under iron excess and to a lesser extent also under iron limitation. This region, which spans about 187 kb, was identified as the prophage region CGP3 (19). Its G+C content is significantly lower than the overall G+C content of the *C. glutamicum* genome (53.8%), the insertion site is a tRNA-Val gene indicated by the presence of a direct repeat flanking the CGP3 element, and it contains a phage-type integrase gene at the left border, which appears to be disrupted by a frameshift mutation. With few exceptions, e.g., NCgl1646, encoding a secretory serine protease, and NCgl1703 to NCgl1705, encoding a type II restriction-modification system, the genes within CGP3 encode hypothetical proteins.

Table 2 lists a subset of the genes with ≥2-fold-altered mRNA level in the Δ*dtxR* mutant, i.e., those presumably involved in iron acquistion, storage, or metabolism (group I), those known to be RipA targets (group II), those encoding transcriptional regulators (group III), and those further genes showing a ≥10-fold-increased mRNA level in the Δ*dtxR* mutant (group IV).

Group I includes 26 genes, 22 of which encode proteins presumably involved in heme uptake, in heme degradation (*hmuO*), or in iron acquisition via siderophores. All of these 22 genes showed increased expression in the Δ*dtxR* mutant under iron excess, whereas under iron limitation their mRNA levels are unaltered or increased to a lower extent. The latter situation indicates that even under our conditions of iron limitation there is still some active DtxR protein present in the wild type. Overall the expression pattern corresponds to the expectation that these genes are repressed by DtxR under iron excess but not, or more weakly, under iron limitation. Two genes of group I (*sufB* and *sufD*) encode components involved in the formation of iron-sulfur clusters. Their mRNA levels were decreased under both iron excess and iron starvation. Similar to the situation with *M. tuberculosis* (12, 17), the genes encoded by the *suf* operon may constitute the only iron-sulfur cluster assembly machinery in *C. glutamicum*. Finally, group I included the two genes of the *C. glutamicum* genome that are involved in iron storage, i.e., the *ftn* gene encoding ferritin and the *dps* gene encoding a protein that protects DNA from oxidative damage by nonspecific binding to DNA and catalyzing the oxidation of ferrous iron and its mineralization as a ferric

TABLE 2. Selection of genes whose average mRNA ratio was altered ≥2-fold (*P* value, ≤0.05) under iron excess or under iron limitation in at least two independent experiments[a]

Category and NCgl gene no.	Description of product and gene designation	mRNA ratio	
		Fe excess	Fe limitation
Genes presumably involved in iron acquisition, storage, or metabolism			
NCgl0377	Put. secreted heme transport associated protein, C-term. TMH	16.82	5.00
NCgl0378	Heme ABC transporter, secreted lipoprotein, *hmuT*	3.54	2.64*
NCgl0379	Heme ABC transporter, permease, *hmuU*	9.33	3.98
NCgl0381	Put. secreted heme transport associated protein, C-term. TMH	17.66	5.99
NCgl0382	Put. secreted heme transport associated protein, C-term. TMH	13.99	6.51*
NCgl0482	Put. siderophore ABC transporter, ATPase	5.72	1.73
NCgl0483	Put. siderophore ABC transporter, permease, FecCD family	6.43	1.55*
NCgl0635	Put. soluble, cytoplasmic siderophore-interacting protein	6.53	1.70
NCgl0636	Put. siderophore ABC transporter, ATPase	6.78	1.62
NCgl0637	Put. siderophore ABC transporter, permease, FecCD family	5.70	1.74
NCgl0638	Put. siderophore ABC transporter, permease, FecCD family	2.35	1.42
NCgl0639	Put. siderophore ABC transporter, secreted lipoprotein	7.85	1.72
NCgl0773	Put. soluble, cytoplasmic siderophore-interacting protein	11.63	2.38
NCgl0774	Put. siderophore ABC transporter, secreted lipoprotein	8.43	2.51
NCgl0776	Put. siderophore ABC transporter, secreted lipoprotein	4.16	1.17*
NCgl0779	Put. siderophore ABC transporter, ATPase	4.21	1.27*
NCgl1200	Put. soluble, cytoplasmic siderophore-interacting protein	4.76	2.42*
NCgl1209	Put. siderophore ABC transporter, secreted lipoprotein	3.31	1.94*
NCgl1502	Fe-S cluster assembly protein, *sufD*	0.47	0.43
NCgl1503	Fe-S cluster assembly protein, *sufB*	0.48	0.43
NCgl1959	Put. secreted siderophore binding lipoprotein	8.48	3.26
NCgl2146	Heme oxygenase, *hmuO*	4.02	3.17
NCgl2439	Ferritin, *ftn*	1.07*	2.54
NCgl2897	Starvation-inducible DNA-binding protein, *dps*	1.28**	6.39**
NCgl2969	Transporter of major facilitator superfamily	4.35	1.43
NCgl2970	Put. secreted siderophore binding lipoprotein	4.94	1.37
Genes known to be regulated by RipA			
NCgl0251	Catalase, *katA*	0.27	3.06
NCgl0359	Succinate dehydrogenase, *sdhC*	0.16	0.46*
NCgl0360	Succinate dehydrogenase, *sdhA*	0.08	0.28*
NCgl0361	Succinate dehydrogenase, *sdhB*	0.18	0.46
NCgl1141	Nitrate reductase, β subunit, *narH*	0.21	0.24*
NCgl1142	Nitrate reductase, α subunit, *narG*	0.10	0.41
NCgl1143	Nitrate/nitrite transporter, *narK*	0.34	0.60*
NCgl1262	3-Isopropylmalate dehydratase, large subunit, *leuC*	0.28	0.50*
NCgl1263	3-Isopropylmalate dehydratase small subunit, *leuD*	0.28	0.59*
NCgl1482	Aconitase, *acn*	0.29	0.63*
NCgl2319	Catechol 1,2-dioxygenase, *catA*	0.05	0.14
NCgl2657	Phosphotransacetylase, *pta*	0.26	1.10*
Genes encoding transcriptional regulators			
NCgl0358	Transcriptional regulator, *ramB*	0.39	0.67*
NCgl0430	Transcriptional regulator, ArsR family	6.68	7.39
NCgl0943	Transcriptional regulator, AraC family, *ripA*	12.16	4.13
Further genes with a >10-fold increased mRNA level in the Δ*dtxR* mutant			
NCgl0122	Hypothetical protein	31.33	21.49*
NCgl0123	Hypothetical protein	20.93	10.76
NCgl1618	Hypothetical protein	5.88	17.48
NCgl1635	Hypothetical protein	24.00	20.55
NCgl1646	Secretory serine protease	33.09	11.92
NCgl1651	Hypothetical exported protein	13.72	11.53
NCgl1677	Hypothetical protein	7.47	14.78
NCgl1678	Hypothetical protein	23.04	10.11
NCgl1679	Hypothetical protein	16.00	9.27*
NCgl1680	Hypothetical protein	14.99	9.97
NCgl1682	Hypothetical protein	10.40	8.04
NCgl1685	Hypothetical protein	12.54	9.10
NCgl2450	Put. 2-methylcitrate dehydratase	10.10	11.52

[a] The mRNA ratios (Δ*dtxR* mutant/wild type) represent average values obtained from four (iron excess) or three (iron limitation) DNA microarray experiments performed with RNA isolated from four or three independent cultures in CGXII minimal medium containing either 100 μM $FeSO_4$ or 1 μM $FeSO_4$. Ratios labeled with a single asterisk could be analyzed in only a single experiment; for the ratios labeled with two asterisks, the *P* value was above 0.05. A list of all genes showing twofold-altered mRNA levels in the Δ*dtxR* mutant is provided in Table S2 in the supplemental material. Put., putative; TMH, transmembrane helix.

core inside the protein (1). Both the *ftn* and *dps* mRNA levels were unaltered under iron excess but increased in the Δ*dtxR* mutant under iron limitation.

Group II includes 12 genes previously shown to be repressed by the RipA protein under iron limitation (40). Most of them encode iron-containing proteins (catalase, succinate dehydrogenase, nitrate reductase, isopropylmalate dehydratase, aconitase, and catechol 1,2-dioxygenase), but some also noniron

proteins (nitrate/nitrite transporter, phosphotransacetylase). The mRNA level of all these genes was 3- to 20-fold decreased in the Δ*dtxR* mutant under iron excess, as expected when *ripA* expression is no longer repressed by DtxR. Under iron limitation, most of the RipA targets still showed decreased mRNA levels, but not as strongly as under iron limitation, again indicating that there is still some active DtxR protein present in the wild type that represses *ripA*. The only exceptions were the mRNA ratios for *pta* and *katA*, whose mRNA levels were unaltered or even increased in the ΔdtxR mutant under iron limitation, respectively, presumably because expression of these genes is controlled by additional regulatory proteins or mechanisms.

Group III includes three genes which encode transcriptional regulators. In our previous work, *ripA* was proposed to be a target of DtxR, since its expression is induced under iron limitation (24) and DtxR binds to the *ripA* promoter region (40). In agreement with this model, the *ripA* gene showed a strongly (>10-fold) increased mRNA level in the Δ*dtxR* mutant under iron excess, confirming its control by DtxR. Under iron limitation, the *ripA* mRNA level was still increased but to a significantly lesser extent than under iron excess. The *ripA* expression pattern fits perfectly with that of its target genes (see above). The *ramB* gene encodes a regulator which is involved in the control of carbon metabolism in *C. glutamicum* (13). Its mRNA level was decreased in the Δ*dtxR* mutant under iron excess and to a lesser extent also under iron limitation, indicating that its expression in the wild type is positively influenced by DtxR. The NCgl0430 gene encodes a transcriptional regulator of the ArsR family, whose mRNA level was strongly increased in the Δ*dtxR* mutant under both iron excess and iron limitation. The function of the regulator encoded by NCgl0430 and its target genes are not yet known.

Group IV includes 11 further genes whose mRNA levels were more than 10-fold increased in the Δ*dtxR* mutant under iron excess and which do not obviously belong to group I, II, or III. With three exceptions, all these genes are located in the CGP3 prophage region (see above). Nine of the genes encode hypothetical proteins, one encodes a putative secreted serine protease, and one a putative 2-methylcitrate dehydratase.

Identification and testing of putative DtxR boxes in *C. glutamicum*. Besides the transcriptome comparison of the wild type and the Δ*dtxR* mutant, we used a second, completely independent approach for the identification of putative DtxR target genes. We searched for potential DtxR operators in the *C. glutamicum* genome, amplified the corresponding DNA regions by PCR, and tested them for their ability to bind purified DtxR. A 19-bp consensus binding site of the *C. diphtheriae* DtxR protein has been defined as TWAGGTWAGSCTWAC CTWA (36) and is probably also correct for DtxR from *C. glutamicum*, since *C. glutamicum* DtxR was shown to repress the *C. diphtheriae tox* promoter in an iron-dependent manner (28). Using the ERGO software suite (Integrated Genomics), we searched the *C. glutamicum* genome for sequences deviating in maximally five positions from the consensus and allowing neither insertions nor deletions. As shown in Table S3 in the supplemental material, 117 putative DtxR binding sites could be identified that fulfilled the given criteria. Seventy of these sites were located maximally 500 bp upstream or maximally 100 bp downstream of the start codon of the neighboring gene and were thought to be physiologically the most relevant.

To test whether DtxR binds in vitro to the potential binding sites, DNA fragments covering 74 of the corresponding sequences were amplified by PCR and used for gel shift assays with the purified *C. glutamicum* DtxR protein. For this purpose, the DtxR protein was overproduced in *E. coli* and isolated by means of a carboxy-terminal histidine tag as described previously. For the gel shift assays, the DNA fragments (8 to 20 nM) were mixed with various concentrations of the DtxR protein (0 to 4 μM dimeric form) and then separated on 15% native polyacrylamide gels. Mn^{2+} was included in all reactions instead of Fe^{2+} on account of its redox stability. As a negative control, all reactions included a promoter fragment of *acn*, *pta*, *katA*, or *porB* which was not shifted by DtxR. As shown in Fig. 2, the DtxR protein shifted 51 of the 74 tested DNA fragments containing a putative DtxR box, albeit with different affinities. In Table 3, the DtxR boxes present within the shifted fragments, the neighboring genes, the distances of the DtxR boxes to the neighboring genes, and the relative affinities are summarized. According to the affinity, three classes of DtxR binding sites were distinguished: those requiring a 25-fold molar excess of dimeric DtxR for a complete shift (indicated by "++" in Table 3), those requiring a 50-fold excess for a complete shift ("+"), and those requiring a 200-fold molar excess for a complete or a partial shift ["(+)"]. There was no correlation between the binding affinity and individual positions in the DtxR binding site; however, there was a correlation between binding affinity and the number of deviations from the consensus binding site: 3.9 on average for those with high affinity, 4.5 on average for those with intermediate affinity, and always 5 for those with low affinity. The genes located adjacent to the DtxR binding sites were ordered into four groups. The first group includes 17 genes coding for proteins involved in iron acquistion, e.g., siderophore binding proteins, siderophore ABC uptake systems, and heme uptake ABC transporters. Most of the corresponding binding sites showed a high affinity for DtxR, with DtxR-DNA complex formation being observed at a 15- to 25-fold molar excess of dimeric DtxR (data not shown). The second group includes the genes for the iron storage proteins ferritin and Dps. Whereas the DtxR binding site in front of the *dps* gene showed a high affinity similar to that of the iron uptake genes, the DNA fragment covering the ferritin promoter region showed a lower affinity, requiring a 200-fold molar excess of DtxR for a complete shift. The third group consists of eight genes coding for transcriptional regulators, including *ramB*, *ripA*, *sufR*, and *cgtR11*. The corresponding DNA fragments showed various affinities for DtxR: in the cases of *ramB*, NCgl0430, *ripA*, *sufR*, *cgtR11* and NCgl2877, a 50-fold molar excess of dimeric DtxR was sufficient for a complete shift, whereas in the cases of NCgl0120 and NCgl1127, even a 200-fold molar excess of dimeric DtxR was not sufficient for a complete shift. The fourth group, designated as "others," includes genes encoding proteins of various functions, e.g., two cation-transporting ATPases, a fatty acid synthase, two secreted serine proteases, the SecD subunit of the Sec protein translocase, a glycogen phosphorylase, and others. The corresponding DNA fragments showed various affinities for DtxR, requiring a 50- to 200-fold molar excess of dimeric DtxR for a complete shift. Binding of DtxR to all of these fragments was

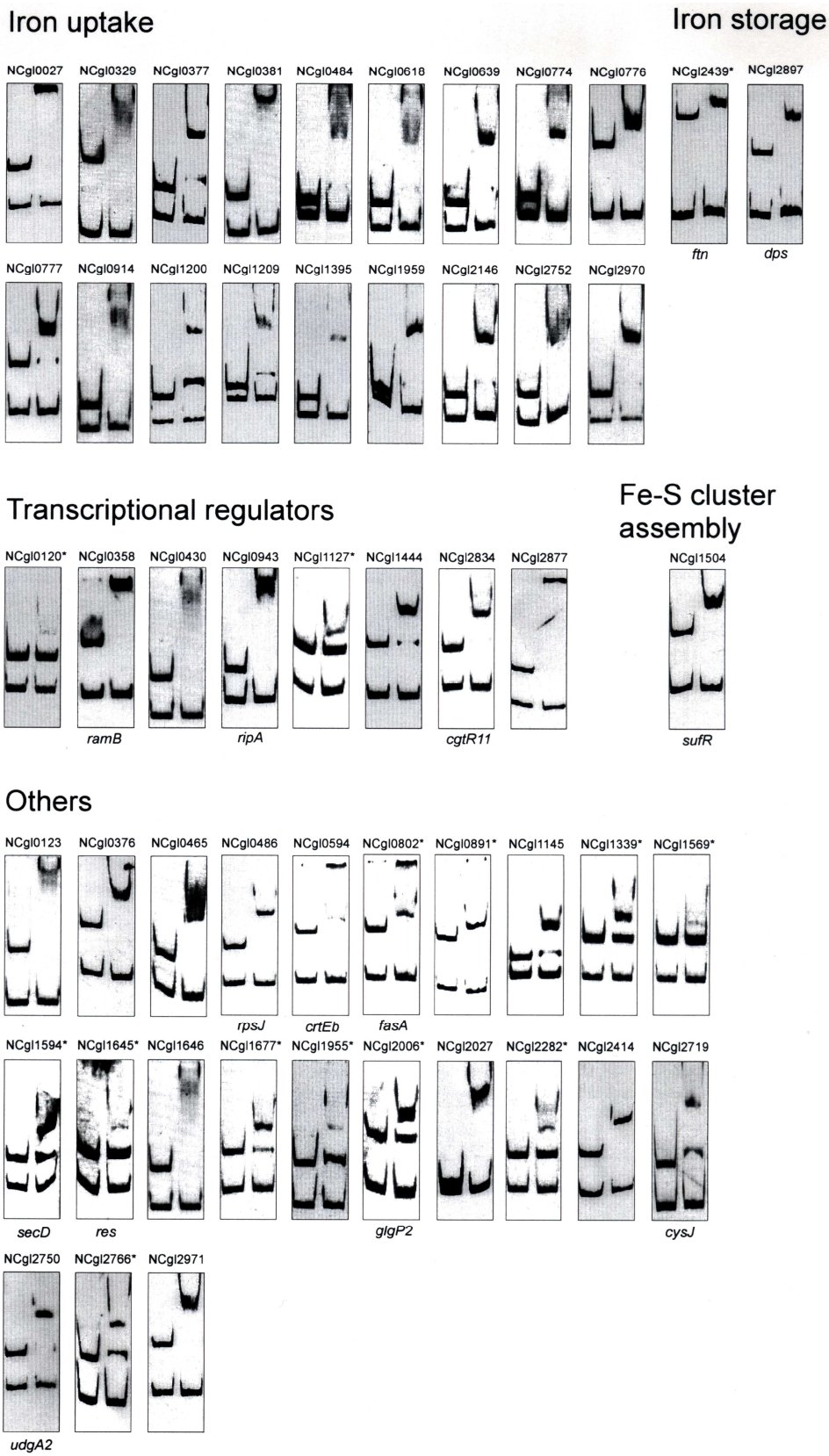

FIG. 2. Binding of DtxR to the predicted DtxR boxes. DNA fragments (200 to 400 bp in size; final concentration, 10 to 20 nM) covering promoter regions with putative DtxR binding sites were incubated for 30 min at room temperature without DtxR (left lanes) or with a 50-fold or a 200-fold (labeled with an asterisk) molar excess of purified DtxR protein (dimeric form) (right lanes) before separation by native polyacrylamide (15%) gel electrophoresis and staining with SybrGreen I. DNA fragments (100 to 200 bp) covering the promoter regions of *acn*, *pta*, and *katA*, which do not contain putative DtxR binding sites, served as negative controls.

TABLE 3. DtxR binding sites in the *C. glutamicum* genome verified by bandshift analysis[a]

NCgl gene no. or description	DtxR binding site	Category of neighboring gene	Annotated function of neighboring gene	Shift	Location
Consensus site of *C. diphtheriae*	TWAGGTWAGSCTWACCTWA				
NCgl0027	**TTT**G**C**GC**AGGCTAACCTTT**	Iron acquisition	ABC transporter, permease	++	+125.5
NCgl0329	**TAAGGATA**A**CCTT**G**CCTTA**	Iron acquisition	Secreted siderophore binding lipoprotein	++	−42.5
NCgl0377	**TTA**A**GTTAGC**A**TA**G**CCTTA**	Iron acquisition	Heme transport-associated protein	++	−150.5
NCgl0381	**TAAGGTTA**C**CCTA**C**CCT**CT	Iron acquisition	Heme transport-associated protein	++	−90.5
NCgl0484	**TTAG**T**AAAGGCTCACCTAA**	Iron acquisition	Siderophore ABC transporter, permease	+	−100.5
NCgl0618	A**TAGGATAGGT**T**AACCTG**A	Iron acquisition	Secreted siderophore binding lipoprotein	++	−34.5
NCgl0639	GTC**GGG**C**AGCCTAACCTAA**	Iron acquisition	Siderophore ABC transporter, secreted lipoprotein	++	−49.5
NCgl0774	**TAAGGTTTGCCTAA**T**GTTT**	Iron acquisition	Secreted siderophore binding lipoprotein	+	−39.5
NCgl0776	**TT**TAG**GTAACCTAACCTCA**	Iron acquisition	Secreted siderophore binding lipoprotein	++	−73.5
NCgl0777	**TTAGGTTAGGCT**C**TAATAT**	Iron acquisition	Siderophore ABC transporter, permease	++	−182.5
NCgl0914	**TTAAGT**C**AG**T**GTTACCTAA**	Iron acquisition	Siderophore export ABC transporter, permease	++	−92.5
NCgl1200	**TTTTGTTAGGCTTGCCTA**G	Iron acquisition	Siderophore-interacting protein	+	−42.5
NCgl1209	**TTAGGTAAGGTTTGCATA**C	Iron acquisition	Secreted siderophore binding lipoprotein	+	−40.5
NCgl1395	**TTAGGTTAGGCAAGCCATA**	Iron acquisition	Cytoplasmic siderophore-interacting protein	++	−48.5
NCgl1959	**TTAGGC**A**AGGCTA**C**CTTTT**	Iron acquisition	Secreted siderophore binding lipoprotein	++	−19.5
NCgl2146	G**TAGGT**G**TGGGTAACCTAA**	Iron acquisition	Heme oxygenase	+	−129.5
NCgl2752	**TAAGGCAAGCCTAA**A**TTA**G	Iron acquisition	Hyp. exported protein, heme transport	++	−106.5
NCgl2970	**TT**GC**GTTAGGATAGCCTAA**	Iron acquisition	Secreted siderophore binding lipoprotein	++	−8.5
NCgl2439	**TTA**T**GC**TGC**GCTAACCTA**T	Iron storage	Ferritin, *ftn*	(+)	−46.5
NCgl2897	**TCAGGATAGGA**C**AACCTAA**	Iron storage	DNA protection during starvation protein, *dps*	++	−70.5
NCgl1504	**TTGGCTTAGGG**T**TCGCTTA**	Iron-sulfur cluster assembly	Fe-S cluster assembly, *suf* operon	++	−141.5
NCgl0120	**TTGGCTA**T**GGTTTACCTA**T	Transcriptional regulator	Transcriptional repressor	(+)	+13.5
NCgl0358	**TTAGGA**T**AGCCTTAC**T**TTA**	Transcriptional regulator	Transcriptional regulator, *ramB*	++	−390.5
NCgl0430	**TTAGGC**T**TGCCATACCTA**T	Transcriptional regulator	ArsR-type transcriptional regulator	++	−25.5
NCgl0943	T**GAGGTTAGC**G**TAACCTA**C	Transcriptional regulator	AraC-type transcriptional regulator, *ripA*	++	−42.5
NCgl1127	**TAAGGCAA**T**TG**T**AATCTAA**	Transcriptional regulator	Transcriptional regulator, Crp family	(+)	−353.5
NCgl1444	**TTAGGGA**C**GCTTTACCT**GC	Transcriptional regulator	Put. transcriptional regulator	++	−87.5
NCgl2834	ATGA**GTAAGGCTA**G**ACTAA**	Transcriptional regulator	Response regulator, *cgtR11*	+	−95.5
NCgl2877	**TTTGGC**A**AG**A**CTTACC**G**AC**	Transcriptional regulator	Transcriptional regulator, PadR-like family	++	−110.5
NCgl0123	A**ATGGTTAGGCTAACCTTA**	Other	Hypothetical protein	++	+10.4
NCgl0376	**TAAGGC**T**ATGCTAAC**T**TAA**	Other	Copper-transporting P-type ATPase	++	−79.5
NCgl0465	**TA**G**GGAAAGCCC**A**TCCTTA**	Other	Copper-transporting P-type ATPase	++	−31.5
NCgl0486	G**TTGGTAAGGC**A**AACATGA**	Other	Ribosomal protein S10, *rpsJ*	+	−378.5
NCgl0594	**TTTGGT**C**TGGCCTACCTA**T	Other	Lycopene elongase, *crtEb*	+	+78.5
NCgl0802	**TTCGGCTA**C**GCTCACGTAA**	Other	Fatty acid synthase, *fasA*	+	−73.5
NCgl0891	**TGAGGTA**C**GC**G**TTACCT**GT	Other	Hypothetical protein	+	−186.5
NCgl1145	CGT**GGGAAGCCTAAC**T**TAA**	Other	Putative secreted serine protease	+	−51.5
NCgl1339	**TTAGGGAAGGA**A**AACA**T**AT**	Other	Putative secreted lipoprotein	(+)	+7.5
NCgl1569	**TT**CC**GTA**C**GGCTA**T**GCTTA**	Other	Putative Holliday junction resolvase	(+)	−130.5
NCgl1594	**TATGGGAAGGC**A**AAACTA**C	Other	Protein translocase, *secD*	(+)	−160.5
NCgl1645	**TAA**C**TTAAGCCTCACATA**C	Other	Putative resolvase, *res*	(+)	−759.5
NCgl1646	**TTAGGTAA**A**GCTTGCCTA**T	Other	Secretory serine protease	++	−183.5
NCgl1677	**TTAGGTTA**T**GT**C**AA**A**GTTA**	Other	Hypothetical protein	+	−563.5
NCgl1955	**TTAGA**T**AAGCCTGACA**TC**A**	Other	Predicted endonuclease	(+)	−342.5
NCgl2006	C**AA**TC**TTAGGCTTA**G**TTTA**	Other	Glycogen phosphorylase, *glgP2*	+	−14.5
NCgl2027	**TCAAGTAAGGT**T**TACCTTA**	Other	SAM-dependent methyltransferase	++	−8.5
NCgl2282	**TTAGGT**C**AAGCTTGCATTT**	Other	Hypothetical membrane-spanning protein	+	−29.5
NCgl2414	**TAATGTA**T**GCCTTGACTTG**	Other	Xanthosine triphosphate pyrophosphatase	+	−227.5
NCgl2719	**TTAGGTTAGGT**T**CACCGTG**	Other	Putative sulfite reductase, *cysJ*	+	−213.5
NCgl2750	A**TTGGTA**C**GGGTTACCTTG**	Other	Predicted UDP-glucose 6-dehydrogenase, *udgA2*	++	+24.5
NCgl2766	**TTA**A**CTTTGCCC**T**ACCTAA**	Other	Putative permease	+	−199.5
NCgl2971	**TT**GCA**TTAGGCTA**T**CCTAA**	Other	Putative Zn-dependent oxidoreductase	++	−173.5

[a] The DtxR binding sites shown in this table were identified by a motif search of the *C. glutamicum* genome using the consensus sequence TWAGGTWAGSCT WACCTWA from *C. diphtheriae* and allowing up to five mismatches, but no insertions or deletions. All binding sites fulfilling the applied criteria are listed in Table S3 in the supplemental material. This table includes only those sites that were successfully shifted by purified DtxR protein. The column labelled "Shift" indicates whether DtxR showed a high (++), medium (+), or low [(+)] affinity to the corresponding DNA fragment. The position of the center of the binding sites relative to the predicted translation start site of the neighboring gene is given by the numbers in the "Location" column. Boldface indicates consensus.

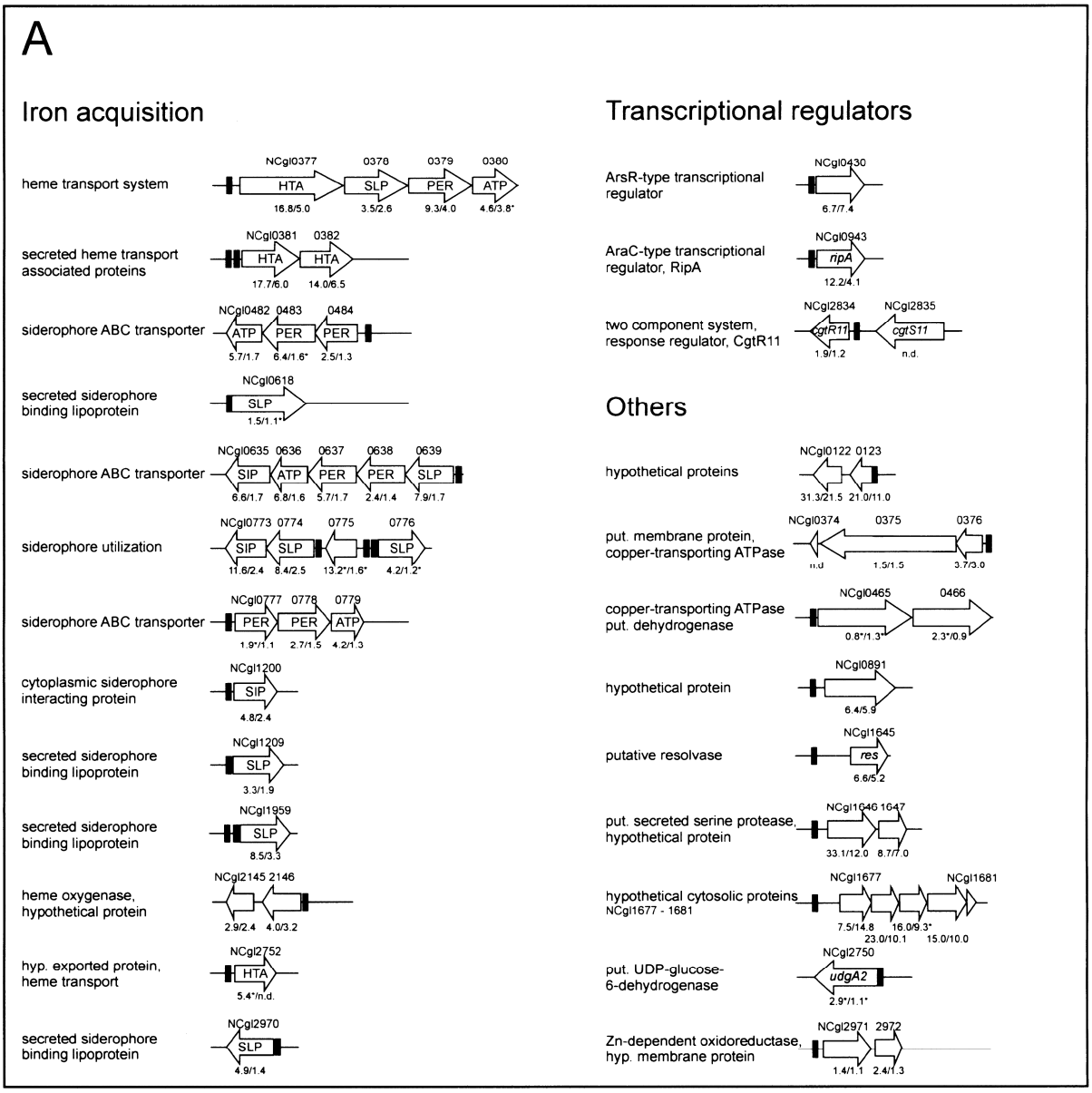
A
Iron acquisition
heme transport system
NCgl0377 0378 0379 0380
HTA SLP PER ATP
16.8/5.0 3.5/2.6 9.3/4.0 4.6/3.8*
secreted heme transport associated proteins
NCgl0381 0382
HTA HTA
17.7/6.0 14.0/6.5
siderophore ABC transporter
NCgl0482 0483 0484
ATP PER PER
5.7/1.7 6.4/1.6* 2.5/1.3
secreted siderophore binding lipoprotein
NCgl0618
SLP
1.5/1.1*
siderophore ABC transporter
NCgl0635 0636 0637 0638 0639
SIP ATP PER PER SLP
6.6/1.7 6.8/1.6 5.7/1.7 2.4/1.4 7.9/1.7
siderophore utilization
NCgl0773 0774 0775 0776
SIP SLP SLP
11.6/2.4 8.4/2.5 13.2*/1.6* 4.2/1.2*
siderophore ABC transporter
NCgl0777 0778 0779
PER PER ATP
1.9*/1.1 2.7/1.5 4.2/1.3
cytoplasmic siderophore interacting protein
NCgl1200
SIP
4.8/2.4
secreted siderophore binding lipoprotein
NCgl1209
SLP
3.3/1.9
secreted siderophore binding lipoprotein
NCgl1959
SLP
8.5/3.3
heme oxygenase, hypothetical protein
NCgl2145 2146
2.9/2.4 4.0/3.2
hyp. exported protein, heme transport
NCgl2752
HTA
5.4*/n.d.
secreted siderophore binding lipoprotein
NCgl2970
SLP
4.9/1.4
Transcriptional regulators
ArsR-type transcriptional regulator
NCgl0430
6.7/7.4
AraC-type transcriptional regulator, RipA
NCgl0943
ripA
12.2/4.1
two component system, response regulator, CgtR11
NCgl2834 NCgl2835
cgtR11 cgtS11
1.9/1.2 n.d.
Others
hypothetical proteins
NCgl0122 0123
31.3/21.5 21.0/11.0
put. membrane protein, copper-transporting ATPase
NCgl0374 0375 0376
n.d 1.5/1.5 3.7/3.0
copper-transporting ATPase put. dehydrogenase
NCgl0465 0466
0.8*/1.3* 2.3*/0.9
hypothetical protein
NCgl0891
6.4/5.9
putative resolvase
NCgl1645
res
6.6/5.2
put. secreted serine protease, hypothetical protein
NCgl1646 1647
33.1/12.0 8.7/7.0
hypothetical cytosolic proteins NCgl1677 - 1681
NCgl1677 NCgl1681
7.5/14.8 16.0/9.3* 23.0/10.1 15.0/10.0
put. UDP-glucose-6-dehydrogenase
NCgl2750
udgA2
2.9*/1.1*
Zn-dependent oxidoreductase, hyp. membrane protein
NCgl2971 2972
1.4/1.1 2.4/1.3
B
Iron metabolism
cytoplasmic siderophore-interacting protein
NCgl1395
SIP
0.6/1.1*
SUF machinery
NCgl1498 1499 1500 1501 1502 1503 1504
sufS sufC sufD sufB sufR
0.4/0.5 1.2/1.0 0.6/0.7 0.5/0.4 0.5/0.4 0.64/0.6
0.6/0.7*
Others
put. secreted lipoprotein
NCgl1339
0.3/0.6*
put. Holliday junction resolvase
NCgl1569
0.6/0.6
Transcriptional regulators
transcriptional regulator, RamB
NCgl0358 NCgl0359 0360 0361
ramB sdhC sdhA sdhB
0.4/0.7 0,2/0.5* 0,1/0,3* 0,2/0,5
put. transcriptional regulator, HTH-motif
NCgl1444
0.2*/0.8
transcriptional regulator, PadR-like family
NCgl2877
0.6/1.0

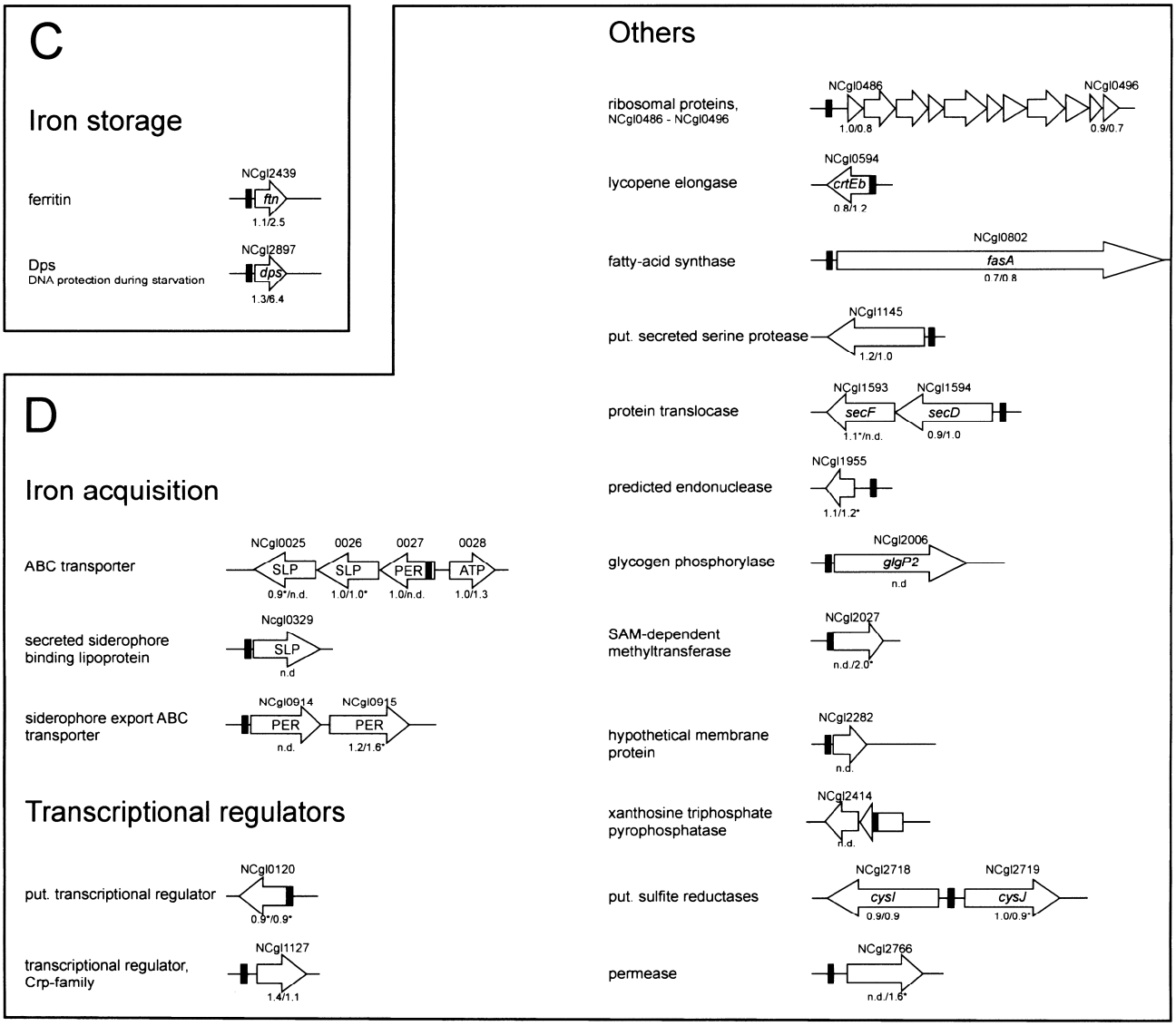

FIG. 3. Overview of *C. glutamicum* operons preceded by a functional DtxR binding site. The black boxes indicate the positions of the identified DtxR boxes. The mRNA ratios (Δ*dtxR* mutant versus wild type) obtained from the DNA microarray experiments are shown below the corresponding gene. The first value gives the ratio under iron excess, and the second value gives the ratio under limitation. It has to be taken into account that for the majority of genes the indicated function was derived from the genome annotation rather than from experimental data. The genes/operons were separated in four groups. Group A contains genes whose mRNA level was at least 1.5-fold increased in the Δ*dtxR* mutant under iron excess. These genes are presumably repressed by DtxR. Group B comprises genes whose mRNA level was at least 1.5-fold decreased in the Δ*dtxR* mutant under iron excess. These genes might be activated by DtxR. Group C contains two genes whose mRNA levels were almost unaltered in the Δ*dtxR* mutant under iron excess but were increased under iron limitation. How DtxR controls expression of these genes is not clear yet. Group D contains all genes whose mRNA ratios could not be determined and those whose mRNA levels were altered less than 1.5-fold in the Δ*dtxR* mutant. Whether these genes are indeed regulated by DtxR requires further studies.

strictly dependent on the presence of Mn^{2+} ions, since in the absence of Mn^{2+} no shift was observed even at a 200-fold molar excess of dimeric DtxR (data not shown).

Combining gel shift and DNA microarray data for the identification of the DtxR target genes. The transcriptome comparison of the wild type and the Δ*dtxR* mutant identified genes and operons whose mRNA levels were altered as a consequence of the *dtxR* deletion; however, this approach was not able to distinguish between genes that are directly controlled by DtxR and those whose expression is indirectly influenced by the absence of DtxR. In contrast, the gel shift assay with purified DtxR and DNA regions containing potential DtxR binding sites was able to identify putative direct target genes of DtxR, but this approach gave no information on the influence of DtxR on the expression of these genes in vivo. To identify genes or operons that are probably directly regulated by DtxR in vivo, we analyzed which of the genes/operons containing a functional DtxR binding site in their promoter region showed

more than 1.5-fold-altered mRNA levels in the Δ*dtxR* mutant and which did not. Based on this analysis, four groups of genes were identified, which are shown in Fig. 3.

The first group (Fig. 3A) includes 51 genes organized in 27 putative operons which are presumably repressed by DtxR, since they show an increased mRNA level in the Δ*dtxR* mutant under iron excess. The majority of these genes are obviously involved in iron acquisition, three encode transcriptional regulators, i.e., the AraC-type regulator RipA (40), the response regulator CgtR11 (23), and an ArsR-type regulator, and the others encode proteins of diverse or unknown functions. Three DtxR-repressed operons are located within the CGP3 prophage region.

The second group (Fig. 3B) comprises 12 genes that show a decreased mRNA level in the Δ*dtxR* mutant under iron excess. These genes could be activated by DtxR, as previously reported for the *bfrA* gene of *M. tuberculosis* (14). Interestingly, this group included the *suf* operon (NCgl1504 to NCgl1498), whose products are involved in formation and repair of iron-sulfur clusters, and several genes for transcriptional regulators, including RamB, which is involved in the regulation of acetate metabolism (13). In the case of *ramB*, the situation is exceptional, since this gene is located upstream and divergent to the RipA-controlled *sdhCAB* operon encoding succinate dehydrogenase (Fig. 3B). The DtxR binding site dedicated to *ramB* is located 390 bp upstream of the translation start of *ramB* and 105 bp upstream of the transcription start site of *sdhC*, which we recently identified by primer extension to be located 15 bp upstream of the *sdhC* start codon (S. Degraf and M. Bott, unpublished data). Although *sdhCAB* expression followed the same pattern as that of the other RipA target genes, the possibility that DtxR directly activates *sdhCAB* expression under iron excess cannot be excluded from our data.

The third group (Fig. 3C) contains two genes, *ftn* and *dps*, which are of particular importance for iron homoeostasis, since they encode proteins capable of iron storage, namely ferritin and Dps (for a review see reference 1). The mRNA levels of these genes were almost unaltered in the Δ*dtxR* mutant under iron excess but increased under iron limitation, a behavior not yet understood.

The fourth group (Fig. 3D) includes 32 genes organized in 18 putative operons that contain a functional DtxR binding site but whose mRNA levels could not be determined or were changed less than 1.5-fold in the Δ*dtxR* mutant. With few exceptions, most of the corresponding genes show no obvious connection to iron metabolism. The influence of DtxR on the expression of these genes in vivo is unclear, since small changes in expression might remain undetected with the DNA microarray method used.

On average, high mRNA ratios (Δ*dtxR* mutant/wild type) under iron excess correlated with high in vitro binding affinities of the respective DtxR binding sites and low mRNA ratios with low in vitro binding affinities.

DISCUSSION

The transcriptional regulator DtxR was first identified in *C. diphtheriae*, where it controls the expression of the diphtheria toxin gene carried by corynebacteriophage β in an iron-dependent manner (4, 33). Subsequent studies with DtxR and its ortholog IdeR from *Mycobacterium* species revealed that DtxR plays a key role in the control of iron metabolism and thus is a functional equivalent of the Fur protein from gram-negative and low-G+C gram-positive bacteria (2, 11, 16). In this work, we performed a genome-wide search for DtxR-regulated genes in *C. glutamicum* by comparing the gene expression profiles of the wild type and a Δ*dtxR* mutant and by testing the functionality of 74 putative DtxR binding sites with electrophoretic mobility shift assays with purified DtxR protein from *C. glutamicum*. Genes which are preceded by a functional DtxR binding site and which show an at least 1.5-fold-altered mRNA level in the Δ*dtxR* mutant are considered probable direct target genes of DtxR.

As expected, the majority of the target genes are repressed by DtxR (increased mRNA level in the Δ*dtxR* mutant) and are involved in iron acquisition (Fig. 3A). One operon (NCgl0377 to NCgl0380) is homologous to the *hmu* operon of *C. diphtheriae* (7) and encodes an ABC transporter for heme uptake. Three other genes are predicted to encode proteins that are also involved in heme transport, all of which contain a signal peptide and a putative C-terminal transmembrane helix (NCgl0381-NCgl0382 and NCgl2752). A further gene repressed by DtxR and probably also required for heme utilization is *hmuO*, encoding heme oxygenase (NCgl2146), an enzyme converting protoheme to biliverdin IXα and free iron. Nineteen genes repressed by DtxR encode proteins presumably involved in the acquisition of iron from siderophores. They include three ABC transporters (permeases and ATPases), seven secreted siderophore-binding lipoproteins, and three cytoplasmic siderophore-interacting proteins. In contrast to the high number of genes involved in siderophore utilization, none of the genes repressed by DtxR was annotated to be involved in siderophore biosynthesis, in contrast, for example, to *M. smegmatis* or *M. tuberculosis* (8, 14, 30). Inspection of the *C. glutamicum* ATCC 13032 genome sequence (20) failed to reveal genes that are obviously involved in siderophore biosynthesis. Thus, the strategy of *C. glutamicum* ATCC 13032 for coping with iron starvation is to make use of a variety of siderophores produced by other microbes and perhaps also of heme compounds. However, since another strain of *C. glutamicum*, ATCC 14067, produces the cyclic catecholate siderophore corynebactin (5), strain-specific differences exist with respect to siderophore production.

In addition to its function in repressing iron starvation genes, we recently provided evidence for another role of DtxR, namely, its influence on the expression of several prominent iron-containing proteins via the AraC-type regulator RipA (40). We proposed that *ripA* expression is controlled by DtxR, since this protein binds to a well-conserved binding site upstream of *ripA* (40). This proposal was clearly confirmed in this work. The *ripA* mRNA level was more than 10-fold increased in the Δ*dtxR* mutant, whereas the mRNA level of the RipA target genes was strongly reduced in the Δ*dtxR* mutant (Table 2). The fact that the RipA protein synthesized in the Δ*dtxR* mutant repressed its target genes in the presence of excess iron indicates that RipA repressor activity is not directly controlled by iron, in contrast to the case with DtxR.

Besides *ripA*, two further genes for transcriptional regulators are likely to be repressed by DtxR, i.e., NCgl0430 and *cgtR11*. The mRNA level of NCgl0430, encoding an ArsR-type regulator, was sevenfold increased in the Δ*dtxR* mutant under both

iron excess and iron starvation. Members of the SmtB/ArsR family usually repress the expression of genes required to cope with stress-inducing concentrations of di- and multivalent heavy metal ions. Depression results from direct binding of metal ions to the homodimeric repressors (6). The metal ion that might be sensed by the NCgl0430 protein as well as its target genes are not yet known. The mRNA level of *cgtR11* was about twofold increased in the ΔdtxR mutant under iron excess. This gene encodes the response regulator of the CgtSR11 two-component system of *C. glutamicum* (23). Since the DtxR binding site is located upstream of *cgtR11* (Fig. 3A), only this gene, but not the upstream *cgtS11* gene, appears to be under direct control of DtxR. The CgtS11 and CgtR11 proteins show high sequence identity to the *C. diphtheriae* proteins encoded by the genes DIP2268 (56% identity) and DIP2267 (86%), respectively, and weaker similarity to the sensor kinase ChrS (30%) and the response regulator ChrA (50%) from *C. diphtheriae*. Since the ChrAS two-component system was recently shown to control the expression of the *hmuO* gene encoding heme oxygenase (3), the CgtSR11 two-component system might also be involved in the control of genes required for heme utilization.

Studies with *M. tuberculosis* indicate that DtxR can function not only as a transcriptional repressor but also as a transcriptional activator (14). In the course of our studies, a number of genes were identified that were preceded by a functional DtxR binding site and which showed a decreased mRNA level in the Δ*dtxR* mutant (Fig. 3B). Thus, expression of these genes appears to be activated by DtxR. One interesting operon belonging to this group was the *suf* operon, which includes seven genes (NCgl1504 to NCgl1498). A DtxR box upstream of NCgl1504, designated here as *sufR*, was able to bind purified DtxR (Fig. 2), whereas a second putative DtxR box localized upstream of NCgl1501 was not. With the exception of the promoter-proximal *sufR*, the genes of this operon encode proteins involved in the assembly and repair of iron-sulfur clusters, which form the so-called SUF machinery. As in *M. tuberculosis* (17), the SUF machinery appears to be the exclusive system for this function in *C. glutamicum*. The SufR protein of *C. glutamicum*, which is a DeoR-type transcriptional regulator, might have the same function as the SufR protein from *Synechocystis* sp. strain PCC6803 (38). In *Synechocystis*, SufR functions as a repressor of the *sufBCDS* operon, and it was proposed that SufR senses the levels of iron-sulfur clusters in the cell through its own unstable iron-sulfur cluster: if the cluster is present, SufR binds to its operator and represses the *suf* operon; if it is oxidatively damaged or absent, repression is relieved. If the *C. glutamicum* SufR protein functions in a similar fashion, the *C. glutamicum suf* operon is under dual transcriptional control, i.e., positive control by DtxR and negative control by SufR.

Genes of particular importance for iron homeostasis are those encoding iron storage proteins. The genome of *C. glutamicum* harbors two such genes, i.e., *ftn* (NCgl2439), encoding a ferritin (NCgl2439), and *dps* (NCgl2897), encoding a protein of the Dps family. Both genes contain a functional DtxR binding site in the 5′ noncoding region and showed almost unchanged mRNA levels in the Δ*dtxR* mutant under iron excess but increased mRNA levels under iron limitation (Fig. 3C). The simplest explanation would assume that DtxR represses *ftn* and *dps* under iron limitation, which is physiologically meaningful, since iron storage proteins are probably required in only minute amounts under these conditions. However, purified DtxR bound with high affinity to the *dps* promoter and with low affinity to the *ftn* promoter only in the presence of Mn^{2+} but not in its absence. Thus, further studies are required to understand how DtxR attenuates *ftn* and *dps* expression under iron limitation.

In summary, the results presented here indicate that about 60 genes are likely to be directly controlled by DtxR and thus form the DtxR regulon. Since several of these themselves encode transcriptional regulators, such as *ripA*, a multitude of further genes is controlled indirectly by DtxR. Thus, DtxR was shown to be the master regulator of iron-dependent gene expression in *C. glutamicum*.

ACKNOWLEDGMENTS

We thank Hermann Sahm for continuous support, Volker Wendisch for establishing the DNA chip technique in our institute, and Melanie Brocker for help with DNA microarray analyses.

ADDENDUM IN PROOF

After this article was accepted for publication, another study on the identification of DtxR target genes in *Corynebacterium glutamicum* was published (I. Brune, H. Werner, A. T. Hüser, J. Kalinowski, A. Pühler, and A. Tauch, BMC Genomics **7**:21, 2006).

REFERENCES

1. **Andrews, S. C., A. K. Robinson, and F. Rodriguez-Quinones.** 2003. Bacterial iron homeostasis. FEMS Microbiol. Rev. **27**:215–237.
2. **Baichoo, N., T. Wang, R. Ye, and J. D. Helmann.** 2002. Global analysis of the *Bacillus subtilis* Fur regulon and the iron starvation stimulon. Mol. Microbiol. **45**:1613–1629.
3. **Bibb, L. A., N. D. King, C. A. Kunkle, and M. P. Schmitt.** 2005. Analysis of a heme-dependent signal transduction system in *Corynebacterium diphtheriae*: deletion of the *chrAS* genes results in heme sensitivity and diminished heme-dependent activation of the *hmuO* promoter. Infect. Immun. **73**:7406–7412.
4. **Boyd, J., M. N. Oza, and J. R. Murphy.** 1990. Molecular cloning and DNA sequence analysis of a diphtheria tox iron-dependent regulatory element (*dtxR*) from *Corynebacterium diphtheriae*. Proc. Natl. Acad. Sci. USA **87**: 5968–5972.
5. **Budzikiewicz, H., A. Bossenkamp, K. Taraz, A. Pandey, and J. M. Meyer.** 1997. Corynebactin, a cyclic catecholate siderophore from *Corynebacterium glutamicum* ATCC 14067 (*Brevibacterium* sp. DSM 20411). Z. Naturforsch. **52c**:551–554.
6. **Busenlehner, L. S., M. A. Pennella, and D. P. Giedroc.** 2003. The SmtB/ArsR family of metalloregulatory transcriptional repressors: structural insights into prokaryotic metal resistance. FEMS Microbiol. Rev. **27**:131–143.
7. **Drazek, E. S., C. A. Hammack, and M. P. Schmitt.** 2000. *Corynebacterium diphtheriae* genes required for acquisition of iron from haemin and haemoglobin are homologous to ABC haemin transporters. Mol. Microbiol. **36**:68–84.
8. **Dussurget, O., M. Rodriguez, and I. Smith.** 1996. An *ideR* mutant of *Mycobacterium smegmatis* has derepressed siderophore production and an altered oxidative-stress response. Mol. Microbiol. **22**:535–544.
9. **Eggeling, L., and M. Bott.** 2005. Handbook of Corynebacterium glutamicum. CRC Press, Inc., Boca Raton, Fla.
10. **Eikmanns, B. J., N. Thum-Schmitz, L. Eggeling, K. U. Lüdtke, and H. Sahm.** 1994. Nucleotide sequence, expression and transcriptional analysis of the *Corynebacterium glutamicum gltA* gene encoding citrate synthase. Microbiology **140**:1817–1828.
11. **Escolar, L., J. Perez-Martin, and V. de Lorenzo.** 1999. Opening the iron box: transcriptional metalloregulation by the Fur protein. J. Bacteriol. **181**:6223–6229.
12. **Fontecave, M., S. O. Choudens, B. Py, and F. Barras.** 2005. Mechanisms of iron-sulfur cluster assembly: the SUF machinery. J. Biol. Inorg. Chem. **10**: 713–721.
13. **Gerstmeir, R., A. Cramer, P. Dangel, S. Schaffer, and B. J. Eikmanns.** 2004. RamB, a novel transcriptional regulator of genes involved in acetate metabolism of *Corynebacterium glutamicum*. J. Bacteriol. **186**:2798–2809.

14. **Gold, B., G. M. Rodriguez, S. A. Marras, M. Pentecost, and I. Smith.** 2001. The *Mycobacterium tuberculosis* IdeR is a dual functional regulator that controls transcription of genes involved in iron acquisition, iron storage and survival in macrophages. Mol. Microbiol. **42:**851–865.
15. **Hanahan, D.** 1985. Techniques for transformation of *E. coli*, p. 109–135. *In* D. M. Glover (ed.), DNA cloning: a practical approach, vol. 1. IRL-Press, Oxford, United Kingdom.
16. **Hantke, K.** 2001. Iron and metal regulation in bacteria. Curr. Opin. Microbiol. **4:**172–177.
17. **Huet, G., M. Daffe, and I. Saves.** 2005. Identification of the *Mycobacterium tuberculosis* SUF machinery as the exclusive mycobacterial system of [Fe-S] cluster assembly: evidence for its implication in the pathogen's survival. J. Bacteriol. **187:**6137–6146.
18. **Ishige, T., M. Krause, M. Bott, V. F. Wendisch, and H. Sahm.** 2003. The phosphate starvation stimulon of *Corynebacterium glutamicum* determined by DNA microarray analyses. J. Bacteriol. **185:**4519–4529.
19. **Kalinowski, J.** 2005. The genomes of amino acid-producing corynebacteria, p. 37–56. *In* L. Eggeling and M. Bott (ed.), Handbook of *Corynebacterium glutamicum*. CRC Press, Boca Raton, Fla.
20. **Kalinowski, J., B. Bathe, D. Bartels, N. Bischoff, M. Bott, A. Burkovski, N. Dusch, L. Eggeling, B. J. Eikmanns, L. Gaigalat, A. Goesmann, M. Hartmann, K. Huthmacher, R. Kramer, B. Linke, A. C. McHardy, F. Meyer, B. Mockel, W. Pfefferle, A. Puhler, D. A. Rey, C. Ruckert, O. Rupp, H. Sahm, V. F. Wendisch, I. Wiegrabe, and A. Tauch.** 2003. The complete *Corynebacterium glutamicum* ATCC 13032 genome sequence and its impact on the production of L-aspartate-derived amino acids and vitamins. J. Biotechnol. **104:**5–25.
21. **Keilhauer, C., L. Eggeling, and H. Sahm.** 1993. Isoleucine synthesis in *Corynebacterium glutamicum*: molecular analysis of the *ilvB-ilvN-ilvC* operon. J. Bacteriol. **175:**5595–5603.
22. **Kinoshita, S., S. Udaka, and M. Shimono.** 1957. Studies on the amino acid fermentation. I. Production of L-glutamic acid by various microorganisms. J. Gen. Appl. Microbiol. **3:**193–205.
23. **Kocan, M., S. Schaffer, T. Ishige, U. Sorger-Herrmann, V. F. Wendisch, and M. Bott.** 2006. Two-component systems of *Corynebacterium glutamicum*: deletion analysis and involvement of the PhoS-PhoR system in the phosphate starvation response. J. Bacteriol. **188:**724–732.
24. **Krug, A., V. F. Wendisch, and M. Bott.** 2005. Identification of AcnR, a TetR-type repressor of the aconitase gene *acn* in *Corynebacterium glutamicum*. J. Biol. Chem. **280:**585–595.
25. **Lange, C., D. Rittmann, V. F. Wendisch, M. Bott, and H. Sahm.** 2003. Global expression profiling and physiological characterization of *Corynebacterium glutamicum* grown in the presence of L-valine. Appl. Environ. Microbiol. **69:**2521–2532.
26. **Möker, N., M. Brocker, S. Schaffer, R. Kramer, S. Morbach, and M. Bott.** 2004. Deletion of the genes encoding the MtrA-MtrB two-component system of *Corynebacterium glutamicum* has a strong influence on cell morphology, antibiotics susceptibility and expression of genes involved in osmoprotection. Mol. Microbiol. **54:**420–438.
27. **Niebisch, A., and M. Bott.** 2001. Molecular analysis of the cytochrome bc_1-aa_3 branch of the *Corynebacterium glutamicum* respiratory chain containing an unusual diheme cytochrome c_1. Arch. Microbiol. **175:**282–294.
28. **Oguiza, J. A., X. Tao, A. T. Marcos, J. F. Martin, and J. R. Murphy.** 1995. Molecular cloning, DNA sequence analysis, and characterization of the *Corynebacterium diphtheriae dtxR* homolog from *Brevibacterium lactofermentum*. J. Bacteriol. **177:**465–467.
29. **Polen, T., D. Rittmann, V. F. Wendisch, and H. Sahm.** 2003. DNA microarray analyses of the long-term adaptive response of *Escherichia coli* to acetate and propionate. Appl. Environ. Microbiol. **69:**1759–1774.
30. **Rodriguez, G. M., M. I. Voskuil, B. Gold, G. K. Schoolnik, and I. Smith.** 2002. *ideR*, an essential gene in *Mycobacterium tuberculosis*: role of IdeR in iron-dependent gene expression, iron metabolism, and oxidative stress response. Infect. Immun. **70:**3371–3381.
31. **Sambrook, J., E. F. Fritsch, and T. Maniatis.** 1989. Molecular cloning. a laboratory manual. Cold Spring Harbor Laboratory Press, Cold Spring Harbor, N.Y.
32. **Schäfer, A., A. Tauch, W. Jäger, J. Kalinowski, G. Thierbach, and A. Pühler.** 1994. Small mobilizable multi-purpose cloning vectors derived from the *Escherichia coli* plasmids pK18 and pK19: selection of defined deletions in the chromosome of *Corynebacterium glutamicum*. Gene **145:**69–73.
33. **Schmitt, M. P., and R. K. Holmes.** 1991. Iron-dependent regulation of diphtheria toxin and siderophore expression by the cloned *Corynebacterium diphtheriae* repressor gene *dtxR* in *C. diphtheriae* C7 strains. Infect. Immun. **59:**1899–1904.
34. **Stackebrandt, E., F. A. Rainey, and N. L. WardRainey.** 1997. Proposal for a new hierarchic classification system, Actinobacteria classis nov. Int. J. Syst. Bacteriol. **47:**479–491.
35. **Studier, F. W., and B. A. Moffatt.** 1986. Use of bacteriophage T7 RNA polymerase to direct selective high-level expression of cloned genes. J. Mol. Biol. **189:**113–130.
36. **Tao, X., and J. R. Murphy.** 1994. Determination of the minimal essential nucleotide sequence for diphtheria tox repressor binding by in vitro affinity selection. Proc. Natl. Acad. Sci. USA **91:**9646–9650.
37. **van der Rest, M. E., C. Lange, and D. Molenaar.** 1999. A heat shock following electroporation induces highly efficient transformation of *Corynebacterium glutamicum* with xenogeneic plasmid DNA. Appl. Microbiol. Biotechnol. **52:**541–545.
38. **Wang, T., G. Shen, R. Balasubramanian, L. McIntosh, D. A. Bryant, and J. H. Golbeck.** 2004. The *sufR* gene (sll0088 in *Synechocystis* sp. strain PCC 6803) functions as a repressor of the *sufBCDS* operon in iron-sulfur cluster biogenesis in cyanobacteria. J. Bacteriol. **186:**956–967.
39. **Wendisch, V. F.** 2003. Genome-wide expression analysis in *Corynebacterium glutamicum* using DNA microarrays. J. Biotechnol. **104:**273–285.
40. **Wennerhold, J., A. Krug, and M. Bott.** 2005. The AraC-type regulator RipA represses aconitase and other iron proteins from *Corynebacterium* under iron limitation and is itself repressed by DtxR. J. Biol. Chem. **280:**40500–40508.

JOURNAL OF BACTERIOLOGY, Feb. 2007, p. 1145–1149 Vol. 189, No. 3
0021-9193/07/$08.00+0 doi:10.1128/JB.01061-06

NOTES

RamB, the Transcriptional Regulator of Acetate Metabolism in *Corynebacterium glutamicum*, Is Subject to Regulation by RamA and RamB[▽]

Annette Cramer,[1] Marc Auchter,[1] Julia Frunzke,[2] Michael Bott,[2] and Bernhard J. Eikmanns[1]*

Department of Microbiology and Biotechnology, University of Ulm, 89069 Ulm,[1] and Institute of Biotechnology 1, Research Center Jülich, D-52425 Jülich,[2] Germany

Received 19 July 2006/Accepted 5 November 2006

In *Corynebacterium glutamicum*, the transcriptional regulator RamB negatively controls the expression of genes involved in acetate metabolism. Here we show that RamB represses its own expression by direct interaction with a 13-bp motif in the *ramB* promoter region. Additionally, *ramB* expression is subject to carbon source-dependent positive control by RamA.

Corynebacterium glutamicum is an aerobic gram-positive soil bacterium well known for its use in large-scale biotechnological production of L-glutamate and lysine (10–14). We are interested in acetate metabolism and its regulation in this organism (7), and we recently identified and characterized two regulatory proteins, designated *r*egulator of *a*cetate *m*etabolism *A* and *B* (RamA and RamB, respectively) from *C. glutamicum* ATCC 13032 (4, 6). RamA binds to single or tandem stretches of A/C/TG$_{4-6}$T/C or AC$_{4-5}$A/G/T and thereby acts as an activator of the *pta*, *ack*, *aceA*, and *aceB* genes, encoding phosphotransacetylase, acetate kinase, isocitrate lyase, and malate synthase, all involved in acetate metabolism of *C. glutamicum*. RamA was also shown to activate transcription of the surface layer protein gene (*cspB*) in *C. glutamicum* ATCC 14067 (9). Furthermore, RamA was shown to bind to the promoter region of its own gene and to act as a repressor there (3). The RamB protein specifically binds to a highly conserved 13-bp motif (AA/GAACTTTGCAAA) and represents a repressor of the *pta*, *ack*, *aceA*, and *aceB* genes when *C. glutamicum* is grown on glucose as a carbon and energy source (6). Inspection of the *ramB* promoter region revealed the presence of putative RamA and RamB binding sites, and this observation prompted us to study expression of *ramB* in cells growing in media containing glucose and/or acetate and to test for a regulatory function of RamA and RamB in *ramB* expression.

The bacterial strains and the plasmids, their relevant characteristics and sources, and the oligonucleotides used in this study are given in Table 1. The media used and the methods not outlined explicitly (DNA preparation, promoter binding assays with hexahistidyl-tagged RamA and RamB fusion proteins, enzyme assays, RNA preparation and identification of the transcriptional start site by the RACE [rapid amplification of cDNA ends] method, generation of polyclonal antibodies, and Western blotting) were described previously (3, 4, 6).

Western blot experiments with RamB-specific antibodies and crude extracts from *C. glutamicum* wild-type (WT) cells grown in minimal medium containing glucose, glucose plus acetate, and acetate showed that RamB is present in cells grown on either carbon source (Fig. 1). In agreement with the results of DNA affinity chromatography experiments (4), the largest amounts of RamB were observed in the cells grown on glucose alone.

To test for *ramB* promoter activities in *C. glutamicum* cells grown in minimal media with glucose and/or acetate, we constructed reporter gene fusions by cloning a 593-bp *ramB* promoter fragment (covering the region 521 bp upstream to 72 bp downstream of the *ramB* start codon) into the promoter test vector pET2, resulting in plasmid p*ramB*p1. This vector was transformed into *C. glutamicum* WT, and the plasmid-bound *ramB* promoter activity of *ramB* was then tested in *C. glutamicum* (p*ramB*p1) by measuring the specific activities of the reporter gene product chloramphenicol acetyltransferase (CAT). As shown in Table 2, *C. glutamicum* (p*ramB*p1) showed about fourfold-lower specific CAT activity when grown in medium containing acetate or a mixture of both carbon sources instead of glucose. To exclude copy number or titration effects, we also tested the *ramB*p1-*cat* fusion after monocopy integration into the chromosome of WT *C. glutamicum*. For this purpose, the PCR-generated fragment *ramB*p1 (Fig. 2A) was ligated into plasmid pRIM2, and the resulting plasmid was integrated into the chromosome as described elsewhere (17). As in the case of the multicopy *ramB*p1-*cat* fusion, the specific CAT activity was about fourfold lower when the cells were grown on glucose instead of acetate (0.004 and 0.001 U/mg protein, respectively). These result show the presence of a promoter on the *ramB*p1 fragment and indicates transcriptional regulation of *ramB*, i.e., induction or derepression when cells are grown on glucose as the sole carbon and energy source and/or repression when acetate is present in the growth medium. Taken together, the

* Corresponding author. Mailing address: Department of Microbiology and Biotechnology, University of Ulm, 89069 Ulm, Germany. Phone: 49 731 50 22707. Fax: 49 731 50 22719. E-mail: bernhard.eikmanns@uni-ulm.de.

▽ Published ahead of print on 17 November 2006.

TABLE 1. Bacterial strains, plasmids, and oligonucleotides used in this study

Strain, plasmid, or oligonucleotide	Relevant characteristics or sequence[a]	Source, reference, or purpose
Strains		
E. coli DH5	*supE44 hsdR17 recA1 endA1 gyrA96 thi-1 relA1*	8
E. coli BL21 (DE)	*ompT hsdS*$_B$ (r_B^- m_B^-) *gal dcm* (DE3)	5
C. glutamicum WT	Wild-type strain ATCC 13032	American Type Culture Collection
C. glutamicum RG1	WT *C. glutamicum* with truncated *ramB* gene, shortened by 775 bp	6
C. glutamicum RG2	WT *C. glutamicum* with truncated *ramA* gene, shortened by 364 bp	4
Plasmids		
pET2	Multicopy promoter probe vector carrying the promoterless *cat* gene; Km^r	17
pRIM2	Integrative promoter probe vector carrying the promoterless *cat* gene; Km^r	17
pET28-RamAx6His	pET28 containing the *ramA* structural gene	4
pET29-RamBx6His	pET29 containing the *ramB* structural gene	6
p*ramB*p1	pET2 containing the 593-bp *ramB* promoter fragment	This work
p*ramB*p3	pET2 containing the 370-bp *ramB* promoter fragment	This work
p*ramB*p3b	pET2 containing the 211-bp *ramB* promoter fragment	This work
p*ramB*p3c	pET2 containing the 135-bp *ramB* promoter fragment	This work
pRIM-*ramB*p1	pRIM containing the 593-bp *ramB* promoter fragment	This work
pRIM-*ramB*p3c	pRIM containing the 135-bp *ramB* promoter fragment	This work
pDrive	Cloning vector; Km^r Amp^r *lacZ*α *ori*f1 *ori*-pUC	QIAGEN GmbH, Hilden, Germany
pDrive *ramB*pRACE	pDrive derivative plasmid containing the *ramB* PCR-amplified fragment from the RACE assay	This work
Oligonucleotides[b]		
*ramB*pLF forw	5′-ACGCGTCGACCTAACAGTCATGGCACCTCCAGTGTGG-3′	*ramB*p1and *ramB*p5
*ramB*pLF rev	5′-CGCGGATCCCAAGGGTTGCTGCTAAGGATGCCTG-3′	*ramB*p1, *ramB*p3, *ramB*p3a, *ramB*p3b, *ramB*p3c
*ramB*p forw	5′-AGCGAAAATCAACAAGTTTGCAACACCTCAGT-3′	*ramB*p 13-bp motif
*ramB*p rev	5′-ACTGAGGTGTTGCAAACTTGTTGATTTTCGCT-3′	*ramB*p 13-bp motif
*ramB*pKF forw	5′-ACGCGTCGACGCTTCCTCACAGGATACCGA-3′	*ramB*p3
*ramB*p3a forw	5′-CAGGGAGCAACTTTGCGCAG-3′	*ramB*p3a
*ramB*p3b forw	5′-ACGCGTCGACGATGTGGCCCGACCACGCCG-3′	*ramB*p3b
*ramB*p3c forw	5′-ACGCGTCGACCTCAGTGCCAAGAGTGGTTA-3′	*ramB*p3c
*ramB*p5 rev	5′-CGCAGGTAGAGCACACTCAAT-3′	*ramB*p5
CM4	5′-GAAAATCTCGTCGAAGCTCG-3′	cDNA synthesis; 5′-RACE *ramA* and *ramB* transcriptional start site determination
Oligonucleotide dT anchor primer	5′-GACCACGCGTATCGATGTCGACTTTTTTTTTTTTTTTV-3′	Amplification of dA-tailed cDNA (Roche, 5′/3′ RACE kit)

[a] Restriction sites in the oligonucleotides are underlined. V represents an A, C, or G.
[b] forw., forward; rev, reverse.

results indicate that the amount of RamB protein in *C. glutamicum* is dependent on the carbon source in the growth medium and that the respective control is due to transcriptional regulation of the *ramB* gene.

To identify the *ramB* transcriptional initiation site (TS) and to localize the respective promoter, total RNA from *C. glutamicum* (p*ramB*p1) was isolated, and cDNA of the 5′ end of the *ramB* transcript was generated with reverse transcriptase. Subsequently, this cDNA was amplified and subcloned into the vector pDrive, and the resulting plasmid, pDrive *ramB*pRACE

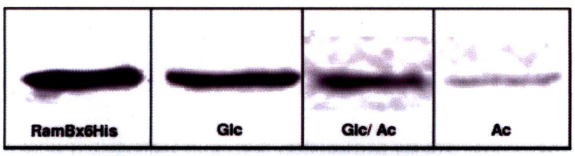

FIG. 1. Western blot using specific antibodies against RamB and cell extracts of *C. glutamicum* WT (100 μg total protein) grown in minimal medium containing glucose (Glc), glucose and acetate (Glc/Ac), or acetate (Ac). The presence of RamB in the extracts was tested by incubation with specific mouse antibodies followed by incubation with peroxidase-conjugated goat anti-mouse immunoglobulin G Fab fragments and visualization by chemiluminescence. Purified RamB protein (RamBx6His; 0.2 μg) was used as a control.

TABLE 2. Specific CAT activities of *C. glutamicum* grown in minimal medium (MM) containing glucose and/or acetate as the carbon and energy source

C. glutamicum strain	CAT sp act (U/mg protein)[a] on MM with:		
	Glucose	Glucose + acetate	Acetate
WT(p*ramB*p1)	0.28 ± 0.02	0.07 ± 0.01	0.06 ± 0.01
RG1(p*ramB*p1) (Δ*ramB*)	0.45 ± 0.03	0.21 ± 0.01	0.15 ± 0.02
RG2(p*ramB*p1) (Δ*ramA*)	0.08 ± 0.01	0.08 ± 0.01	NG
WT(p*ramB*p3)	0.28 ± 0.03	0.09 ± 0.01	0.10 ± 0.01
WT(p*ramB*p3b)	0.14 ± 0.01	0.05 ± 0.01	0.05 ± 0.01
WT(p*ramB*p3c)	0.45 ± 0.02	0.22 ± 0.01	0.16 ± 0.02

[a] Values are means ± standarsd deviations obtained from at least three independent cultivations and two determinations per experiment. NG, no growth.

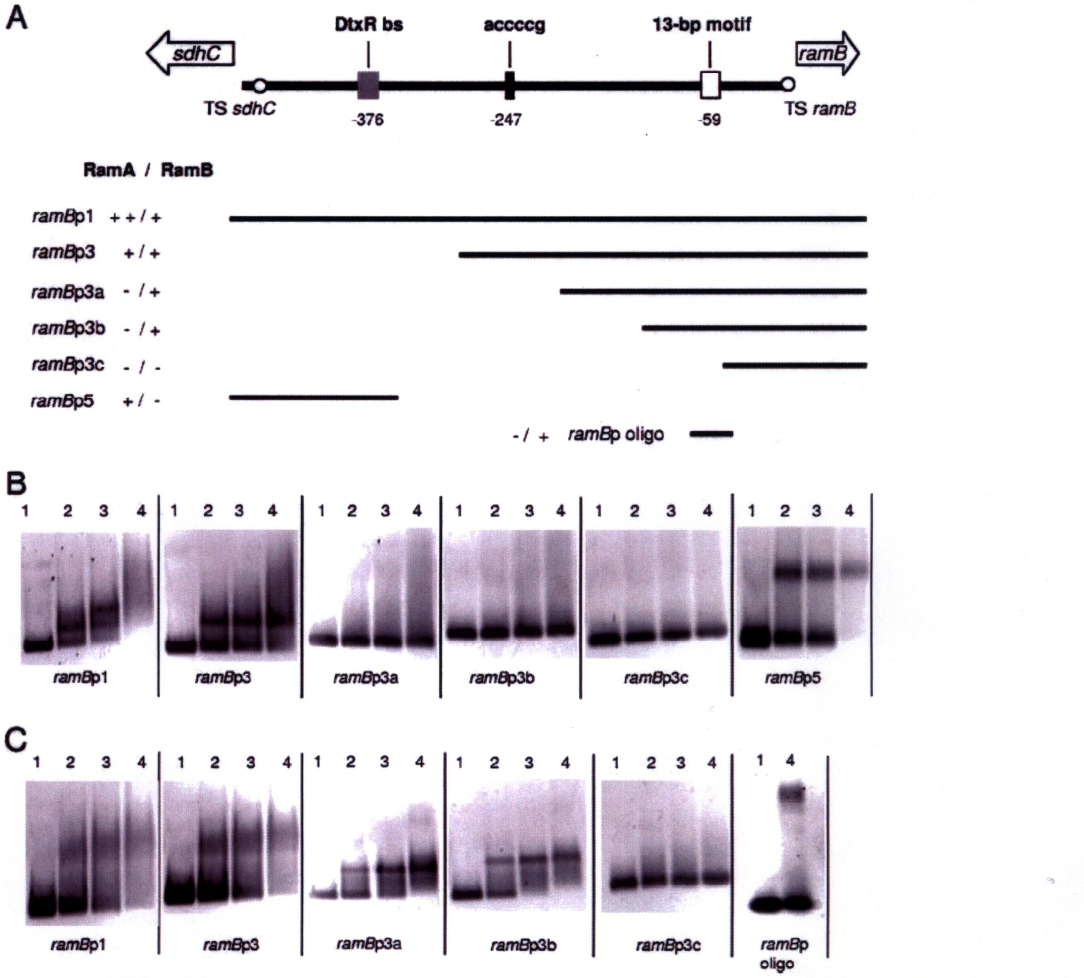

FIG. 2. Genomic locus of the *ramB* promoter region and DNA fragments used for mapping the relevant RamA and RamB binding loci (A) and representative EMSAs using various DNA fragments and RamA protein (B) and RamB protein (C). *sdhC* codes for a protein annotated as a membrane anchor protein of the succinate dehydrogenase. The transcriptional start sites for the *ramB* gene and the *sdhC* gene are designated TS *ramB* and TS *sdhC*, respectively. (A) The RamB binding site is designated as a 13-bp motif. The nucleotide sequence of the putative RamA binding site is given above the black box. The putative DtxR binding site (DtxR bs) is indicated by a dark gray box. The numbers indicate the positions of the centers of these sites relative to the *ramB* TS site. The fragments used for the binding assays are shown as narrow bars. Also indicated are binding (+) and lack of binding (−) of RamA and RamB. Lanes 1 to 4 (B and C) show EMSAs using 0, 0.25, 0.5, and 1.0 μg of RamA or RamB, respectively.

was sequenced, leading to the identification of the TS for *ramB*. In four independently obtained pDrive *ramB*pRACE clones, the TS of *ramB* was found to be an A residue which is identical to the translational start site proposed (11) (NCBI accession number NC_006958). Such leaderless transcripts are not uncommon in *C. glutamicum* and other actinomycetes (16). Inspection of the upstream region of the TS led to the identification of a potential −10 box (TATAGT) which is conserved in five of six nucleotides relative to the −10 consensus sequence described for corynebacteria (TA[C/T]AAT) (15). No apparent −35 region (TTGCCA) could be recognized, which also is a common feature of *C. glutamicum* promoters (15, 16).

Inspection of the *ramB* promoter region revealed the presence of a typical 13-bp RamB binding motif (ACAAGTTTG CAAC; mismatches underlined), centered 59 bp upstream of the *ramB* TS. Furthermore, a nucleotide sequence resembling the RamA binding site was also found, centered 247 bp upstream of the *ramB* TS (Fig. 2A). Further possible RamA binding sites are located in the region near the *sdhC* transcriptional start site (not shown in Fig. 2A). To test whether expression of *ramB* in *C. glutamicum* in fact is subject to transcriptional control by RamA and/or RamB, the *ramB* promoter activities were determined in the *ramB* and *ramA* deletion mutants *C. glutamicum* RG1 and RG2. For this purpose, plasmid p*ramB*p1 (see above) was transformed into both mutants, and after growth in minimal medium containing glucose and/or acetate, the *ramB* promoter activities were tested by measuring the specific CAT activity and compared to that of *C. glutamicum* WT (p*ramB*p1). The *C. glutamicum* RG2 derivative did not grow on minimal medium containing acetate as the sole carbon source, a phenotype which was previously found for the parental strain RG2 (4).

C. glutamicum RG1 (p*ramB*p1) cells showed about twofold-higher specific CAT activities than *C. glutamicum* WT (p*ramB*p1) cells on glucose and about threefold-higher activities in the presence of acetate (Table 2). On the other hand, only very low CAT activity was observed in *C. glutamicum* RG2 (p*ramB*p1) cells independent of the presence or absence of glucose. These results indicate that (i) *ramB* transcription is negatively autoregulated by RamB under all conditions tested and (ii) *ramB* expression is positively regulated by RamA when glucose is the sole carbon and energy source. Since the *ramB* mutant RG1 (p*ramB*p1), in spite of a deregulation, showed different CAT activities when grown in medium with glucose alone, glucose plus acetate, or acetate alone (Table 2), it must be concluded that either RamA is responsible for the induction (or derepression) of the *ramB* gene in the presence of glucose or another regulatory factor is involved.

Wennerhold and Bott (18) and Brune et al. (2) identified a binding site for the iron regulator DtxR centered 376 bp upstream of the *ramB* TS. However, although this binding site is closer (105 bp) to the TS of the neighboring succinate dehydrogenase subunit C gene *sdhC* (Fig. 2A), we speculated about a function of this motif for control of *ramB* or *sdhC* (18). To test for involvement of DtxR in the regulation of *ramB* expression, we determined CAT activities in WT *C. glutamicum* (p*ramB*p1) and in *C. glutamicum* Δ*dtxR* (17) transformed with plasmid p*ramB*p1. Both strains showed identical CAT activities in glucose minimal medium under iron limitation (1 μM) and iron excess (100 μM) conditions (data not shown). These results suggest that DtxR is not involved as a transcriptional regulator in the control of *ramB* expression.

Electrophoretic mobility shift assays (EMSAs) with hexahistidyl-tagged RamA and RamB fusion proteins and a series of *ramB* promoter fragments (Fig. 2A) were performed to assay for direct binding of RamA and/or RamB to the putative RamA and RamB binding sites observed within the *ramB* promoter region. Different amounts of purified RamA or RamB protein were incubated with the *ramB* promoter fragments and separated on an agarose gel. The relevant results of these EMSAs with the *ramB* fragments and RamA and RamB protein are shown in Fig. 2B and C, respectively.

The promoter fragments *ramB*p1, *ramB*p3, and *ramB*p5 were retarded effectively by RamA (Fig. 2B). Retardation in all three cases was complete with 1 μg of RamA protein, corresponding to molar excesses (protein/DNA) of about 50. The fragment *ramB*p1 formed two RamA/DNA complexes, while the fragments *ramB*p3 and *ramB*p5 formed only one RamA/DNA complex. No retardation was observed with fragments lacking the putative RamA binding sites (i.e., *ramB*p3a, *ramB*p3b, and *ramB*p3c). These results show relatively tight binding of RamA to the *ramB* promoter region.

As shown in Fig. 2C, the *ramB* promoter fragments containing the putative 13-bp motif (i.e., *ramB*p1, *ramB*p3, *ramB*p3a, and *ramB*p3b) were retarded by RamB, while the fragment *ramB*p3c (without this motif) showed no retardation. A 32-bp oligonucleotide covering the 13-bp motif also revealed retardation, corroborating our conclusion that this motif in fact is responsible for the specific binding of RamB to the *ramB* promoter.

The fragments *ramB*p3, *ramB*p3b, and *ramB*p3c were also tested for *ramB* promoter activity. For this purpose, we constructed respective reporter gene fusions in the promoter test vector pET2, resulting in plasmids p*ramB*p3, p*ramB*p3b, and p*ramB*p3c. The promoter activities of these fragments were tested in *C. glutamicum* WT by measuring specific CAT activity. As shown in Table 2, p*ramB*p3 conferred the same promoter activity to *C. glutamicum* as p*ramB*p1, on all media tested. This result shows that the RamA bindings site located near the *sdhC* TS site has no influence on *ramB* expression. Plasmid p*ramB*p3b, lacking the RamA binding site 247 bp upstream of the *ramB* TS, conferred about twofold-lower promoter activity in glucose medium than p*ramB*p1 and p*ramB*p3, and the activities of WT *C. glutamicum* carrying p*ramB*p3b were comparable to those of the RamA-negative mutant RG2(p*ramB*p1). These results indicate that RamA activates *ramB* expression in *C. glutamicum* by direct binding to the *ramB* promoter region when cells are grown in glucose medium.

The lack of the RamB binding site in plasmid p*ramB*p3c [WT *C. glutamicum*(p*ramB*p3c)] resulted in high *ramB* promoter activities similar to those observed in the *ramB* mutant *C. glutamicum* RG1(p*ramB*p1). In accordance, the specific CAT activity of a *ramB*p3c-*cat* fusion after monocopy integration into the chromosome of *C. glutamicum* WT (tested by ligating fragment *ramB*p3c [Fig. 2A] into plasmid pRIM2 and integration) was significantly higher than that of the *ramB*p1-*cat* fusion, independent of the carbon source used (0.014 and 0.004 U/mg protein on glucose and 0.007 and 0.001 U/mg protein on acetate as the carbon sources). These results show that RamB negatively autoregulates its expression by direct binding to the 13-bp motif located 59 bp upstream of the *ramB* TS.

In conclusion, we provide evidence that expression of the *ramB* gene as well as the amount of RamB protein is significantly higher in glucose-grown cells than in acetate-grown cells, that both RamA and RamB bind to the *ramB* promoter region, and that *ramB* expression is subject to negative control by RamB and to carbon source-dependent positive control by RamA. Since RamA negatively controls the expression of its own gene (3) and additionally positively influences the expression of *ramB*, it can be concluded that RamA is a master regulator of acetate metabolism in *C. glutamicum*. A model summarizing the present knowledge on the regulation network involving RamA and RamB in *C. glutamicum* is shown in Fig. 3. It is interesting that genes encoding orthologs of *ramA* and *ramB* have been found in other corynebacteria, such as *C. efficiens*, *C. diphtheriae*, and *C. jeikeium* (1). In the former two species, the *ramB* ortholog is preceded by a motif resembling the 13-bp motif (centered 59 and 275 bp, respectively, upstream of the postulated translational start codons) and by several motifs similar to the *C. glutamicum* RamA binding sites. These observations may indicate similar regulation of *ramB* expression by RamB itself and by RamA in *C. efficiens* and *C. diphtheriae*.

We thank J. Kalinowski (University of Bielefeld) for helpful comments on our manuscript.

The support of the BMBF (grants 031U213D and 0313105 "Genome research on bacteria relevant for agriculture, environment and biotechnology") and of the Degussa AG is gratefully acknowledged.

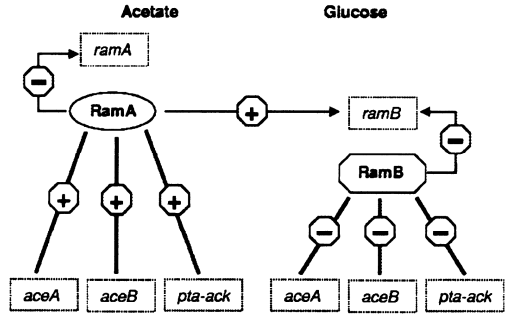

FIG. 3. Model of the regulatory network involving RamA and RamB in *C. glutamicum* grown in medium containing either glucose or acetate as the carbon source. The model is based on previous data (3, 4, 6, 7) and on data obtained here. Activation and repression are indicated by plus and minus signs, respectively. The thickness of the lines give a rough indication of the strength of activation/repression.

REFERENCES

1. **Brune, I., K. Brinkrolf, J. Kalinowski, A. Pühler, and A. Tauch.** 2005. The individual and common repertoire of DNA-binding transcriptional regulators of *Corynebacterium glutamicum*, *Corynebacterium efficiens*, *Corynebacterium diphtheriae*, and *Corynebacterium jeikeium* deduced from the complete genome sequence. BMC Genomics **6:**86.
2. **Brune, I., H. Werner, A. T. Hüser, J. Kalinowski, A. Pühler, and A. Tauch.** 2006. The DtxR protein acting as dual transcriptional regulator directs a global regulatory network involved in iron metabolism of *Corynebacterium glutamicum*. BMC Genomics **7:**21.
3. **Cramer, A., and B. J. Eikmanns.** 2007. RamA, the transcriptional regulator of acetate metabolism in *Corynebacterium glutamicum* is subject to negative autoregulation. J. Mol. Microbiol. Biotechnol. **12:**49–57.
4. **Cramer, A., R. Gerstmeir, S. Schaffer, M. Bott, and B. J. Eikmanns.** 2006. Identification of RamA, a novel LuxR-type transcriptional regulator of genes involved in acetate metabolism of *Corynebacterium glutamicum*. J. Bacteriol. **188:**2554–2567.
5. **Dubendorff, J. W., and F. W. Studier.** 1991. Controlling basal expression in an inducible T7 expression system by blocking the target T7 promoter with *lac* repressor. J. Mol. Biol. **219:**45–59.
6. **Gerstmeir, R., A. Cramer, P. Dangel, S. Schaffer, and B. J. Eikmanns.** 2004. RamB, a novel transcriptional regulator of genes involved in acetate metabolism of *Corynebacterium glutamicum*. J. Bacteriol. **186:**2798–2809.
7. **Gerstmeir, R., V. F. Wendisch, S. Schnicke, H. Ruan, M. Farwick, D. Reinscheid, and B. J. Eikmanns.** 2003. Acetate metabolism and its regulation in *Corynebacterium glutamicum*. J. Biotechnol. **104:**99–122.
8. **Hanahan, D.** 1983. Studies on transformation of *Escherichia coli* with plasmids. J. Mol. Biol. **166:**557–580.
9. **Hansmeier, N., A. Albersmeier, A. Tauch, T. Damberg, R. Ros, D. Anselmetti, A. Pühler, and J. Kalinowski.** 2006. The surface (S)-layer gene *cspB* of *Corynebacterium glutamicum* is transcriptionally activated by a LuxR-type regulator and located on a 6 kb genomic island absent from the type strain ATCC 13032. Microbiology **152:**923–935.
10. **Hermann, T.** 2003. Industrial production of amino acids by coryneform bacteria. J. Biotechnol. **104:**155–172.
11. **Kalinowski, J., B. Bathe, D. Bartels, M. Bischoff, M. Bott, A. Burkovski, N. Dusch, L. Eggeling, B. J. Eikmanns, L. Gaigalat, A. Goesmann, M. Hartmann, K. Huthmacher, R. Krämer, B. Linke, A. C. McHardy, F. Meyer, B. Möckel, W. Pfefferle, A. Pühler, D. Rey, C. Rückert, O. Rupp, H. Sahm, V. F. Wendisch, I. Wiegräbe, and A. Tauch.** 2003. The complete *Corynebacterium glutamicum* ATCC 13032 genome sequence and its impact on the production of L-aspartate-derived amino acids and vitamins. J. Biotechnol. **104:**5–25.
12. **Kelle, R., T. Hermann, and B. Bathe.** 2005. L-Lysine production, p. 465–488. *In* L. Eggeling and M. Bott (ed.), Handbook of *Corynebacterium glutamicum*. CRC Press, Boca Raton, FL.
13. **Kimura, E.** 2005. L-Glutamate production, p. 439–463. *In* L. Eggeling and M. Bott (ed.), Handbook of *Corynebacterium glutamicum*. CRC Press, Boca Raton, FL.
14. **Liebl, W.** 2005. *Corynebacterium* taxonomy, p. 9–34. *In* L. Eggeling and M. Bott (ed.), Handbook of *Corynebacterium glutamicum*. CRC Press, Boca Raton, FL.
15. **Patek, M., B. J. Eikmanns, J. Patek, and H. Sahm.** 1996. Promoters from *Corynebacterium glutamicum*: cloning, molecular analysis and search for a consensus motif. Microbiology **142:**1297–1309.
16. **Patek, M., J. Nesvera, A. Guyonvarch, O. Reyes, and G. Leblon.** 2003. Promoters of *Corynebacterium glutamicum*. J. Biotechnol. **104:**311–323.
17. **Vasicova, P., Z. Abrhamova, J. Nesvera, M. Patek, H. Sahm, and B. Eikmanns.** 1998. Integrative and autonomously replicating vectors for analysis of promoters in *Corynebacterium glutamicum*. Biotechnol. Techniques **12:** 743–746.
18. **Wennerhold, J., and M. Bott.** 2006. The DtxR regulon of *Corynebacterium glutamicum*. J. Bacteriol. **188:**2907–2918.

Evidence for the involvement of the two-component system CgtSR11 in the regulation of heme homeostasis in *Corynebacterium glutamicum*

Julia Frunzke & Michael Bott*

Institut of Biotechnology 1, Research Centre Jülich, Germany

*Correspondence: Michael Bott, Institute of Biotechnology 1, Research Centre Jülich, D52425 Jülich, Germany. Tel.:(+49) 2461 615515 ; fax : (+49) 2461 612710 ; e-mail: m.bott@fz-juelich.de

Keywords : *Corynebacterium glutamicum*, two-component system, CgtSR11, heme, iron, regulation

Abstract

The response regulator CgtR11 belonging to the CgtSR11 two-component system was previously shown to be repressed by the iron-dependent regulator DtxR in *Corynebacterium glutamicum*. Deletion of *cgtSR11* genes resulted in a decreased expression of the *hmuO* gene encoding heme oxygenase, an enzyme involved in the utilization of heme as an iron source. Indeed, it was shown that *C. glutamicum* is able to grow on heme as iron source. Besides *hmuO*, the putative *ctaE-qcrCAB* operon coding for subunit III of cytochrome aa_3 oxidase and the three subunits of the cytochrome bc_1 complex also showed a decreased mRNA level in the Δ*cgtSR11* mutant. In contrast, the mRNA level of the heme biosynthesis genes *hemA* (glutamyl-tRNA reductase) and *hemE* (uroporphyrinogen decarboxylase) was increased in the mutant. Purified CgtR11 protein was shown to bind to the promoter regions of *hmuO*, *hemA* and *ctaE*. These results suggest an involvement of the CgtSR11 two-component system in the control of heme homeostasis in *C. glutamicum*.

Introduction

Iron is a critical element for bacteria, being essential as a co-factor in a multitude of enzymes, poorly soluble in its oxidized form, and dangerous by catalyzing the formation of reactive oxygen species. Therefore, most cells possess sophisticated regulatory systems to ensure a sufficient supply of iron but to avoid high levels of free Fe^{2+}, the form responsible for hydroxyl radical production via the Fenton reaction. We and others recently demonstrated that the transcriptional regulator DtxR is the master regulator of iron-dependent gene expression in *Corynebacterium glutamicum*, a non-pathogenic Gram-positive soil bacterium, which is used industrially for large scale amino acid production. Furthermore, *C. glutamicum* serves as model organism for the suborder *Corynebacterineae* within the order *Actinomycetales* (Brune *et al.*, 2006a; Wennerhold and Bott, 2006). When the iron supply is sufficient, DtxR in complex with Fe^{2+} represses more than fifty genes, the majority of which are involved in iron acquisition. Simultaneously, a number of genes are activated by DtxR, such as those encoding the iron storage proteins ferritin and Dps (Brune *et al.*, 2006a). When iron becomes limiting, Fe^{2+} dissociates from DtxR and the protein looses its DNA-binding ability.

Table 1. Strains and plasmids used in this work.

Strains or plasmids	Relevant characteristics	Source or reference
Strains		
C. glutamicum		
ATCC 13032	Biotin-auxotrophic wild type	(Kinoshita *et al.*, 1957)
Δ*cgtSR11*	ATCC 13032 derivative with an in-frame deletion of the *cgtSR11* genes	(Kocan *et al.*, 2006b)
E. coli		
DH5α	*supE44* Δ*lacU169* (ϕ80*lacZ*DM15) *hsdR17 recA1 endA1 gyrA96 thi-1 relA1*	Invitrogen
BL21(DE3)	F^- *ompT hsdS*$_B$($r_B^-m_B^-$) *gal dcm* (DE3)	(Studier and Moffatt, 1986)
Plasmids		
pET28b	Kan^R; vector for overexpression of genes in *E. coli*, adding an N-terminal or a C-terminal hexahistidine tag to the synthesized protein (pBR322 *ori*$V_{E.c.}$, P_{T7}, *lacI*)	Novagen
pET28b-cgtR11	Kan^R; pET28b-Streptag derivative for over-production of CgtR11 with an N-terminal hexa-histidine tag.	This study

An interesting feature elucidated in our previous work was the finding that three of the target genes repressed by DtxR under iron excess encode itself transcriptional regulators, which are the AraC-type regulator RipA, the ArsR-type regulator Cg0527 and the response regulator CgtR11. Whereas RipA was shown to be involved in the repression of several genes encoding prominent iron-containing proteins (*e.g.* aconitase and succinate dehydrogenase) under iron limitation (Wennerhold *et al.*, 2005), the function of Cg0527 and CgtR11 is still unclear. The genome of *C. glutamicum* encodes 13 two-component systems some of which (MtrA/B and PhoR/S) have already been characterized to some extend (Brocker and Bott, 2006; Kocan *et al.*, 2006c; Möker *et al.*, 2004a; Schaaf and Bott, 2007). In this work we analyzed the function of the CgtSR11 two-component system in *C. glutamicum* and provide evidence that it controls the expression of the genes involved in heme utilization and heme biosynthesis, but also genes for heme-containing proteins.

Material and Methods

Bacterial strains, media and growth conditions

Bacterial strains and plasmids used or constructed in this work are listed in Table 1. For growth experiments or DNA microarray analysis 5 ml of brain heart infusion (BHI) medium (Difco Laboratories, Detroit, MI) were inoculated with colonies from a fresh BHIS agar plate (BHI agar with 0.5 M sorbitol) and incubated for 6 hours at 30°C and 170 rpm. This first preculture was used to inoculate a 500-ml shake flask containing 50 ml CGXII minimal medium (Keilhauer et al., 1993) with 4% glucose added as carbon source. The second preculture was cultivated overnight at 30°C and then used to inoculate the main culture to an optical density at 600 nm (OD_{600}) of ~1. For DNA microarray analysis cells were harvested at an OD_{600} of 5-6. Escherichia coli DH5α or BL21(DE3) were grown aerobically in LB medium on a rotary shaker (150 rpm) or on LB agar plates at 37°C (Sambrook, 1989). If appropriate, kanamycin was added to final concentrations of 25 μg ml^{-1} (C. glutamicum) or 50 μg ml^{-1} (E. coli).

Recombinant DNA work

Standard methods like PCR, restriction or ligation were carried out according to established protocols (Sambrook, 1989). *Escherichia coli* was transformed by the RbCl method (Inoue *et al.*, 1990). DNA sequencing was performed with a 3100-Avant genetic analyzer (Applied Biosystems, Darmstadt, Germany). Sequencing reactions were carried out with the ABI PRISM™ Big Dye Terminator Cycle Sequencing Kit (Applied Biosystems). The oligonucleotides used in this study were

Table 2. Oligonucleotides used in this study.

Oligonucleotide	Sequence (5´→ 3´) and properties[a]
Oligonucleotides for overexpression of *cgtR11* in *E. coli*	
cgtR11-for	ATA TAT CAT ATG ATT CGC GTG CTG CTT GCT GAT G (NdeI)
cgtR11-rev	ATA TAT CTC GAG CTA CAG CAG CCC CTG CTC ACG TGC G (XhoI)
Oligonucleotides used for quantitative Real-Time PCR	
hmuO_standard-for	ACTTCCGCTTGGCAGCGACCG
hmuO_standard-rev	GGGCAAAGATCAGGGAACTCCC
hmuO-RT-(cDNA)	AACTTGCTGATTAAACCTGAACGC
hmuO-LC-for	CCGCTACCTGGGTGATTTGTCC
hmuO-LC-rev	GCACGGTAATTATCCTTGTACGG
hemA_standard-for	AGGGATGTCGCACAGGTCTGC
hemA_standard-rev	TGGTGGCAAGTTTGGATCCTCG
hemA-RT-(cDNA)	GCAGTTCTGACGCGTTGACG
hemA-LC-for	AGACATCGATGATGCTTGTGCG
hemA-LC-rev	CCAACTCTTCCCGAACAATCGC
qcrC_standard-for	ATGCCCTTCACTTCCACAGTCG
qcrC_standard-rev	CTCATCGCGTTGAGTTCTTGGG
qcrC-RT-(cDNA)	GAGGACCAAGATGCCGAATACC
qcrC-LC-for	ATGTTGCAGCTAATGGCGGTGG
qcrC-LC-rev	GGCAGGATGCACAGTTCAGGC
ddh-for	ACGTGCTGTTCCTGTGCATGG
ddh-rev	GCTCGGCTAAGACTGCCGCT
Oligonucleotides for generating PCR products used in gel shift assays	
hmuO-prom-for	GCGGAAAATTGTTCCAACTAAGGG
hmuO-prom-rev	CCTCCGATAGGTCGCTGTTGCTTGC
hmuO-2-for	AAGGGACTATATGTAGGTGTGGG
hmuO-3-for	GGTAACCTAAGTTAATCTTTTGTG
hemA-prom-for	CCGATAATGGATATCTCCATTGAG
hemA-prom-rev	GCTTAAAGACGCCCTACCCAGGAG
ctaE-prom-for	TGATCACCGTGACGAAACTATCC
ctaE-prom-rev	GTTCAGTGCCGCAACACGTTGTG
0994-prom-for	TCTGCCCTGGGGATCGAGGACGC
0994-prom-rev	CTGGAATTGGCAAGTAGCCAACG

[a] In some cases oligonucleotides were designed to introduce recognition sites for restriction endonucleases (recognition sites underlined, restriction endonucleases indicated in parentheses).

obtained from Operon (Cologne, Germany) and are listed in Table 2. For overproduction and purification of CgtR11 with an N-terminal hexahistidine tag the corresponding coding region was cloned into the expression vector pET28b (Novagen). The CgtR11 protein encoded by this plasmid contains 20 additional amino acids (MGSSHHHHHHSSGLVPRGSH) at the amino terminus. For overproduction the plasmid was transferred into *E. coli* BL21(DE3).

DNA microarray analysis

For preparation of total RNA, cultures of the wild type and the Δ*cgtSR11* mutant were grown in CGXII minimal medium containing 4% (w/v) glucose under iron excess (100 µM $FeSO_4$), iron limitation (1 µM $FeSO_4$) or with heme (2.5 µM) as iron source. In the exponential growth phase at an OD_{600} of 4-6, 25 ml of the cultures were used for the preparation of total RNA as described previously (Möker *et al.*, 2004a). Isolated RNA samples were analyzed for quantity and quality by UV spectrophotometry and denaturing formaldehyde agarose gel electrophoresis (Sambrook, 1989), respectively, and stored at -20°C until use. The generation of whole-genome DNA microarrays (Wendisch, 2003), synthesis of fluorescently labelled cDNA from total RNA, microarray hybridization, washing and data analysis were performed as described previously (Ishige *et al.*, 2003; Lange *et al.*, 2003; Polen *et al.*, 2003). Genes that exhibited significantly changed mRNA levels ($p < 0.05$ in a Student's t-test) by at least a factor of 2 were determined in three series of DNA microarray experiments: (i) two comparisons of the wild type and the Δ*cgtSR11* mutant cultivated under iron excess (100 µM $FeSO_4$); (ii) three comparisons of the wild type and the Δ*cgtSR11* mutant grown under iron limitation (1 µM $FeSO_4$) and (iii) three comparisons of the wild type and the Δ*cgtSR11* mutant cultivated with 2.5 µM heme as iron source.

Quantitative real-time RT-PCR

Purified total RNA of *C. glutamicum* wild type or Δ*cgtSR11* mutant was transcribed into cDNA using the Omniskript RT Kit (Qiagen, Cologne). Subsequently, 2 µl of the cDNA sample were added as template for real-time PCR using the Quanti-Tect SYBR Green PCR Kit (Qiagen) and a LightCycler instrument (Roche Diagnostics). Oligonucleotides used for standard preparation, reverse transcription and real-time PCR are listed in Table 2. Differences in gene expression were determined by comparing the concentrations of two samples measured in at least three independent experiments. Concentrations were calculated using a standard curve obtained from several dilutions of a defined standard template (1 ng/µl-100 fg/µl) covering the coding region of the corresponding gene.

Overproduction and purification of CgtR11

E. coli BL21(DE3) carrying the plasmid pET28b-cgtR11 was grown in 100 ml LB medium with 50 µg/ml kanamycin at 30°C. Expression was induced at an OD_{600} of ~0.5 with 1 mM IPTG. Four hours after induction cells were harvested by centrifugation and stored at –20°C. For cell extract preparation, cells were resuspended in 10 ml of TNI-5 buffer (20 mM Tris/HCl, pH 7.9, 300 mM NaCl and 5 mM imidazol) containing 1 mM diisopropylfluorophosphate and 1 mM phenylmethylsulfonyl fluoride as protease inhibitors. CgtR11 present in the supernatant was purified by using nickel-activated nitrilotriacetic acid-agarose (Novagen). After washing the column with TNI-20 buffer (containing 20 mM imidazole) CgtR11 protein was eluted with TNI-200 buffer (200 mM imidazole). Fractions containing CgtR11 were pooled and the elution buffer was exchanged against TG buffer (20 mM Tris/HCl, pH 7.5, 10% glycerol).

Gel shift assays

For testing the binding of CgtR11 to putative target promoters, purified protein (130-520 nM) was mixed with DNA fragments (230-550bp, final concentration 13-38 nM) in a total volume of 20 µl. The binding buffer contained 20 mM Tris/HCl (pH 7.5), 50 mM KCl, 10 mM $MgCl_2$, 5% (v/v) glycerol, 0.5 mM EDTA. Approximately 13 nM of promoter regions of putative non-target genes (*cg1179*, *acn* and *sdh*) were used as negative controls. The reaction mixture was incubated at room temperature for 20 min and then loaded onto a 10% nondenaturating polyacrylamide gel. Electrophoresis was performed at room temperature and 170 V using 1xTBE (89 mM Tris base, 89 mM boric acid, 2 mM EDTA) as electrophoresis buffer. The gels were subsequently stained with Sybr Green I (Sigma-Aldrich, Taufkirchen, Germany). All PCR products used in the gel shift assays were purified with the PCR purification Kit (Qiagen).

Results and Discussion

The CgtSR11 two-component system – genomic organization and sequence similarities

The gene *cgtS11* (cg3248) encoding the sensor kinase CgtS11 is located upstream of *cgtR11* (*cg3247*) coding for the response regulator CgtR11. The two genes are separated by an intergenic region of 98 bp. We previously showed that *cgtR11* is repressed by the iron-dependent regulator DtxR under conditions of sufficient iron supply and that purified DtxR binds to a DNA fragment covering the intergenic region (Brune *et al.*, 2006a; Wennerhold and Bott, 2006). The most convincing DtxR binding site (ATGAGTAA-GGCTAGACTAA) is centred at position –97 bp upstream of the start codon of *cgtR11* and partially overlaps with the coding region of *cgtS11*. Thus, only expression of *cgtR11*, but not of *cgtS11* is regulated by DtxR in dependency of iron availability.

The derepression of *cgtR11* under iron limitation is an indication that the CgtSR11 system might be involved in some aspect related to iron acquisition. A search for proteins homologous to CgtS11 and CgtR11 resulted in the identification of the two-component systems HrrAS and ChrAS of *C. diphtheriae*. CgtS11 shows 56% and 30% sequence identity to HrrS and ChrS, respectively, and CgtR11 shows 86% and 50% sequence identity to HrrA and ChrA,

respectively. Both two-component systems of *C. diphtheriae* were recently shown to be involved in the heme-dependent activation of *hmuO* expression (Bibb *et al.*, 2005; Bibb *et al.*, 2007). The *hmuO* gene encodes heme oxygenase, which catalyzes the oxygen-dependent conversion of hemin to biliverdin, carbon monoxide, and free iron. It thus allows the utilization of heme as an iron source. In contrast to *cgtR11*, neither *hrrAS* nor *chrAS* were reported to be controlled by DtxR and inspection of the corresponding promoter regions failed to reveal the presence of a DtxR binding motif. A deletion of *chrAS* in *C. diphtheriae* resulted in an increased heme sensitivity of the resulting mutant. In the case of the HrrAS system, a *hrrS* deletion mutant required a heme source in the growth medium for optimal growth, whereas a Δ*hrrSA* mutant did not exhibit such a requirement (Bibb *et al.*, 2007).

Heme as an iron source for *C. glutamicum*

The sequence similarity to HrrAS and ChrAS indicated that the CgtSR11 two-component system might also be involved in the control of genes required for heme utilization. To follow this assumption, we first tested whether *C. glutamicum* is able to use heme as an iron source. The type strain ATCC 13032 was cultivated in CGXII minimal medium with 4% glucose either without an iron source or with $FeSO_4$ (1 µM) or with heme (2.5 µM or 10 µM). As shown in Fig. 1, the cultures containing either 1 µM $FeSO_4$ or 2.5 µM heme grew with almost identical growth rates up to an OD_{600} of about 30, whereas the culture without an iron source stopped growth at an OD_{600} of less than 3. This result indicated that *C. glutamicum* is able to use heme as an iron source. The culture containing 10 µM heme started to grow only after a lag phase of 10-15 hours, but then reached the same growth rate ($\mu = 0.37\ h^{-1}$) and the same final OD_{600} of ~60 as the culture containing $FeSO_4$ in excess. This growth behaviour indicates that 10 µM heme is toxic for *C. glutamicum*, presumably due to partitioning into membranes and promotion of non-enzymatic redox reactions, but that growth is possible by suppressor mutations which have not yet been characterized. *C. diphtheriae* was reported to tolerate 10 µM heme (Bibb *et al.*, 2005), which might be an adaptation to its pathogenic life style where heme is abundant and a coveted iron source.

Comparison of the expression profiles of a Δ*cgtSR11* mutant and wild type

To search for the target genes of the CgtSR11 two-component system, we investigated the effect of a *cgtSR11* deletion on global gene expression. The construction of a Δ*cgtSR11* mutant of *C. glutamicum* ATCC 13032 has been described previously (Kocan *et al.*, 2006c). The transcriptomes of the Δ*cgtSR11* mutant and the wild type were compared using DNA microarray analysis. For this purpose the strains were cultivated in CGXII minimal medium under iron excess (100 µM $FeSO_4$), or under iron limitation (1 µM $FeSO_4$) or with heme (2.5 µM) as iron source. Each comparison was performed in triplicate, starting from three independent cultivations. Genes which showed a more than two-fold altered mRNA level in the Δ*cgtSR11* mutant compared to the wild type in at least one of the three experiments are summarized in Table 3.

The microarray data indicated that the Δ*cgtSR11* mutant shows a stronger iron starvation response than the wild type when cultivated with heme as iron source. Several genes belonging to the DtxR regulon showed higher mRNA levels in the *cgtSR11* deletion

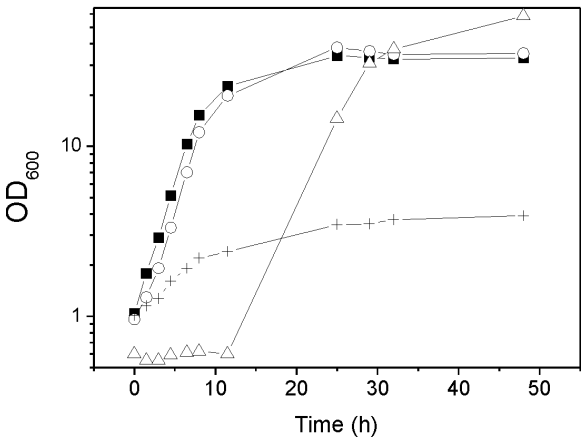

Fig. 1. Growth of *C. glutamicum* on heme as an iron source. *C. glutamicum* type strain ATCC 13032 was cultivated in CGXII minimal medium with 4% glucose and different iron sources: 1 µM $FeSO_4$ (■); 2.5 µM heme (○); 10 µM heme (Δ); or no iron at all (+).

mutant whereas several genes coding for iron-containing proteins, *e.g.* succinate dehydrogenase or catechol 1,2-dioxygenase, showed lower mRNA levels in the mutant. This behaviour might be caused by a reduced rate of iron acquisition from heme due to a lower activity of heme oxygenase. The corresponding *hmuO* gene, despite being a target of DtxR repression, showed a 3-fold decreased in the Δ*cgtSR11* mutant compared to the wild type when the cells were grown with heme as iron source. In contrast, the mRNA levels of other target genes of the iron regulator DtxR were increased in this mutant (Table 3). This result supported our assumption that the CgtSR11 system could be involved in heme-dependent activation of *hmuO* expression as previously described for the HrrAS and ChrAS systems of *C. diphtheriae*. To confirm the microarray data for *hmuO*, quantitative real-time RT-PCR was used to analyze the *hmuO* mRNA levels in wild-type and Δ*cgtSR11* mutant cells. As shown in Fig. 2, the data obtained by this method agreed with the microarray data. When heme was added as iron source, the *hmuO* mRNA was 6.5-fold higher in the wild type compared to the Δ*cgtSR11* mutant, whereas a 4-fold increased level was measured in the wild type under iron limitation (1 µM $FeSO_4$). Under conditions of sufficient iron supply (100 µM $FeSO_4$) only a 1.5-fold increased level was observed in the wild type.

Despite the lowered *hmuO* mRNA level, the Δ*cgtSR11* mutant grew like the wild type in CGXII minimal medium with 2.5 µM heme as iron source (data not shown). This indicates that either the heme oxygenase activity of the mutant is still sufficient to allow growth rates like the wild type or that alternative heme-degrading enzymes might be present. Such enzymes have been reported in several organisms and share no significant sequence similarities with heme oxygenases (Puri and O'Brian, 2006; Wu *et al.*, 2005). It a recent study it was shown that in *Corynebacterium ulcerans* a deletion of *hmuO* abolished heme utilization, whereas *hmuO* mutant strains *C. diphtheriae* were only partially defective in heme utilization or even not at all (Kunkle and Schmitt, 2007). This indicates that *C. diphtheriae* possess additional proteins besides heme oxygenase that allow to use heme as an iron source. The observation that the *C. glutamicum* Δ*cgtSR11* mutant shows a clear

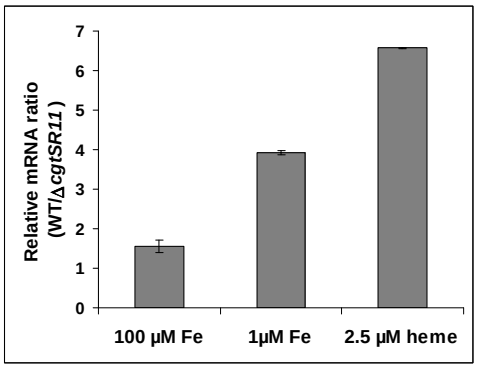

Fig. 2. Relative *hmuO* expression determined by quantitative real-time RT-PCR. For preparation of total RNA *C. glutamicum* wild type and the Δ*cgtSR11* mutant were grown in CGXII minimal medium with 4% glucose and iron sources added as indicated in the graph. Synthesis of cDNA and quantitative real-time PCR were carried out as described in Material and Methods.

iron starvation response when cultivated with heme as iron source suggests that in this species heme oxygenase is required for the acquisition of heme iron.

Besides *hmuO*, also several other genes involved in heme metabolism were differentially expressed in the Δ*cgtSR11* mutant. Under iron excess, but not under iron limitation or with 2.5 µM heme as iron source, the heme biosynthesis genes *hemA* and *hemE* encoding glutamyl-tRNA reductase and uroporphyrinogen decarboxylase showed about twofold increased mRNA levels in the Δ*cgtSR11* mutant. Thus, CgtSR11 is most likely involved in the repression of these genes under certain conditions, either directly or indirectly. In *C. diphtheriae*, the *hemA* gene was also shown to be negatively regulated by HrrAS and ChrAS, but also in this case it is not yet clear whether the influence is direct or indirect (Bibb *et al.*, 2007).

A third group of genes related to heme metabolism which showed altered expression in the Δ*cgtSR11* mutant were those coding for subunit III of cytochrome aa_3 oxidase (*ctaE*) and the three subunits of the cytochrome bc_1 complex (*qcrCAB*), which presumably form an operon. It was recently shown that in *C. glutamicum* the cytochrome bc_1 complex and cytochrome aa_3 oxidase form a supercomplex and that cytochrome c_1 contains two covalently bound heme *c* moieties rather than only one (Niebisch and Bott, 2001). In the Δ*cgtSR11*

Table 3. Differential gene expression in a Δ*cgtSR11* mutant compared with *C. glutamicum* WT.

Categorie and Cg number	Gene	Annotation	mRNA ratio[a] iron excess	iron limitation	Heme
cg3247	*cgtR11*	Two-component system, response regulator	0.17	0.08	0.14
cg3248	*cgtS11*	Two-component system, sensor kinase	0.80	0.66	0.38
Iron starvation response					
DtxR regulon					
cg0159		Hypothetical protein	1.80	2.30	2.40
cg0470		Secreted heme transport-associated protein	1.48	3.67	5.75
cg0471		Secreted heme transport-associated protein	2.00	2.35	4.37
cg0588		Hypothetical protein	1.10	1.38	2.19
cg0589		Siderophore ABC transporter, ATP-binding protein	1.21	1.53	2.45
cg0590		Siderophore ABC transporter, permease protein	0.96	1.20	2.26
cg0768		Siderophore ABC transporter, ATP-binding protein	1.72	1.61	2.49
cg0776		Secreted siderophore-binding lipoprotein	2.35	1.32	1.51
cg0921		Cytoplasmic siderophore-interacting protein	1.38	1.71	2.19
cg0922		Secreted siderophore-binding lipoprotein	1.28	1.64	2.42
cg0924		Secreted siderophore-binding lipoprotein	1.15	1.50	2.15
cg1695		Putative transcriptional regulator	0.62	0.73	0.47
cg1930		Secretory serine protease	1.33	1.67	3.08
cg1931		Hypothetical secreted protein	1.51	1.53	2.48
cg2234		Secreted siderophore binding lipoprotein	1.42	1.62	2.21
cg2445	*hmuO*	Heme oxygenase	1.05	0.67	0.33
cg2782	*ftn*	Ferritin	0.87	0.83	2.09
cg2796		Hypothetical protein	1.50	1.86	3.33
RipA regulon					
cg0445	*sdhC*	Succinate dehydrogenase, cytochrome *b* subunit	0.39	0.40	0.31
cg0446	*sdhA*	Succinate dehydrogenase, flavoprotein	0.30	0.41	0.36
cg0447	*sdhB*	Succinate dehydrogenase, FeS protein	0.39	0.43	0.34
cg2636	*catA*	Catechol 1,2-dioxygenase	0.62	0.46	0.28
Heme metabolism					
Heme containing proteins					
cg2403	*qcrB*	Cytochrome bc_1 complex, cytochrome *b* subunit	0.47	0.60	0.61
cg2404	*qcrA*	Cytochrome bc_1 complex, Rieske iron-sulfur protein	0.48	0.6	0.34
cg2405	*qcrC*	Cytochrome bc_1 complex, cytochrome c_1 subunit	0.41	0.57	0.54
cg2406	*ctaE*	Cytochrome aa_3 oxidase, subunit III	0.36	0.40	0.38
Heme biosynthesis					
cg0497	*hemA*	Glutamyl-tRNA reductase, *hemA*	1.82	1.17	1.32
cg0516	*hemE*	Uroporphyrinogen decarboxylase	2.09	1.22	1.23
Others					
cg0228		Sensor protein fixL	0.76	0.57	0.46
cg0629		LSU ribosomal protein L6P	1.04	2.74	0.87
cg0642		Hypothetical protein / PEP-utilizing enzyme	1.56	0.84	0.40
cg0762	*prpC2*	2-Methylcitrate synthase	0.43	0.43	0.43
cg0828		Putative dihydrofolate reductase	0.86	0.82	0.52
cg1081		ABC transporter ATP-binding protein	2.50	1.58	1.48
cg1147		FMN reductase	1.57	1.37	1.96
cg1179		Sensor protein, GGDEF/EAL family protein	0.34	0.21	0.16
cg1181		N-Acetylglucosaminyltransferase	0.38	0.17	0.19
cg1193		4-Carboxymuconolactone decarboxylase	1.75	0.82	0.46
cg1218		Putative mutator mutT protein	2.37	1.44	2.28
cg1227		ABC transporter, permease component	1.07	2.41	1.22
cg1228		ABC transporter, ATP binding component	0.87	2.00	0.84

Table 3 (continued). Differential gene expression in a Δ*cgtSR11* mutant compared with *C. glutamicum* WT.

			mRNA ratio[a]		
Categorie and Cg number	**Gene**	**Annotation**	**iron excess**	**iron limitation**	**Heme**
cg1230		Adenylate kinase and related kinases	1.28	1.99	1.07
cg1231	*chaA*	Calcium/proton antiporter	0.97	1.63	0.97
cg1377	*ssuC*	Aliphatic sulfonates transporter, permease protein	2.21	2.27	3.56
cg1476	*thiC*	Thiamine biosynthesis protein	1.04	2.64	1.00
cg1514		Hypothetical secreted protein	1.33	1.19	2.07
cg1612		Acetyltransferase	0.73	0.46	0.40
cg1883		Hypothetical secreted protein	0.35	0.47	0.32
cg1884		Putative copper resistance protein C	0.33	0.33	0.10
cg1918		Hypothetical secreted protein	1.95	1.69	3.24
cg2079		Hypothetical protein	2.40	1.15	1.60
cg2202		ABC transporter permease protein	9.02	2.98	2.35
cg2556		Uncharacterized iron-regulated membrane protein	0.95	0.87	0.49
cg2559	*aceB*	Malate synthase	0.59	0.51	0.41
cg2560	*aceA*	Isocitrate lyase	0.42	0.33	0.47
cg2630	*pcaG*	Protocatechuate 3,4-dioxygenase, alpha subunit	0.72	0.59	0.45
cg2750		Hypothetical membrane protein	0.78	0.90	0.46
cg2808		Transposase	3.28	1.26	2.16
cg2836	*sucD*	Succinyl-CoA synthetase, alpha subunit	1.01	0.64	0.48
cg2837	*sucC*	Succinyl-CoA synthetase, beta subunit	0.72	0.53	0.42
cg2893		Permease, major facilitator superfamily I	3.00	2.43	2.50
cg2894		Transcriptional regulator, TetR family	3.81	2.80	2.64
cg3044		Hypothetical membrane protein	n.d.	n.d.	0.30
cg3049	*fprA*	Ferredoxin:NADP reductase	0.71	n.d.	0.45
cg3096		Aldehyde dehydrogenase	0.48	0.37	0.36
cg3169	*pck*	Phosphoenolpyruvate carboxykinase	2.16	1.61	1.40
cg3195		Flavin-containing monooxygenase	0.36	0.22	0.32
cg3225		Hypothetical cytosolic protein	1.76	1.27	0.23
cg3249		Putative secreted protein	0.83	0.61	0.50
cg3255		Universal stress protein, uspA	1.08	n.d.	0.49
cg4005		Putative secreted protein	1.36	1.29	2.04
NCgl0627		2-Methylisocitrate synthase (EC 5.3.3.-)	0.45	0.48	0.46

[a)] These columns include those genes which showed a ≥2-fold altered mRNA level (Δ*cgtSR11*/wild type) when cultivated in CGXII minimal medium under iron excess (100 µM $FeSO_4$), iron limitation (1 µM $FeSO_4$) or with 2.5 µM heme as iron source (p-value ≤ 0.05). The mRNA ratios represent average values obtained from two or three independent DNA microarray experiments performed with RNA isolated from two or three independent cultivations.

mutant the *ctaE-qcrCAB* mRNA levels were about twofold lower than in the wild type under all conditions tested, suggesting that they might be positively regulated by the CgtSR11 system in a direct or indirect manner. In *C. diphtheriae*, an influence of HrrAS or ChrAS on the expression of the homologous genes has not been reported yet. According to the results described above, CgtSR11 might carry out a dual function by acting as an activator of heme oxygenase and heme-containing proteins and as repressor of genes involved in heme biosynthesis.

Besides, the genes related to heme metabolism, a variety of additional genes showed altered mRNA levels in the Δ*cgtSR11* mutant (Table 3). However, it is not yet possible to give reasonable explanations for these expression differences.

Identification of direct target genes of CgtR11

In order to test whether some of the genes showing an altered mRNA level in the Δ*cgtSR11* mutant are direct target genes of the response regulator CgtR11, binding of purified CgtR11 protein to the promoter regions of selected genes was tested in gel shift assays. For this purpose, CgtR11 containing an N-terminal hexahistidine

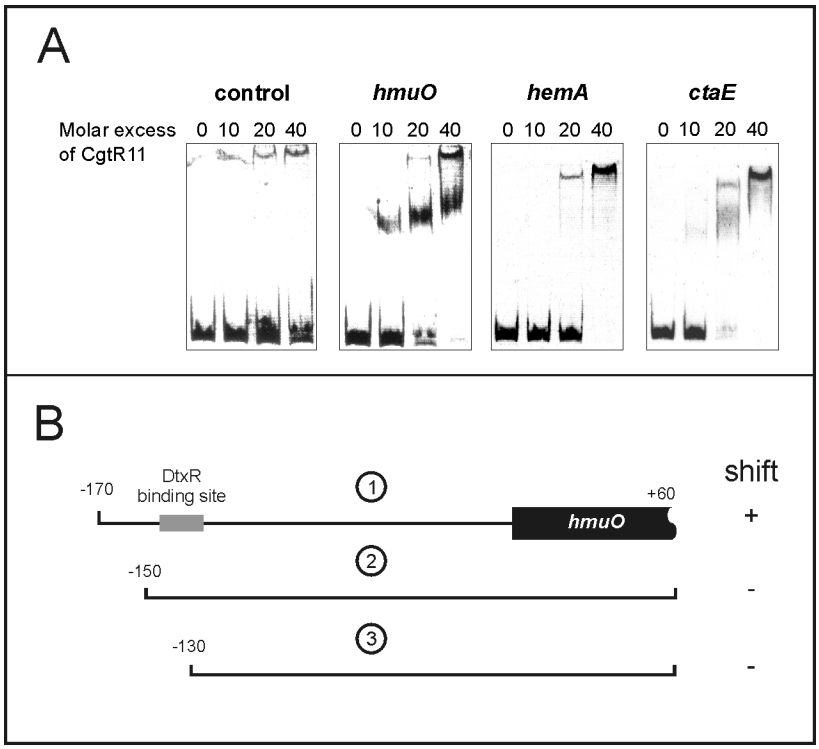

Fig. 3. Binding of CgtR11 to the promoter regions of *hmuO*, *hemA* and *ctaE*. (A) DNA fragments (230-550 bp; final concentration 14-35 nM) covering the promoter regions of *hmuO*, *hemA*, *ctaE* were incubated for 20 min at room temperature with different concentrations of purified CgtR11 protein. The samples were separated by nondenaturating 10% polyacrylamide gel electrophoresis and stained with SybrGreen I. A fragment (550 bp; 14 nM) covering the promoter region of *acn* served as a negative control. Oligonucleotides used for amplification of the corresponding DNA fragments are listed in (Table 2). (B) DNA fragments used to localize CgtR11 binding within the *hmuO* promoter region. The numbers indicate the ends of the fragment with respect to the *hmuO* start codon. All fragments were tested in gel retardation assays with purified CgtR11 protein as described above. The already identified DtxR binding site is indicated as grey box. The column "shift" indicates whether the fragment was shifted by CgtR11 (+) or not (-).

tag was overproduced in *E. coli* and purified by Ni^{2+}-chelate affinity chromatography as described in Materials and Methods. As shown in Fig. 3A, CgtR11 was able to bind to the promoter regions of *hmuO*, *hemA* and *ctaE*. A complete shift was observed at a 20 to 40-fold molar excess of CgtR11. Subsequently, binding of CgtR11 to subfragments of the *hmuO* promoter was tested to confine the CgtR11 binding region. Reduction of the original *hmuO* fragment by 20 bp (-150 to +60 with respect to the proposed start codon) completely abolished binding of CgtR11 to the *hmuO* promoter (Fig. 4B). Therefore, it can be concluded that the CgtR11 binding site is localized immediately upstream of the previously identified DtxR binding site, which is centred at position -130.5 with respect to the start codon. The promoter regions of the genes *cg1179*, *cg0641*, *cg2894*, *cg0228* and *hemL* as well as the tested negative controls (*acn* and *sdhC*) were not bound by CgtR11 up to an 80-fold molar excess of protein under the specified conditions. At a molar excess of 100 and above, a presumably unspecific binding was observed for all DNA fragments tested. Further studies are required to investigate the effect of phosphorylation of CgtR11 on binding and affinity to its target promoters.

Conclusions

The studies described in this work suggest an involvement of the two-component system CgtSR11 in the control of heme homeostasis through the coordinate regulation of genes involved in heme degradation (*hmuO*) and heme biosynthesis (*hemA*) and of hemoproteins (*qcrB*, *qcrC*) in *C. glutamicum*. Since the strongest effect of CgtSR11 on *hmuO* expression was

observed in the presence of heme, a scenario can be envisaged in which the membrane integral sensor kinase CgtS11 becomes activated in the presence of heme and subsequently activates the response regulator CgtR11 by phosphorylation. This heme-dependency was not observed in the case of the other identified target genes hemA and *ctaE-qcrCA*). For a more complete understanding of the system, further studies are required targeting the recognition of the (heme)-signal by the sensor kinase and the identification of the exact binding motif of CgtR11 in its target promoter regions.

Acknowledgements

We thank Volker Wendisch and Tino Polen for establishing the DNA microarray technique at our institute.

References

Bibb, L.A., King, N.D., Kunkle, C.A., and Schmitt, M.P. (2005) Analysis of a heme-dependent signal transduction system in *Corynebacterium diphtheriae*: deletion of the *chrAS* genes results in heme sensitivity and diminished heme-dependent activation of the *hmuO* promoter. *Infect Immun* **73**: 7406-7412.

Bibb, L.A., Kunkle, C.A., and Schmitt, M.P. (2007) The ChrA-ChrS and HrrA-HrrS Signal Transduction Systems Are Required for Activation of the *hmuO* Promoter and Repression of the hemA Promoter in *Corynebacterium diphtheriae*. *Infect Immun* **75**: 2421-2431.

Brocker, M., and Bott, M. (2006) Evidence for activator and repressor functions of the response regulator MtrA from *Corynebacterium glutamicum*. *FEMS Microbiol Lett* **264**: 205-212.

Brune, I., Werner, H., Hüser, A.T., Kalinowski, J., Pühler, A., and Tauch, A. (2006) The DtxR protein acting as dual transcriptional regulator directs a global regulatory network involved in iron metabolism of *Corynebacterium glutamicum*. *BMC Genomics* **7**: 21.

Inoue, H., Nojima, H., and Okayama, H. (1990) High efficiency transformation of *Escherichia coli* with plasmids. *Gene* **96**: 23-28.

Ishige, T., Krause, M., Bott, M., Wendisch, V.F., and Sahm, H. (2003) The phosphate starvation stimulon of *Corynebacterium glutamicum* determined by DNA microarray analyses. *J Bacteriol* **185**: 4519-4529.

Keilhauer, C., Eggeling, L., and Sahm, H. (1993) Isoleucine synthesis in *Corynebacterium glutamicum*: molecular analysis of the *ilvB-ilvN-ilvC* operon. *J Bacteriol* **175**: 5595-5603.

Kinoshita, S., Udaka, S., and Shimono, M. (1957) Studies on the amino acid fermentation: I. Production of L-glutamic acid by various microorganisms. *J. Gen. Appl. Microbiol.* **3**: 193-205.

Kocan, M., Schaffer, S., Ishige, T., Sorger-Herrmann, U., Wendisch, V.F., and Bott, M. (2006b) Two-component systems of *Corynebacterium glutamicum*: deletion analysis and involvement of the PhoS-PhoR system in the phosphate starvation response. *J Bacteriol* **188**: 724-732.

Kunkle, C.A., and Schmitt, M.P. (2007) Comparative analysis of *hmuO* function and expression in *Corynebacterium* species. *J Bacteriol* **189**: 3650-3654.

Lange, C., Rittmann, D., Wendisch, V.F., Bott, M., and Sahm, H. (2003) Global expression profiling and physiological characterization of *Corynebacterium glutamicum* grown in the presence of L-valine. *Appl Environ Microbiol* **69**: 2521-2532.

Möker, N., Brocker, M., Schaffer, S., Krämer, R., Morbach, S., and Bott, M. (2004) Deletion of the genes encoding the MtrA-MtrB two-component system of *Corynebacterium glutamicum* has a strong influence on cell morphology, antibiotics susceptibility and expression of genes involved in osmoprotection. *Mol Microbiol* **54**: 420-438.

Niebisch, A., and Bott, M. (2001) Molecular analysis of the cytochrome bc1-aa3 branch of the *Corynebacterium glutamicum* resp-iratory chain containing an unusual diheme cytochrome c1. *Arch Microbiol* **175**: 282-294.

Niebisch, A., and Bott, M. (2003) Purification of a cytochrome bc_1-aa_3 supercomplex with quinol oxidase activity from *Corynebacterium glutamicum*. Identification of a fourth subunity of cytochrome aa3 oxidase and mutational analysis of diheme cytochrome c_1. *J Biol Chem* **278**: 4339-4346.

Polen, T., Rittmann, D., Wendisch, V.F., and Sahm, H. (2003) DNA microarray analyses of the long-term adaptive response of *Escherichia coli* to acetate and propionate. *Appl Environ Microbiol* **69**: 1759-1774.

Puri, S., and O'Brian, M.R. (2006) The *hmuQ* and *hmuD* genes from *Bradyrhizobium japonicum* encode heme-degrading enzymes. *J Bacteriol* **188**: 6476-6482.

Sambrook, J., Fritsch, E.F., and Maniatis, T. (1989) Molecular Cloning. A Laboratory Manual. *Cold Spring Harbor, NY: Cold Spring Harbor Laboratoy Press.*

Schaaf, S., and Bott, M. (2007) Target Genes and DNA-Binding Sites of the Response Regulator PhoR from *Corynebacterium glutamicum*. *J Bacteriol* **189**: 5002-5011.

Studier, F.W., and Moffatt, B.A. (1986) Use of bacteriophage T7 RNA polymerase to direct selective high-level expression of cloned genes. *J Mol Biol* **189**: 113-130.

Wendisch, V.F. (2003) Genome-wide expression analysis in *Corynebacterium glutamicum* using DNA microarrays. *J Biotechnol* **104**: 273-285.

Wennerhold, J., Krug, A., and Bott, M. (2005) The AraC-type regulator RipA represses aconitase and other iron proteins from *corynebacterium* under iron limitation and is itself repressed by DtxR. *J Biol Chem* **280**: 40500-40508.

Wennerhold, J., and Bott, M. (2006) The DtxR regulon of *Corynebacterium glutamicum*. *J Bacteriol* **188**: 2907-2918.

Wu, R., Skaar, E.P., Zhang, R., Joachimiak, G., Gornicki, P., Schneewind, O., and Joachimiak, A. (2005) Staphylococcus aureus IsdG and IsdI, heme-degrading enzymes with structural similarity to monooxygenases. *J Biol Chem* **280**: 2840-2846.

Genome heterogeneity in *Corynebacterium glutamicum* ATCC 13032 caused by the prophage CGP3

Julia Frunzke[1], Marc Bramkamp[2], Jens-Eric Schweitzer[1], and Michael Bott[1]*

[1] *Institute of Biotechnology 1, Research Centre Jülich, D-52425 Jülich, Germany.*

[2] *Institute of Biochemistry, University of Cologne, Germany*

Summary

The genome of the *Corynebacterium glutamicum* type strain ATCC 13032 contains three prophages named CGP1, CGP2 and CGP3. In a recent study we observed that many genes located within the CGP3 prophage region showed increased mRNA levels in a mutant lacking the *dtxR* gene encoding the master regulator of iron homeostasis in *C. glutamicum*. Here, we provide evidence that this effect is due to an increased induction of the prophage CGP3 in the Δ*dtxR* mutant compared to the wild type, possibly triggered by oxidative stress caused by an elevated intracellular iron concentration. Upon induction, the CGP3 prophage region becomes excised from the genome producing a covalently closed circular form of the phage DNA. Using quantitative real-time PCR an average copy number of about 0.1 per chromosome was determined for the circular CGP3 molecules in *C. glutamicum* wild-type cells. This copy number increased about 15-fold in the *dtxR* deletion mutant. In order to visualize the CGP3 DNA within single cells, a derivative of the wild-type strain was constructed which contained an array of *tet* operators integrated within the CGP3 region and a plasmid-encoded YFP-TetR fusion protein. As expected 1-2 fluorescent foci were detected in the majority of cells, representing the chromosomally integrated CGP3 prophage. However, in a small fraction of the population (~2-4%) 4-10 CGP3 DNA molecules could be observed in a single cell. The presence of many CGP3 copies in one cell was often accompanied by an efflux of chromosomal DNA, indicating lysis of the corresponding cell. Evidence for the formation of functional infective CGP3 phage particles could not be obtained yet.

*For correspondence. E-mail m.bott@fz-juelich.de; Tel. (+49) 2461 615515; Fax (+49) 2461 612710.

Introduction

In the course of bacterial genome sequencing it was recognized that the genomes of many species contain integrated prophages which usually can be recognized due to differences in GC content, oligonucleotide frequencies or codon usage as well as the presence of genes with bacteriophage homologs of known function (*e.g.* integrases) (Casjens, 2003). A search in the genome of *Corynebacterium glutamicum* ATCC 13032 (Eggeling and Bott, 2005), a Gram-positive soil bacterium belonging to the actinomycetes, using the above-mentioned criteria revealed the existence of four potential prophages (CGP1, CGP2, CGP3 and CGP4), highly diverse in size and grade of degeneration (Kalinowski *et al.*, 2003; Kalinowski, 2005c) The smaller prophages CGP1 and CGP2 (13.5 and 3.9 kbp, respectively) are most probably highly degenerated and no longer able to form functional bacteriophages. In contrast, the CGP3 element is one of the largest known prophages (~187 kbp), constituting ~6% of the entire *C. glutamicum* ATCC 13032 genome. The insertion site of the CGP3 prophage, a tRNA-Val gene, is easily detectable by a 26-bp direct repeat flanking the CGP3 element, a cluster of tRNA genes at its left border and a phage-type integrase at its right border (´*int2*). The *C. glutamicum* ATCC 13032 genome was sequenced independently also as a collaboration between the Kyowa Hakko company and Kitasato University. One major difference between the two available genome sequences (Degussa-Bielefeld and Kyowa Hakko-Kitasato

University) is the insertion of another prophage (CGP4) into the CGP3 element in the Kyowa Hakko-Kitasato University sequence and a duplicated gene region containing a second *'int2* gene at its end.

The isolation of bacteriophages was reported for several *C. glutamicum* strains, which were previously designated as *Brevibacterium flavum*, but to our knowledge not for the strain ATCC 13032 (Moreau *et al.*, 1995; Patek *et al.*, 1985; Sonnen *et al.*, 1990). Most of the so far characterized corynephages are temperate phages, which have been isolated after UV induction (Kato *et al.*, 1984; Moreau *et al.*, 1995; Patek *et al.*, 1985).

In a recent study we determined the regulon of the transriptional regulator DtxR of *C. glutamicum.* This protein was first identified in *Corynebacterium diphtheriae* where it represses transcription of the *tox* gene (encoding diphtheria toxin) as well as a variety of genes involved in iron acquisition (Kunkle and Schmitt, 2003; Schmitt and Holmes, 1991b). Our studies revealed that DtxR is the master regulator in a complex regulatory network controlling iron homeostasis in *C. glutamicum* (Brune *et al.*, 2006b; Wennerhold and Bott, 2006). Remarkably, transcriptome comparisons of *C. glutamicum* wild type and a *dtxR* deletion mutant showed that the mRNA levels of more than 50 genes located within the CGP3 prophage region (*cg1890-cg2071*) were significantly increased in the *dtxR* deletion mutant (Wennerhold and Bott, 2006). Based on this finding, we wondered whether this effect might be due to an induction of the CGP3 prophage in the mutant.

In this work we provide evidence that the CGP3 prophage is still able to excise from the *C. glutamicum* genome and exists as a circular phage DNA molecule, whose copy number is strongly increased in the *dtxR* deletion mutant compared to the wild type. Fluorescence microscopy was used as a novel approach to visualize the number of CGP3 DNA molecules within single cells and to complement the data obtained by molecular genetic studies.

Results

Evidence for CGP3 prophage induction in a dtxR *deletion mutant*

Previous work revealed that the transcriptional regulator DtxR is the master regulator of iron homeostasis in *C. glutamicum* (Brune *et al.*, 2006b; Wennerhold and Bott, 2006). In the course of these studies, we compared the transcriptomes of *C. glutamicum* WT and a Δ*dtxR* mutant. Besides many genes that were later identified as direct target genes of DtxR, a large set of genes showed a more than two-fold increased mRNA level in the Δ*dtxR* mutant all of which were located within the CGP3 prophage region of the ATCC 13032 genome (Wennerhold and Bott, 2006). The vast majority of the 146 open reading frames located within the CGP3 region encode hypothetical proteins and only few

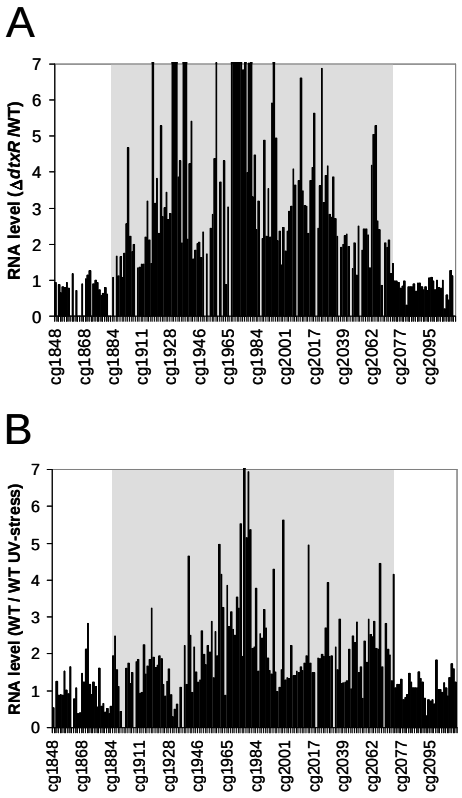

Fig. 1. Increased mRNA levels of genes within the *C. glutamicum* ATCC 13032 CGP3 prophage region in a *dtxR* deletion mutant (A) or after exposure of the wild type to UV light (B). The graphs show the mRNA ratio of genes within or adjacent to the CGP3 prophage region in the *C. glutamicum* genome (*cg1848-cg2109*) as determined by DNA microarray analysis. A, Transcriptome comparison of a *C. glutamicum dtxR* deletion mutant and WT cultivated in CGXII minimal medium with 4% glucose under iron excess (100 µM $FeSO_4$). B, Transcriptome comparison of *C. glutamicum* WT before and after exposure to UV light (see Experimental procedures). The CGP3 prophage region is shaded in grey.

Table 1. Genes within the CGP3 prophage region coding for proteins with known or putative functions.

Cg Number	Gene	Annotation
cg1893		Acetyltransferase
cg1907		Phosphopantothenoylcystein decarboxylase
cg1929	*res*	Site-specific recombinase, resolvase family
cg1930		Putative sectretory serine protease
cg1932		Putative protein tyrosine phosphatase
cg1935	*gntR2*	Transcriptional regulator, GntR family
cg1950		Transposase
cg1951		Transposase
cg1956	*recJ*	Single-stranded-DNA-specific exonuclease
cg1959	*priP*	Prophage DNA primase
cg1961		Phage-related protein
cg1963		Phage-related DNA helicase
cg1980		Putative ATPase, MoxR-like protein
cg1982	*clpE*	ATP-dependent Clp protease, ATP-binding subunit
cg1996	*cglIM*	Type II restriction-modification system methylation subunit
cg1997	*cglIR*	Type II restriction-modification system restriction subunit
cg1998	*cglIIR*	Type II restriction-modification system restriction subunit
cg2003		Phage-related helicase, superfamily II DNA/RNA helicases
cg2004		Phage-related protein, similar to 232 protein-*Lactobacillus* bacteriophage g1e
cg2009		Putative ATPase Clp-like protein
cg2040		Putative transcriptional regulator
cg2043		Periplasmic serine protease
cg2064		DNA topoisomerase I
cg2065		Superfamily I DNA and RNA helicases
cg2066		Pentapeptide repeat protein
cg2069	*psp1*	Putative secreted protein
cg2070	*'int2*	Putative phage integrase, C-terminal fragment
cg2071	*int2'*	Putative phage integrase, N-terminal fragment

code for proteins with known or putative functions, *e.g.* those for a restriction modification system (*cglIM*, *cglIR*, *cglIIR*) (Schäfer *et al.*, 1997), transposases and proteins with known phage homologs such as phage primase and the phage-type integrase `*int2*) (for an overview see Table 1). Fig. 1 clearly shows that the mRNA concentration of nearly all genes located within the CGP3 region (*cg1980-cg2071*) was strongly increased in the *dtxR* deletion mutant, whereas the mRNA levels of genes located at the left (*cg1849-cg1979*) or at the right border (*cg2072-cg2109*) were about the same as in the wild type. Since only two of the genes within the prophage region were identified as direct target genes of DtxR (*cg1930*, *cg1931*), we came up with the assumption that the increased mRNA level of the CGP3 genes in the *dtxR* deletion mutant might be the result of an induction and subsequent replication of the prophage DNA.

A search in our in-house microarray database (Polen and Wendisch, 2004) resulted in the identification of several other experiments in which the mRNA level of genes within the CGP3 region was slightly increased. However, in no case this effect was as convincing as in the Δ*dtxR* mutant. Interestingly, the second best hit was an experiment where the transcriptome of *C. glutamicum* WT was compared before and after exposure to ultraviolet light (final intensity, 800 J/m^2). This finding corroborated the postulated induction of the CGP3 prophage, since exposure to UV light is known to be one of the most efficient methods for prophage induction.

CGP3 phage DNA exists as a self-contained circular molecule

To confirm the postulated prophage induction, the presence of circular CGP3 DNA molecules and the absence of the CGP3 region in the genome was tested by PCR using several combinations of oligonucleotides and identical amounts (see Experimental procedures) of total DNA isolated from the wild type and the Δ*dtxR*

mutant (Fig. 2). Amplification using oligonucleotides 1 and 2 resulted in a PCR product of ~2.5 kbp in size in the Δ*dtxR* mutant and with lower yield also in *C. glutamicum* wild type. This product can only be obtained if the ends of the CGP3 prophage are closed to a circular phage DNA molecule. Sequence analysis of this PCR fragment confirmed the existence of circular phage DNA molecules in *C. glutamicum*. The ends of the phage DNA were connected via the direct repeat flanking the CGP3 element (GTGGTCCTAGCTGGGT TCGAACCAGC). PCR with oligonucleotides 3 and 6 led to a product of about 200 bp in the Δ*dtxR* mutant, but with lower yield in the wild type. This product can only be obtained if the CGP3 region is excised from the *C. glutamicum* genome. Sequence analysis of this fragment confirmed the excision of the CGP3 prophage region, leaving just one of the direct repeats back in the chromosome. Further PCRs performed with oligonucleotides 3+4 and 5+6 led to products of about 500 bp and 1200 bp, respectively. These fragments can only be formed from genomic DNA containing the integrated CGP3 prophage.

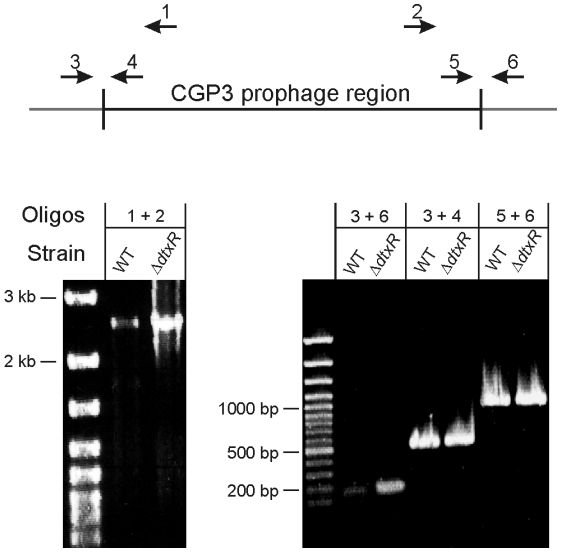

Fig. 2. Evidence for the presence of self-contained circular CGP3 phage DNA molecules in *C. glutamicum* ATCC 13032. PCRs with the indicated combinations of oligonucleotides (Table 4) and total DNA isolated from the wild type or the Δ*dtxR* mutant were used to test whether the CGP3 prophage exists as a circular DNA molecule (primer combination 1+2) and is excised from *C. glutamicum* genome (primer combinations 3+6, 3+4 and 5+6). The PCR products were separated on 1% agarose gels and stained with ethidium bromide.

A comparison of the yields of PCR products obtained indicated that in the majority of genomes present in the total DNA preparation the prophage was still integrated. In summary, these results clearly show that in a small fraction of wild-type cells and in a higher fraction of Δ*dtxR* mutant cells the CGP3 prophage is excised from the genome and exists as a double-stranded circular phage DNA molecule (Fig. 3).

Determination of the average copy number of circular CGP3 DNA molecules

Quantitative real-time PCR (qRT-PCR) was previously described as a valuable tool for the determination of plasmid copy numbers in bacteria (Lee *et al.*, 2006). Therefore, we used this method to determine the copy number of the circular CGP3 phage DNA molecule in *C. glutamicum* WT and the Δ*dtxR* mutant and to quantify the differences observed between both strains. To ensure that only the circular phage DNA molecule served as template for copy number determination, the oligonucleotides used for qRT-PCR were designed to anneal in the CGP3 element at the very left and right border, respectively, pointing into opposite directions. As a consequence, no product will be obtained from the integrated prophage. The oligonucleotide pair used for quantification of genomic DNA targeted the gene *ddh* (*cg2900*) encoding *meso*-diaminopimelate dehydrogenase. Different dilutions of total DNA of *C. glutamicum* WT or the Δ*dtxR* mutant were used as a template for amplification. DNA was extracted from cells cultivated in CGXII minimal medium with 4% glucose under iron excess (100 µM $FeSO_4$) or under iron limitation (1 µM $FeSO_4$) and harvested in the early exponential phase (OD_{600} of 5-6), following the conditions used for the previous DNA microarray experiments (Wennerhold and Bott, 2006). With this method the average copy number per genome of circular CGP3 DNA was determined to be 0.10 and 0.07 for *C. glutamicum* WT grown under iron excess or under iron limitation, respectively (Table 2). In the Δ*dtxR* mutant the copy number of the circular phage DNA was increased about 15-fold under iron excess (1.74) and 8-fold under iron limitation (0.59). These results confirm our postulation that in a very small fraction of the cells induction of CGP3 prophage also takes place in

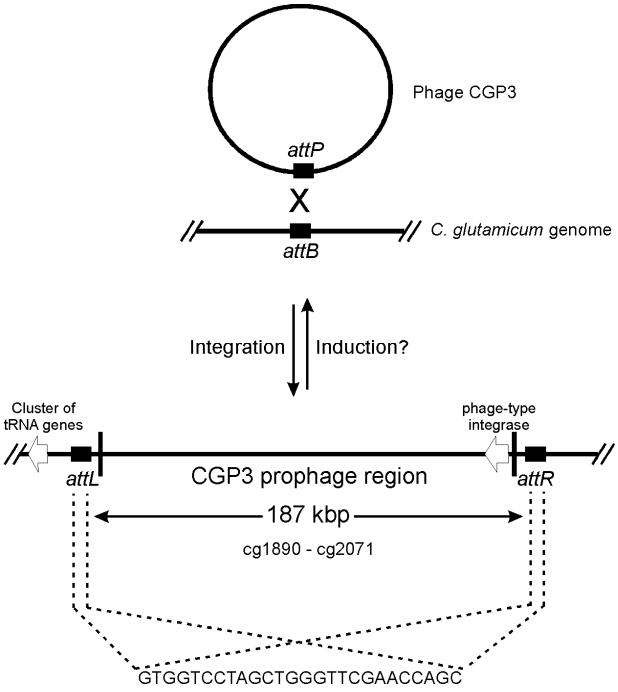

Fig. 3: Preliminary model of CGP3 integration and induction in *C. glutamicum*. The lower part of the figure shows CGP3 in its prophage state integrated into the *C. glutamicum* ATCC 13032 genome as known from the genome sequence. The insertion site is detectable as a direct repeat flanking the CGP3 element (black boxes, sequence given below). After induction of the CGP3 prophage, recombination takes place most probably at the direct repeats, resulting in excision of a self-contained circular phage DNA molecule.

C. glutamicum WT. This fraction increases up to 15-fold in the Δ*dtxR* mutant, which also explains the significant increase of the mRNA level of CGP3 genes observed in the DNA microarray experiments (Fig. 1).

As control we also determined the copy number of the *hom* gene (*cg1337*) encoding homoserine dehydrogenase in the *C. glutamicum* strain MH20-22B-DR17 (Reinscheid *et al.*, 1994). In this strain the *hom* gene is present in four copies in the genome. qRT-PCR gave a copy number of 4.20 ± 0.6, confirming the reliability of the method.

Fluorescence microscopy of C. glutamicum *WT with an YFP-tagged CGP3 element*

The determination of the average copy number of the circular phage DNA molecule (0.1) by qRT-PCR revealed the existence of about one molecule in every tenth cell in a population of *C. glutamicum* wild type. If we assume this to be the result of a partial induction of the CGP3 prophage, a very small fraction of the bacteria probably contains several copies of circular phage DNA rather than every tenth cell one copy. In order to visualize the CGP3 element within the cells and to estimate the copy number per cell, an array of approximately 120 *tet* operator regions (*tetO* array) were inserted into the intergenic region between *cg1905* and *cg1906* within the CGP3 prophage. Subsequently, cells were transformed with plasmid pEKEx2-yfp-tetR which contains a gene encoding a fusion protein of the yellow fluorescent protein (YFP) and the repressor TetR under the control of a *tac* promoter. This fusion protein should bind specifically to the integrated *tetO* arrays (Lau *et al.*, 2003). Synthesis of this fusion protein, which is monitored by the appearance of fluorescent foci within cells, is controlled by the IPTG concentration (0-1 mM) added to the culture.

Positions and quantity of CGP3 molecules were visualized in *C. glutamicum* WT cells grown in CGXII minimal medium with 4% glucose. After cells had been induced to synthesize YFP-TetR fusion protein with 0.1 mM IPTG for 30 min, fluorescent foci were monitored immediately (see Experimental procedures). As expected in most cells (>80%) one or two fluorescent foci were detected, most likely representing the chromosomally integrated prophage (Fig. 4A). In these cells the chromosomal DNA (stained with DAPI) is easy detectable as a distinct region within the cell (Fig. 4B, row 1). In about 6% of the cells, three fluorescent foci were observed and in about 5% four to 10 foci (Fig. 4B row 2-3 and Fig. 4C). Interestingly, this observation often came along with a clear efflux of chromosomal DNA, indicating lysis of at least one cell in the corresponding area.

Table 2. Copy number of the circular CGP3 DNA molecule in *C. glutamicum* ATCC 13032 determined by quantitative real-time PCR. The values represent means ± standard deviation from at least three independent cultivations. For extraction of total DNA, *C. glutamicum* WT and the Δ*dtxR* mutant were grown in CGXII minimal medium with 4% glucose under iron excess (100 µM $FeSO_4$) or iron limitation (1 µM $FeSO_4$).

	Average Copy number	
Strain	iron excess	iron limitation
ATCC 13032	0.11 ± 0.03	0.07 ± 0.01
ATCC 13032 Δ*dtxR*	1.74 ± 0.32	0.59 ± 0.15

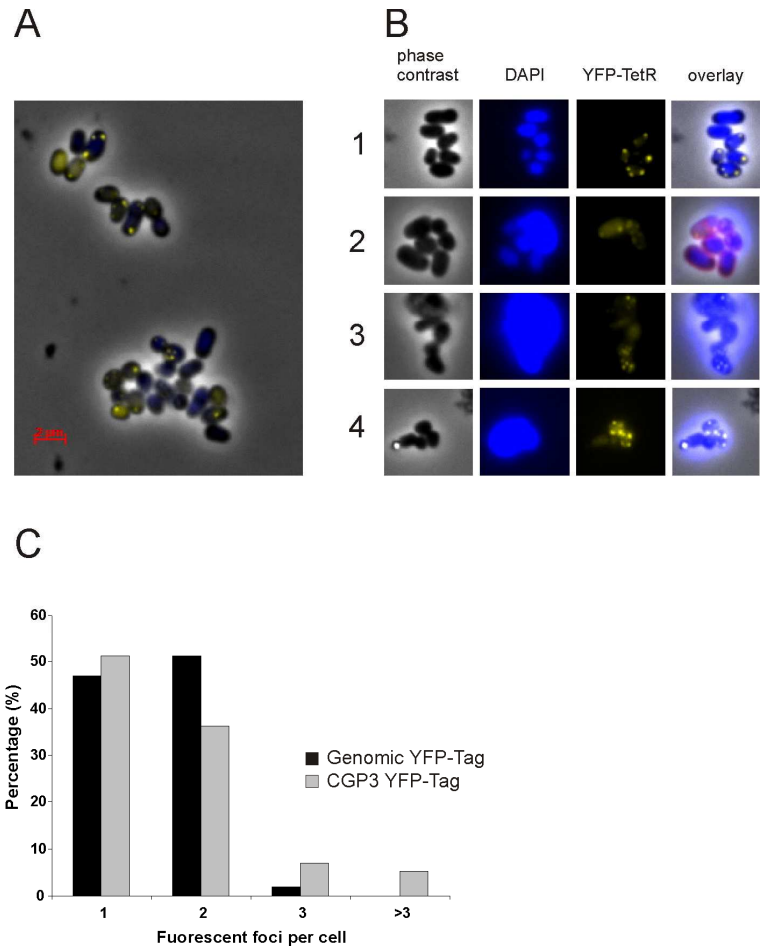

Fig. 4: Fluorescence microscopy of *C. glutamicum* WT cells containing a *tetO* array integrated within the CGP3 (pro)phage region (between *cg1905* and *cg1906*) and a plasmid (pEKEX2-yfp-tetR) encoding a YFP-TetR fusion protein under the control of the *tac* promoter. Cells were grown in CGXII minimal medium with 4% glucose to an OD_{600} of ~2 and then synthesis of the fusion protein was induced with 0.1 mM IPTG until fluorescent foci appeared (20-40 min). Additionally, the nucleoid was stained with DAPI (blue) and in some cases membranes were stained with Nile red (row 2, last column). The cells shown in (A) are representative for the various types of cells observed. In most cases zero to three CGP3 foci could be detected per cell (B, row 1) and in these cells the nucleoid is visible as a distinct region. In a few cases, 4-10 CGP3 foci were observed in a single cell (B, row 2-4). This finding often came along with an efflux of DNA, indicating lysis of the cells as a result of induction of the CGP3 phage. In panel C, the fluorescent foci per cell were counted in the strain containing the tetO array within the CGP3 region (CGP3 YFP tag, grey bars) and in a control strain containing the *tetO* array inserted outside the CGP3 region between *cg1859* and *cg1857* (Genomic YFP tag, black bars). Four classes of cells were defined (1, 2, 3 or >3 foci per cell) and the percentage of each class in both strains is given in the graph. Approximately 200 cells were evaluated for each of the two strains.

As a negative control a strain was constructed where the *tetO* arrays were inserted outside, but in close vicinity of the CGP3 element. For this purpose the intergenic region between *cg1859* and *cg1857* was chosen. With this control strain we were able to visualize the number of genomes within one *C. glutamicum* cell, in order to exclude the possibility that the multiple foci observed in the strain carrying the *tetO* arrays in the CGP3 region were due to the existence of multiple genomes within one cell. More than 80% of the cells of the control strain contained one or two fluorescent foci (approximately 200 cells were counted in total) (Fig. 4C). The maximal number of foci visible in the control strain was three in about 2% the cells.

These results confirmed our assumption of CGP3 prophage induction happening spontaneously in a small fraction of *C. glutamicum* WT cells. Although some of these cells appeared to have become leaky as indicated by the efflux of chromosomal DNA, neither lysis of liquid cultures nor plaque formation on lawns has been observed during many years of experimental work with this strain, arguing against the formation of infective CGP3 phage particles.

Discussion

In this work we provide strong evidence for a spontaneous induction of the CGP3 prophage in a small fraction of *C. glutamicum* ATCC 13032 cells. Primarily this finding based on the observation that the mRNA level of genes located within the CGP3 region was significantly increased in a *dtxR* deletion mutant or after exposure of the wild type to UV light (Fig. 1). Subsequently, it could be shown that this is due to an induction of the CGP3 prophage in *C. glutamicum*. Upon induction, the CGP3 element becomes excised from the genome and exists as a double-stranded DNA phage with cohesive ends, like the majority of other known corynephages (Bukovska *et al.*, 2006; Moreau *et al.*, 1995; Patek *et al.*, 1985; Sonnen *et al.*, 1990). Until now, the CGP3 phage was supposed to exist exclusively in its lysogenic form as a large prophage (~187 kbp) integrated into the *C. glutamicum* genome. Additionally, fluorescence microscopy of cells with an YFP-tagged CGP3 region was used to throw light on the heterogeneity of a typical *C. glutamicum* WT culture. Whereas in most cells zero, one or two fluorescent foci were detected, a small fraction of the bacteria contained up to ten foci within one single cell. In the absence of CGP3 induction, two to maximally four foci can be explained by the ongoing replication of the chromosomal DNA in exponentially growing cells. The existence of more than four fluorescent foci within one cell, however, must be due to an induction of the CGP3 prophage and subsequent replication of its circularized genome. In several cells no fluorescent foci at all were detectable. This finding is most likely caused by an insufficient induction of the *yfp-tetR* gene in the corresponding cells. Alternatively, it could be due to the loss of the CGP3 phage DNA by cell division immediately after prophage induction.
Furthermore, fluorescent microscopy experiments revealed lysis of cells containing many phage-DNA molecules, detectable by an obvious efflux of chromosomal DNA (DAPI stained) from these cells (Fig. 4B, row 2-4). Double-stranded DNA phages usually accomplish lysis by expression of a muralytic enzyme, called endolysin, encoded by the phage genome, which degrades the bacterial cell wall (Loessner, 2005; Young *et al.*, 2000). Additionally, the action of endolysins depends on so-called holins, small membrane proteins which permeabilize the membrane and thereby allow the corresponding endolysin to attack the peptidoglycan (Wang *et al.*, 2000). Genes encoding putative holins or endolysins located within the CGP3 region of *C. glutamicum* have not been identified yet. Also homologs of typical phage morphogenic genes, *e.g.* genes encoding coat proteins, tail fibres or shaft building proteins), could not be identified so far. As stated before only few genes of the CGP3 region code for proteins of known or putative functions (Table 1), whereas the majority of open reading frames lack any similarity to known phage or bacterial genes. However, the extreme diversity of phage genomes in bacterial genome sequences is a known feature of dsDNA phages (Casjens, 2003; Hendrix *et al.*, 1999). Other examples exist where prophages contain a majority of novel genes with unknown function, *e.g.* >75% of the genes of the prophage RadMu in the *Deinococcus radiodurans* R1 genome have no known homolog (Morgan *et al.*, 2002).

The site of integration of the CGP3 prophage into the *C. glutamicum* genome, a tRNA-Val gene, can be easily identified due to the direct 26-bp repeats flanking the CGP3 prophage (GTGGTCCTAGCTGGGTTCGAACCAGC). The specific site of integration site into a bacterial genome is primarily determined by the integrase enzyme, which catalyzes site-specific recombination between the phage recognition site (*attP*) and a short sequence of bacterial DNA (*attB*) (for a preliminary model see Fig. 3) (Groth and Calos, 2004). The gene encoding the integrase of the CGP3 prophage is located at the right border and seems to be disrupted by a frame-shift mutation (*int2'* encoding the N-terminal part, *'int2* encoding the C-terminal part). However, the finding that the CGP3 prophage is still able to excise from the *C. glutamicum* genome indicates that a functional integrase can still be formed. The above-mentioned direct repeat was shown to be the connection site of the circular phage DNA molecule and one repeat remained in the bacterial genome after excision of the CGP3 prophage. Thus, it is very likely that crossing-over occurs at these 26-bp sites, which form a so-called core-type binding site that is recognized by the phage integrase (Groth and Calos, 2004).

DNA microarray analysis as well as determination of the copy number of the circular

phage DNA molecule revealed that the fraction of cells with an induced CGP3 prophage increases about 15-fold in a *dtxR* deletion mutant (Fig. 1A, Table 2). In this mutant expression of several genes encoding high-affinity iron uptake system is strongly increased (Brune *et al.*, 2006b; Wennerhold and Bott, 2006) even under conditions of sufficient iron supply. As a consequence, the mutant cells might be faced with elevated intracellular iron concentrations and a resulting increase of iron-induced oxidative stress (Pierre and Fontecave, 1999). Additionally, exposure to UV light probably also leads to prophage induction (Fig. 1B). Thus, oxidative stress caused by an increased intracellular iron concentration or by exposure to UV light seems to be good candidate for induction of the CGP3 prophage in a distinct fraction of the bacteria.

Up to now it remains unclear whether intact and fully functional CGP3 phage particles are formed and released by lysis of the cell. Neither obvious lysis of cells in liquid cultures nor the formation of plaques on lawns was observed in growth experiments with strains derived from *C. glutamicum* ATCC 13032. However, this does not exclude the formation of functional phage particles, since our experiments revealed a spontaneous prophage induction in only about 2-4% of *C. glutamicum* wild type cells. If functional CGP3 phages were formed, they could not infect and lyse other cells of the culture because they are resistant due to their integrated CGP3 prophage.

Fluorescence microscopy with an YFP-tagged CGP3 region was found to be a valuable tool for the observation of culture heterogeneity. This approach also revealed that a small fraction of *C. glutamicum* WT cells even might have got rid of the CGP3 prophage, most probably by cell division shortly after prophage induction, inheriting the CGP3 phage DNA molecule to the other daughter cell. These cells would then have a strong advantage in comparison to *C. glutamicum* cells still carrying the large CGP3 genome (~187 kbp). The fact that *C. glutamicum* has not managed to get completely rid of the CGP3 prophage indicates either the existence of essential *C. glutamicum* genes dislocated into the CGP3 element or indeed the formation of intact phage particles which can infect these cells.

Experimental procedures

Bacterial strains, media and growth conditions

All strains and plasmids used in this work are listed in Table 3. The *C. glutamicum* type strain ATCC 13032 (Kinoshita *et al.*, 1957) was used as wild type (WT). Strain Δ*dtxR* is a derivative containing an in-frame deletion of the gene *cg2103* (Wennerhold and Bott, 2006). For growth experiments, 5 ml of brain heart infusion (BHI) medium (Difco Laboratories, Detroit, MI) was inoculated with colonies from a fresh BHI agar plate and incubated for 6 hours at 30°C and 170 rpm. After washing with 5 ml 0.9% (w/v) NaCl, the cells of this first preculture were used to inoculate a 500-ml shake flask containing 60 ml CGXII minimal medium (Keilhauer *et al.*, 1993) with 4% (w/v) glucose and either 1 µM $FeSO_4$ (iron starvation) or 100 µM $FeSO_4$ (iron excess). This second preculture was incubated overnight at 30°C and then used to inoculate the main culture to an optical density at 600 nm (OD_{600}) of ~1. The main culture contained the same iron concentration as the second preculture. The trace element solution with iron salts omitted and the $FeSO_4$ solution were always added after autoclaving. Additionally, the medium was supplemented with 30 mg/l 3,4-dihydroxybenzoate as iron chelator. For all cloning purposes, *E. coli* DH5α (Invitrogen) was used as host. *E. coli* strains were cultivated aerobically in LB medium at 37°C. When appropriate, the media contained kanamycin (25 µg/ml for *C. glutamicum*, 50 µg/ml for *E. coli*) or spectinomycin (250 µg/ml for *C. glutamicum*, 100 µg/ml for *E. coli*).

General DNA techniques

The enzymes for recombinant DNA work were obtained from Roche Diagnostics (Mannheim, Germany) or New England Biolabs (Frankfurt, Germany). The oligonucleotides used in this study are listed in Table 4 and were obtained from Operon (Cologne, Germany). Routine methods like PCR, restriction or ligation were carried out according to standard protocols (Sambrook, 1989). Plasmids from *E. coli* were isolated with the QIAprep spin Miniprep Kit

Table 3. Strains and plasmids used in this work

Strains or plasmids	Relevant characteristics	Source or reference
Strains		
C. glutamicum		
ATCC13032	Biotin-auxotrophic wild type	(Kinoshita *et al.*, 1957)
13032Δ*dtxR*	In-frame deletion of the *dtxR* gene	(Wennerhold and Bott, 2006)
E. coli		
DH5α	*supE44* Δ*lacU169* (ϕ80*lacZ*DM15) *hsdR17 recA1 endA1 gyrA96 thi-1 relA1*	Invitrogen
Plasmids		
pEKEx2	Kan^R; *C. glutamicum*/*E. coli* shuttle vector for regulated gene expression (P_{tac}, $lacI^Q$, pBL1 $oriV_{Cg.}$, pUC18 $oriV_{E.c.}$)	(Eikmanns *et al.*, 1991a)
pEKEx3	$Spec^R$, pEKEx2 derivative containing a spectinomycin resistance instead of the kanamycin resistance gene.	
pEKEx2-yfp-tetR	Kan^R; pEKEx2 derivative containing *yfp-tetR* encoding a YFP-TetR fusion protein under control of the *tac* promoter.	This work
pLAU44	Amp^R; Gm^R; plasmid containing two sets of *tetO* arrays	(Lau *et al.*, 2003)
pLAU44-CGP3-Spec	$Spec^R$, pLAU44 derivative containing a 500-bp insert of the *cg1905-1906* intergenic region for recombination into the genome.	This work
pLAU44-control-Spec	$Spec^R$, pLAU44 derivative containing a 500-bp insert of the *cg1859-1857* intergenic region for recombination into the genome.	This work

(Qiagen, Hilden, Germany). *E. coli* was transformed by the RbCl method (Hanahan, 1985), *C. glutamicum* by electroporation (van der Rest *et al.*, 1999). DNA sequencing was performed with a Genetic Analyzer 3100-Avant (Applied Biosystems, Darmstadt, Germany). Sequencing reactions were carried out with the BigDye Terminator v3.1 Cycle Sequencing kit (Applied Biosystems). Construction of an in-frame *dtxR* deletion mutant was described previously (Wennerhold and Bott, 2006).

Isolation of chromosomal and phage DNA

Chromosomal DNA from *C. glutamicum* was prepared as described (Eikmanns *et al.*, 1994). Plasmids from *E. coli* were isolated with the QIAprep spin Miniprep Kit (Qiagen, Hilden, Germany). For isolation of circular CGP3 phage DNA 0.5 g (wet weight) cells of the Δ*dtxR* mutant were disrupted as described for the isolation of chromosomal DNA (Eikmanns *et al.*, 1994), and the DNA was isolated with the reagents of the QIAprep spin Miniprep Kit used for plasmid isolation. After denaturation of protein and chromosomal DNA, the phage DNA was precipitated with 0.9 volumes of cooled isopropanol and centrifuged (20 min, 15.000 x *g*, 4℃). Subsequently, the pellet was washed with 500 µl 70% (v/v) ethanol. After centrifugation (15 min, 15.000 x *g*, 4℃) the pellet was air-dried (approx. 30 min at room temperature) and resuspended in 100-200 µl EB buffer (10 mM Tris/HCl, pH 8.5).

Plasmid construction

For tagging of the CGP3 prophage region with *tetO* arrays a 500-bp region from the intergenic region of *cg1905* and *cg1906* was amplified using oligonucleotides (CGP3-tetO-for and CGP3-tetO-rev) introducing an XhoI and a PstI restriction site. Additionally, a region containing the spectinomycin resistance cassette from pEKEx3 was amplified and restriction sites for PstI and NheI were introduced (Spec-tetO-for and Spec-tetO-rev). Both PCR products were cloned into the vector pLAU44, resulting in the plasmid pLAU44-CGP3-Spec. Construction and assembly of the *tetO* arrays contained in pLAU44 has been performed by the group of Prof. David J. Sherratt (Lau *et al.*, 2003). Since plasmid pLAU44-CGP3-Spec lacks an origin for *C. glutamicum,* integration into the chromosome *via* homologous recombination with the *cg1905-1906* intergenic region was obligatory for growth on BHI plates supplemented with 250 µg/ml spectinomycin. Transformants were assayed for correct integration of the *tetO* arrays by PCR using the primer pair control-tetO-for and Spec-tetO-rev.

Table 4. Oligonucleotides used in this work.

Oligonucleotide	Sequence (5´→ 3´) and properties
Oligonucleotides for overexpression of YFP-tetR	
tetR-YFP-for	TATATAGGATCCAAGGAGATATAGATATGGTGTCTAGATTAGATAAAAG (BamHI)
tetR-YFP-rev	TATATAGAATTCTTATCTAGACTTGTACAGCTCGTCC (EcoRI)
CGP3-tetO-for	TATATACTCGAGATCTGGTGTTTACAGATAGCAAGG (XhoI)
CGP3-tetO-rev	TATATACTGCAGTTTCCCCTGAAATATTAGATTGC (PstI)
control-tetO-for	TATATA CTCGAG GTTCTAAGCCCCTCTTCTTTCAAC (XhoI)
control-tetO-rev	TATATA CTGCAG TTCCTGGATCCTTCATTTCAGAG (PstI)
Spec-tetO-for	TATATACTGCAGTATCTAGATAAAAAATTTAGAAGCC (PstI)
Spec-tetO-rev	TATATAGCTAGCACCAATTAGAATGAATATTTCCC (NheI)
Oligonucleotides for investigation of prophage induction	
prophage-1-for	GCAGAGTTCGCACGAGTGTTGAGCG
prophage-2-rev	CACGTACTTTGCACGGATTCGTCGG
prophage-3-for	GGTGAGCTGGGGGAGTTGCGAGGCG
prophage-4-rev	CCGCAAGGTCCTATGGCTCAGTGG
prophage-5-for	CATCCCTTGAAAAGCTGAAGAAGC
prophage-6-rev	CACGTACTTTGCACGGATTCGTCGG
Oligonucleotides used for real-Time PCR	
Phage-LC-for	CCCACGTTCACCCCACAAACG
Phage-LC-rev	CTAAAATGAAGCCATCGCGACC
ddh-LC-for	ACGTGCTGTTCCTGTGCATGG
ddh-LC-rev	GCTCGGCTAAGACTGCCGCT
hdh-LC-for	AGCCGCAAACGTTGACCTGTAC
hdh-LC-rev	AAGTTGGTGGTGCCGTTAACG

For expression of a YFP-TetR fusion protein under control of the *tac* promoter, *yfp-tetR* was amplified by PCR using the oligonucleotides tetR-YFP-for and tetR-YFP-rev and the vector pLAU53 as template (Lau *et al.*, 2003). The resulting PCR product was cloned into the vector pEKEx2 (Eikmanns *et al.*, 1991a) and the recombinant plasmid pEKEx2-yfp-tetR was used to transform *C. glutamicum* WT::pLAU44-CGP3-Spec. Transformants were selected for kanamycin and spectinomycin resistance.

Global gene expression analysis

In previous studies transcriptome comparisons of *C. glutamicum* WT and a Δ*dtxR* mutant grown in CGXII minimal medium containing 4% (w/v) glucose under iron excess (100 µM $FeSO_4$) or iron limitation (1 µM $FeSO_4$) was performed using DNA microarray analysis (Wennerhold and Bott, 2006). Additionally, the transcriptomes of WT cells before and after exposure to UV light were compared. For this purpose, cells were grown in LB medium with 4% glucose to an OD_{600} of 3.5. Then two 8-ml samples were taken one of which was used immediately for RNA preparation, whereas the second one was poured into a sterile glass petri dish and incubated under UV irradiation (0.4 W/m^2) at 30℃ with stirring at 600 rpm. After 30 min (corresponding to a final intensity of 800 J/m^2) the cells were harvested and used for the preparation of total RNA as described previously (Möker *et al.*, 2004a). Isolated RNA samples were analyzed for quantity and quality by UV spectrophotometry and stored at -70 ℃ until use (Sambrook, 1989).

The generation of whole-genome DNA microarrays (Wendisch, 2003), synthesis of fluorescently labelled cDNA from total RNA, microarray hybridization, washing and data analysis were performed as described previously (Ishige *et al.*, 2003; Lange *et al.*, 2003; Polen *et al.*, 2003).

Copy number determination using quantitative real-time PCR

The copy number of the circular phage DNA molecule was determined by quantitative real-time PCR as described (Lee *et al.*, 2006). Each sample contained 1 µg template DNA, 10 µl of 2x QuantiTect SYBR Green PCR Master Mix (Qiagen, Cologne, Germany), specific forward and reverse primers (final concentration 0.5 µM, Table 4) and was filled up with dH_2O to a final volume of 20 µl. Amplification was carried out in Lightcycler capillaries (20 µl) (Roche, Grenzach, Germany) using the LightCycler instrument (Roche Diagnostics). Serial ten-fold dilutions (1 ng/µl-100 fg/µl) of a phage and a genomic DNA solution of a given concentration (10 ng/µl) were used to establish a standard curve. A negative control was set up by substituting the template DNA with dH_2O in order to determine the lower detection limit. Real-time PCR was

performed with the following cycling conditions: pre-incubation at 95℃ for 15 min, followed by 50 cycles of 94℃ for 15 s, 62℃ for 20 s, 72℃ for 15 s, 80℃ for 15 s, and 72℃ for 5 s. Upon completion of 50 cycles a melting curve analysis was performed (from 60℃ to 95℃ in 15 min) to confirm specific amplification of PCR products. Subsequently, the copy number was calculated for each sample using the following equation:

$$\text{Copy number per genome} = \frac{\text{size of chromosomal DNA (bp) x amount of plasmid DNA (pg)}}{\text{size of plasmid DNA (bp) x amount of genomic DNA (pg)}}$$

In order to check whether the derived copy number values were reliable, a positive control was performed using a template of known copy number. For this purpose, the copy number of the *hom* gene (*cg1337*) in strain *C. glutamicum* MH20-22B-DR17 was determined. This strain is known to contain four *hom* copies in the genome (Reinscheid *et al.*, 1994). An average copy number of 4.2 ± 0.3 was determined by qRT-PCR.

Fluorescence microscopy

Cells for microscopy were grown in CGXII minimal medium with 4% glucose under iron excess (100 µM $FeSO_4$) to an OD_{600} of 2, when they were induced with 0.1 mM IPTG until fluorescent foci appeared (approx. 30 min). For phase contrast and fluorescence microscopy 1-3 µl of a culture sample was placed on a microscope slide coated with a thin agarose (1%) layer and covered by a coverslip. For membrane or DNA staining a 10-µl culture sample was mixed with 1 µl Nile red (Molecular Probes, Paisley, UK) (12.5 µg ml^{-1}) or 2 µl DAPI (Sigma, Munich, Germany) solution (1 µg ml^{-1} 50 % glycerol), respectively. Images were taken on a Zeiss AxioImager Z1 equipped with a Zeiss AxioCam MRm camera. YFP fluorescence was monitored using an FITC filter set. An EC Plan-Neofluar 100x/1,3 Oil Ph3 objective was used. Digital images were acquired and analyzed with the AxioVision software (Zeiss, Göttingen, Germany). Final image preparation was done in Adobe Photoshop 6.0 (Adobe Systems Incorporated).

Acknowledgements

We thank Prof. David Sherrat and Dr. Xindang Wang (University of Oxford) for sending us the plasmids pLAU44 and pLAU53 and Volker Wendisch for stimulating discussions at the initial phase of this project.

References

Brune, I., Werner, H., Hüser, A.T., Kalinowski, J., Pühler, A., and Tauch, A. (2006) The DtxR protein acting as dual transcriptional regulator directs a global regulatory network involved in iron metabolism of *Corynebacterium glutamicum*. *BMC Genomics* 7: 21.

Bukovska, G., Klucar, L., Vlcek, C., Adamovic, J., Turna, J., and Timko, J. (2006) Complete nucleotide sequence and genome analysis of bacteriophage BFK20--a lytic phage of the industrial producer *Brevibacterium flavum*. *Virology* 348: 57-71.

Casjens, S. (2003) Prophages and bacterial genomics: what have we learned so far? *Mol Microbiol* 49: 277-300.

Eggeling, L., and Bott, M. (2005) *Handbook of Corynebacterium glutamicum.* Inc., Boca Raton, FL: Academic Press.

Eikmanns, B.J., Kleinertz, E., Liebl, W., and Sahm, H. (1991) A family of *Corynebacterium glutamicum*/*Escherichia coli* shuttle vectors for cloning, controlled gene expression, and promoter probing. *Gene* 102: 93-98.

Eikmanns, B.J., Thum-Schmitz, N., Eggeling, L., Lüdtke, K.U., and Sahm, H. (1994) Nucleotide sequence, expression and transcriptional analysis of the *Corynebacterium glutamicum gltA* gene encoding citrate synthase. *Microbiology* 140: 1817-1828.

Groth, A.C., and Calos, M.P. (2004) Phage integrases: biology and applications. *J Mol Biol* 335: 667-678.

Hanahan (1985) Techniques for transformation of *E. coli*. In *DNA-cloning*. Vol. 1. M., G.D. (ed). Oxford/Washington DC: IRL-Press, pp. 109-135.

Hendrix, R.W., Smith, M.C., Burns, R.N., Ford, M.E., and Hatfull, G.F. (1999) Evolutionary

relationships among diverse bacteriophages and prophages: all the world's a phage. *Proc Natl Acad Sci U S A* 96: 2192-2197.

Ishige, T., Krause, M., Bott, M., Wendisch, V.F., and Sahm, H. (2003) The phosphate starvation stimulon of *Corynebacterium glutamicum* determined by DNA microarray analyses. *J Bacteriol* 185: 4519-4529.

Kalinowski, J., Bathe, B., Bartels, D., Bischoff, N., Bott, M., Burkovski, A., Dusch, N., Eggeling, L., Eikmanns, B.J., Gaigalat, L., Goesmann, A., Hartmann, M., Huthmacher, K., Krämer, R., Linke, B., McHardy, A.C., Meyer, F., Möckel, B., Pfefferle, W., Pühler, A., Rey, D.A., Rückert, C., Rupp, O., Sahm, H., Wendisch, V.F., Wiegräbe, I., and Tauch, A. (2003) The complete *Corynebacterium glutamicum* ATCC 13032 genome sequence and its impact on the production of L-aspartate-derived amino acids and vitamins. *J Biotechnol* 104: 5-25.

Kalinowski, J. (2005) The genomes of amino-acid producing bacteria. In *Handbook of Corynebacterium glutamicum*. Eggeling, L. and Bott, M. (eds). Inc., Boca Raton, FL: Academic Press.

Kato, F., Yoshimi, M., araki, K., Motomura, Y., Matsufune, Y., Nobunaga, H., and Murata, A. (1984) Screening of bacteriocins in amino acid or nucleic acid producing bacteria and related species. *Agric Biol Chem* 48: 193-200.

Keilhauer, C., Eggeling, L., and Sahm, H. (1993) Isoleucine synthesis in *Corynebacterium glutamicum*: molecular analysis of the *ilvB-ilvN-ilvC* operon. *J Bacteriol* 175: 5595-5603.

Kinoshita, S., Udaka, S., and Shimono, M. (1957) Studies on the amino acid fermentation: I. Production of L-glutamic acid by various microorganisms. *J Gen Appl Microbiol* 3: 193-205.

Kunkle, C.A., and Schmitt, M.P. (2003) Analysis of the *Corynebacterium diphtheriae* DtxR regulon: identification of a putative siderophore synthesis and transport system that is similar to the Yersinia high-pathogenicity island-encoded yersiniabactin synthesis and uptake system. *J Bacteriol* 185: 6826-6840.

Lange, C., Rittmann, D., Wendisch, V.F., Bott, M., and Sahm, H. (2003) Global expression profiling and physiological characterization of *Corynebacterium glutamicum* grown in the presence of L-valine. *Appl Environ Microbiol* 69: 2521-2532.

Lau, I.F., Filipe, S.R., Soballe, B., Okstad, O.A., Barre, F.X., and Sherratt, D.J. (2003) Spatial and temporal organization of replicating *Escherichia coli* chromosomes. *Mol Microbiol* 49: 731-743.

Lee, C.L., Ow, D.S., and Oh, S.K. (2006) Quantitative real-time polymerase chain reaction for determination of plasmid copy number in bacteria. *J Microbiol Methods* 65: 258-267.

Loessner, M.J. (2005) Bacteriophage endolysins--current state of research and applications. *Curr Opin Microbiol* 8: 480-487.

Möker, N., Brocker, M., Schaffer, S., Krämer, R., Morbach, S., and Bott, M. (2004) Deletion of the genes encoding the MtrA-MtrB two-component system of *Corynebacterium glutamicum* has a strong influence on cell morphology, antibiotics susceptibility and expression of genes involved in osmoprotection. *Mol Microbiol* 54: 420-438.

Moreau, S., Leret, V., Le Marrec, C., Varangot, H., Ayache, M., Bonnassie, S., Blanco, C., and Trautwetter, A. (1995) Prophage distribution in coryneform bacteria. *Res Microbiol* 146: 493-505.

Morgan, G.J., Hatfull, G.F., Casjens, S., and Hendrix, R.W. (2002) Bacteriophage Mu genome sequence: analysis and comparison with Mu-like prophages in *Haemophilus*, *Neisseria* and *Deinococcus*. *J Mol Biol* 317: 337-359.

Patek, M., Ludvik, J., Benada, O., Hochmannova, J., Nesvera, J., Krumphanzl, V., and Bucko, M. (1985) New bacteriophage-like particles in *Corynebacterium glutamicum*. *Virology* 140: 360-363.

Pierre, J.L., and Fontecave, M. (1999) Iron and activated oxygen species in biology: the basic chemistry. *Biometals* 12: 195-199.

Polen, T., Rittmann, D., Wendisch, V.F., and Sahm, H. (2003) DNA microarray analyses of the long-term adaptive response of *Escherichia coli* to acetate and propionate. *Appl Environ Microbiol* 69: 1759-1774.

Polen, T., and Wendisch, V.F. (2004) Genomewide expression analysis in amino acid-producing bacteria using DNA microarrays. *Appl Biochem Biotechnol* 118: 215-232.

Reinscheid, D.J., Kronemeyer, W., Eggeling, L., Eikmanns, B.J., and Sahm, H. (1994) Stable Expression of *hom-1-thrB* in *Corynebacterium glutamicum* and Its Effect on the Carbon Flux to Threonine and Related Amino Acids. *Appl Environ Microbiol* 60: 126-132.

Sambrook, J., Fritsch, E.F., and Maniatis, T. (1989) Molecular Cloning. A Laboratory

Manual. *Cold Spring Harbor, NY: Cold Spring Harbor Laboratoy Press.*

Schäfer, A., Tauch, A., Droste, N., Pühler, A., and Kalinowski, J. (1997) The *Corynebacterium glutamicum cglIM* gene encoding a 5-cytosine methyltransferase enzyme confers a specific DNA methylation pattern in an McrBC-deficient *Escherichia coli* strain. *Gene* 203: 95-101.

Schmitt, M.P., and Holmes, R.K. (1991) Iron-dependent regulation of diphtheria toxin and siderophore expression by the cloned *Corynebacterium diphtheriae* repressor gene *dtxR* in *C. diphtheriae* C7 strains. *Infect Immun* 59: 1899-1904.

Sonnen, H., Schneider, J., and Kutzner, H.J. (1990) Corynephage Cog, a virulent bacteriophage of *Corynebacterium glutamicum*, and its relationship to phi GA1, an inducible phage particle from *Brevibacterium flavum*. *J Gen Virol* 71 (Pt 8): 1629-1633.

van der Rest, M.E., Lange, C., and Molenaar, D. (1999) A heat shock following electroporation induces highly efficient transformation of *Corynebacterium glutamicum* with xenogeneic plasmid DNA. *Appl. Microbiol. Biotechnol.* 52: 541-545.

Wang, I.N., Smith, D.L., and Young, R. (2000) Holins: the protein clocks of bacteriophage infections. *Annu Rev Microbiol* 54: 799-825.

Wendisch, V.F. (2003) Genome-wide expression analysis in *Corynebacterium glutamicum* using DNA microarrays. *J Biotechnol* **104**: 273-285.

Wennerhold, J., and Bott, M. (2006) The DtxR regulon of *Corynebacterium glutamicum*. *J Bacteriol* 188: 2907-2918.

Young, I., Wang, I., and Roof, W.D. (2000) Phages will out: strategies of host cell lysis. *Trends Microbiol* 8: 120-128.

Book Chapter in: "*Corynebacteria*: Genomics and molecular biology" (Burkovski A., ed.), Horizon Scientific Press, Norwich, UK, in press.

Regulation of iron homeostasis in *Corynebacterium glutamicum*

Julia Frunzke und Michael Bott

Institut für Biotechnologie 1, Forschungszentrum Jülich, D-52425 Jülich

Corresponding author: Prof. Dr. Michael Bott, Institut für Biotechnologie 1, Forschungszentrum Jülich, D-52425 Jülich. Phone +49 (0)2461 615515. Fax +49 (0)2461 612710. E-mail m.bott@fz-juelich.de.

Abstract

The relevance of iron to corynebacteria was first noticed in the 1930s, when the synthesis of diphtheria toxin by *Corynebacterium diphtheriae* was shown to be dependent on the iron supply. Meanwhile, the DtxR protein responsible for this regulation has been intensively characterized biochemically. It functions as an intracellular Fe^{2+} sensor and, when its low-affinity iron-binding site is occupied, as a transcriptional regulator. In *C. diphtheriae*, several DtxR targets have been identified and thoroughly characterized, but no genome-wide studies were performed yet. In the non-pathogenic *Corynebacterium glutamicum*, on the other hand, the DtxR regulon has been determined by genome-wide studies including transcriptome comparisons of wild type and *dtxR* deletion mutants using DNA microarrays. By this approach, more than 50 genes were found to be repressed by DtxR under iron excess, most of which encode proteins involved in iron acquisition, notably several ABC transporters for siderophores. Moreover, genes which are presumably activated by DtxR have been identified, such as iron storage proteins and proteins responsible for iron-sulfur cluster assembly. Three of the target genes repressed by DtxR in *C. glutamicum* (*ripA*, *cgtR11*, *cg0527*) encode themselves transcriptional regulators. The AraC-type regulator RipA has been shown to repress a set of genes which encode prominent iron proteins of the cell, such as aconitase, succinate dehydrogenase or catalase. In this way, the iron demand of the cell is reduced, possibly allowing prolonged survival under iron limitation. In the case of the response regulator CgtR11, evidence for its involvement in heme utilization has been obtained, whereas the function of Cg0527 is not yet known. In summary, key players of a complex regulatory network controlling iron homeostasis in *C. glutamicum* have been elucidated in recent years.

1. Iron – essential but dangerous

Iron is an essential element for almost all organisms as constituent of proteins containing heme, iron-sulfur clusters, or mono- or binuclear iron species. Such proteins play important roles in many biological processes, such as electron transport, the tricarboxylic acid (TCA) cycle or gene regulation. Although iron is one of the most abundant elements in the earth crust, it is not readily available, since the predominant form of iron under aerobic conditions is the ferric state (Fe^{3+}) which has has been reported to have a solubility of 1.4×10^{-9} M at neutral pH (Chipperfield and Ratledge, 2000), in contrast to the ferrous state (0.1 M at pH 7.0). To cope with this problem, many microbes have evolved complex systems to solubilize iron from their environment. Besides being essential, iron can also be harmful to cells, mainly due to its reaction with hydrogen peroxide, a by-product of aerobic metabolism. In the Fenton reaction, Fe^{2+} reacts with H_2O_2 to yield Fe^{3+}, OH^- and the highly reactive and strongly damaging hydroxyl radical $\cdot OH$ (Pierre and Fontecave, 1999). Thus, cells have to cope with poor iron solubility on one hand and to avoid high levels of free intracellular Fe^{2+} on the other hand. As pointed out by Andrews et al. (Andrews et al., 2003), five major strategies are used by bacteria to deal with these problems: (i) high-affinity iron transport systems for scavenging iron from the environment; (ii) intracellular iron storage proteins providing an iron source when the external ones are transiently unavailable; (iii) redox stress resistance mechanisms such as degradation of reactive oxygen species and repair of damaged molecules; (iv) reduction of the cellular iron demand by partial repression of iron-containing proteins; and (v) a sophisticated regulatory system that controls all of the above-mentioned processes according to iron availability.

This chapter deals predominantly with iron homeostasis in the non-pathogenic Gram-positive soil bacterium *C. glutamicum*, but includes also relevant data from *C. diphtheriae*. First we will give an overview on the possibilities of *C. glutamicum* for iron acquisition and then we summarize current knowlege on a recently discovered complex regulatory network which controls iron homeostasis.

2. Iron acquisition by *Corynebacterium glutamicum*

Iron dependency of growth. Early studies showed that growth of *C. glutamicum* (formerly *Micrococcus glutamicus*) in synthetic medium depends on a sufficient supply of iron, which could be provided e.g. in form of ferrichrome (10 mg/l), or by high concentrations of iron salts (0.5 – 2.0 g/l). Moreover, a synergistic action between iron and several chelating agents on growth was demonstrated (Nakayama et al., 1964a; Nakayama et al., 1964b). Twenty-five years later, two studies addressed once more the problem of iron acquisition by *C. glutamicum* when a defined medium was required for metabolic studies. Von der Osten et al. showed that 0.1% (3.9 mM) citrate (provided as sodium salt) in combination with ≥20 mg/l $FeSO_4 \times 7\ H_2O$ (72 µM) allowed good growth (von der Osten et al., 1989). Interestingly, citrate was consumed before glucose, but the depletion had no negative effect on the growth rate. The authors therefore suggested that iron is accumulated intracellularly in the early

stages of cultivation. Liebl et al. (1989) confirmed the results of von der Osten et al., but noticed that the high concentrations of citrate required might be undesirable in metabolic studies. They could show that low concentrations (10 µM) of protocatechuate (3,4-dihydroxybenzoate) or catechol in combination with 72 µM $FeSO_4$ suffice to achieve the same growth as 0.1% citrate (Liebl *et al.*, 1989b). The standard minimal medium used in our and several other laboratories, called CGXII (Keilhauer et al., 1993), contains 30 mg/l (195 µM) protocatechuate. Like in the case of citrate (Polen et al.), also protocatechuate is used as a carbon source by *C. glutamicum* (Merkens et al., 2005). Again, accumulation of iron in the initial growth phase might be responsible for maintaining a high growth rate when protocatechuate has been consumed. According to the studies described above, *C. glutamicum* is able to take up ferrichrome, ferric citrate and iron complexes of protocatechuate and catechol. The overall iron content of *C. glutamicum* cells has been determined to vary between 0.04 iron/g cell dry weight on CGIII complex medium and 0.3 - 0.5 mg iron/g cell dry weight on BMCG and CGXII minimal medium used for cultivation (Liebl *et al.*, 1989a).

Except for the studies described above and a very recent report (Dertz et al., 2006), no experimental data on iron transport in *C. glutamicum* appear to exist. Therefore, the current knowledge on iron acquisition is primarily based on the annotated genome sequence (Kalinowski et al., 2003) and on DNA microarray studies in which global gene expression was analyzed in cells grown with different iron supplies or in mutant cells lacking regulators of iron metabolism (Brune *et al.*, 2006a; Krug *et al.*, 2005; Wennerhold *et al.*, 2005; Wennerhold and Bott, 2006).

C. glutamicum ***does not synthesize siderophores by itself.*** To overcome the poor solubility of ferric iron, many microorganisms synthesize and excrete low molecular mass (<1000 Da) compounds called siderophores that are characterized by their high specificity and affinity ($K_d \sim 10^{-30}$ M^{-1}) towards ferric iron. More than 500 different siderophores are currently known and formation of iron complexes usually involves either hydroxamate groups, or catechol rings, or hydroxy acids. Upon import of iron siderophore complexes into the bacterial cytoplasm, the iron is released either by the reduction to Fe^{2+} catalyzed by ferri-siderophore reductases (Schröder et al., 2003) or by breaking down the siderophore structure as described for several siderophores, *e.g.* bacillibactin (Miethke et al., 2006) or enterobactin (Lin et al., 2005). In 1997, Budzikiewicz and co-workers (Budzikiewicz et al., 1997) reported the isolation of a cyclic catecholate siderophore from *C. glutamicum* strain ATCC14067 which they named corynebactin. A siderophore of identical structure was later isolated from *Bacillus subtilis* and designated bacillibactin (May et al., 2001). Moreover, the genes *dhbABCEF* responsible for bacillibactin synthesis were identified (May et al., 2001). Analysis of the genome sequence of *C. glutamicum* strain ATCC13032 revealed a gene homologous to *dhbC* (encoding isochorismate synthetase), but there were no genes present that are homologous to *dhbA*, *dhbB*, *dhbE* or *dhbF*. Moreover, no other genes obviously involved in siderophore biosynthesis were identified, leading to the conclusion that at least the type strain ATCC13032 does not produce siderophores (Wennerhold and Bott, 2006). Recently, Raymond and coworkers

reinvestigated corynebactin (alias bacillibactin) synthesis by *C. glutamicum* ATCC14067 and failed to detect the production of this siderophore (Dertz et al., 2006). The strain was also negative in the Chrome Azurol S (CAS) assay, which indicates the inability to synthesize siderophores that remove iron from the CAS chromophore. Finally, the strain did not take up ^{55}Fe-labeled bacillibactin, which would be expected for a strain that synthesises and excretes this siderophore. Thus, *C. glutamicum* ATCC14067 like the type strain ATCC13032 does not produce siderophores (Dertz et al., 2006).

C. glutamicum ***has a large arsenal of genes for siderophore utilization.*** In contrast to the inability to synthesize siderophores by itself, *C. glutamicum* has a substantial arsenal of more than 25 genes annotated to be involved in the acquisition of iron from different siderophores. These include five ABC transporters, nine secreted siderophore-binding lipoproteins, and five cytoplasmic siderophore-interacting proteins (Table 1). Thus, it can be suggested that *C. glutamicum* is able to benefit in its natural habitat from siderophores produced by other organisms. However, as none of these transport components has been studied yet, their substrate specificity is still unknown. According to the results described in the preceding paragraph, ferrichrome and ferric citrate belong to the substrates accepted by these transporters.

Gram-negative bacteria have developed a sophisticated mechanism to transport ferric siderophores through the outer membrane. High-affinity receptor proteins located within the outer membrane (*e.g.* FhuA, FecA or FepA) are supplied with energy from the cytoplasmic membrane by the Ton complex (TonB, ExbB and ExbD, for review see (Postle and Kadner, 2003)), thereby allowing transport of the bound ligand. In the periplasm, the ferric siderophores are captured by soluble periplasmic binding proteins and subsequently transported through the cytoplasmic membrane (Faraldo-Gomez and Sansom, 2003). Especially the uptake systems for the siderophores enterobactin (FepABCD) and ferrichrome (FhuACDB) as well as ferric citrate (FecABCD) have been studied intensely in Gram-negative species. Homologs of FhuA, FecA, FepA, TonB, ExbB and ExbD are not present in corynebacteria. However, there is evidence that these bacteria and other members of the suborder *Corynebacterinae* possess a structure with functional similarity to the outer membrane of Gram-negative bacteria (Bayan et al., 2003; Puech et al., 2001). This structure is composed in particular of mycolic acids (2-alkyl-3-hydroxy acids of variable chain length), either linked to the cell wall sugar polymer arabinogalactan or esterified with trehalose. The question how siderophores and other iron complexes pass this hydrophobic layer has not been addressed yet. Porins may play a role in this process (Costa-Riu et al., 2003; Hünten et al., 2005).

Table 1: Transport systems possibly involved in iron acquisition in *Corynebacterium glutamicum* ATCC13032.

Gene	Protein	Molecular mass, kDa	Function	DtxR binding site	Pfam domain and further information
Ferric-siderophore uptake systems					
cg0052		32.3	siderophore ABC transporter, permease protein		PF01032, FecCD transport family
cg0053		28.3	siderophore ABC transporter, ATP-binding protein		PF00005, ABC transporter
cg0054		31.0	cytoplasmic siderophore-interacting protein	-	PF04954, siderophore-interacting protein PF08021, siderophore-interacting FAD- binding domain
cg0405		34.0	secreted siderophore binding lipoprotein	-	PF01497, periplasmic binding protein
cg0591		35.4	siderophore ABC transporter, permease protein		PF01032, FecCD transport family
cg0590		41.1	siderophore ABC transporter, permease protein	+	PF01032, FecCD transport family
cg0589		28.9	siderophore ABC transporter, ATP-binding protein		PF00005, ABC transporter
cg0748		35.1	secreted siderophore binding lipoprotein	+	PF01497, periplasmic binding protein
cg0771		37.4	secreted siderophore binding lipoprotein		PF01497, periplasmic binding protein
cg0770		37.8	siderophore ABC transporter, permease protein		PF01032, FecCD transport family
cg0769		35.3	siderophore ABC transporter, permease protein		PF01032, FecCD transport family
cg0768		29.1	siderophore ABC transporter, ATP-binding protein	+	PF00005, ABC transporter
cg0767		32.5	cytoplasmic siderophore-interacting protein		PF04954, siderophore-interacting protein PF08021, siderophore-interacting FAD- binding domain
cg0778		34.7	siderophore ABC transporter, permease protein		PF01032, FecCD transport family
cg0777		27.7	siderophore ABC transporter, ATP-binding protein	-	PF00005, ABC transporter
cg0776		33.8	secreted siderophore binding lipoprotein		PF01497, periplasmic binding protein
cg0922		33	secreted siderophore binding lipoprotein	+	PF01497, periplasmic binding protein

Table 1: (continued) Transport systems possibly involved in iron acquisition in *Corynebacterium glutamicum* ATCC13032.

Gene	Protein	Molecular mass, kDa	Function	DtxR binding site	Pfam domain and further information
cg0921		30.8	cytoplasmic siderophore-interacting protein		PF04954, siderophore-interacting protein PF08021, siderophore-interacting FAD-binding domain
cg0924		35.7	secreted siderophore binding lipoprotein	+	PF01497, periplasmic binding protein
cg0926		36.0	siderophore ABC transporter, permease protein		PF01032, FecCD transport family
cg0927		40.8	siderophore ABC transporter, permease protein	+	PF01032, FecCD transport family
cg0928		27.9	siderophore ABC transporter, ATP-binding protein		PF00005, ABC transporter
cg1405		31.2	cytoplasmic siderophore-interacting protein	+	PF04954, siderophore-interacting protein PF08021, siderophore-interacting FAD-binding domain
cg1418		35.9	secreted siderophore binding lipoprotein	+	PF01497, periplasmic binding protein
cg1642		27.1	cytoplasmic siderophore-interacting protein	+	PF04954, siderophore-interacting protein PF08021, siderophore-interacting FAD-binding domain
cg2234		33.0	secreted siderophore binding lipoprotein	+	PF01497, periplasmic binding protein
cg3404		36.6	secreted siderophore binding lipoprotein	+	PF01497, periplasmic binding protein high similarity to FagD of *C. pseudotuberculosis* (Billington et al. 2002)
Heme transport systems					
cg0466	HtaA	62.1	secreted heme-transport associated protein	+	PF04213, Htaa
cg0467	HmuT	37.3	hemin-binding periplasmic protein precursor		PF01497, periplasmic binding protein
cg0468	HmuU	37.1	hemin transport system, permease protein		PF01032, FecCD transport family
cg0469	HmuV	28.5	hemin transport system, ATP-binding protein		
cg0470		33.6	secreted heme-transport associated protein	+	PF04213, Htaa
cg0471		29	secreted heme-transport associated protein		PF04213, Htaa

Table 1: (continued) Transport systems possibly involved in iron acquisition in *Corynebacterium glutamicum* ATCC13032.

Gene	Protein	Molecular mass, kDa	Function	DtxR binding site	Pfam domain and further information
cg3156		26.9	secreted heme-transport associated protein	+	PF04213, Htaa
Vitamin B12, heme or siderophore transport systems					
cg1832		37.3	permease of ABC transporter		PF01032, FecCD transport family
cg1833		33.5	secreted binding lipoprotein	-	PF01494, periplasmic binding protein
cg1834		27.7	ATP-binding protein of ABC transporter		PF00005, ABC transporter
cg2315		12.4	ATP-binding protein of ABC transporter		PF01497, periplasmic binding protein
cg2317		35.8	permease of ABC transporter	-	PF01032, FecCD transport family
cg2318		27.1	putative secreted vitamin B12 binding lipoprotein		PF00005, ABC transporter
Putative Fe^{2+}, Mn^{2+} or Zn^{2+} ABC transporter					
cg0043		23.7	ATP-binding protein of ABC transporter,		PF00005, ABC transporter
cg0042		29.8	permease of ABC transporter	+	PF00950, ABC 3 transport family PF01032, FecCD transport family
cg0041		33.6	secreted Fe^{2+}, Mn^{2+} or Zn^{2+}-binding lipoprotein		PF01227, periplasmic solute binding protein family
Putative Fe^{3+} ABC transporter					
cg0508		37.9	secreted binding lipoprotein		PF01547, extracellular solute-binding protein
cg0507		55.6	permease of ABC transporter	-	PF00528, binding-protein-dependent transport system, inner membrane component
cg0506		37.8	ATP-binding protein of ABC transporter,		PF00005, ABC transporter

C. glutamicum ***can utilize heme as iron source.*** Besides siderophores many bacteria can also acquire iron from heme. Following the transport of heme into the cytoplasm *via* specific heme transporters, the iron is extracted by heme oxygenases that degrade the tetrapyrrole ring. Up to now heme uptake in Gram-positive organisms has rarely been studied, however, heme uptake systems of *C. diphtheriae* and *Corynebacterium ulcerans* and have recently been documented (Drazek et al., 2000; Schmitt and Drazek, 2001). The heme transporter of *C. diphtheriae* encoded by the *hmu* operon shows similarity to heme-dependent ABC transporters of Gram-negative bacteria (Drazek et al., 2000). The *hmu* operon consists of five genes including *htaA*, *hmuT*, *hmuU*, *hmuV* and an ORF of unknown function. The promoter-proximal *htaA* gene encodes a protein with a signal sequence and a putative membrane spanning region, suggesting that HtaA is secreted and possibly anchored to the cell surface. Its exact function is not yet known. The heme-dependent ABC transport system consists of the binding protein HmuT, the permease HmuU and the ATPase component HmuV (Drazek et al., 2000). Based on experimental data it has been proposed that HmuT is a heme- and hemoglobin-binding lipoprotein, sharing ~25% sequence identity to the periplasmic heme binding proteins (PBPs) from *Yersinia* species (Hornung et al., 1996; Wandersman and Stojiljkovic, 2000). The genome of *C. glutamicum* contains a putative operon (*cg0466-cg0469*) showing the same gene order as reported for the *hmu* operon of *C. diphtheriae*. The encoded proteins share about 50% sequence identity with the *C. diphtheriae* homologs. Additionally, the *C. glutamicum* genome contains three other genes predicted to encode proteins involved in heme transport, all of which contain a signal peptide and a putative C-terminal transmembrane helix (*cg0470*, *cg0471*, *cg3156*), and a heme oxygenase (*cg2445*) (Table 1). All these genes were recently shown to be repressed in *C. glutamicum* by the global iron regulator DtxR under conditions of sufficient iron supply (Brune *et al.*, 2006a; Wennerhold and Bott, 2006). The presence of the abovementioned genes and their iron-dependent regulation suggests that *C. glutamicum* is able to import heme and use it as an iron source. In fact, recent experiments in our laboratory have confirmed that *C. glutamicum* can grow with heme as sole iron source (Frunzke and Bott, unpublished results).

Survey of the **C. glutamicum** ***genome for the presence of putative ferrous and ferric iron transporters.*** Cells can acquire iron not only in form of iron complexes, but also in an uncomplexed state as ferric or ferrous ions. Analysis of the *C. glutamicum* genome revealed an apparent operon (*cg0508-cg0507-cg0506*) whose protein products share some similarity (25 - 30%) with the SfuABC system of *Serratia marcescens*, which has been described as the first siderophore-independent ferric iron ABC transporter (Angerer et al., 1990; Schryvers et al., 1998). Whether the proteins encoded by *cg0508-cg0507-cg0506* also catalyze ferric iron transport in *C. glutamicum* remains to be analyzed. As no DtxR binding site was identified in the promoter region of *cg0508-0506*, these genes presumably do not belong to the DtxR regulon.

So far several systems have been described which mediate the uptake of ferrous iron and other divalent cations, like Mn^{2+}, Co^{2+}, Ni^{2+} or Mg^{2+} in various bacterial species (Koster, 2005). The Feo system of *Escherichia coli* was one of the first ferrous iron transport systems

identified in bacteria (Cartron et al., 2006). Homologs of *feoB* and *feoA* are widely distributed in bacteria, but absent from the genome of *C. glutamicum*. MntH, an Nramp-like protein (natural resistance associated macrophage proteins) of *E. coli*, has also been described as divalent cation transporter, but with a preference for Mn^{2+}. Whereas the genome of *C. glutamicum* ATCC13032 does not encode proteins with significant identity to Nramp-like proteins, the genome of *C. glutamicum* strain R (Yukawa et al., 2007) encodes a protein (CgR_0158) which shares some sequence identity (34%) to *E. coli* MntH. In contrast to the Nramp proteins of various eukaryotes, the MntH proteins in bacteria seem to be of minor importance for the transport of ferrous iron under physiological conditions (Courville et al., 2006; Makui et al., 2000; Patzer and Hantke, 2001).

Several bacterial species use the Sit ABC transport system to mediate transport of Mn^{2+} and Fe^{2+}. In *C. glutamicum* the genes *cg0041* (secreted binding lipoprotein), *cg0042* (permease) and *cg0043* (ATP-binding protein) encode an ABC transporter whose proteins display some sequence identity (~30 %) with those encoded by *sitABCD* from *Enterobacterianeae* species (Janakiraman and Slauch, 2000). The *cg0043* gene is located upstream and divergent to *cg0042-cg0041*. A functional DtxR binding site has been identified in the intergenic region of *cg0042* and *cg0043*, but in DNA microarray studies no effect on the transcription of these genes has been observed in a *dtxR* deletion mutant (Wennerhold and Bott, 2006). However, transcriptome analysis of *C. glutamicum* wild type cells cultivated with different iron concentrations revealed a decreased mRNA level of this operon under iron limitation (Krug et al., 2005). As for the genes described above, further studies are required to determine the metal ion substrate(s) of this ABC transporter and its iron-dependent regulation.

3. Control of iron homeostasis in *Corynebacterium glutamicum*

DtxR, the repressor of the* Corynebacterium diphtheriae *tox gene. In the early 1930s it was demonstrated that high levels of iron in the growth medium repressed the production of diphtheria toxin by *C. diphtheriae* (Pappenheimer and Johnson, 1936). About 60 years later, this effect was shown to be mediated by the transcriptional regulator DtxR (diphtheria toxin regulator) (Boyd *et al.*, 1990; Schmitt and Holmes, 1991a). Under iron excess, DtxR in complex with Fe^{2+} represses transcription of the *tox* gene. When iron becomes limiting, Fe^{2+} dissociates from DtxR and apo-DtxR becomes inactive, causing derepression of the *tox* gene. In contrast to diphtheria toxin, which is encoded in the genome of some corynephages, DtxR is encoded by the *C. diphtheriae* genome (locus tag DIP1414; (Cerdeno-Tarraga et al., 2003)). Meanwhile, it has been shown that DtxR is not a specific regulator of the *tox* gene, but controls many genes involved in iron acquisition in *C. diphtheriae* (Kunkle and Schmitt, 2003). Homologs of DtxR are widely distributed in bacteria and some have been characterized, *e.g.* the IdeR protein of *Mycobacterium tuberculosis* (Gold et al., 2001).

Metal ion activation of DtxR. The protein structures of DtxR from *C. diphtheriae* and IdeR from *M. tuberculosis* have been intensively investigated and provided important knowledge about the mechanism of metal ion activation of DtxR-like proteins (D'Aquino et al., 2005; Ranjan et al., 2006). The active form of DtxR is a homodimer, with each monomer consisting

of two domains connected by a flexible tether of 23 amino acids that contains a proline-rich region (Qiu et al., 1995; Schiering et al., 1995). The N-terminal domain contains the helix-turn-helix motif responsible for DNA binding as well as two metal ion binding sites (Fig. 1). The ancillary binding site (site 1) binds Fe^{2+} with high affinity (K_d = 2 x 10^{-7} M for Ni^{2+}, (D'Aquino et al., 2005)) and, when occupied, stabilizes the monomeric form of the repressor. When the iron concentration increases, the primary binding site (site 2), a low affinity Fe^{2+} binding site (K_d = 6.3 x 10^{-4} M for Ni^{2+}, (D'Aquino et al., 2005)), is occupied, leading to conformational changes in the N-terminal region and subsequently dimerization of the protein. Besides Fe^{2+}, several other divalent metal ions can activate the binding of DtxR to its target promoters *in vitro*, preferred in the following order Fe^{2+} ~ Ni^{2+} > Co^{2+} >> Mn^{2+} (Spiering et al., 2003; Tao and Murphy, 1992). The C-terminal domain has been shown to be structurally similar to eukaryotic SH3 domains (Qiu *et al.*, 1995). So far, the function of this domain is not completely understood. Although contributing two ligands (Glu170 and Gln173) to the ancillary ion binding site, studies with mutants lacking this domain indicate that it is not essential for DNA binding (Posey et al., 1999).

Crystal structures of the complex of metal-ion activated DtxR and a DNA fragment containing the *tox* operator have shown that two DtxR dimers interact with the target DNA at almost opposite sites of the DNA and do not interact with each other (Pohl et al., 1999; White et al., 1998). The minimal essential nucleotide sequence for DtxR binding is a 9-bp inverted repeat with an 1-bp gap (TWAGGTWAGSCTWACCTWA, Fig. 1) (Tao and Murphy, 1994).

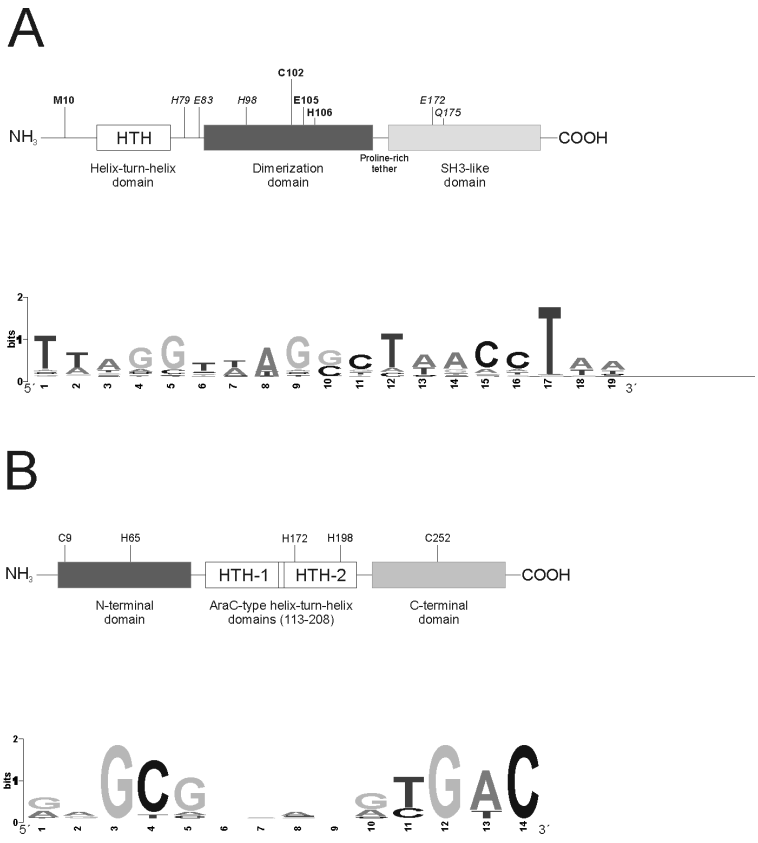

Fig. 1: Domain structure and consensus DNA binding site of DtxR (A) and RipA (B) from *C. glutamicum*. In the structure of DtxR, amino acids printed in *italic* are ligands of the ancillary metal-binding site (site 1) and amino acids printed in bold constitute the primary binding site (site 2). The functional significance of the cysteine and histidine residues in the domain structure of RipA is not clear yet. They could be involved in binding of a metal ion. The presentation of the consensus binding sites were obtained using the WEBLOGO tool (Crooks et al., 2004). In the case of DtxR, the 52 binding sites shown in Table 3 of (Wennerhold and Bott, 2006) were used to derive a consensus motif; in the case of RipA the 13 binding sites shown in Fig. 7 of (Wennerhold et al., 2005).

The DtxR regulon of* C. glutamicum*: genes repressed by DtxR. The genome of the *C. glutamicum* type strain ATCC13032 (Ikeda and Nakagawa, 2003; Kalinowski et al., 2003) contains a gene (*cg2103*) encoding a transcriptional regulator with 72% sequence identity to the diphtheria toxin repressor DtxR of *C. diphtheriae*. Therefore, it has been assumed that this regulator might carry out a similar regulatory function as DtxR from *C. diphtheriae*. In fact, the corresponding protein from *C. glutamicum* strain ATCC13869 (previously designated "*Brevibacterium lactofermentum*") was shown to bind the diphtheria *tox* promoter/operator in an iron-dependent manner (Oguiza et al., 1995). Recently, the DtxR regulon of *C. glutamicum* ATCC13032 has been determined in two independent studies using comparative transcriptome analysis of *dtxR* deletion mutants with the wild type in combination with computer-based approaches and *in vitro* binding studies in order to identify functional DtxR binding sites in the genome (Brune *et al.*, 2006a; Wennerhold and Bott, 2006). The results of these studies revealed that more than 50 genes are repressed by DtxR (Fig. 2).

The majority of these genes encode proteins involved in iron acquisition, such as four ABC transporters (permease and ATPase) for siderophore uptake, seven secreted siderophore-binding lipoproteins, three cytoplasmic siderophore interacting proteins, one ABC transporter for heme uptake (permease and ATPase), a secreted heme-binding lipoprotein, four proteins presumably associated in an unknown manner with heme transport, and heme oxygenase. Several genes repressed by DtxR encode proteins that are not obviously related to iron metabolism. These include two putative copper-transporting P-type ATPases, a putative resolvase, a putative secretory serine protease, a putative UDP-glucose-6-dehydrogenase, or a putative Zn-dependent oxidoreductase. The genes *cysI* (*cg3118*) and *cysJ* (*cg3119*) encode a putative sulfite reductase and a putative NADPH-ferredoxin reductase, respectively, and showed increased mRNA levels in one of the *dtxR* deletion mutants analyzed (Brune *et al.*, 2006a). Further studies are required to understand the increased expression of these genes under iron limitation. Interestingly, three genes repressed by DtxR encode themselves transcriptional regulators, adding a further level of complexity to the DtxR regulon. These are *ripA* (*cg1120*), *cg0527* encoding an ArsR-type regulator, and the response regulator *cgtR11* belonging to the CgtSR11 two-component signal transduction system (Kocan *et al.*, 2006a). Whereas the regulons of Cg0527 and CgtR11 are not yet known, that of RipA was identified recently and will be described in detail later in this chapter (Wennerhold et al., 2005).

The DtxR regulon of* C. glutamicum*: genes presumably activated by DtxR. The studies on the DtxR regulon revealed that this regulator can function not only as a transcriptional repressor but presumably also as an activator (Brune *et al.*, 2006a; Wennerhold and Bott, 2006). For example the genes *dps* (*cg3327*) and *ftn* (*cg2782*) had an about 10-fold decreased mRNA level in one of the *dtxR* deletion mutants (Brune *et al.*, 2006a). As the *C. glutamicum* Dps protein shows more than 50% sequence identity to *Mycobacterium smegmatis* Dps, which has been characterized structurally and functionally (Ceci *et al.*, 2005a; Gupta *et al.*, 2002b; Gupta and Chatterji, 2003a; Roy *et al.*, 2004b), it presumably has a similar function and protects DNA from oxidative damage by sequestering intracellular Fe^{2+} and storing it in the form of Fe^{3+} oxyhydroxide mineral. Dps catalyzes the oxidation of Fe^{2+} by hydrogen

peroxide: 2 Fe^{2+} + H_2O_2 + 2 H^+ → 2 Fe^{3+} + 2 H_2O. In this way, it prevents hydroxyl radical formation by the Fenton reaction and protects DNA from hydroxyl radical-mediated cleavage. Dps binds DNA with no apparent sequence specificity. In contrast to Dps, the sole function of ferritin is presumably restricted to iron storage. In *M. tuberculosis* it has been demonstrated that expression of the bacterioferritin-encoding gene *bfrA* and of the ferritin-encoding gene *bfrB* is activated by binding of the DtxR-homolog IdeR to a double iron box located 106 bp upstream of the transcriptional start site (Gold et al., 2001; Rodriguez and Smith, 2003). In *C. glutamicum* the DtxR binding sites in the promoter regions of *ftn* and *dps* were also located upstream of the -35 region, supporting an activating function of DtxR (Brune *et al*., 2006a).

The synthesis of iron-sulfur clusters is usually also tightly regulated in response to iron availability and oxidative stress, since many iron-sulfur proteins play important roles in central metabolic pathways. A functional DtxR binding site has been identified in the upstream region of the *suf* operon in *C. glutamicum*. This operon consists of seven genes (*cg1765 – cg1759*) which showed an approx. twofold decreased mRNA level in one of the *dtxR* deletion mutants (Wennerhold and Bott, 2006). With the exception of the first gene, designated here as *sufR*, the proteins encoded by this operon are presumably involved in the assembly and repair of iron-sulfur clusters, constituting the so-called SUF operon in *C. glutamicum*. Recently, it has been shown that the SUF proteins of *M. tuberculosis* constitute the sole machinery for iron-sulfur cluster assembly in this organism (Huet et al., 2005). A similar situation can be assumed for *C. glutamicum*, since analysis of the genome sequence gave no evidence for alternative genes involved in iron-sulfur cluster assembly, e.g. genes encoding proteins of the Isc or Nif machinery (Johnson et al., 2005). Activation of the *suf* operon by DtxR might be explained by the fact that under conditions of sufficient iron supply, higher levels of several prominent iron-sulfur-cluster-containing proteins are formed, *e.g*. aconitase or succinate dehydrogenase, requiring higher levels of the SUF machinery. Curiously, the mRNA level of the *suf* genes was decreased in the Δ*dtxR* mutant not only under iron excess, but also under iron limitation (Wennerhold and Bott, 2006). Therefore, the role of DtxR in regulation of the *suf* operon is not completely clear. The first gene of the *C. glutamicum suf* operon encodes a transcriptional regulator of the DeoR family. It might regulate the expression of the *suf* operon in response to the cellular demand for iron-sulfur cluster assembly and repair, similar to the regulators IscR of *E. coli* (Giel et al., 2006; Schwartz et al., 2001; Yeo et al., 2006) or SufR of *Synechocystis* (Wang et al., 2004). Thus, expression of the *suf* operon of *C. glutamicum* is presumably regulated by two regulators, DtxR and SufR.

An interesting gene cluster with respect to iron-dependent regulation in *C. glutamicum* is the *sdhCAB* operon encoding succinate dehydrogenase. A functional DtxR binding site was identified 105 bp (with respect to the center of the 19-bp binding site) upstream of the transcriptional start site of *sdhC*, which suggests a transcriptional activation of *sdhCAB* by DtxR. The *sdhCAB* mRNA level was indeed about 5-fold reduced in the Δ*dtxR* mutant, however, this effect is most likely due to repression by RipA (see below) rather than to a missing activation by DtxR (Brune *et al*., 2006a; Wennerhold and Bott, 2006). Further studies are required to elucidate the direct influence of DtxR on *sdhCAB* expression.

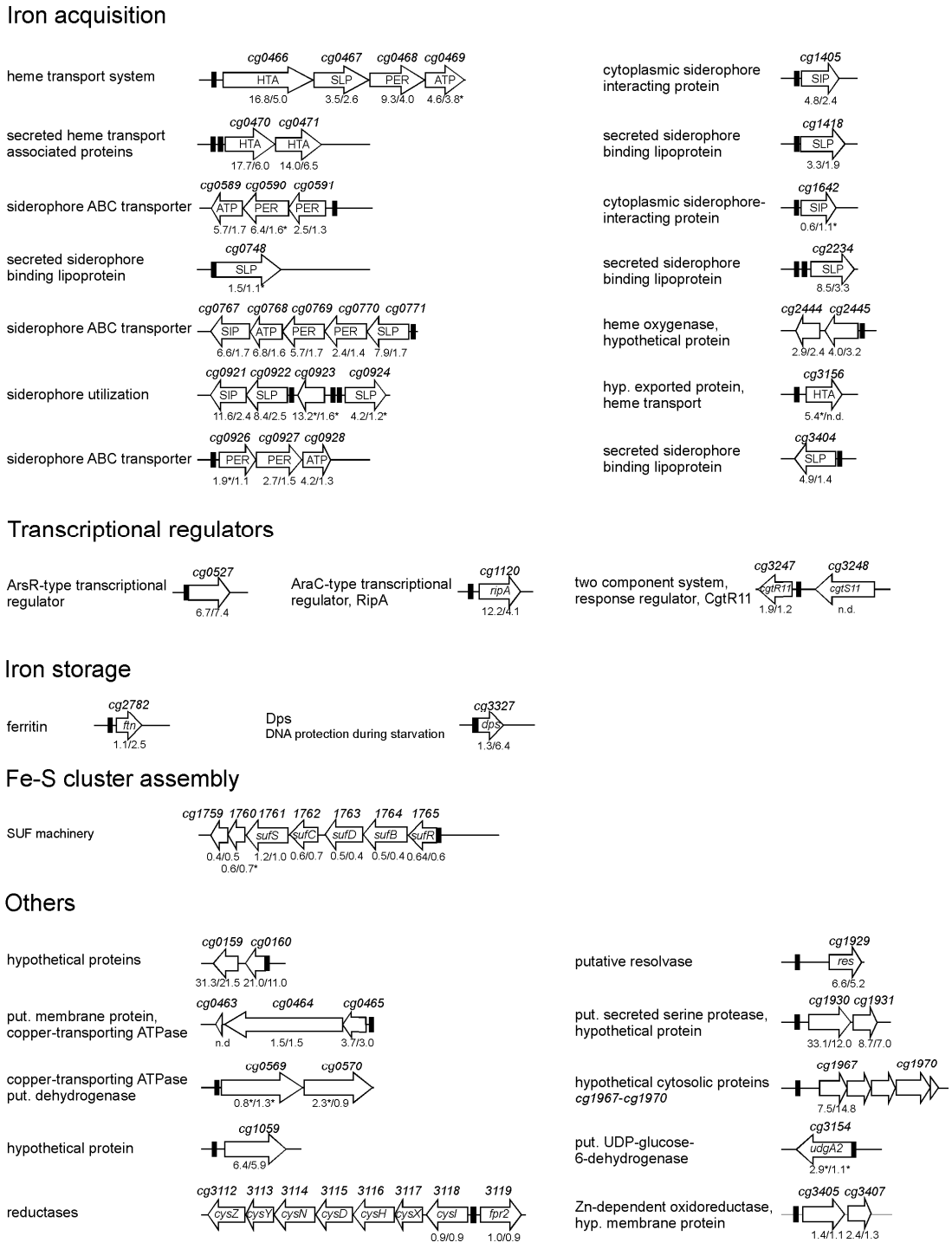

Fig.2: The DtxR regulon of *Corynebacterium glutamicum*. Overview on those *C. glutamicum* genes or gene clusters that are preceded by a functional DtxR binding site and showed altered mRNA levels in a *dtxR* deletion mutant (Wennerhold and Bott, 2006). The black boxes indicate the position of the identified DtxR boxes. The mRNA ratios (Δ*dtxR* mutant *vs.* wild type) obtained from DNA microarray experiments are shown below the corresponding gene. The first value gives the ratio under iron excess (100 µM $FeSO_4$ in the growth medium), the second value gives the ratio under iron limitation (1 µM $FeSO_4$). It has to be taken into account that for the majority of genes the indicated function was derived from the genome annotation rather than from experimental data. Additional genes which are preceded by a functional DtxR binding site have been omitted here, since their mRNA level was unchanged in a *dtxR* deletion mutant (Wennerhold and Bott, 2006). In the case of the genes *cg3115-cg3119*, increased mRNA levels in a Δ*dtxR* mutant were reported by (Brune *et al.*, 2006a).

***DtxR – the master regulator of iron metabolism in* C. glutamicum.** Based on the results described above, DtxR obviously is the master regulator of iron metabolism in *C. glutamicum*, controlling directly more than 60 genes (Fig. 2). Its activity is determined by the occupation of a low affinity Fe^{2+} binding site and therefore by the cytoplasmic Fe^{2+} concentration, which thus seems to represent the decisive signal that reflects the cellular iron supply. Since at least three of the target genes that are repressed by DtxR function as transcriptional regulators (*ripA*, *cgtR11*, *cg0527*) by themselves, a set of further genes is controlled indirectly by DtxR.

RipA, a regulator of iron proteins. The *cg1120* gene of *C. glutamicum* encodes an AraC-type regulator (Fig. 1) and was first noticed in DNA microarray experiments comparing cells grown under iron limitation and iron excess, where the *cg1120* mRNA level was strongly increased under iron limitation (Krug et al., 2005). At the same time, the mRNA of several genes encoding iron-containing proteins (*e.g* aconitase, succinate dehydrogenase and nitrate reductase) was decreased under iron limitation. Therefore, this regulator was considered as a candidate for repressing the iron protein-encoding genes and was subsequently named RipA for "regulator of iron proteins A". A *ripA* deletion mutant showed a growth defect under iron limitation, but not under iron excess (Wennerhold et al. 2005). Under iron limitation, the aconitase activity was ~2-fold higher in the Δ*ripA* mutant (~0.2 U (mg protein)$^{-1}$) than in the wild type (~0.1 U (mg protein)$^{-1}$), whereas it was similar under iron excess (~0.3 U (mg protein)$^{-1}$), supporting a repressor function of RipA. In a transcriptome comparison of Δ*ripA* mutant *vs*. wild type, about a dozen genes showed 2- to 4-fold increased mRNA levels in the mutant under iron limitation, but not under iron excess. This group of genes correlated well with those showing a decreased mRNA level in the wild type under iron limitation and included *acn*, *sdhCAB*, *narKGHJI* (nitrate/nitrite transporter and nitrate reductase), *leuCD* (isopropylmalate dehydratase), *catA* (catechol 1,2-dioxygenase), *pta* (phosphotransacetylase), and *katA* (catalase) (Fig. 3). Except for the transporter NarK, phosphotransacetylase and acetate kinase (the *ackA* gene encoding the latter enzyme is co-transcribed with *pta* and presumably also co-regulated), the enzymes encoded by the other genes are known to contain iron. The function of RipA as a repressor of the abovementioned genes under iron limitation was supported by gel shift assays showing that purified RipA binds to the seven corresponding promoter upstream regions. In all cases, evidence for at least two RipA binding sites was obtained and from 13 experimentally verified binding sites the 14-bp consensus motif RRGCGNNNNRYGAC was derived (Fig. 1). AraC-type regulators (Gallegos et al., 1997; Martin and Rosner, 2001) like RipA contain two adjacent helix-turn-helix (HTH) motifs, which in the case of MarA insert in two adjacent segments of the major groove of the *mar* promoter (Rhee et al., 1998). Thus, one HTH region of RipA might interact with the RRGCG motif and the adjacent HTH region with the RYGAC motif. In Fig. 3C, the location and orientation of the RipA binding sites in the seven target promoters is shown. In the case of the *acn* promoter, the experimentally verified RipA binding sites are centered at positions -146.5 and -203.5 with respect to the transcriptional start site, giving rise to the question how RipA exerts its repressing effect. A third putative RipA binding site which begins immediately downstream of the *acn* start codon might be relevant in this context, although a fragment containing only this site was not bound by RipA. In the case of the

sdhCAB promoter, the two RipA binding sites are centered at -42.5 and -123.5 upstream of the transcription start site that was mapped 15 bp upstream of the *sdhC* start codon (Wennerhold and Bott, 2006; Brune et al. 2006). In this case, RipA might interfere with the binding of RNA polymerase. The presence of at least two DNA-binding sites in each RipA target promoter and the large and varying distances between these binding sites suggest that DNA looping might be involved in the mechanism of action of RipA, as reported e.g. for AraC (Lobell and Schleif, 1990).

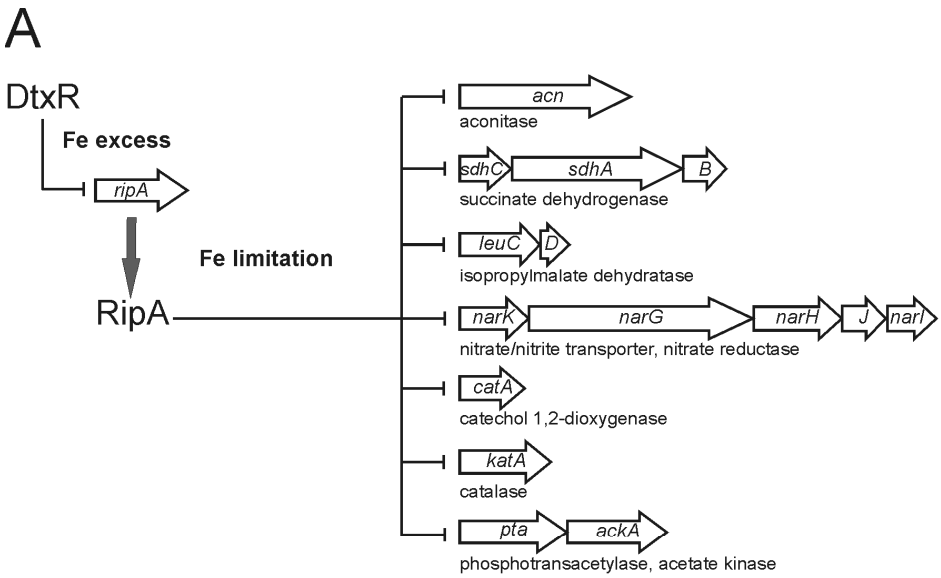

B

Iron cofactors of RipA targets

Aconitase	1x 4Fe-4S cluster
Succinate dehydrogenase	1x 4Fe-4S cluster 1x 3Fe-4S cluster 1x 2Fe-2S cluster 2x heme *b*
Nitrate reductase	3x 4Fe-4S cluster 1x 3Fe-4S cluster 2x heme *b*
Isopropylmalate dehydratase	1x 4Fe-4S cluster
Catechol 1,2-dioxygenase	1Fe per subunit
Catalase	1heme *b* per subunit
Phosphotransacetylase, Acetate kinase	/

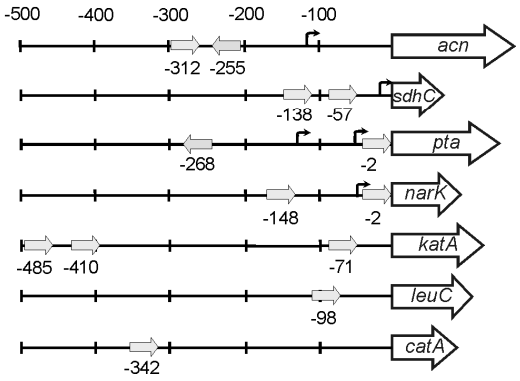

Fig. 3: RipA-dependent regulation of prominent iron proteins in *C. glutamicum*. (A) Under iron excess, DtxR in complex with iron represses transcription of *ripA*. Under iron limitation, the AraC-type regulator RipA is synthesized and represses several genes encoding iron-containing proteins. In this way, RipA reduces the iron expenditure of the cell under iron limitation, which is probably beneficial for survival under this stress condition. (B) Iron cofactors of the proteins controlled by RipA. (C) Localization of the verified RipA binding sites in the promoter regions of its target genes. The orientation of the RipA binding motif within the promoter region is indicated by an arrow. The position beneath the arrows indicates the distance of the center of the binding site to the predicted start codon of the corresponding gene (position +1). For *acn*, *sdhC*, *pta* and *narK*, the transcriptional start sites have been determined experimentally and are indicated by black arrows.

The discovery of RipA as a repressor of iron proteins and its own repression by DtxR has unravelled a new aspect of the regulatory network controlling iron homeostasis in *C. glutamicum*. The reduced synthesis of several important iron proteins of the cell under iron deprivation may serve to reduce iron expenditure and to increase survival. Orthologs of RipA were identified in *Corynebacterium efficiens* (CE1047; 70% sequence identity) and *C. diphtheriae* (DIP0922; 52% sequence identity), but not in *Corynebacterium jeikeium* (Tauch et al., 2005) or *Mycobacterium* species. The *C. efficiens ripA* gene as originally annotated in the genome sequence (Nishio et al., 2003) encodes a protein of 400 amino acids (accession number BAC17857). According to the RipA sequences of *C. glutamicum* and *C. diphtheriae*, it seems more likely that the *C. efficiens* RipA contains only 332 amino acid residues (see accession number Q8FQS2). A well conserved DtxR binding site is centered 50 bp upstream of the ATG start codon of *ripA* (encoding the 332-amino-acid residue RipA protein), indicating repression by DtxR. In *C. diphtheriae*, the annotated genome sequence from strain NCTC13129 predicts that *ripA* (DIP0922) encodes a protein of 335 amino acid residues (Cerdeno-Tarraga et al., 2003). Inspection of the corresponding upstream sequence revealed a putative DtxR binding sites centered 128 bp (TAACCTTAGGCTTGCCTTT) upstream of the proposed start codon. Interestingly, Lee et al. (Lee et al., 1997) previously identified a DtxR-regulated gene region designated IRP3 from *C. diphtheriae* strain C7 which is equivalent to the one described above. The DtxR binding site they identified experimentally by DNase I footprinting (TTAGGTGAGACGCACCCAT) is located upstream of an open reading frame encoding a 124-amino-acid polypeptide showing high identity to regions of *C. glutamicum* RipA (data not shown). The IRP3 DtxR binding site starts 267 bp downstream of the proposed start codon of DIP0922. Further studies are required to determine the relevance of the strain differences and the *in vivo* relevance of the DtxR binding sites. Due to the poor conservation of the RipA binding motif, it is difficult to predict RipA binding sites in *C. efficiens* and *C. diphtheriae* with confidence. Nevertheless, inspection of the promoter regions of potential RipA target genes revealed for example two putative RipA binding sites in front of the *acn* gene of *C. efficiens*, located at position -167 and -308 with respect to the start codon. Therefore, it can be speculated that all *ripA* genes are probably controlled by DtxR and that the RipA proteins presumably have an at least partially overlapping set of target genes.

A regulatory cascade with a similar function as that of DtxR and RipA is found in some Gram-negative bacteria, *e.g. E. coli* or *Pseudomonas aeruginosa* (Masse et al., 2007). In *E. coli* the ferric uptake regulator (Fur) in complex with iron represses a small (s)RNA named RhyB, which stimulates the degradation of mRNAs encoding iron-containing proteins like aconitase A (*acnA*), succinate dehydrogenase (*sdhCDAB*) and the iron storage proteins ferritin (*ftnA*) and bacterioferritin (*bfr*) (Masse et al., 2005).

Possible involvement of the* C. glutamicum *CgtSR11 two-component system in heme-dependent regulation. As described above, *C. glutamicum* possesses genes presumably involved in heme uptake as well as a gene encoding heme oxygenase (*hmuO*), all of which are repressed by DtxR under iron-replete conditions. Heme oxygenases catalyze the degradation of heme to α-biliverdin, accompanied by the liberation of the heme-bound iron. In *C. diphtheriae*, expression of *hmuO* was shown to be repressed by DtxR and induced by

heme or hemoglobin (Schmitt, 1997). Subsequently, a two-component signal transduction system was identified that activated *hmuO* expression in a heme-dependent manner, designated ChrS-ChrA (Schmitt, 1999). However, a significant activation of heme-dependent *hmuO* expression was maintained in *C. diphtheriae* mutants lacking either *chrS* or *chrA*, suggesting the participation of an additional regulatory system in heme- or hemoglobin-dependent regulation (Bibb et al., 2005). Recent studies indeed showed that for full hemoglobin-dependent activation of *hmuO* an additional two-component system is required, designated as HrrS-HrrA, which shares significant sequence similarity to the ChrS-ChrA system (Bibb et al., 2007).

A BLAST search in the *C. glutamicum* genome revealed that both these systems show significant sequence similarity to the two-component system encoded by the *cgtS11-cgtR11* genes. The *cgtR11* gene has already been mentioned as being regulated by DtxR, which binds to a site located in non-coding region between *cgtS11* and *cgtR11*. This indicates the existence of a *cgtR11*-specific promoter. Based on the high sequence identity of CgtS11 to HrrS (56%) and ChrS (30%) and of CgtR11 to HrrA (86%) and ChrA (50%), a function of the *C. glutamicum* CgtS11-CgtR11 system in heme-dependent activation of *hmuO* transcription has been postulated (Wennerhold and Bott, 2006). Recent studies in our laboratory with a *cgtSR11* deletion mutant (Kocan *et al.*, 2006a) supported this suggestion (Frunzke and Bott, unpublished results). Therefore, *hmuO* expression in *C. glutamicum* also appears to be under dual regulation, repressed by DtxR in response to iron availability and activated by the two-component system CgtSR11 in response to heme availability.

3. Concluding remarks and outlook

The large number of *C. glutamicum* genes involved in iron acquisition (Table 1) impressively demonstrates the importance of this element for cellular functionality. Based on the genome sequence, comparative transcriptome analysis, and the definition of the DtxR and RipA regulons, key features of iron metabolism and its regulation in *C. glutamicum* have been elucidated in recent years. These are summarized in the model shown in Fig. 4. However, there are obviously also many aspects that have not been addressed yet, such as the substrate spectrum of the different ABC transporters involved in siderophore transport, the release of iron from the siderophores, the fate of the siderophores after iron release, or the transport of free Fe^{3+} and Fe^{2+}. It is also still unclear how iron is taken up when *C. glutamicum* is grown in the laboratory in a minimal medium with an excess of iron, but without added siderophores, heme, citrate, protocatechuate or catechol. Thus, there is a lot of room for further studies.

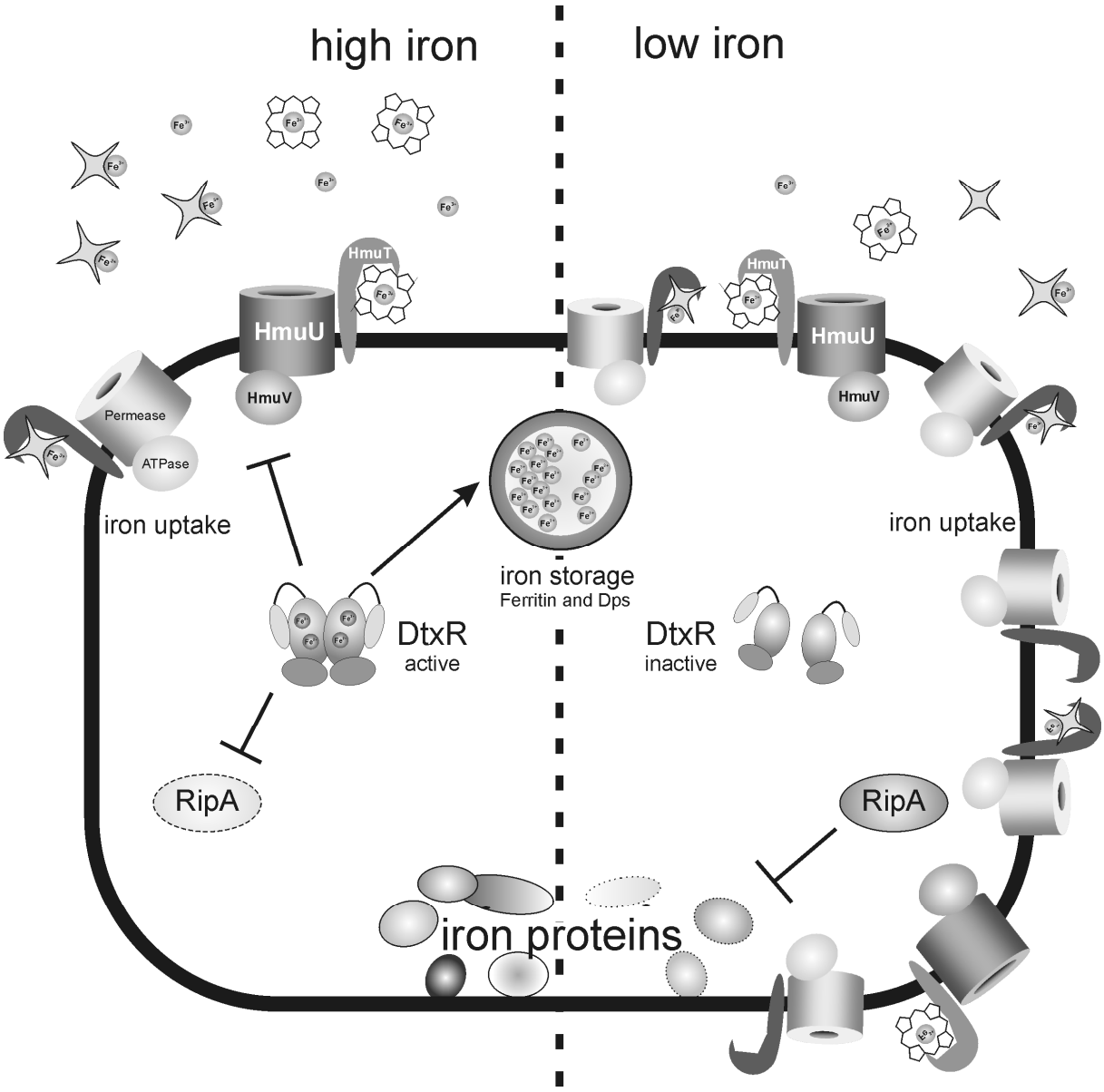

Fig. 4: Model showing key features of iron dependent regulation in *C. glutamicum*. Under iron-replete conditions, DtxR binds iron, dimerizes and becomes active as a transcriptional regulator. It represses genes encoding high affinity iron uptake systems and activates the genes for the iron storage proteins Dps and ferritin. When intracellular iron becomes limiting, Fe^{2+} dissociates at least from the low-affinity primary binding site within DtxR, which then dissociates into its monomeric form and becomes inactive. As a consequence, a large set of proteins involved in iron acquisition is induced, in particular several ABC transporters for siderophores and an ABC transporter for heme, but also the AraC-type regulator RipA. RipA itself is a repressor of genes encoding several prominent iron proteins, *e.g.* aconitase or succinate dehydrogenase, and thereby reduces the iron demand of the cell under iron limitation (see Fig. 3). Blunt-ended lines (⊣) indicate transcriptional repression, arrows (→) stand for transcriptional activation.

References

Alamuri, P., Mehta, N., Burk, A., and Maier, R.J. (2006) Regulation of the *Helicobacter pylori* Fe-S cluster synthesis protein NifS by iron, oxidative stress conditions, and *fur*. *J Bacteriol* 188: 5325-5330.

Alen, C., and Sonenshein, A.L. (1999) *Bacillus subtilis* aconitase is an RNA-binding protein. *Proc Natl Acad Sci U S A* 96: 10412-10417.

Andrews, S.C., Robinson, A.K., and Rodriguez-Quinones, F. (2003) Bacterial iron homeostasis. *FEMS Microbiol Rev* 27: 215-237.

Angerer, A., Gaisser, S., and Braun, V. (1990) Nucleotide sequences of the *sfuA*, *sfuB*, and *sfuC* genes of *Serratia marcescens* suggest a periplasmic-binding-protein-dependent iron transport mechanism. *J Bacteriol* 172: 572-578.

Baichoo, N., Wang, T., Ye, R., and Helmann, J.D. (2002) Global analysis of the *Bacillus subtilis* Fur regulon and the iron starvation stimulon. *Mol Microbiol* 45: 1613-1629.

Banerjee, S., Nandyala, A.K., Raviprasad, P., Ahmed, N., and Hasnain, S.E. (2007) Iron-dependent RNA-binding activity of *Mycobacterium tuberculosis* aconitase. *J Bacteriol* 189: 4046-4052.

Bayan, N., Houssin, C., Chami, M., and Leblon, G. (2003) Mycomembrane and S-layer: two important structures of *Corynebacterium glutamicum* cell envelope with promising biotechnology applications. *J. Biotechnol.* 104: 55-67.

Bibb, L.A., King, N.D., Kunkle, C.A., and Schmitt, M.P. (2005) Analysis of a heme-dependent signal transduction system in *Corynebacterium diphtheriae*: deletion of the *chrAS* genes results in heme sensitivity and diminished heme-dependent activation of the *hmuO* promoter. *Infect Immun* 73: 7406-7412.

Bibb, L.A., Kunkle, C.A., and Schmitt, M.P. (2007) The ChrA-ChrS and HrrA-HrrS Signal Transduction Systems Are Required for Activation of the *hmuO* Promoter and Repression of the hemA Promoter in *Corynebacterium diphtheriae*. *Infect Immun* 75: 2421-2431.

Biville, F., Cwerman, H., Letoffe, S., Rossi, M.S., Drouet, V., Ghigo, J.M., and Wandersman, C. (2004) Haemophore-mediated signalling in *Serratia marcescens*: a new mode of regulation for an extra cytoplasmic function (ECF) sigma factor involved in haem acquisition. *Mol Microbiol* 53: 1267-1277.

Boyd, J., Oza, M.N., and Murphy, J.R. (1990) Molecular cloning and DNA sequence analysis of a diphtheria tox iron-dependent regulatory element (*dtxR*) from *Corynebacterium diphtheriae*. *Proc Natl Acad Sci U S A* 87: 5968-5972.

Brune, I., Werner, H., Hüser, A.T., Kalinowski, J., Pühler, A., and Tauch, A. (2006) The DtxR protein acting as dual transcriptional regulator directs a global regulatory network involved in iron metabolism of *Corynebacterium glutamicum*. *BMC Genomics* 7: 21.

Budzikiewicz, H., Bossenkamp, A., Taraz, K., Pandey, A., and Meyer, J.M. (1997) Corynebactin, a cyclic catecholate siderophore from *Corynebacterium glutamicum* ATCC 14067 (*Brevibacterium* sp. DSM 20411). *Z Naturforsch 52c* 52: 551-554.

Bunny, K., Liu, J., and Roth, J. (2002) Phenotypes of *lexA* mutations in *Salmonella enterica*: evidence for a lethal *lexA* null phenotype due to the Fels-2 prophage. *J Bacteriol* 184: 6235-6249.

Busenlehner, L.S., Pennella, M.A., and Giedroc, D.P. (2003) The SmtB/ArsR family of metalloregulatory transcriptional repressors: Structural insights into prokaryotic metal resistance. *FEMS Microbiol Rev* 27: 131-143.

Cartron, M.L., Maddocks, S., Gillingham, P., Craven, C.J., and Andrews, S.C. (2006) Feo - transport of ferrous iron into bacteria. *Biometals* 19: 143-157.

Casjens, S. (2003) Prophages and bacterial genomics: what have we learned so far? *Mol Microbiol* 49: 277-300.

Ceci, P., Ilari, A., Falvo, E., Giangiacomo, L., and Chiancone, E. (2005) Reassessment of protein stability, DNA binding, and protection of *Mycobacterium smegmatis* Dps. *J. Biol. Chem.* 280: 34776-34785.

Cerdeno-Tarraga, A.M., Efstratiou, A., Dover, L.G., Holden, M.T.G., Pallen, M., Bentley, S.D., Besra, G.S., Churcher, C., James, K.D., De Zoysa, A., Chillingworth, T., Cronin, A., Dowd, L., Feltwell, T., Hamlin, N., Holroyd, S., Jagels, K., Moule, S., Quail, M.A., Rabbinowitsch, E., Rutherford, K.M., Thomson, N.R., Unwin, L., Whitehead, S., Barrell, B.G., and Parkhill, J. (2003) The complete genome sequence and analysis of *Corynebacterium diphtheriae* NCTC13129. *Nucleic Acids Res.* 31: 6516-6523.

Chipperfield, J.R., and Ratledge, C. (2000) Salicylic acid is not a bacterial siderophore: a theoretical study. *Biometals* 13: 165-168.

Cornell, R.M., and Schwertmann, U. (2003) *The Iron Oxides: Structure, Properties, Reactions, Occurrences and Uses*: Wiley-VCH.

Costa-Riu, N., Burkovski, A., Krämer, R., and Benz, R. (2003) PorA represents the major cell wall channel of the Gram-positive bacterium *Corynebacterium glutamicum*. *J. Bacteriol.* 185: 4779-4786.

Courville, P., Chaloupka, R., and Cellier, M.F. (2006) Recent progress in structure-function analyses of Nramp proton-dependent metal-ion transporters. *Biochem Cell Biol* 84: 960-978.

Cox, M.M. (2007) Regulation of bacterial RecA protein function. *Crit Rev Biochem Mol Biol* 42: 41-63.

Crooks, G.E., Hon, G., Chandonia, J.M., and Brenner, S.E. (2004) WebLogo: A sequence logo generator. *Genome Res.* 14: 1188-1190.

D'Aquino, J.A., Tetenbaum-Novatt, J., White, A., Berkovitch, F., and Ringe, D. (2005) Mechanism of metal ion activation of the diphtheria toxin repressor DtxR. *Proc Natl Acad Sci U S A* 102: 18408-18413.

Delany, I., Rappuoli, R., and Scarlato, V. (2004) Fur functions as an activator and as a repressor of putative virulence genes in *Neisseria meningitidis*. *Mol Microbiol* 52: 1081-1090.

Dertz, E.A., Stintzi, A., and Raymond, K.N. (2006) Siderophore-mediated iron transport in *Bacillus subtilis* and *Corynebacterium glutamicum*. *J Biol Inorg Chem* 11: 1087-1097.

Drazek, E.S., Hammack, C.A., and Schmitt, M.P. (2000) *Corynebacterium diphtheriae* genes required for acquisition of iron from haemin and haemoglobin are homologous to ABC haemin transporters. *Mol Microbiol* 36: 68-84.

Edelman, L.M., Cheong, R., and Kahn, J.D. (2003) Fluorescence resonance energy transfer over approximately 130 basepairs in hyperstable lac repressor-DNA loops. *Biophys J* 84: 1131-1145.

Eggeling, L., and Bott, M. (2005) *Handbook of Corynebacterium glutamicum*. Inc., Boca Raton, FL: Academic Press.

Eisenstein, R.S. (2000) Iron regulatory proteins and the molecular control of mammalian iron metabolism. *Annu Rev Nutr* 20: 627-662.

Escolar, L., Perez-Martin, J., and de Lorenzo, V. (1999) Opening the iron box: transcriptional metalloregulation by the Fur protein. *J Bacteriol* 181: 6223-6229.

Faraldo-Gomez, J.D., and Sansom, M.S. (2003) Acquisition of siderophores in gram-negative bacteria. *Nat Rev Mol Cell Biol* 4: 105-116.

Fontecave, M., Choudens, S.O., Py, B., and Barras, F. (2005) Mechanisms of iron-sulfur cluster assembly: the SUF machinery. *J Biol Inorg Chem*: 1-9.

Gallegos, M.T., Schleif, R., Bairoch, A., Hofmann, K., and Ramos, J.L. (1997) Arac/XylS family of transcriptional regulators. *Microbiol Mol Biol Rev* 61: 393-410.

Giel, J.L., Rodionov, D., Liu, M.Z., Blattner, F.R., and Kiley, P.J. (2006) IscR-dependent gene expression links iron-sulphur cluster assembly to the control of O_2-regulated genes in *Escherichia coli*. *Mol. Microbiol.* 60: 1058-1075.

Gold, B., Rodriguez, G.M., Marras, S.A., Pentecost, M., and Smith, I. (2001) The *Mycobacterium tuberculosis* IdeR is a dual functional regulator that controls transcription of genes involved in iron acquisition, iron storage and survival in macrophages. *Mol Microbiol* 42: 851-865.

Gupta, S., Pandit, S.B., Srinivasan, N., and Chatterji, D. (2002) Proteomics analysis of carbon-starved *Mycobacterium smegmatis*: induction of Dps-like protein. *Protein Eng.* 15: 503-511.

Gupta, S., and Chatterji, D. (2003) Bimodal protection of DNA by *Mycobacterium smegmatis* DNA-binding protein from stationary phase cells. *J. Biol. Chem.* 278: 5235-5241.

Hantke, K. (2001) Iron and metal regulation in bacteria. *Curr Opin Microbiol* 4: 172-177.

Hornung, J.M., Jones, H.A., and Perry, R.D. (1996) The *hmu* locus of *Yersinia pestis* is essential for utilization of free haemin and haem-protein complexes as iron sources. *Mol. Microbiol.* 20: 725-739.

Huet, G., Daffe, M., and Saves, I. (2005) Identification of the *Mycobacterium tuberculosis* SUF machinery as the exclusive mycobacterial system of [Fe-S] cluster assembly: evidence for its implication in the pathogen's survival. *J Bacteriol* 187: 6137-6146.

Hünten, P., Costa-Riu, N., Palm, D., Lottspeich, F., and Benz, R. (2005) Identification and characterization of PorH, a new cell wall channel of *Corynebacterium glutamicum*. *Biochim. Biophys. Acta* 1715: 25-36.

Ikeda, M., and Nakagawa, S. (2003) The *Corynebacterium glutamicum* genome: features and impacts on biotechnological processes. *Appl Microbiol Biotechnol* 62: 99-109.

Janakiraman, A., and Slauch, J.M. (2000) The putative iron transport system SitABCD encoded on SPI1 is required for full virulence of *Salmonella typhimurium*. *Mol Microbiol* 35: 1146-1155.

Johnson, A.D., Poteete, A.R., Lauer, G., Sauer, R.T., Ackers, G.K., and Ptashne, M. (1981) lambda Repressor and cro--components of an efficient molecular switch. *Nature* 294: 217-223.

Johnson, D.C., Dean, D.R., Smith, A.D., and Johnson, M.K. (2005) Structure, function, and formation of biological iron-sulfur clusters. *Annu Rev Biochem* 74: 247-281.

Kalinowski, J., Bathe, B., Bartels, D., Bischoff, N., Bott, M., Burkovski, A., Dusch, N., Eggeling, L., Eikmanns, B.J., Gaigalat, L., Goesmann, A., Hartmann, M., Huthmacher, K., Krämer, R., Linke, B., McHardy, A.C., Meyer, F., Möckel, B., Pfefferle, W., Pühler, A., Rey, D.A., Rückert, C., Rupp, O., Sahm, H., Wendisch, V.F., Wiegräbe, I., and Tauch, A. (2003) The complete *Corynebacterium glutamicum* ATCC 13032 genome sequence and its impact on the production of L-aspartate-derived amino acids and vitamins. *J Biotechnol* 104: 5-25.

Keilhauer, C., Eggeling, L., and Sahm, H. (1993) Isoleucine synthesis in *Corynebacterium glutamicum*: molecular analysis of the *ilvB-ilvN-ilvC* operon. *J Bacteriol* 175: 5595-5603.

Kelley, W.L. (2006) Lex marks the spot: the virulent side of SOS and a closer look at the LexA regulon. *Mol Microbiol* 62: 1228-1238.

Kim, B., and Little, J.W. (1993) LexA and lambda Cl repressors as enzymes: specific cleavage in an intermolecular reaction. *Cell* 73: 1165-1173.

King, N.D., Kirby, A.E., and Connell, T.D. (2005) Transcriptional control of the *rhuIR-bhuRSTUV* heme acquisition locus in *Bordetella avium*. *Infect Immun* 73: 1613-1624.

Kinoshita, S., Udaka, S., and Shimono, M. (1957) Studies on the amino acid fermentation: I. Production of L-glutamic acid by various microorganisms. *J Gen Appl Microbiol* 3: 193-205.

Klausner, R.D., and Rouault, T.A. (1993) A double life: cytosolic aconitase as a regulatory RNA binding protein. *Mol Biol Cell* 4: 1-5.

Kocan, M., Schaffer, S., Ishige, T., Sorger-Herrmann, U., Wendisch, V.F., and Bott, M. (2006) Two-component systems of *Corynebacterium glutamicum*: deletion analysis and involvment of the PhoS-PhoR system in the phosphate starvation response. *J Bacteriol* 188: in press.

Koster, W. (2005) Cytoplasmic membrane iron permease systems in the bacterial cell envelope. *Front Biosci* 10: 462-477.

Krug, A. (2004) Identifizierung und Charakterisierung eines Transkriptionsregulators der Aconitase von *Corynebacterium glutamicum*. In *Mathematisch-Naturwissenschaftlische-Fakultät* Düsseldorf: Heinrich-Heine Universität.

Krug, A., Wendisch, V.F., and Bott, M. (2005) Identification of AcnR, a TetR-type repressor of the aconitase gene *acn* in *Corynebacterium glutamicum*. *J Biol Chem* 280: 585-595.

Kunkle, C.A., and Schmitt, M.P. (2003) Analysis of the *Corynebacterium diphtheriae* DtxR regulon: identification of a putative siderophore synthesis and transport system that is similar to the Yersinia high-pathogenicity island-encoded yersiniabactin synthesis and uptake system. *J Bacteriol* 185: 6826-6840.

Kunkle, C.A., and Schmitt, M.P. (2005) Analysis of a DtxR-regulated iron transport and siderophore biosynthesis gene cluster in *Corynebacterium diphtheriae*. *J Bacteriol* 187: 422-433.

Lamont, I., Brumby, A.M., and Egan, J.B. (1989) UV induction of coliphage 186: prophage induction as an SOS function. *Proc Natl Acad Sci U S A* 86: 5492-5496.

Lee, J.H., Wang, T., Ault, K., Liu, J., Schmitt, M.P., and Holmes, R.K. (1997) Identification and characterization of three new promoter/operators from *Corynebacterium diphtheriae* that are regulated by the diphtheria toxin repressor (DtxR) and iron. *Infect Immun* 65: 4273-4280.

Lee, J.W., and Helmann, J.D. (2007) Functional specialization within the Fur family of metalloregulators. *Biometals* 20: 485-499.

Liebl, W., Klamer, R., and Schleifer, K.H. (1989) Requirement of chelating compounds for the growth of *Corynebacterium glutamicum* in synthetic media. *Appl Microbiol Biotechnol* 32: 205-210.

Lin, H., Fischbach, M.A., Liu, D.R., and Walsh, C.T. (2005) *In vitro* characterization of salmochelin and enterobactin trilactone hydrolases IroD, IroE, and Fes. *J. Am. Chem. Soc.* 127: 11075-11084.

Little, J.W., and Mount, D.W. (1982) The SOS regulatory system of *Escherichia coli*. *Cell* 29: 11-22.

Little, J.W. (1984) Autodigestion of lexA and phage lambda repressors. *Proc Natl Acad Sci U S A* 81: 1375-1379.

Lobell, R.B., and Schleif, R.F. (1990) DNA looping and unlooping by AraC protein. *Science* 250: 528-532.

Lyubchenko, Y.L., Jacobs, B.L., Lindsay, S.M., and Stasiak, A. (1995) Atomic force microscopy of nucleoprotein complexes. *Scanning Microsc* 9: 705-724; discussion 724-707.

Makui, H., Roig, E., Cole, S.T., Helmann, J.D., Gros, P., and Cellier, M.F. (2000) Identification of the *Escherichia coli* K-12 Nramp orthologue (MntH) as a selective divalent metal ion transporter. *Mol. Microbiol.* 35: 1065-1078.

Malik, M., Zhao, X., and Drlica, K. (2006) Lethal fragmentation of bacterial chromosomes mediated by DNA gyrase and quinolones. *Mol Microbiol* 61: 810-825.

Mardanov, A.V., and Ravin, N.V. (2007) The antirepressor needed for induction of linear plasmid-prophage N15 belongs to the SOS regulon. *J Bacteriol* 189: 6333-6338.

Martin, R.G., and Rosner, J.L. (2001) The AraC transcriptional activators. *Curr Opin Microbiol* 4: 132-137.

Masse, E., and Gottesman, S. (2002) A small RNA regulates the expression of genes involved in iron metabolism in *Escherichia coli*. *Proc Natl Acad Sci U S A* 99: 4620-4625.

Masse, E., Vanderpool, C.K., and Gottesman, S. (2005) Effect of RyhB small RNA on global iron use in *Escherichia coli*. *J Bacteriol* 187: 6962-6971.

Masse, E., Salvail, H., Desnoyers, G., and Arguin, M. (2007) Small RNAs controlling iron metabolism. *Curr Opin Microbiol* 10: 140-145.

Matthews, K.S. (1992) DNA looping. *Microbiol Rev* 56: 123-136.

May, J.J., Wendrich, T.M., and Marahiel, M.A. (2001) The *dhb* operon of *Bacillus subtilis* encodes the biosynthetic template for the catecholic siderophore 2,3-dihydroxybenzoate-glycine-threonine trimeric ester bacillibactin. *J Biol Chem* 276: 7209-7217.

McHugh, J.P., Rodriguez-Quinones, F., Abdul-Tehrani, H., Svistunenko, D.A., Poole, R.K., Cooper, C.E., and Andrews, S.C. (2003) Global iron-dependent gene regulation in *Escherichia coli*. A new mechanism for iron homeostasis. *J Biol Chem* 278: 29478-29486.

Merkens, H., Beckers, G., Wirtz, A., and Burkovski, A. (2005) Vanillate metabolism in *Corynebacterium glutamicum*. *Curr. Microbiol.* 51: 59-65.

Miethke, M., Klotz, O., Linne, U., May, J.J., Beckering, C.L., and Marahiel, M.A. (2006) Ferri-bacillibactin uptake and hydrolysis in *Bacillus subtilis*. *Mol Microbiol* 61: 1413-1427.

Nakayama, K., Kinoshita, S., and Sato, Z. (1964a) Growth of glutamic acid producing bacterium and related bacteria. 1. Effect of iron salts, ferrichrome, amino acids and some other compounds. *J. Gen. Appl. Microbiol.* 10: 143-155.

Nakayama, K., Sato, Z., Kinoshita, S., and Tanaka, H. (1964b) Growth of glutamic acid producing bacterium and related bacteria. 2. Effect of chelating agent and its relation to inorganic salt. *J. Gen. Appl. Microbiol.* 10: 181-199.

Nishio, Y., Nakamura, Y., Kawarabayasi, Y., Usuda, Y., Kimura, E., Sugimoto, S., Matsui, K., Yamagishi, A., Kikuchi, H., Ikeo, K., and Gojobori, T. (2003) Comparative complete genome sequence analysis of the amino acid replacements responsible for the thermostability of *Corynebacterium efficiens*. *Genome Res.* 13: 1572-1579.

Ochsner, U.A., Wilderman, P.J., Vasil, A.I., and Vasil, M.L. (2002) GeneChip expression analysis of the iron starvation response in *Pseudomonas aeruginosa*: identification of novel pyoverdine biosynthesis genes. *Mol Microbiol* 45: 1277-1287.

Oguiza, J.A., Tao, X., Marcos, A.T., Martin, J.F., and Murphy, J.R. (1995) Molecular cloning, DNA sequence analysis, and characterization of the *Corynebacterium diphtheriae dtxR* homolog from *Brevibacterium lactofermentum*. *J Bacteriol* 177: 465-467.

Oppenheim, A.B., Kobiler, O., Stavans, J., Court, D.L., and Adhya, S. (2005) Switches in bacteriophage lambda development. *Annu Rev Genet* 39: 409-429.

Ortiz de Orue Lucana, D., Zou, P., Nierhaus, M., and Schrempf, H. (2005) Identification of a novel two-component system SenS/SenR modulating the production of the catalase-peroxidase CpeB and the haem-binding protein HbpS in *Streptomyces reticuli*. *Microbiology* 151: 3603-3614.

Pantopoulos, K. (2004) Iron metabolism and the IRE/IRP regulatory system: an update. *Ann N Y Acad Sci* 1012: 1-13.

Pappenheimer, A.M., and Johnson, S.J. (1936) Studies in diphtheria toxin production. I : The effect of iron and copper. *B. J. Exp. Pathol.* 17: 335-341.

Patzer, S.I., and Hantke, K. (2001) Dual repression by Fe(2+)-Fur and Mn(2+)-MntR of the *mntH* gene, encoding an NRAMP-like Mn(2+) transporter in *Escherichia coli*. *J Bacteriol* 183: 4806-4813.

Pierre, J.L., and Fontecave, M. (1999) Iron and activated oxygen species in biology: the basic chemistry. *Biometals* 12: 195-199.

Pohl, E., Holmes, R.K., and Hol, W.G. (1999) Crystal structure of a cobalt-activated diphtheria toxin repressor-DNA complex reveals a metal-binding SH3-like domain. *J Mol Biol* 292: 653-667.

Polen, T., Schluesener, D., Poetsch, A., Bott, M., and Wendisch, V.F. Characterization of citrate utilization in *Corynebacterium glutamicum* by transcriptome and proteome analysis. *FEMS Microbiol. Lett.* in press.

Polen, T., Schluesener, D., Poetsch, A., Bott, M., and Wendisch, V.F. (2007) Characterization of citrate utilization in *Corynebacterium glutamicum* by transcriptome and proteome analysis. *FEMS Microbiol Lett* 273: 109-119.

Posey, J.E., Hardham, J.M., Norris, S.J., and Gherardini, F.C. (1999) Characterization of a manganese-dependent regulatory protein, TroR, from *Treponema pallidum*. *Proc Natl Acad Sci U S A* 96: 10887-10892.

Postle, K., and Kadner, R.J. (2003) Touch and go: tying TonB to transport. *Mol Microbiol* 49: 869-882.

Puech, V., Chami, M., Lemassu, A., Laneelle, M.A., Schiffler, B., Gounon, P., Bayan, N., Benz, R., and Daffe, M. (2001) Structure of the cell envelope of corynebacteria: importance of the non-covalently bound lipids in the formation of the cell wall permeability barrier and fracture plane. *Microbiology* 147: 1365-1382.

Puig, S., Askeland, E., and Thiele, D.J. (2005) Coordinated remodeling of cellular metabolism during iron deficiency through targeted mRNA degradation. *Cell* 120: 99-110.

Qiu, X., Verlinde, C.L., Zhang, S., Schmitt, M.P., Holmes, R.K., and Hol, W.G. (1995) Three-dimensional structure of the diphtheria toxin repressor in complex with divalent cation co-repressors. *Structure* 3: 87-100.

Que, Q., and Helmann, J.D. (2000) Manganese homeostasis in *Bacillus subtilis* is regulated by MntR, a bifunctional regulator related to the diphtheria toxin repressor family of proteins. *Mol Microbiol* 35: 1454-1468.

Quinones, M., Kimsey, H.H., and Waldor, M.K. (2005) LexA cleavage is required for CTX prophage induction. *Mol Cell* 17: 291-300.

Ranjan, S., Yellaboina, S., and Ranjan, A. (2006) IdeR in mycobacteria: from target recognition to physiological function. *Crit Rev Microbiol* 32: 69-75.

Rhee, S., Martin, R.G., Rosner, J.L., and Davies, D.R. (1998) A novel DNA-binding motif in MarA: the first structure for an AraC family transcriptional activator. *Proc Natl Acad Sci U S A* 95: 10413-10418.

Rodriguez, G.M., Voskuil, M.I., Gold, B., Schoolnik, G.K., and Smith, I. (2002) *ideR*, An essential gene in *Mycobacterium tuberculosis*: role of IdeR in iron-dependent gene expression, iron metabolism, and oxidative stress response. *Infect Immun* 70: 3371-3381.

Rodriguez, G.M., and Smith, I. (2003) Mechanisms of iron regulation in mycobacteria: role in physiology and virulence. *Mol Microbiol* 47: 1485-1494.

Rodriguez, G.M. (2006) Control of iron metabolism in *Mycobacterium tuberculosis*. *Trends Microbiol* 14: 320-327.

Rouault, T.A. (2006) The role of iron regulatory proteins in mammalian iron homeostasis and disease. *Nat Chem Biol* 2: 406-414.

Roy, S., Gupta, S., Das, S., Sekar, K., Chatterji, D., and Vijayan, M. (2004) X-ray analysis of *Mycobacterium smegmatis* Dps and a comparative study involving other Dps and Dps-like molecules. *J. Mol. Biol.* 339: 1103-1113.

Rudolph, G., Hennecke, H., and Fischer, H.M. (2006) Beyond the Fur paradigm: iron-controlled gene expression in rhizobia. *FEMS Microbiol Rev* 30: 631-648.

Saiz, L., and Vilar, J.M. (2006) DNA looping: the consequences and its control. *Curr Opin Struct Biol* 16: 344-350.

Schiering, N., Tao, X., Zeng, H., Murphy, J.R., Petsko, G.A., and Ringe, D. (1995) Structures of the apo- and the metal ion-activated forms of the diphtheria *tox* repressor from *Corynebacterium diphtheriae*. *Proc Natl Acad Sci U S A* 92: 9843-9850.

Schmitt, M.P., and Holmes, R.K. (1991) Iron-dependent regulation of diphtheria toxin and siderophore expression by the cloned *Corynebacterium diphtheriae* repressor gene *dtxR* in *C. diphtheriae* C7 strains. *Infect Immun* 59: 1899-1904.

Schmitt, M.P. (1997) Utilization of host iron sources by *Corynebacterium diphtheriae*: identification of a gene whose product is homologous to eukaryotic heme oxygenases and is required for acquisition of iron from heme and hemoglobin. *J Bacteriol* 179: 838-845.

Schmitt, M.P. (1999) Identification of a two-component signal transduction system from *Corynebacterium diphtheriae* that activates gene expression in response to the presence of heme and hemoglobin. *J Bacteriol* 181: 5330-5340.

Schmitt, M.P., and Drazek, E.S. (2001) Construction and consequences of directed mutations affecting the hemin receptor in pathogenic *Corynebacterium* species. *J Bacteriol* 183: 1476-1481.

Schröder, I., Johnson, E., and de Vries, S. (2003) Microbial ferric iron reductases. *FEMS Microbiol Rev* 27: 427-447.

Schryvers, A.B., Bonnah, R., Yu, R.H., Wong, H., and Retzer, M. (1998) Bacterial lactoferrin receptors. *Adv Exp Med Biol* 443: 123-133.

Schwartz, C.J., Giel, J.L., Patschkowski, T., Luther, C., Ruzicka, F.J., Beinert, H., and Kiley, P.J. (2001) IscR, an Fe-S cluster-containing transcription factor, represses expression of *Escherichia coli* genes encoding Fe-S cluster assembly proteins. *Proc. Natl. Acad. Sci. USA* 98: 14895-14900.

Shearwin, K.E., Brumby, A.M., and Egan, J.B. (1998) The Tum protein of coliphage 186 is an antirepressor. *J Biol Chem* 273: 5708-5715.

Simpson, W., Olczak, T., and Genco, C.A. (2000) Characterization and expression of HmuR, a TonB-dependent hemoglobin receptor of *Porphyromonas gingivalis*. *J Bacteriol* 182: 5737-5748.

Spiering, M.M., Ringe, D., Murphy, J.R., and Marletta, M.A. (2003) Metal stoichiometry and functional studies of the diphtheria toxin repressor. *Proc Natl Acad Sci U S A* 100: 3808-3813.

Tang, Y., and Guest, J.R. (1999) Direct evidence for mRNA binding and post-transcriptional regulation by *Escherichia coli* aconitases. *Microbiology* 145 (Pt 11): 3069-3079.

Tao, X., and Murphy, J.R. (1992) Binding of the metalloregulatory protein DtxR to the diphtheria *tox* operator requires a divalent heavy metal ion and protects the palindromic sequence from DNase I digestion. *J. Biol. Chem.* 267: 21761-21764.

Tao, X., and Murphy, J.R. (1994) Determination of the minimal essential nucleotide sequence for diphtheria tox repressor binding by in vitro affinity selection. *Proc Natl Acad Sci U S A* 91: 9646-9650.

Tauch, A., Kaiser, O., Hain, T., Goesmann, A., Weisshaar, B., Albersmeier, A., Bekel, T., Bischoff, N., Brune, I., Chakraborty, T., Kalinowski, J., Meyer, F., Rupp, O., Schneiker, S., Viehoever, P., and Pühler, A. (2005) Complete genome sequence and analysis of the multiresistant nosocomial pathogen *Corynebacterium jeikeium* K411, a lipid-requiring bacterium of the human skin flora. *J. Bacteriol.* 187: 4671-4682.

von der Osten, C.H., Gioannetti, C., and Sinskey, A.J. (1989) Design of a defined medium for growth of *Corynebacterium glutamicum* in which citrate facilitates iron uptake. *Biotechnol. Lett.* 11: 11-16.

Waldor, M.K., and Friedman, D.I. (2005) Phage regulatory circuits and virulence gene expression. *Curr Opin Microbiol* 8: 459-465.

Walker, G.C. (1987) The SOS response of *Escherichia coli*. In *Escherichia coli and Salmonella typhimurium*. Ingraham, J.L., Low, K.B., Magasanik, B., Schaechter, M. and Umbarger, H.E. (eds). Washington, DC: American Society for Microbiology, pp. 1346-1357.

Wandersman, C., and Stojiljkovic, I. (2000) Bacterial heme sources: the role of heme, hemoprotein receptors and hemophores. *Curr Opin Microbiol* 3: 215-220.

Wang, T., Shen, G., Balasubramanian, R., McIntosh, L., Bryant, D.A., and Golbeck, J.H. (2004) The *sufR* gene (sll0088 in *Synechocystis* sp. strain PCC 6803) functions as a repressor of the *sufBCDS* operon in iron-sulfur cluster biogenesis in cyanobacteria. *J Bacteriol* 186: 956-967.

Wennerhold, J., Krug, A., and Bott, M. (2005) The AraC-type regulator RipA represses aconitase and other iron proteins from *corynebacterium* under iron limitation and is itself repressed by DtxR. *J Biol Chem* 280: 40500-40508.

Wennerhold, J., and Bott, M. (2006) The DtxR regulon of *Corynebacterium glutamicum*. *J Bacteriol* 188: 2907-2918.

White, A., Ding, X., vanderSpek, J.C., Murphy, J.R., and Ringe, D. (1998) Structure of the metal-ion-activated diphtheria toxin repressor/tox operator complex. *Nature* 394: 502-506.

Wilson, T.J., Bertrand, N., Tang, J.L., Feng, J.X., Pan, M.Q., Barber, C.E., Dow, J.M., and Daniels, M.J. (1998) The *rpfA* gene of *Xanthomonas campestris* pathovar campestris, which is involved in the regulation of pathogenicity factor production, encodes an aconitase. *Mol Microbiol* 28: 961-970.

Wong, D.K., Lee, B.Y., Horwitz, M.A., and Gibson, B.W. (1999) Identification of *fur*, aconitase, and other proteins expressed by *Mycobacterium tuberculosis* under conditions of low and high concentrations of iron by combined two-dimensional gel electrophoresis and mass spectrometry. *Infect Immun* 67: 327-336.

Yang, J., Sangwan, I., Lindemann, A., Hauser, F., Hennecke, H., Fischer, H.M., and O'Brian, M.R. (2006) *Bradyrhizobium japonicum* senses iron through the status of haem to regulate iron homeostasis and metabolism. *Mol Microbiol* 60: 427-437.

Yellaboina, S., Ranjan, S., Chakhaiyar, P., Hasnain, S.E., and Ranjan, A. (2004) Prediction of DtxR regulon: identification of binding sites and operons controlled by Diphtheria toxin repressor in *Corynebacterium diphtheriae*. *BMC Microbiol* 4: 38.

Yeo, W.S., Lee, J.H., Lee, K.C., and Roe, J.H. (2006) IscR acts as an activator in response to oxidative stress for the *suf* operon encoding Fe-S assembly proteins. *Mol. Microbiol.* 61: 206-218.

Yukawa, H., Omumasaba, C.A., Nonaka, H., Kos, P., Okai, N., Suzuki, N., Suda, M., Tsuge, Y., Watanabe, J., Ikeda, Y., Vertes, A.A., and Inui, M. (2007) Comparative analysis of the *Corynebacterium glutamicum* group and complete genome sequence of strain R. *Microbiology* 153: 1042-1058.

4 Discussion

4.1 Control of iron homeostasis in *C. glutamicum*

The basic principle of bacterial iron homeostasis is to keep the intracellular pool of free iron at a level that provides sufficient supply for iron proteins of important biological pathways, such as the TCA cycle, electron transport or DNA biosynthesis, but is not toxic for the cell. To maintain iron homeostasis many organisms have evolved a complex regulatory network that coordinately controls expression of high affinity iron uptake systems, iron storage proteins, iron-containing proteins and redox stress resistance mechanisms in response to iron availability (Andrews *et al.*, 2003).

In this work a hierarchical regulatory system has been uncovered which controls iron homeostasis in the Gram-positive soil bacterium *C. glutamicum*. This system is composed of four transcriptional regulators, namely the global iron regulator DtxR, the regulator of iron proteins (RipA), the response regulator CgtR11 of the CgtSR11 two-component system and the ArsR-type regulator Cg0527. DNA microarray studies with a *dtxR* deletion mutant revealed that expression of more than 100 genes is regulated in an iron-dependent manner. In other organisms (*e.g. E. coli, Pseudomonas aeruginosa,* or *B. subtilis*) global analyses of iron-dependent gene expression revealed effects in a similar range (Baichoo *et al.*, 2002; McHugh *et al.*, 2003; Ochsner *et al.*, 2002). In *C. glutamicum* these genes not only encode proteins with a direct connection to iron metabolism, but also proteins of various or unknown function. These results underline the important influence of the trace element iron on global gene expression.

The general strategies to maintain iron homeostasis are similar in many organisms. However, the way how these strategies are being followed and especially their coordinated regulation can differ considerably. Whereas the regulatory processes described in this work affect gene expression at the transcriptional level, the control of iron homeostasis in mammals is achieved by posttranscriptional regulation (Eisenstein, 2000; Rouault, 2006). This control is exerted by iron-regulatory proteins (IRP1 and 2). Under conditions of sufficient iron supply IRP1 functions as the cytoplasmic isoform of aconitase, containing a 4Fe-4S cluster. When iron becomes limiting the apoprotein without its iron-sulfur cluster binds with high affinity to a specific iron regulatory element (IRE) on the mRNA of several genes, *e.g.* those encoding the transferrin receptor and ferritin (Klausner and Rouault, 1993;

Pantopoulos, 2004). Depending on the position of the IRE, IRP-binding either stabilizes or inhibits translation of the corresponding transcript. During the last few years evidence increased that also in several bacterial species aconitases occupy a regulatory role under iron deprivation (Alen and Sonenshein, 1999; Tang and Guest, 1999; Wilson *et al.*, 1998). Recently it has been reported that upon iron depletion aconitase of *M. tuberculosis*, a pathogenic relative of *C. glutamicum*, binds to specific IREs located at the 3'-untranslated region (UTR) of thioredoxin and the 5'-UTR of the iron-dependent regulator (*ideR*) (Banerjee *et al.*, 2007). First experiments with an *acn* deletion mutant did not reveal a regulatory effect of *C. glutamicum* aconitase on expression of genes involved in iron metabolism (Krug, 2004). However, these experiments were carried out under conditions of sufficient iron supply, which presumably do not allow the detection of regulatory effects of aconitase. Therefore, further investigations are required to identify putative IREs in the genome of *C. glutamicum* and to test RNA-binding capability of the *C. glutamicum* aconitase under iron limitation before this additional control mechanism can be discarded.

The following sections will now focus in more detail on the regulatory role of the four transcriptional regulators which constitute the hierarchical regulatory network controlling iron homeostasis in *C. glutamicum*.

4.1.1 The global iron regulator DtxR

In many Gram-positive bacteria with high GC content DtxR-like transcriptional regulators function as global iron-dependent regulators (Andrews *et al.*, 2003; Hantke, 2001). Inspection of the *C. glutamicum* genome revealed a gene (*cg2103*) encoding a transcriptional regulator with 72% sequence identity to the diphtheria toxin repressor DtxR of *C. diphtheriae* (Ikeda and Nakagawa, 2003; Kalinowski *et al.*, 2003). The corresponding protein from *C. glutamicum* strain ATCC13869 (designated "*Brevibacterium lactofermentum*" before) had previously been shown to bind the *C. diphtheriae tox* promoter/operator in an iron-dependent manner (Oguiza *et al.*, 1995). Therefore, it was assumed that this regulator might carry out a similar regulatory function as DtxR from *C. diphtheriae*. In this work the regulon of DtxR in *C. glutamicum* has been investigated using two independent approaches. On the one hand the transcriptome of a *dtxR* deletion mutant was compared with that of the wild type using DNA microarray analysis. On the other hand we used a computer-based approach together with *in vitro* binding studies with purified DtxR protein to identify functional DtxR binding sites in the *C. glutamicum* genome. Combination of the results of these studies revealed that

more than 50 genes are repressed by DtxR and additionally indicated that in some cases DtxR might also function as an activator of gene expression.

Interestingly, three genes repressed by DtxR encode themselves transcriptional regulators, adding a further level of complexity to the DtxR regulon. These are *ripA* (*cg1120*), *cg0527* encoding an ArsR-type regulator, and the response regulator *cgtR11* belonging to the CgtSR11 two-component signal transduction system (Kocan *et al.*, 2006b). Whereas the function of Cg0527 is not yet known, the regulatory role of RipA and CgtR11 are discussed in the following sections.

Repression of high affinity iron uptake systems

As expected, the majority of genes repressed by DtxR encode proteins involved in iron uptake, such as ABC transporters, secreted siderophore-binding lipoproteins putatively involved in siderophore uptake, and cytoplasmic siderophore-interacting proteins. Additionally, a presumptive heme ABC transporter, secreted heme-binding lipoproteins and heme oxygenase were shown to be repressed by DtxR, too. These data indicated at first, that *C. glutamicum* might be able to utilize heme as an alternative iron source under iron limitation; an assumption which has been later confirmed in studies targeting the function of the two-component system CgtSR11. Analysis of the *C. glutamicum* genome led to the identification of several genes encoding transport systems putatively involved in iron uptake, but which are so far not characterized biochemically. However, the majority of these systems were shown to be repressed by DtxR, which already indicates a function of these transporters in iron acquisition in *C. glutamicum* (section 3.6, Table 1). Although several ABC transporters for siderophores were identified, inspection of the *C. glutamicum* genome did not reveal genes encoding putative siderophore biosynthesis proteins. In this respect, *C. glutamicum* can be regarded as a cadger that uses the siderophores synthesized by other microorganisms present in its natural habitat. In *C. diphtheriae* and *M. tuberculosis* siderophore biosynthesis genes are present and were shown to be repressed by DtxR and IdeR, respectively (Kunkle and Schmitt, 2005; Rodriguez *et al.*, 2002). Due to the pathogenic lifestyle of these two species, the possibility to produce siderophores is likely to be more important than for a non-pathogenic soil bacterium.

Activation of genes encoding iron storage proteins

Important agents in the control of the intracellular concentration of free iron are iron storage proteins, like ferritin, bacterioferritin or Dps. The genome of *C. glutamicum* contains two

genes probably involved in iron storage, *ftn* encoding a ferritin-like protein and *dps*. The *C. glutamicum* Dps protein shows more that 50% sequence identity to Dps of *Mycobacterium smegmatis*, which has already been characterized structurally and functionally (Ceci *et al.*, 2005b; Gupta *et al.*, 2002a; Gupta and Chatterji, 2003b; Roy *et al.*, 2004a). It was shown to protect DNA from oxidative damage by sequestering intracellular Fe^{2+} and storing it in form of Fe^{3+} oxyhydroxide mineral. Dps catalyzes the oxidation of Fe^{2+} by hydrogen peroxide: $2\ Fe^{2+} + H_2O_2 + 2\ H^+ \rightarrow 2\ Fe^{3+} + 2\ H_2O$. In this way, it prevents hydroxyl radical formation by the Fenton reaction and protects the DNA from hydroxyl radical-mediated cleavage. In contrast to Dps, the sole function of ferritin is presumably restricted to iron storage.

In *M. tuberculosis* it has been demonstrated that expression of the bacterioferritin-encoding gene *bfrA* and the ferritin-encoding gene *bfrB* is directly activated by the DtxR homolog IdeR, which binds to tandem iron boxes located 100 to 106 bp upstream of the transcriptional start site (Gold *et al.*, 2001; Rodriguez and Smith, 2003). In the *dtxR* deletion mutant constructed in this work, the genes encoding ferritin (*ftn*) and Dps (*dps*) showed similar mRNA levels as the wild type under iron excess, but higher mRNA levels than the wild type under iron starvation. This result is not compatible with an activating function of DtxR under iron excess. In contrast, studies with another *dtxR* deletion mutant (strain IB2103) carried out in the lab of Dr. Jörn Kalinowski (Universität Bielefeld) revealed an about 10-fold lower mRNA level of *ftn* and *dps* under iron excess in strain IB2103 compared to the wild type (Brune *et al.*, 2006a). This result, together with the fact that the DtxR binding sites in the promoter regions of *ftn* and *dps* are located upstream of the -35 region, support an activating function of DtxR for these genes. The question arises why such drastic differences in *ftn* and *dps* expression were observed between the two *dtxR* deletion mutants. In this context, it is important to take into account that the Δ*dtxR* mutant described by Brune *et al.* was unable to grow in regular CGXII minimal medium and had to be cultivated in low-iron CGXII medium. In contrast, the Δ*dtxR* mutant constructed in this work showed nearly the same growth behaviour as *C. glutamicum* wild type even in the presence of high iron concentrations (100 µM $FeSO_4$). Thus, it can be speculated, that, due to second-site suppressor mutations, expression of *ftn* and *dps* is constitutively high in this mutant. By this means the mutant might be able to avoid toxically high intracellular iron concentrations resulting from the increased expression of a high affinity iron uptake systems usually repressed by DtxR. Such toxic effects are likely to be responsible for the growth defect of the mutant IB2103 in medium containing a regular iron concentration. Assuming that *ftn* and *dps* expression is normally activated by DtxR under iron excess, a constitutively high expression

of *ftn* and *dps* in our *dtxR* mutant can explain why their mRNA level was similar to the wild type under iron excess, but higher under iron limitation, where activation by DtxR is lost in the wild type. Further experiments, such as sequence analysis of the *ftn* and *dps* promoter regions of our *dtxR* mutant and quantitative real-time-PCR of these genes in wild type and mutant, are required to fully understand these effects.

Control of iron sulfur cluster biosynthesis

The synthesis of iron-sulfur clusters is usually also tightly regulated in response to iron availability and oxidative stress, since many iron-sulfur proteins play important roles in central metabolic pathways. A functional DtxR binding site has been identified in the upstream region of the *suf* operon in *C. glutamicum*. This operon consists of seven genes (*cg1765-cg1759*) which showed an approximatively twofold decreased mRNA level in the *dtxR* deletion mutant constructed in this work. Recently, it has been shown that the Suf proteins of *M. tuberculosis* constitute the sole machinery for iron-sulfur cluster assembly in this organism (Huet *et al.*, 2005). A similar situation can be assumed for *C. glutamicum*, since analysis of the genome sequence gave no evidence for alternative genes involved in iron-sulfur cluster assembly, *e.g.* genes encoding proteins of the Isc or Nif machinery (Johnson *et al.*, 2005). In *E. coli* the Suf machinery is involved in [Fe-S] cluster biosynthesis under stressful conditions, *e.g.* iron limitation or oxidative stress. Under conditions of sufficient iron supply expression of the *suf* genes is repressed by the global iron regulator Fur (Fontecave *et al.*, 2005; Johnson *et al.*, 2005). Consistently, expression of the *suf* operon of *M. tuberculosis* was also shown to be increased under iron limitation, but in an IdeR-independent manner (Rodriguez *et al.*, 2002). Previous DNA microarray analysis performed in our lab also showed an increased mRNA level of the *suf* genes under iron limitation (8 µM $FeSO_4$) compared to iron excess (500 µM $FeSO_4$) (Krug, 2004). Curiously, in our studies the mRNA level of the *suf* genes was lower in the Δ*dtxR* mutant than in the wild type, both under iron excess and iron limitation. However, similar observations were also made in *C. diphtheriae*. The promoter region of the *C. diphtheriae suf* operon also contains a functional DtxR binding site (Kunkle and Schmitt, 2003; Yellaboina *et al.*, 2004). Furthermore, transcriptional analysis of the *suf* operon carried out in *C. diphtheriae* strain C7(-) and strain C7βhm723, a *dtxR* mutant also revealed decreased transcription of these genes in the *dtxR* mutant strain under both conditions, iron excess and iron limitation. Thus, it is most likely that the *suf* operon of *C. glutamicum* is indeed under control of DtxR, but in a manner not yet understood. Expression of the *C. glutamicum suf* operon is controlled by at least one additional regulator.

The first gene of this operon encodes a transcriptional regulator of the DeoR family (designated *sufR*), which might regulate the expression of the *suf* operon in response to the cellular demand for iron-sulfur cluster assembly and repair, similar to SufR of *Synechocystis* (Wang *et al.*, 2004).

DtxR – the master regulator of iron metabolism in *C. glutamicum.*

Based on the results described above, DtxR obviously is the master regulator of iron metabolism in *C. glutamicum*; coordinately regulating genes involved in iron uptake, iron storage and [Fe-S] cluster biosynthesis as well as several other genes which are not obviously connected with iron metabolism. The activity of DtxR is determined by the occupation of a low affinity Fe^{2+} binding site and therefore by the cytoplasmic Fe^{2+} concentration, which thus seems to represent the decisive signal that reflects the cellular iron supply. Since at least three of the target genes that are repressed by DtxR function as transcriptional regulators (*ripA*, *cgtR11*, *cg0527*) by themselves, a set of further genes is controlled indirectly by DtxR.

4.1.2 RipA – regulator of iron proteins

The gene encoding the AraC-type regulator RipA (regulator of iron proteins A) was also shown to be under negative control by the iron regulator DtxR. Under iron limitation RipA is involved in the down-regulation of several prominent iron-containing proteins and thereby plays an important role in the reduction of the cellular iron demand under these conditions. In this work 15 target genes of RipA, organized in 7 operons, were identified, including *acn* (aconitase), *sdhCAB* (succinate dehydrogenase), *narKGHJI* (nitrate/nitrite transporter and nitrate reductase), *leuCD* (isopropylmalate dehydratase), *catA* (catechol 1,2-dioxygenase), *pta* (phosphotransacetylase), and *katA* (catalase). Except for the transporter NarK, phosphotransacetylase and acetate kinase (the *ackA* gene is co-transcribed with *pta* and presumably also co-regulated (Reinscheid *et al.*, 1999)), the enzymes encoded by all other genes are known to contain iron (Figure 4.1 A). In all cases evidence for the existence of at least two RipA binding sites in each promoter region was obtained. In Figure 4.1 B, location and orientation of the RipA binding sites in the promoter regions of its target genes is shown. So far 13 RipA binding sites were identified and a 14-bp RipA consensus motif could be derived (RRGCGNNNNRYGAC). In several cases RipA binding sites are located far upstream of the identified transcription start site of the corresponding gene (*e.g. acn*: -146.5 and –203.5; *sdhC*: -42.5 and –123.5), giving rise to the question how RipA exerts its repressing effect. Based on the location of RipA binding sites in the promoters of *pta* and *narK*

A

Iron cofactors of RipA targets

Aconitase	1x 4Fe-4S cluster
Succinate dehydrogenase	1x 4Fe-4S cluster 1x 3Fe-4S cluster 1x 2Fe-2S cluster 2x heme *b*
Nitrate reductase	3x 4Fe-4S cluster 1x 3Fe-4S cluster 2x heme *b*
Isopropylmalate dehydratase	1x 4Fe-4S cluster
Catechol 1,2-dioxygenase	1Fe per subunit
Catalase	1heme *b* per subunit
Phosphotransacetylase, Acetate kinase	/

B

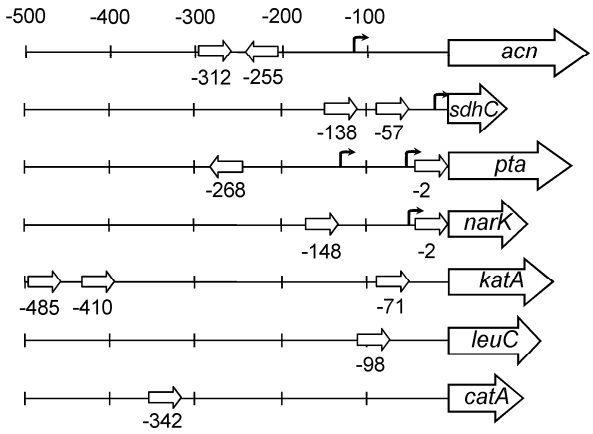

Figure 4.1. RipA-dependent regulation of prominent iron proteins in *C. glutamicum*. (A) Iron cofactors of the proteins controlled by RipA. (B) Localization of the verified RipA binding sites in the promoter regions of its target genes. The orientation of the RipA binding motif within the promoter region is indicated by an arrow. The position beneath the arrows indicates the distance of the center of the binding site to the predicted start codon of the corresponding gene (position +1). For *acn*, *sdhC*, *pta* and *narK*, the transcriptional start sites have been determined experimentally and are indicated by black arrows (Brune *et al.*, 2006a; Gerstmeir *et al.*, 2003; Krug *et al.*, 2005; Takeno *et al.*, 2007).

interference with the binding of RNA polymerase is a possible mechanism of RipA-mediated repression of these genes. Due to the presence of multiple RipA binding sites in each RipA target promoter and the large and varying distances between these binding sites it can be suggested that DNA looping might be involved in the mechanism of RipA action, as reported *e.g.* for AraC (Lobell and Schleif, 1990; Matthews, 1992; Saiz and Vilar, 2006). A first approach to visualize putative RipA-mediated DNA loops was the use of atomic force microscopy (AFM) (Lyubchenko *et al.*, 1995). For this purpose, a DNA fragment covering the *acn* promoter region with both identified RipA binding sites (-450 to +190 with respect to the transcription start site) was incubated with different amounts of purified RipA protein, comparable to that used in gel shift assays. Subsequently, the nucleoprotein complex was immobilized on freshly spliced mica and used for AFM (cooperation with Dr. Dirk Mayer, Institute of Thin Films and Interfaces, Research Centre Jülich). However, no DNA loop formation could be observed under the chosen conditions (data not shown). One explanation could be the existence of further RipA binding sites required for DNA looping, but missing on the tested DNA fragment. Another way of testing the formation of RipA-mediated DNA loops would be the measurement of fluorescence resonance energy transfer (FRET) between fluorophores attached on opposite sides of the DNA loop; a method already applied to

assess geometry and protein conformation in LacI-mediated DNA loops (Edelman *et al.*, 2003).

In subsequent studies it was shown that expression of RipA itself is repressed by the global iron regulator DtxR, as already mentioned in the previous section. These results have unravelled a new aspect of the regulatory network controlling iron homeostasis in *C. glutamicum*, namely the down-regulation of several iron containing proteins when iron becomes limiting. By means of this strategy the cell is able to save the scarce iron for other important iron-requiring processes, such as respiration or DNA biosynthesis. In fact, genes encoding iron-containing subunits of the electron transport chain (cytochrome bc_1 complex, cytochrome aa_3 oxidase or cytochrome *bd* complex) did not reveal a decreased mRNA level in DNA microarray analyses comparing the transcriptomes of cells grown under iron limitation (8 µM $FeSO_4$) and iron excess (500 µM $FeSO_4$) (Krug *et al.*, 2005).

Interestingly, in the case of the *sdhCAB* operon a functional DtxR binding site was identified 105 bp (with respect to the centre of the 19-bp binding site) upstream of the transcriptional start site of *sdhC*, which suggests a transcriptional activation of *sdhCAB* by DtxR. The *sdhCAB* mRNA level was indeed about 5-fold reduced in the Δ*dtxR* mutant, however, this effect is most likely due to repression by RipA rather than to a missing activation by DtxR (Brune *et al.*, 2006a). Nevertheless, due to the close vicinity of the DtxR binding site to one of the RipA binding sites (centered at -119.5) DtxR might be involved in displacing RipA from its binding site upon a shift from iron limitation to conditions of sufficient iron supply. Further studies are required to investigate whether the activation of *sdhCAB* by DtxR is caused by the interference with the repressor RipA or depends on an independent mechanism. The question of how RipA repression is abolished when the cell has overcome iron limitation is yet unanswered. One possibility to inactivate RipA would be for example iron-dependent proteolysis or the binding of an iron cofactor. The latter mechanism would be a reverse mechanism to that described for DtxR, where iron is essential for its activity. Although first spectroscopic analyses of RipA protein produced heterologously in *E. coli* did not reveal the existence of an iron cofactor, further investigations are required to test this possibility.

Orthologs of RipA were identified in *Corynebacterium efficiens* (CE1047; 70% sequence identity) and *C. diphtheriae* (DIP0922; 52% sequence identity), but not in *Corynebacterium jeikeium* (Tauch *et al.*, 2005) or *Mycobacterium* species. Inspection of the promoter region of the *ripA* genes in *C. efficiens* and *C. diphtheriae* also revealed well conserved DtxR binding sites

(for further details see the discussion section of the corresponding publication). Due to the high variability of the RipA binding motif, it is difficult to predict RipA binding sites in *C. efficiens* and *C. diphtheriae* with confidence. Nevertheless, inspection of the promoter regions of potential RipA target genes revealed for example two putative RipA binding sites in front of the *acn* gene of *C. efficiens*, located at position -167 and -308 with respect to the start codon. Therefore, it can be speculated that all *ripA* genes are probably controlled by DtxR and that the RipA proteins presumably have an at least partially overlapping set of target genes.

A regulatory cascade with a similar function as that of DtxR and RipA is found in some Gram-negative bacteria, *e.g. E. coli* or *P. aeruginosa* (Masse *et al.*, 2007). In *E. coli* the ferric uptake regulator (Fur) in complex with iron represses a small (s)RNA named RhyB, which stimulates the degradation of mRNAs encoding iron-containing proteins like aconitase A (*acnA*), succinate dehydrogenase (*sdhCDAB*), the iron storage protein ferritin (*ftnA*) and superoxide dismutase (*sodB*) (Masse *et al.*, 2005). Similar regulatory mechanisms to overcome iron limitation were also described in other organisms. In *Saccharomyces cerevisiae* the Cth2 protein coordinates the response of iron-dependent metabolic pathways by directly targeting mRNAs encoding iron-requiring proteins for degradation (Puig *et al.*, 2005). In the human pathogen *N. meningitidis* the global iron regulator Fur itself activates expression of iron-using proteins (Delany *et al.*, 2004). These examples just give a rough impression of the great regulatory variety which organisms have evolved to pursue one major strategy of iron homeostasis: The down-regulation of iron-requiring proteins under iron limitation.

4.1.3 The two-component system CgtSR11

As mentioned above, the genome of *C. glutamicum* contains genes coding for a putative heme ABC transporter, heme-binding proteins and heme oxygenase (*hmuO*), all of which are repressed by DtxR under iron-replete conditions. Heme oxygenases are involved in the utilization of heme as iron source by catalyzing the degradation of the tetrapyrrole ring to α-biliverdin, CO_2 and free iron. Growth experiments confirmed our postulation that *C. glutamicum* is able to use heme as an alternative iron source, since no differences in growth were observed when either $FeSO_4$ (1 μM) or heme (2.5 μM) were added as iron source in CGXII minimal medium. In *C. diphtheriae* the expression of heme oxygenase was shown to be repressed by DtxR and induced by heme or hemoglobin (Schmitt, 1997). In this organism the two-component systems HrrAS and ChrAS were shown to be involved in the heme-

dependent activation of *hmuO* (Bibb *et al.*, 2005; Bibb *et al.*, 2007). Interestingly, both systems show significant sequence similarity to the two-component system encoded by the *cgtS11-cgtR11* genes in *C. glutamicum*. Therefore, a function of the *C. glutamicum* CgtSR11 system in heme-dependent activation of *hmuO* transcription was postulated.

The *cgtR11* gene has already been mentioned as being regulated by DtxR, which binds to a site located in the non-coding region between *cgtS11* and *cgtR11*. This indicates the existence of a *cgtR11*-specific promoter. In DNA microarray analysis comparing the transcriptomes of a Δ*cgtSR11* mutant and *C. glutamicum* wild type *hemA* and *hemE* encoding the heme biosynthesis enzymes glutamyl-tRNA reductase and uroporphyrinogen decarboxylase showed an increased mRNA level in the mutant. In contrast, the mRNA level of genes coding for heme-containing proteins (*e.g. qcrCAB* encoding the cytochrome bc_1 complex) and heme oxygenase was decreased in the Δ*cgtSR11* mutant. Evidence for a direct regulation of these genes by CgtR11 was obtained by showing an interaction of purified CgtR11 with the promoter regions of *hmuO*, *hemA* and *qcrC* via gel shift assays. In the case of *hmuO* the strongest effect of a *cgtSR11* deletion was observed under iron limitation, but in the presence of heme. Based on these findings a very similar mechanism of heme-dependent *hmuO* activation can be assumed as already proposed for *C. diphtheriae hmuO* (Figure 4.2) (Schmitt, 1999). The sensor kinase CgtS11, located in the cytoplasmic membrane, is most likely involved in the detection of extracellular or membrane-associated heme, leading to the autophosphorylation of the conserved histidine residue (H260). This phosphoryl group can then be transferred to CgtR11 (D54), which subsequently activates or represses its target genes. Under iron excess transcription of *cgtR11* (and also of *hmuO*) is repressed by DtxR whereas neither *chrA* nor *hrrA C. diphtheriae* seem to be controlled in this way.

The role of CgtSR11 in the regulation of *hemA* and *qcrC* is not completely clear yet. For these genes, about 2-fold changed mRNA levels were observed in the Δ*cgtSR11* mutant under iron excess (100 µM $FeSO_4$), iron limitation (1 µM $FeSO_4$) and with heme (2.5 µM) added as iron source. These results indicate a regulatory effect of the CgtSR11 system under all three tested conditions, but no heme-dependency was observed in these experiments. These findings do not fit into our proposed model of *hmuO* regulation *via* CgtSR11 and thus indicate a more complex regulatory network as proposed so far (Figure 4.2). As described for *C. diphtheriae* a putative cross talk with additional two-component systems has to be kept in mind. The two-component system CgtSR8, whose function is not yet known, shares high sequence identity (~50%) with the CgtSR11 system (Kocan *et al.*, 2006b). Therefore, further

studies are required to fully understand the mechanism of CgtSR11 action and to search for other systems involved in this signal transduction cascade.

The results described in this work indicate on the one hand an involvement of CgtSR11 in the down-regulation of heme biosynthesis (*hemA* and *hemE*) and on the other hand an induction of heme-containing proteins, when extracellular heme is available. Recent studies in *C. diphtheriae* also revealed heme-dependent repression of *hemA* by ChrAS and HrrAS (Bibb *et al.*, 2007), but so far no influence of these systems on the expression of heme-containing proteins was observed.

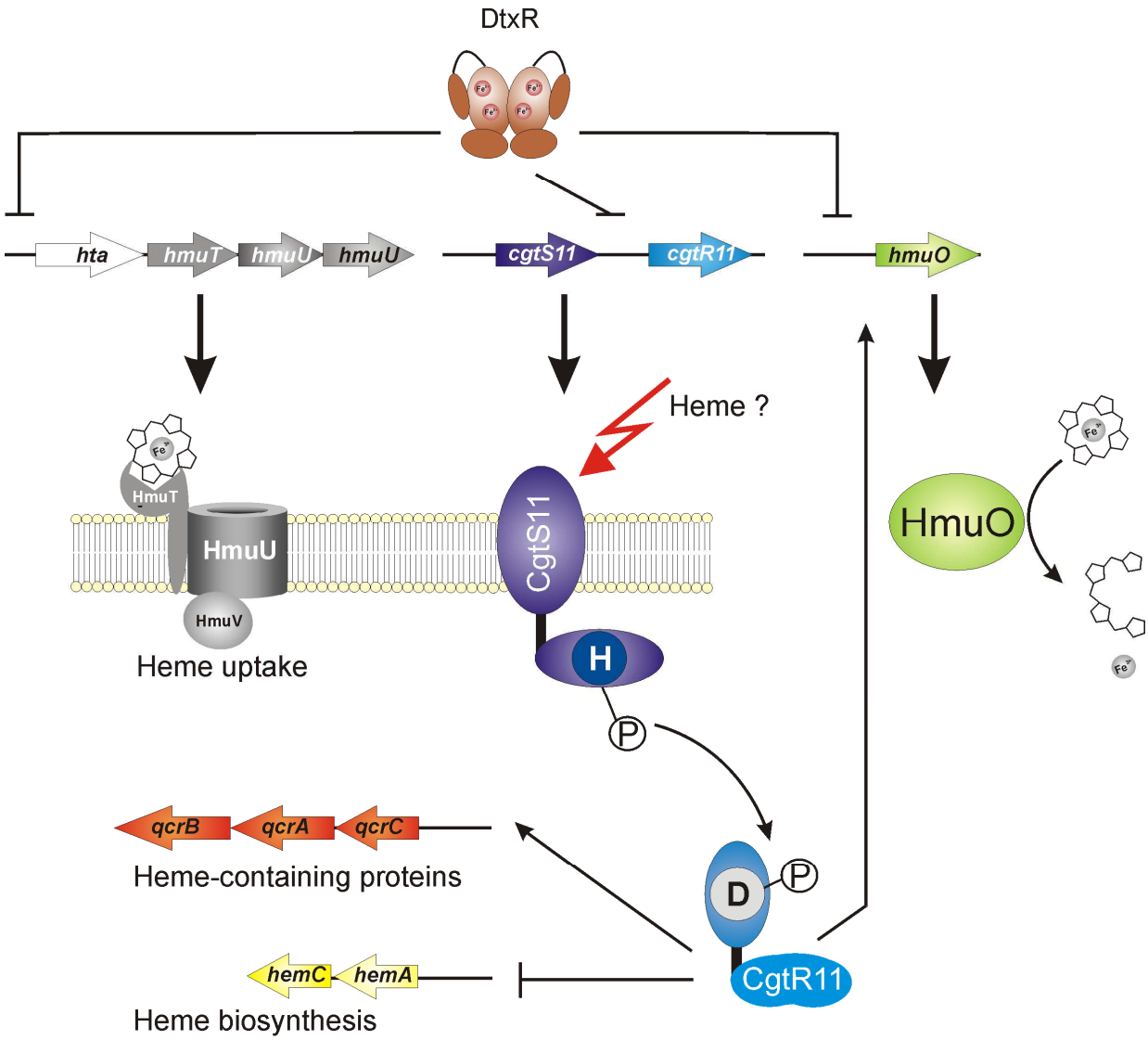

Figure 4.2. Postulated control of heme homeostasis in *C. glutamicum* mediated by a regulatory cascade including the global iron regulator DtxR and the two-component system CgtSR11.

Recently, a further two-component system which shares high sequence identity to CgtSR11 has been described in *Streptomyces reticuli* (Ortiz de Orue Lucana *et al.*, 2005). In this organism the SenRS system negatively modulates expression of a heme-dependent catalase (CpeB) and the heme-binding protein HbpS. However, like for the ChrAS, HrrAS and CgtSR11 the exact signal activating this system is yet unknown. Besides these two-component systems several other heme-responsive transcriptional regulators are known (Biville *et al.*, 2004; King *et al.*, 2005; Simpson *et al.*, 2000). An interesting example is the transcriptional regulator Irr, a member of the Fur superfamily, originally identified in *Bradyrhizobium japonicum* (Yang *et al.*, 2006). This regulator plays an important role in maintaining iron homeostasis in rhizobia (Rudolph *et al.*, 2006). Amongst others Irr represses transcription of *hemB*, the gene encoding the heme biosynthesis enzyme δ-aminolevulinic acid dehydratase. Irr was shown to be degraded upon binding of ferric heme to a heme regulatory motif.

Altogether the results described in this section indicate that CgtSR11 is at least partially responsible for the down-regulation of proteins involved in heme biosynthesis and for induction of heme oxygenase as well as heme-containing proteins. By these means, the cell is able to coordinate heme biosynthesis, production of heme-containing proteins and utilization of heme as an iron source in dependency of iron supply and heme availability.

4.1.4 The ArsR-type regulator Cg0527 – Subject of investigations

The third transcriptional regulator repressed by DtxR is the ArsR-type regulator Cg0527. Members of this family often act as repressors of genes encoding proteins involved in the efflux and/or sequestration of excess metal ions, such as Zn(II), As(III), Ni(II) or Cd(II) (Busenlehner *et al.*, 2003). Repression mediated by ArsR-type regulators is normally alleviated when the concentration of the corresponding metal ion exceeds a tolerable level in the cell. Homologs of Cg0527 can be found in *C. diphtheriae* (DIP0415, 46% identity) and *C. efficiens* (CE0466; 53% identity), but not in *Mycobacterium* species. Inspection of the corresponding promoter regions revealed the presence of a well conserved DtxR binding site centred 21 bp upstream to the start codon of *dip0415* (TTAGCTTAACCTTGCCTAT) and 65 bp upstream of *ce0466* (ATAGCTTAGGCTTACCTGC). Therefore, a similar regulatory cascade as in *C. glutamicum* is likely to exist in these organisms. The way, in which Cg0527 contributes to the maintenance of iron homeostasis or more generally of metal homeostasis in *C. glutamicum*, is subject of further investigations.

In Figure 4.3 the current knowledge on the complex regulatory network controlling iron homeostasis is summarized, giving an overview of the function of the transcriptional regulators DtxR, RipA, CgtR11, and Cg0527 in *C. glutamicum*.

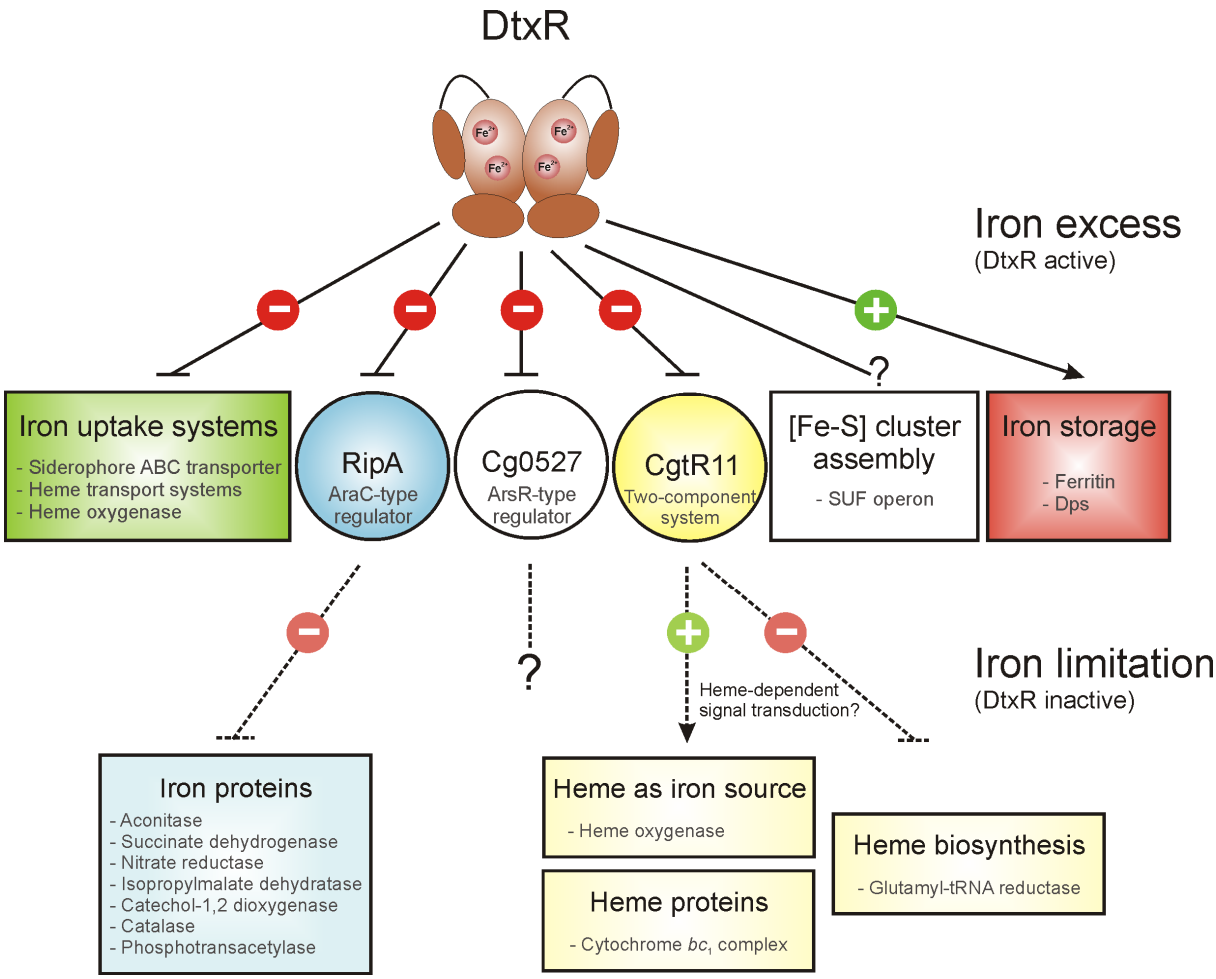

Figure 4.3. The hierarchical regulatory network controlling iron homeostasis in *C. glutamicum*. Under conditions of sufficient iron supply, DtxR in complex with Fe^{2+} represses transcription of high affinity iron uptake systems and of three transcriptional regulators, RipA, Cg0527 and the response regulator CgtR11. On the other hand DtxR seems to act as a direct activator of genes encoding the iron storage proteins ferritin and Dps. Furthermore, an activatory effect of DtxR on *sdhCAB* (encoding succinate dehydrogenase) was postulated, which is not included in this figure. When iron becomes limiting the AraC-type regulator RipA is involved in the reduction of the cellular iron demand by the repression of genes encoding several prominent iron proteins. Additionally, the two-component system CgtSR11 most likely functions in the control of heme homeostasis by coordinately regulating heme biosynthesis, production of heme containing proteins and expression of heme oxygenase in response to iron and heme availability.

4.2 Further putative metal-dependent regulators in *C. glutamicum*

Members of the Fur and DtxR family of transcriptional regulators are widely distributed in bacterial species. As described in the Introduction section the ferric uptake regulator Fur acts as a global iron regulator in many Gram-negative and Gram-positive organisms with low

GC content, whereas an analogous role is carried out by DtxR-type regulators in Gram-positive species with high GC content (Andrews *et al.*, 2003; Hantke, 2001). However, not all members of these families are involved in iron-dependent gene regulation. Especially in the case of the Fur family an impressive diversity of metal ion selectivity and function has been described, with members sensing iron (Fur), zinc (Zur), manganese (Mur) and nickel (Nur) (Lee and Helmann, 2007). Last but not least, the regulators Irr and PerR, which are also members of the Fur family, both use metal catalyzed oxidation to sense the availability of heme or oxidative stress, respectively (Lee and Helmann, 2007). In the case of DtxR-family, two members are known to control expression of target genes in a strictly manganese-dependent manner, namely MntR of *B. subtilis* and TroR of *Treponema pallidum* (Posey *et al.*, 1999; Que and Helmann, 2000).

The genome of *C. glutamicum* contains, apart from *dtxR* itself (*cg2103*), two further genes encoding DtxR-type regulators, *cg0741* (*sirR*) and *cg2784* and in addition one gene (*cg2502*, *fur*) coding for a transcriptional regulator of the Fur family (Table 1) (Ikeda and Nakagawa, 2003; Kalinowski *et al.*, 2003). Both *sirR* and *cg2784* are most likely co-transcribed with integral membrane proteins which might be involved in transport of the corresponding metal. With the exception of *dtxR* (see page 91), no experimental data exist for the other regulators. Most likely, they are not involved in the regulation of iron homeostasis, but sense other metal ions like manganese or zinc.

Table 1: Putative metalloregulators of the DtxR and Fur family in *C. glutamicum*.

Gene ID	Gene Name	kDa	Family	Predicted Operon
cg2103	*dtxR*	25.5	DtxR	*cg2103, dtxR* *cg2104, galE,* UDP-glucose-4-epimerase
cg0741	*sirR*	24.6	DtxR	*cg0739*, putative integral membrane protein *cg0740*, predicted membrane protein *cg0741, sirR*
cg2784		22.8	DtxR	*cg2785*, putative membrane protein *cg2784*, transcriptional regulator
cg2502	*fur*	15.7	Fur	*cg2500*, ArsR-type transcriptional regulator *cg2502*, *fur*

4.3 Induction of the CGP3 prophage in *C. glutamicum*

The genome of *C. glutamicum* ATCC 13032 contains four putative prophage elements (CGP1, CGP2, CGP3 and CGP4), which have been recognized due to differences in base composition and the presence of genes encoding typical phage-type proteins, *e.g.* integrase (Kalinowski, 2005b). So far it was assumed that these phages exist exclusively as integrated prophages within the *C. glutamicum* genome, since no successful induction of one of these prophages has yet been reported. In this work we were able to show that induction of the prophage CGP3 occurs apparently spontaneously in a small fraction of *C. glutamicum* wild-type cells. This finding was the first clue for an at least partially functional temperate bacteriophage present in *C. glutamicum* strain ATCC 13032.

Induction of prophages can happen randomly, but specific signals can cause simultaneous induction of the prophage in nearly every single cell of a culture (Casjens, 2003). For *C. glutamicum* ATCC 13032 we observed a significant increase of the induction rate in a *dtxR* deletion mutant or after exposure of the wild type to ultraviolet light. In several organisms induction of a specific prophage is linked to the SOS response system (Walker, 1987). Usually, the integrated prophage is maintained in a quiescent state due to the binding of a phage-encoded repressor, like CI of bacteriophage λ or coliphage 186, which represses the early phage genes. Depletion of the phage repressor leads to a switch from lysogeny to lytic development. For a more detailed view the reader is referred to a review focusing on the genetic switch of bacteriophage λ between lysogenic and lytic state (Oppenheim *et al.*, 2005). The ultimate signal for activation of the SOS response is the formation of single-stranded DNA by various routes, resulting in an activation of the RecA protein which subsequently promotes autocleavage of CI repressor in several lambdoid phages (Cox, 2007; Kim and Little, 1993; Little, 1984). Additionally, RecA interaction leads to autoproteolysis of the LexA protein, which represses transcription of a number of genes involved in DNA repair and recombination, as well as *recA* and *lexA* itself (Kelley, 2006; Little and Mount, 1982).

In generel this mechanism of phage induction, where an activated RecA protein promotes autocleavage of the main phage repressor, is also conceivable for induction of CGP3. The genome of *C. glutamicum* encodes homologs of RecA and LexA (*cg2141* and *cg2114*, respectively), which most probably carry out similar functions as described for other organisms. In the case of LexA first experimental data revealed a role of this protein in the regulation of genes involved in DNA repair and recombination, such as *uvrA* and *recN*

(*cg1560* and *cg1602*, respectively; https://www.cebitec.uni-bielefeld.de/groups/gi/software/coryneregnet/v3/). Interestingly, the region containing the alanine-glycine bond (A^{84}-G^{85}) of *E. coli* LexA which is cleaved during autodigestion, is also highly conserved in the homologous protein of *C. glutamicum*. Furthermore, inspection of the genomic region constituting the CGP3 element revealed two genes encoding transcriptional regulators (*cg1935* and *cg2040*), which theoretically could function as phage repressors maintaining the lysogenic state of CGP3. However, *cg1935* (*gntR2*) shows significant sequence identity (78%) to *cg2783* (*gntR1*) located on the bacterial chromosome and is most probably the product of a gene duplication event of *cg2783*. Recently, we could show that both GntR1 and GntR2 are involved in the coordinated regulation of gluconate metabolism and sugar uptake in *C. glutamicum* (a publication focusing on this topic is included in the Appendix of this thesis). A Blast search with the amino acid sequence of the second putative regulator encoded by the CGP3 region (Cg2040) revealed significant similarity to several phage-type regulators belonging to the Cro/CI family of transcriptional regulators (Pfam: PF01381) (Johnson *et al.*, 1981; Oppenheim *et al.*, 2005). Thus, the Cg2040 protein is a good candidate for a CGP3 phage repressor and could be involved in maintaining the prophage in a quiescent state. Further genes located within the CGP3 element encoding putative transcriptional regulators could not be identified.

Besides the above-mentioned mechanism of phage induction, based on direct autocleavage of the phage repressor, several alternative scenarios were reported for other phages. In the case of coliphage 186 the Tum protein functions as an antirepressor which binds to the phage repressor resulting in the induction of lytic growth (Lamont *et al.*, 1989; Shearwin *et al.*, 1998). Expression of *tum* itself is under control of host LexA, and thereby phage induction is again linked to the SOS response system of the bacteria. Similar mechanisms were also described for the linear plasmid-prophage N15 of *E. coli* and the *Salmonella enterica* phage Fels-2 (Bunny *et al.*, 2002; Mardanov and Ravin, 2007). Another interesting example is the induction of the CTX prophage of *Vibrio cholerae*, which encodes cholera toxin. Here, expression of the genes required for virion production is directly regulated by host LexA which binds just upstream of the phage-encoded repressor RstR. Again SOS induction results in the production of phage particles due to RecA-mediated autodigestion of LexA, which most probably destabilizes binding of RstR (Quinones *et al.*, 2005; Waldor and Friedman, 2005). Thus, exposure of the host cell to DNA-damaging agents that challenge cell survival and lead to the induction of the SOS response often results in derepression of resident prophages, and subsequently "the rats desert the sinking ship".

Single-stranded DNA, the ultimate signal for SOS induction, can be formed by various routes, *e.g.* exposure to ultraviolet light or treatment with certain drugs, notably quinolones (Malik *et al.*, 2006). The induction rate of CGP3 in *C. glutamicum* was significantly increased in a deletion mutant lacking the transcriptional regulator DtxR. In this mutant expression of high-affinity iron uptake systems is strongly increased and might lead to an increased intracellular Fe^{2+} concentration. By the Fenton reaction, Fe^{2+} catalyzes the formation of the highly reactive hydroxyl radical (·OH), which induces DNA strand breakage, resulting in the formation of single-stranded DNA. However, so far no complete induction of the CGP3 prophage was observed. Even under conditions of increased prophage induction lysis of the *C. glutamicum* culture was not detected. By fluorescence microscopy of cells with a YFP-tagged (yellow fluorescent protein) CGP3 element, obvious lysis of cells containing multiple copies of the phage-DNA was observed. These cells accounted for only about 2-4% of a *C. glutamicum* wild type culture und thus lysis might have been overlooked in normal growth experiments. However, the majority of genes located within the CGP3 element has no known homolog. So far genes encoding putative endolysins or even phage coat proteins have not been discovered yet, but might be of course amongst the multiplicity of genes encoding hypothetical proteins located within the CGP3 element.

The discovery of spontaneous induction of the CGP3 prophage in *C. glutamicum* strain ATCC 13032 raised many questions to be answered in future studies. A main focus will be set on the question whether functional phage particles of CGP3 are formed upon induction and if these phage particles are able to infect other *C. glutamicum* strains not carrying the CGP3 prophage, such as *C. glutamicum* strain R.

5 References

Alamuri, P., Mehta, N., Burk, A., and Maier, R.J. (2006) Regulation of the *Helicobacter pylori* Fe-S cluster synthesis protein NifS by iron, oxidative stress conditions, and *fur*. *J Bacteriol* **188**: 5325-5330.

Alen, C., and Sonenshein, A.L. (1999) *Bacillus subtilis* aconitase is an RNA-binding protein. *Proc Natl Acad Sci U S A* **96**: 10412-10417.

Andrews, S.C., Robinson, A.K., and Rodriguez-Quinones, F. (2003) Bacterial iron homeostasis. *FEMS Microbiol Rev* **27**: 215-237.

Baichoo, N., Wang, T., Ye, R., and Helmann, J.D. (2002) Global analysis of the *Bacillus subtilis* Fur regulon and the iron starvation stimulon. *Mol Microbiol* **45**: 1613-1629.

Banerjee, S., Nandyala, A.K., Raviprasad, P., Ahmed, N., and Hasnain, S.E. (2007) Iron-dependent RNA-binding activity of *Mycobacterium tuberculosis* aconitase. *J Bacteriol* **189**: 4046-4052.

Bibb, L.A., King, N.D., Kunkle, C.A., and Schmitt, M.P. (2005) Analysis of a heme-dependent signal transduction system in *Corynebacterium diphtheriae*: deletion of the *chrAS* genes results in heme sensitivity and diminished heme-dependent activation of the *hmuO* promoter. *Infect Immun* **73**: 7406-7412.

Bibb, L.A., Kunkle, C.A., and Schmitt, M.P. (2007) The ChrA-ChrS and HrrA-HrrS Signal Transduction Systems Are Required for Activation of the *hmuO* Promoter and Repression of the hemA Promoter in *Corynebacterium diphtheriae*. *Infect Immun* **75**: 2421-2431.

Biville, F., Cwerman, H., Letoffe, S., Rossi, M.S., Drouet, V., Ghigo, J.M., and Wandersman, C. (2004) Haemophore-mediated signalling in *Serratia marcescens*: a new mode of regulation for an extra cytoplasmic function (ECF) sigma factor involved in haem acquisition. *Mol Microbiol* **53**: 1267-1277.

Boyd, J., Oza, M.N., and Murphy, J.R. (1990) Molecular cloning and DNA sequence analysis of a diphtheria tox iron-dependent regulatory element (*dtxR*) from *Corynebacterium diphtheriae*. *Proc Natl Acad Sci U S A* **87**: 5968-5972.

Brune, I., Werner, H., Hüser, A.T., Kalinowski, J., Pühler, A., and Tauch, A. (2006) The DtxR protein acting as dual transcriptional regulator directs a global regulatory network involved in iron metabolism of *Corynebacterium glutamicum*. *BMC Genomics* **7**: 21.

Budzikiewicz, H., Bossenkamp, A., Taraz, K., Pandey, A., and Meyer, J.M. (1997) Corynebactin, a cyclic catecholate siderophore from *Corynebacterium glutamicum* ATCC 14067 (*Brevibacterium* sp. DSM 20411). *Z Naturforsch 52c* **52**: 551-554.

Bunny, K., Liu, J., and Roth, J. (2002) Phenotypes of *lexA* mutations in *Salmonella enterica*: evidence for a lethal *lexA* null phenotype due to the Fels-2 prophage. *J Bacteriol* **184**: 6235-6249.

Busenlehner, L.S., Pennella, M.A., and Giedroc, D.P. (2003) The SmtB/ArsR family of metalloregulatory transcriptional repressors: Structural insights into prokaryotic metal resistance. *FEMS Microbiol Rev* **27**: 131-143.

Casjens, S. (2003) Prophages and bacterial genomics: what have we learned so far? *Mol Microbiol* **49**: 277-300.

Ceci, P., Ilari, A., Falvo, E., Giangiacomo, L., and Chiancone, E. (2005) Reassessment of protein stability, DNA binding, and protection of *Mycobacterium smegmatis* Dps. *J Biol Chem* **280**: 34776-34785.

Cerdeno-Tarraga, A.M., Efstratiou, A., Dover, L.G., Holden, M.T.G., Pallen, M., Bentley, S.D., Besra, G.S., Churcher, C., James, K.D., De Zoysa, A., Chillingworth, T., Cronin, A., Dowd, L., Feltwell, T., Hamlin, N., Holroyd, S., Jagels, K., Moule, S., Quail, M.A.,

Rabbinowitsch, E., Rutherford, K.M., Thomson, N.R., Unwin, L., Whitehead, S., Barrell, B.G., and Parkhill, J. (2003) The complete genome sequence and analysis of *Corynebacterium diphtheriae* NCTC13129. *Nucleic Acids Res.* **31**: 6516-6523.

Chipperfield, J.R., and Ratledge, C. (2000) Salicylic acid is not a bacterial siderophore: a theoretical study. *Biometals* **13**: 165-168.

Cornell, R.M., and Schwertmann, U. (2003) *The Iron Oxides: Structure, Properties, Reactions, Occurrences and Uses*: Wiley-VCH.

Cox, M.M. (2007) Regulation of bacterial RecA protein function. *Crit Rev Biochem Mol Biol* **42**: 41-63.

D'Aquino, J.A., Tetenbaum-Novatt, J., White, A., Berkovitch, F., and Ringe, D. (2005) Mechanism of metal ion activation of the diphtheria toxin repressor DtxR. *Proc Natl Acad Sci U S A* **102**: 18408-18413.

Delany, I., Rappuoli, R., and Scarlato, V. (2004) Fur functions as an activator and as a repressor of putative virulence genes in *Neisseria meningitidis*. *Mol Microbiol* **52**: 1081-1090.

Dertz, E.A., Stintzi, A., and Raymond, K.N. (2006) Siderophore-mediated iron transport in *Bacillus subtilis* and *Corynebacterium glutamicum*. *J Biol Inorg Chem* **11**: 1087-1097.

Drazek, E.S., Hammack, C.A., and Schmitt, M.P. (2000) *Corynebacterium diphtheriae* genes required for acquisition of iron from haemin and haemoglobin are homologous to ABC haemin transporters. *Mol Microbiol* **36**: 68-84.

Edelman, L.M., Cheong, R., and Kahn, J.D. (2003) Fluorescence resonance energy transfer over approximately 130 basepairs in hyperstable lac repressor-DNA loops. *Biophys J* **84**: 1131-1145.

Eggeling, L., and Bott, M. (2005) *Handbook of Corynebacterium glutamicum.* Inc., Boca Raton, FL: Academic Press.

Eisenstein, R.S. (2000) Iron regulatory proteins and the molecular control of mammalian iron metabolism. *Annu Rev Nutr* **20**: 627-662.

Escolar, L., Perez-Martin, J., and de Lorenzo, V. (1999) Opening the iron box: transcriptional metalloregulation by the Fur protein. *J Bacteriol* **181**: 6223-6229.

Fontecave, M., Choudens, S.O., Py, B., and Barras, F. (2005) Mechanisms of iron-sulfur cluster assembly: the SUF machinery. *J Biol Inorg Chem*: 1-9.

Gerstmeir, R., Wendisch, V.F., Schnicke, S., Ruan, H., Farwick, M., Reinscheid, D., and Eikmanns, B.J. (2003) Acetate metabolism and its regulation in *Corynebacterium glutamicum*. *J Biotechnol* **104**: 99-122.

Gold, B., Rodriguez, G.M., Marras, S.A., Pentecost, M., and Smith, I. (2001) The *Mycobacterium tuberculosis* IdeR is a dual functional regulator that controls transcription of genes involved in iron acquisition, iron storage and survival in macrophages. *Mol Microbiol* **42**: 851-865.

Gupta, S., Pandit, S.B., Srinivasan, N., and Chatterji, D. (2002) Proteomics analysis of carbon-starved *Mycobacterium smegmatis*: induction of Dps-like protein. *Protein Eng* **15**: 503-512.

Gupta, S., and Chatterji, D. (2003) Bimodal protection of DNA by *Mycobacterium smegmatis* DNA-binding protein from stationary phase cells. *J Biol Chem* **278**: 5235-5241.

Hantke, K. (2001) Iron and metal regulation in bacteria. *Curr Opin Microbiol* **4**: 172-177.

Hornung, J.M., Jones, H.A., and Perry, R.D. (1996) The *hmu* locus of *Yersinia pestis* is essential for utilization of free haemin and haem-protein complexes as iron sources. *Mol. Microbiol.* **20**: 725-739.

Huet, G., Daffe, M., and Saves, I. (2005) Identification of the *Mycobacterium tuberculosis* SUF machinery as the exclusive mycobacterial system of [Fe-S] cluster assembly: evidence for its implication in the pathogen's survival. *J Bacteriol* **187**: 6137-6146.

Ikeda, M., and Nakagawa, S. (2003) The *Corynebacterium glutamicum* genome: features and impacts on biotechnological processes. *Appl Microbiol Biotechnol* **62**: 99-109.

Johnson, A.D., Poteete, A.R., Lauer, G., Sauer, R.T., Ackers, G.K., and Ptashne, M. (1981) lambda Repressor and cro--components of an efficient molecular switch. *Nature* **294**: 217-223.

Johnson, D.C., Dean, D.R., Smith, A.D., and Johnson, M.K. (2005) Structure, function, and formation of biological iron-sulfur clusters. *Annu Rev Biochem* **74**: 247-281.

Kalinowski, J., Bathe, B., Bartels, D., Bischoff, N., Bott, M., Burkovski, A., Dusch, N., Eggeling, L., Eikmanns, B.J., Gaigalat, L., Goesmann, A., Hartmann, M., Huthmacher, K., Krämer, R., Linke, B., McHardy, A.C., Meyer, F., Möckel, B., Pfefferle, W., Pühler, A., Rey, D.A., Rückert, C., Rupp, O., Sahm, H., Wendisch, V.F., Wiegräbe, I., and Tauch, A. (2003) The complete *Corynebacterium glutamicum* ATCC 13032 genome sequence and its impact on the production of L-aspartate-derived amino acids and vitamins. *J Biotechnol* **104**: 5-25.

Kalinowski, J. (2005) The genomes of amino-acid producing *Corynebacteria*. In *Handbook of Corynebacterium glutamicum*. Eggeling, L. and Bott, M. (eds). Inc., Boca Raton, FL: Academic Press.

Keilhauer, C., Eggeling, L., and Sahm, H. (1993) Isoleucine synthesis in *Corynebacterium glutamicum*: molecular analysis of the *ilvB-ilvN-ilvC* operon. *J Bacteriol* **175**: 5595-5603.

Kelley, W.L. (2006) Lex marks the spot: the virulent side of SOS and a closer look at the LexA regulon. *Mol Microbiol* **62**: 1228-1238.

Kim, B., and Little, J.W. (1993) LexA and lambda Cl repressors as enzymes: specific cleavage in an intermolecular reaction. *Cell* **73**: 1165-1173.

King, N.D., Kirby, A.E., and Connell, T.D. (2005) Transcriptional control of the *rhuIR-bhuRSTUV* heme acquisition locus in *Bordetella avium*. *Infect Immun* **73**: 1613-1624.

Kinoshita, S., Udaka, S., and Shimono, M. (1957) Studies on the amino acid fermentation: I. Production of L-glutamic acid by various microorganisms. *J Gen Appl Microbiol* **3**: 193-205.

Klausner, R.D., and Rouault, T.A. (1993) A double life: cytosolic aconitase as a regulatory RNA binding protein. *Mol Biol Cell* **4**: 1-5.

Kocan, M., Schaffer, S., Ishige, T., Sorger-Herrmann, U., Wendisch, V.F., and Bott, M. (2006) Two-component systems of *Corynebacterium glutamicum*: deletion analysis and involvement of the PhoS-PhoR system in the phosphate starvation response. *J Bacteriol* **188**: 724-732.

Krug, A. (2004) Identifizierung und Charakterisierung eines Transkriptionsregulators der Aconitase von *Corynebacterium glutamicum*. In *Mathematisch-Naturwissenschaftlische-Fakultät* Düsseldorf: Heinrich-Heine Universität.

Krug, A., Wendisch, V.F., and Bott, M. (2005) Identification of AcnR, a TetR-type repressor of the aconitase gene *acn* in *Corynebacterium glutamicum*. *J Biol Chem* **280**: 585-595.

Kunkle, C.A., and Schmitt, M.P. (2003) Analysis of the *Corynebacterium diphtheriae* DtxR regulon: identification of a putative siderophore synthesis and transport system that is similar to the Yersinia high-pathogenicity island-encoded yersiniabactin synthesis and uptake system. *J Bacteriol* **185**: 6826-6840.

Kunkle, C.A., and Schmitt, M.P. (2005) Analysis of a DtxR-regulated iron transport and siderophore biosynthesis gene cluster in *Corynebacterium diphtheriae*. *J Bacteriol* **187**: 422-433.

Lamont, I., Brumby, A.M., and Egan, J.B. (1989) UV induction of coliphage 186: prophage induction as an SOS function. *Proc Natl Acad Sci U S A* **86**: 5492-5496.

Lee, J.W., and Helmann, J.D. (2007) Functional specialization within the Fur family of metalloregulators. *Biometals* **20**: 485-499.

Liebl, W., Klamer, R., and Schleifer, K.H. (1989) Requirement of chelating compounds for the growth of *Corynebacterium glutamicum* in synthetic media. *Appl Microbiol Biotechnol* **32**: 205-210.

Lin, H., Fischbach, M.A., Liu, D.R., and Walsh, C.T. (2005) *In vitro* characterization of salmochelin and enterobactin trilactone hydrolases IroD, IroE, and Fes. *J. Am. Chem. Soc.* **127**: 11075-11084.

Little, J.W., and Mount, D.W. (1982) The SOS regulatory system of *Escherichia coli*. *Cell* **29**: 11-22.

Little, J.W. (1984) Autodigestion of lexA and phage lambda repressors. *Proc Natl Acad Sci U S A* **81**: 1375-1379.

Lobell, R.B., and Schleif, R.F. (1990) DNA looping and unlooping by AraC protein. *Science* **250**: 528-532.

Lyubchenko, Y.L., Jacobs, B.L., Lindsay, S.M., and Stasiak, A. (1995) Atomic force microscopy of nucleoprotein complexes. *Scanning Microsc* **9**: 705-724; discussion 724-707.

Malik, M., Zhao, X., and Drlica, K. (2006) Lethal fragmentation of bacterial chromosomes mediated by DNA gyrase and quinolones. *Mol Microbiol* **61**: 810-825.

Mardanov, A.V., and Ravin, N.V. (2007) The antirepressor needed for induction of linear plasmid-prophage N15 belongs to the SOS regulon. *J Bacteriol* **189**: 6333-6338.

Masse, E., and Gottesman, S. (2002) A small RNA regulates the expression of genes involved in iron metabolism in *Escherichia coli*. *Proc Natl Acad Sci U S A* **99**: 4620-4625.

Masse, E., Vanderpool, C.K., and Gottesman, S. (2005) Effect of RyhB small RNA on global iron use in *Escherichia coli*. *J Bacteriol* **187**: 6962-6971.

Masse, E., Salvail, H., Desnoyers, G., and Arguin, M. (2007) Small RNAs controlling iron metabolism. *Curr Opin Microbiol* **10**: 140-145.

Matthews, K.S. (1992) DNA looping. *Microbiol Rev* **56**: 123-136.

May, J.J., Wendrich, T.M., and Marahiel, M.A. (2001) The *dhb* operon of *Bacillus subtilis* encodes the biosynthetic template for the catecholic siderophore 2,3-dihydroxybenzoate-glycine-threonine trimeric ester bacillibactin. *J Biol Chem* **276**: 7209-7217.

McHugh, J.P., Rodriguez-Quinones, F., Abdul-Tehrani, H., Svistunenko, D.A., Poole, R.K., Cooper, C.E., and Andrews, S.C. (2003) Global iron-dependent gene regulation in *Escherichia coli*. A new mechanism for iron homeostasis. *J Biol Chem* **278**: 29478-29486.

Merkens, H., Beckers, G., Wirtz, A., and Burkovski, A. (2005) Vanillate metabolism in *Corynebacterium glutamicum*. *Curr. Microbiol.* **51**: 59-65.

Miethke, M., Klotz, O., Linne, U., May, J.J., Beckering, C.L., and Marahiel, M.A. (2006) Ferri-bacillibactin uptake and hydrolysis in *Bacillus subtilis*. *Mol Microbiol* **61**: 1413-1427.

Nakayama, K., Kinoshita, S., and Sato, Z. (1964a) Growth of glutamic acid producing bacterium and related bacteria. 1. Effect of iron salts, ferrichrome, amino acids and some other compounds. *J. Gen. Appl. Microbiol.* **10**: 143-155.

Nakayama, K., Sato, Z., Kinoshita, S., and Tanaka, H. (1964b) Growth of glutamic acid producing bacterium and related bacteria. 2. Effect of chelating agent and its relation to inorganic salt. *J. Gen. Appl. Microbiol.* **10**: 181-199.

Ochsner, U.A., Wilderman, P.J., Vasil, A.I., and Vasil, M.L. (2002) GeneChip expression analysis of the iron starvation response in *Pseudomonas aeruginosa*: identification of novel pyoverdine biosynthesis genes. *Mol Microbiol* **45**: 1277-1287.

Oguiza, J.A., Tao, X., Marcos, A.T., Martin, J.F., and Murphy, J.R. (1995) Molecular cloning, DNA sequence analysis, and characterization of the *Corynebacterium diphtheriae dtxR* homolog from *Brevibacterium lactofermentum*. *J Bacteriol* **177**: 465-467.

Oppenheim, A.B., Kobiler, O., Stavans, J., Court, D.L., and Adhya, S. (2005) Switches in bacteriophage lambda development. *Annu Rev Genet* **39**: 409-429.

Ortiz de Orue Lucana, D., Zou, P., Nierhaus, M., and Schrempf, H. (2005) Identification of a novel two-component system SenS/SenR modulating the production of the catalase-peroxidase CpeB and the haem-binding protein HbpS in *Streptomyces reticuli*. *Microbiology* **151**: 3603-3614.

Pantopoulos, K. (2004) Iron metabolism and the IRE/IRP regulatory system: an update. *Ann N Y Acad Sci* **1012**: 1-13.

Pappenheimer, A.M., and Johnson, S.J. (1936) Studies in diphtheria toxin production. I : The effect of iron and copper. *B. J. Exp. Pathol.* **17**: 335-341.

Pierre, J.L., and Fontecave, M. (1999) Iron and activated oxygen species in biology: the basic chemistry. *Biometals* **12**: 195-199.

Pohl, E., Holmes, R.K., and Hol, W.G. (1999) Crystal structure of a cobalt-activated diphtheria toxin repressor-DNA complex reveals a metal-binding SH3-like domain. *J Mol Biol* **292**: 653-667.

Polen, T., Schluesener, D., Poetsch, A., Bott, M., and Wendisch, V.F. (2007) Characterization of citrate utilization in *Corynebacterium glutamicum* by transcriptome and proteome analysis. *FEMS Microbiol Lett* **273**: 109-119.

Posey, J.E., Hardham, J.M., Norris, S.J., and Gherardini, F.C. (1999) Characterization of a manganese-dependent regulatory protein, TroR, from *Treponema pallidum*. *Proc Natl Acad Sci U S A* **96**: 10887-10892.

Puig, S., Askeland, E., and Thiele, D.J. (2005) Coordinated remodeling of cellular metabolism during iron deficiency through targeted mRNA degradation. *Cell* **120**: 99-110.

Qiu, X., Verlinde, C.L., Zhang, S., Schmitt, M.P., Holmes, R.K., and Hol, W.G. (1995) Three-dimensional structure of the diphtheria toxin repressor in complex with divalent cation co-repressors. *Structure* **3**: 87-100.

Que, Q., and Helmann, J.D. (2000) Manganese homeostasis in *Bacillus subtilis* is regulated by MntR, a bifunctional regulator related to the diphtheria toxin repressor family of proteins. *Mol Microbiol* **35**: 1454-1468.

Quinones, M., Kimsey, H.H., and Waldor, M.K. (2005) LexA cleavage is required for CTX prophage induction. *Mol Cell* **17**: 291-300.

Ranjan, S., Yellaboina, S., and Ranjan, A. (2006) IdeR in mycobacteria: from target recognition to physiological function. *Crit Rev Microbiol* **32**: 69-75.

Reinscheid, D.J., Schnicke, S., Rittmann, D., Zahnow, U., Sahm, H., and Eikmanns, B.J. (1999) Cloning, sequence analysis, expression and inactivation of the *Corynebacterium glutamicum pta-ack* operon encoding phosphotransacetylase and acetate kinase. *Microbiology* **145 (Pt 2)**: 503-513.

Rodriguez, G.M., Voskuil, M.I., Gold, B., Schoolnik, G.K., and Smith, I. (2002) *ideR*, An essential gene in *Mycobacterium tuberculosis*: role of IdeR in iron-dependent gene expression, iron metabolism, and oxidative stress response. *Infect Immun* **70**: 3371-3381.

Rodriguez, G.M., and Smith, I. (2003) Mechanisms of iron regulation in mycobacteria: role in physiology and virulence. *Mol Microbiol* **47**: 1485-1494.

Rodriguez, G.M. (2006) Control of iron metabolism in *Mycobacterium tuberculosis*. *Trends Microbiol* **14**: 320-327.

Rouault, T.A. (2006) The role of iron regulatory proteins in mammalian iron homeostasis and disease. *Nat Chem Biol* **2**: 406-414.

Roy, S., Gupta, S., Das, S., Sekar, K., Chatterji, D., and Vijayan, M. (2004) X-ray analysis of *Mycobacterium smegmatis* Dps and a comparative study involving other Dps and Dps-like molecules. *J Mol Biol* **339**: 1103-1113.

Rudolph, G., Hennecke, H., and Fischer, H.M. (2006) Beyond the Fur paradigm: iron-controlled gene expression in rhizobia. *FEMS Microbiol Rev* **30**: 631-648.

Saiz, L., and Vilar, J.M. (2006) DNA looping: the consequences and its control. *Curr Opin Struct Biol* **16**: 344-350.

Schiering, N., Tao, X., Zeng, H., Murphy, J.R., Petsko, G.A., and Ringe, D. (1995) Structures of the apo- and the metal ion-activated forms of the diphtheria *tox* repressor from *Corynebacterium diphtheriae*. *Proc Natl Acad Sci U S A* **92**: 9843-9850.

Schmitt, M.P., and Holmes, R.K. (1991) Iron-dependent regulation of diphtheria toxin and siderophore expression by the cloned *Corynebacterium diphtheriae* repressor gene *dtxR* in *C. diphtheriae* C7 strains. *Infect Immun* **59**: 1899-1904.

Schmitt, M.P. (1997) Utilization of host iron sources by *Corynebacterium diphtheriae*: identification of a gene whose product is homologous to eukaryotic heme oxygenases and is required for acquisition of iron from heme and hemoglobin. *J Bacteriol* **179**: 838-845.

Schmitt, M.P. (1999) Identification of a two-component signal transduction system from *Corynebacterium diphtheriae* that activates gene expression in response to the presence of heme and hemoglobin. *J Bacteriol* **181**: 5330-5340.

Schmitt, M.P., and Drazek, E.S. (2001) Construction and consequences of directed mutations affecting the hemin receptor in pathogenic *Corynebacterium* species. *J Bacteriol* **183**: 1476-1481.

Schröder, I., Johnson, E., and de Vries, S. (2003) Microbial ferric iron reductases. *FEMS Microbiol Rev* **27**: 427-447.

Shearwin, K.E., Brumby, A.M., and Egan, J.B. (1998) The Tum protein of coliphage 186 is an antirepressor. *J Biol Chem* **273**: 5708-5715.

Simpson, W., Olczak, T., and Genco, C.A. (2000) Characterization and expression of HmuR, a TonB-dependent hemoglobin receptor of *Porphyromonas gingivalis*. *J Bacteriol* **182**: 5737-5748.

Spiering, M.M., Ringe, D., Murphy, J.R., and Marletta, M.A. (2003) Metal stoichiometry and functional studies of the diphtheria toxin repressor. *Proc Natl Acad Sci U S A* **100**: 3808-3813.

Takeno, S., Ohnishi, J., Komatsu, T., Masaki, T., Sen, K., and Ikeda, M. (2007) Anaerobic growth and potential for amino acid production by nitrate respiration in *Corynebacterium glutamicum*. *Appl Microbiol Biotechnol* **75**: 1173-1182.

Tang, Y., and Guest, J.R. (1999) Direct evidence for mRNA binding and post-transcriptional regulation by *Escherichia coli* aconitases. *Microbiology* **145 (Pt 11)**: 3069-3079.

Tao, X., and Murphy, J.R. (1992) Binding of the metalloregulatory protein DtxR to the diphtheria *tox* operator requires a divalent heavy metal ion and protects the palindromic sequence from DNase I digestion. *J. Biol. Chem.* **267**: 21761-21764.

Tao, X., and Murphy, J.R. (1994) Determination of the minimal essential nucleotide sequence for diphtheria tox repressor binding by in vitro affinity selection. *Proc Natl Acad Sci U S A* **91**: 9646-9650.

Tauch, A., Kaiser, O., Hain, T., Goesmann, A., Weisshaar, B., Albersmeier, A., Bekel, T., Bischoff, N., Brune, I., Chakraborty, T., Kalinowski, J., Meyer, F., Rupp, O., Schneiker, S., Viehoever, P., and Pühler, A. (2005) Complete genome sequence and analysis of the multiresistant nosocomial pathogen *Corynebacterium jeikeium* K411, a lipid-requiring bacterium of the human skin flora. *J. Bacteriol.* **187**: 4671-4682.

von der Osten, C.H., Gioannetti, C., and Sinskey, A.J. (1989) Design of a defined medium for growth of *Corynebacterium glutamicum* in which citrate facilitates iron uptake. *Biotechnol. Lett.* **11**: 11-16.

Waldor, M.K., and Friedman, D.I. (2005) Phage regulatory circuits and virulence gene expression. *Curr Opin Microbiol* **8**: 459-465.

Walker, G.C. (1987) The SOS response of *Escherichia coli*. In *Escherichia coli and Salmonella typhimurium*. Ingraham, J.L., Low, K.B., Magasanik, B., Schaechter, M. and Umbarger, H.E. (eds). Washington, DC: American Society for Microbiology, pp. 1346-1357.

Wandersman, C., and Stojiljkovic, I. (2000) Bacterial heme sources: the role of heme, hemoprotein receptors and hemophores. *Curr Opin Microbiol* **3**: 215-220.

Wang, T., Shen, G., Balasubramanian, R., McIntosh, L., Bryant, D.A., and Golbeck, J.H. (2004) The *sufR* gene (sll0088 in *Synechocystis* sp. strain PCC 6803) functions as a repressor of the *sufBCDS* operon in iron-sulfur cluster biogenesis in cyanobacteria. *J Bacteriol* **186**: 956-967.

Wennerhold, J., and Bott, M. (2006) The DtxR regulon of *Corynebacterium glutamicum*. *J Bacteriol* **188**: 2907-2918.

White, A., Ding, X., vanderSpek, J.C., Murphy, J.R., and Ringe, D. (1998) Structure of the metal-ion-activated diphtheria toxin repressor/tox operator complex. *Nature* **394**: 502-506.

Wilson, T.J., Bertrand, N., Tang, J.L., Feng, J.X., Pan, M.Q., Barber, C.E., Dow, J.M., and Daniels, M.J. (1998) The *rpfA* gene of *Xanthomonas campestris* pathovar campestris, which is involved in the regulation of pathogenicity factor production, encodes an aconitase. *Mol Microbiol* **28**: 961-970.

Wong, D.K., Lee, B.Y., Horwitz, M.A., and Gibson, B.W. (1999) Identification of *fur*, aconitase, and other proteins expressed by *Mycobacterium tuberculosis* under conditions of low and high concentrations of iron by combined two-dimensional gel electrophoresis and mass spectrometry. *Infect Immun* **67**: 327-336.

Yang, J., Sangwan, I., Lindemann, A., Hauser, F., Hennecke, H., Fischer, H.M., and O'Brian, M.R. (2006) *Bradyrhizobium japonicum* senses iron through the status of haem to regulate iron homeostasis and metabolism. *Mol Microbiol* **60**: 427-437.

Yellaboina, S., Ranjan, S., Chakhaiyar, P., Hasnain, S.E., and Ranjan, A. (2004) Prediction of DtxR regulon: identification of binding sites and operons controlled by Diphtheria toxin repressor in *Corynebacterium diphtheriae*. *BMC Microbiol* **4**: 38.

6 Appendix

6.1 Supplemental Material – RipA

Table S1. Bacterial strains and plasmids used in this work.

Strains or plasmids	Relevant characteristics	Source or reference
Strains		
C. glutamicum		
ATCC13032	Biotin-auxotrophic wild type	(46)
13032Δ*ripA*	In-frame deletion of the *ripA* gene	This work
E. coli		
DH5α	*supE44* Δ*lacU169* (ϕ80*lacZ*DM15) *hsdR17* *recA1* *endA1 gyrA96 thi-1 relA1*	Invitrogen
BL21(DE3)	*ompT hsdS*$_B$($r_B^-m_B^-$) *gal dcm* (DE3)	(5)
Plasmids		
pK19*mobsacB*	Kan^R; vector for allelic exchange in *C. glutamicum*; (pK18 *oriV*$_{E.c.}$, *sacB*, *lacZ*α)	(10)
pK19*mobsacB*-Δ*ripA*	Km^R; pK19*mobsacB* derivative containing a crossover PCR product covering the up- and downstream regions of *ripA*	This work
pET24b	Kan^R; vector for overexpression of genes in *E. coli*, adding a C-terminal hexahistidine affinity tag to the synthesized protein (pBR322 *oriV*$_{E.c.}$, P_{T7}, *lacI*)	Novagen
pET24b-*dtxR*-C	Kan^R; pET24b-Streptag derivative for over-production of DtxR with a C-terminal histidine tag	This study
pET28a	Kan^R; vector for overexpression of genes in *E. coli*, adding an N-terminal or a C-terminal hexahistidine tag to the synthesized protein (pBR322 *oriV*$_{E.c.}$, P_{T7}, *lacI*)	Novagen
pET28a-Streptag	Kan^R; pET28a derivative adding an N-terminal StrepTag-II to the synthesized protein	(47)
pET28a-Streptag-*ripA*	Kan^R; pET28a-Streptag derivative for over-production of RipA with an N-terminal StrepTag-II	This study
pJC1	Kan^R; *E. coli*/*C. glutamicum* shuttle vector; *oriV*$_{E.c.}$ from pACYC177, *oriV*$_{C.g.}$ from pHM1519;	(48)
pJC1-*ripA*	Kan^R; pJC1 derivative containing the *ripA* gene including its promoter region (extending 250 bp upstream of the *ripA* start codon)	This study

Table S2. Oligonucleotides used in this study.

Oligonucleotide	Sequence (5´→ 3´) and properties[a]
Oligonucleotides for *ripA* deletion and PCR analysis of the resulting mutants	
1558-amp-for	GTA TTT TCG GTA GCG TAT AAG TCC
1558-amp-rev	CCGGACAGCAGAAGGGAAATT C
1558-A-for	TATATA GAATTC GGATAAGGTCAAATTCTTTCGCTC (EcoRI)
1558-B-rev	*CCCATCCACTAAACTTAAACA* CAAGCTGGCAGAACTCATATCTC
1558-C-for	*TGTTTAAGTTTAGTGGATGGG* GAAGAACTTCTGAACACTCCTGTAC
1558-D-rev	GACGAAGAGGCCTTCGAATACTG (HindIII)
Oligonucleotides for expression of *ripA* in *C. glutamicum*	
ripA+250-for(2)	TAT ATA GTC GAC AGG AGA GTT AGC GCA GCG ACC TGC (SalI)
ripA+250-rev	TATATA CTGCAGTCACATTTGTACAGGTACAGGAG (PstI)
Oligonucleotides for overexpression of *ripA* and *dtxR* in *E. coli*	
ripA-2-for	ATA TAT CAT ATG ATG AGT TCT GCC AGC TTG TTG TG (NdeI)
ripA-2-rev	TAT ATA CTC GAG TCA CAT TTG TAC AGG TAC AGG AG (XhoI)
dtxR-for-1	ATA TAT CAT ATG GTG AAG GAT CTG GTC GAT ACC (NdeI)
dtxR-rev-1	ATA TAT CTC GAG GTG GTG GTG GTG GCC CTC AAC CTT TTC TAC GCG (XhoI)
Oligonucleotides for generating PCR products used in gel shift assays	
Acn-for-3	CAGGTTGGAAGTCATCACTGGAGT
Acn-rev-2	GTCATAGGACTTGTCGCCAACTTC
acn-Prom2-for	ATCCCTCAGGTTGGAAGTCATC
acn-Prom2-rev	TGAAGGTTTTTAGATGATTCCAG
acn-Prom3-for	TTAGTGTCGGGCTCACGAAAGAG
acn-Prom3-rev	GGCGCGTCAATAACGTCATGG
acn-Prom4-for	CAAGAACCCCAACTTTCCCG
acn-Prom4-rev	TAGTCATAGGACTTGTCGCC
acn-Prom5-for	TCTTTTTCCAAAGTCGGAAACTG
acn-Prom5-rev	GACTTTCTATCACCCCCTTACTC
acn-Prom6-for	ACATCACGCACGTACCCATTTCG
acn-Prom6-rev	GCCGGCGTGAGAAAAACATCGG
acn-Prom7-rev	GAGTAAAGTCGGTTCCCGCTC
acn-Prom8-rev	AATGGGTACGTGCGTGATGTGAC
acn-Prom9-for	ATAGAAAGTCACATCACGCACG
acn-Prom10-for	AAAACCTTCATTAGTGTCGGGC
nar-Prom2-for	AGGCCCCACGCCCGTTCCGCCG
nar-Prom2-rev	CGCCATGCAATTTTCGAGTCCC
leuC-Prom-for	TGAACGGATTCGCCGGTGCGCTCC
leuC-Prom-rev	CGACATGGTCGCGCCACACCTTC
catA-Prom-for	TGAAAAGAAGTTGGTATTGCCAC
catA-Prom-rev	CCCGAATCGTGGGCTGTTGGATC
katA-Prom-for	TTTGCGGGGGCGTGCCATGTC
katA-Prom-rev	AACTGGTGCTCCGTTGTGGCGG
sdh-Prom-for	CGGAAGGTTGGGCTGTCTAAAC
sdh-Prom-rev	GACATAAAACCCCACTTATTAGG
pta-Prom-for	CCTGCACCGACAACGGCAACACG
pta-Prom-rev	CGAAGCTGCGGTTGACCGTGGTG
ripA-Prom-for	CTG CTC GCA AAG TTG CTG AAC C
ripA-Prom-rev	GTGAAAATTCTCTCGCCAAA ACG
acn-A.1	GAGTAAAGTCGGTTCCCGGAGTTTCGTGAGCCCGACAC
acn-A.2	GAGTAAAGTCGGTTCGGCCTCTTTCGTGAGCCCGACAC
acn-A.3	GAGTAAACAGGGTTCCCGCTCTTTCGTGAGCCCGACAC
acn-A.4	GAGTAAAGTCGCAAGCCGCTCTTTCGTGAGCCCGACAC
acn-A.5	GAGTATTGTCGGTTCCCGCTCTTTCGTGAGCCCGACAC
acn-B.1	ATAGAAACAGACATCACGCACGTACCCATTTCGAGCAAATCC
acn-B.2	ATAGAAAGTCACATCTGCCACGTACCCATTTCGAGCAAATCC
acn-B.3	ATAGAAAGTCACATCACGGTGCTACCCATTTCGAGCAAATCC

Oligonucleotide	Sequence (5′→ 3′) and properties[a]
acn-A.5	GAGTATTGTCGGTTCCCGCTCTTTCGTGAGCCCGACAC
acn-B.1	ATAGAAACAGACATCACGCACGTACCCATTTCGAGCAAATCC
acn-B.2	ATAGAAAGTCACATCTGCCACGTACCCATTTCGAGCAAATCC
acn-B.3	ATAGAAAGTCACATCACGGTGCTACCCATTTCGAGCAAATCC
acn-B.4	ATAG AAAGTCAGTAGACGCACGTACCCATTTCGAGCAAATCC
acn-B.5	ATAGATTGTCACATCACGCACCAACCCATTTCGAGCAAATCC
sdh-1.1	CTTTATTGTCGTTTGA GCGTCATTTAATTGAGTGTGCTC TACC
sdh-1.2	CTTTATT CAGGTTTGACGCTCATTTAATTG AGTGTGCTCTACC
sdh-1.3	CTTTAAAGTCGTTTGACGCT CTA TTAATTGAGTGTGCTCTACC
sdh-2.1	CATGGGGGA CGCCCCCGTGACTGGTTAATGCC CCGATCTG
sdh-2.2	CATGGGGGAGCGCCCCGT CTGTGGTTAATGCCCCGATCTG
sdh-2.3	CATG GCCGAGCGCCCCGTGACACGTTAATGCCCCGATCTG
katA-A-for	CGGGAACGGATTGTTCCGACTCG
katA-A	ATCCGACACGACATGGCACG CCC
katA-A-M	ATCCGACACGACATGGCAGC GCCCCGCAAATCCA TCGTCGAATACG
katA-B	GTGCGCGCCGAGGAGCGCGCTGC
katA-B-M	GTGCGCGCCGAGCTCCGCGCTGCGAAGCGGGGGAGG
katA-B-rev	TAACGACGCCCACGTCACCG AGC
katA-C	TGATTATTTGGTGGCGCGAA GTG
katA-C-M	TGATTATTTGGTG CGCCGAAGTGACATTCTGATGTA GAC
catA-A-rev	CCCGAGCAAACCCTAGGAAT TC
catA-A	TTTTGCTTTGAAGCGGTGTGTGAC
catA-A-M	TTTTGCTTTGAACGCGTGTGTGACATTTGCGAGCAATTCC
narK-A	ATATTTGTGTCGTAATTCAC TTTATG
narK-A-M	ATATTTGT CAGGTAATTCACTTTATGCAGGT AAACGAATTTG
narK-B	CATGAAGAGGCATCACGTGA CAC
narK-B-M	CATGAAGA CCGATC ACG TGA CAC AAC TCA ACA CCA AAG G
leuC-A	GCATAAATGTCACCTCCCGC CC
leuC-A-M	GCATAAATGTCACCTCC GCGCCAAAATCTTTTTATACCCC CAC
pta-A	GTCTATGAAAGCGCGCAGCG TGAC
pta-A-M	CTATGAAAGC CGCCAGCGTGACAAATCAGACCC CAGCAAAGCC
pta-B	TCTCATTGATGACACTTCAG GCTTG
pta-B-M1	TCTCATTGAT CTGACTTCAGGCTTGTGCCTCCTGGCAC

[a] In some cases oligonucleotides were designed to introduce recognition sites for restriction endonucleases (recognition sites underlined, restriction endonucleases indicated in parentheses) or complementary 21mer sequences for generating cross-over PCR products (printed in italics).

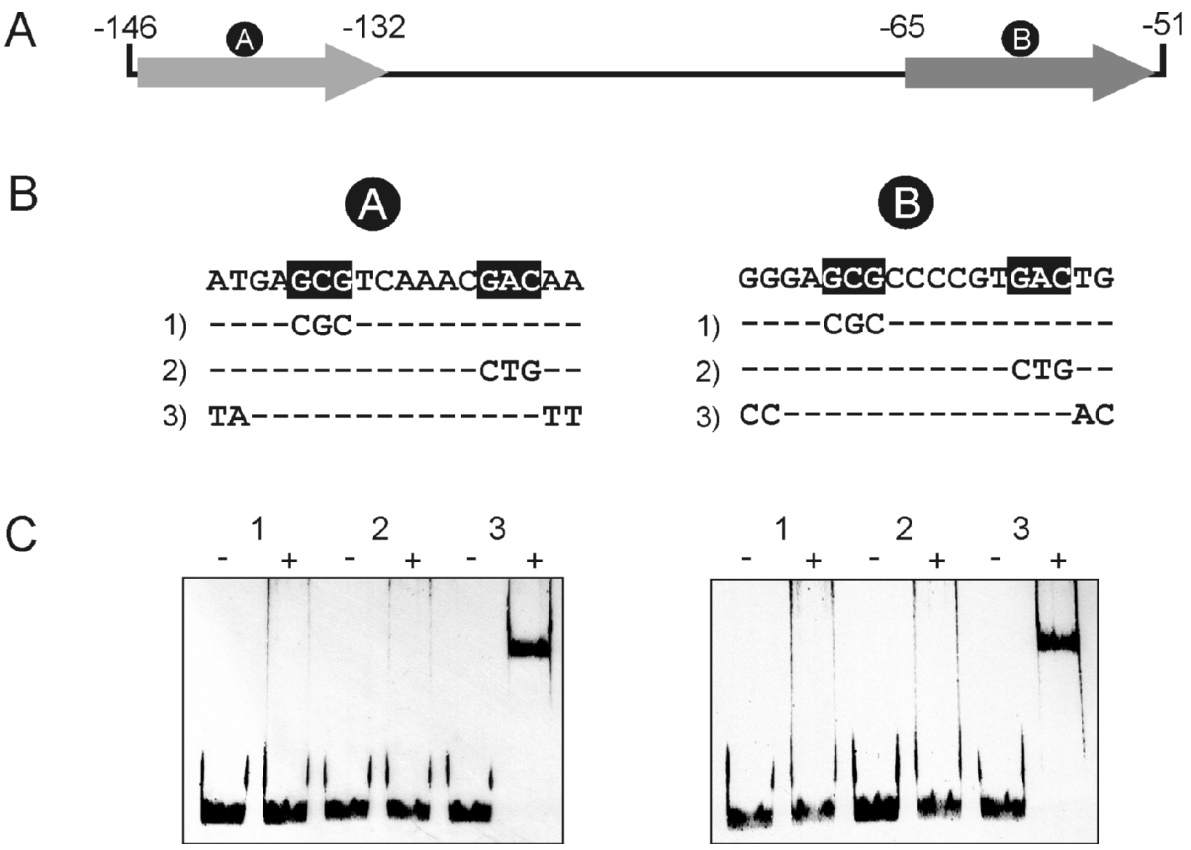

Figure S1. Mutational analysis of the RipA binding sites within the *sdhC* promoter. *A*, the two arrows denoted A and B indicate the two RipA binding sites as deduced from gel shift assays, which show the same orientation. The numbers indicate their position relative to the *sdhC* start codon. *B*, mutations introduced within (1 and 2) and outside (3) the proposed RipA binding sites (A and B) are given below the wild-type sequence. The mutations were introduced using the oligonucleotides sdh-1.1 – sdh-2.1 (Table 2). *C*, gel shift analysis with purified RipA protein and the mutated DNA fragments. Approximately 20 nM of the fragments A1 – A3 and B1 – B3 were incubated for 30 min at room temperature either without RipA (lanes labeled "-") or with 1 µM of RipA protein (lanes labeled "+"). The samples were separated by nondenaturing PAGE (10%) and the gels were stained with SybrGreen I.

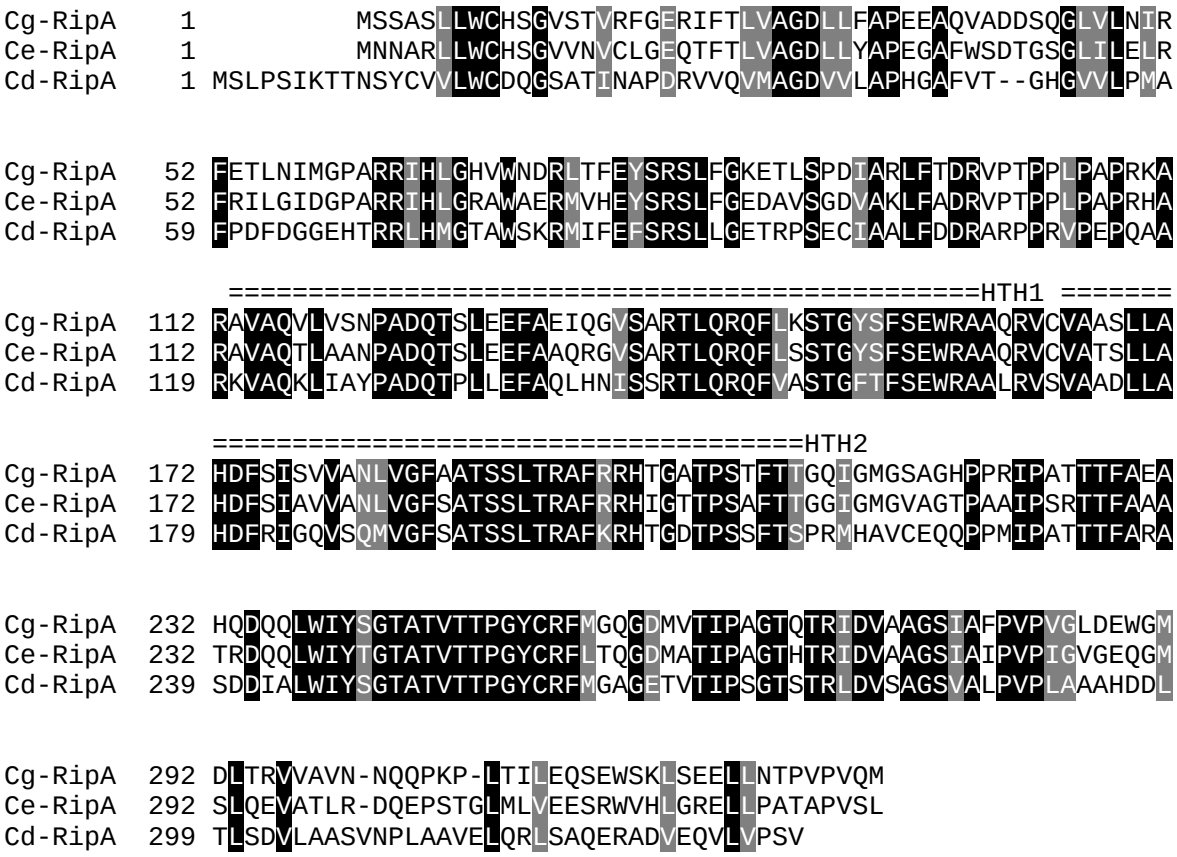

Figure S2. Model of the regulatory cascade involving DtxR and RipA and organization of the RipA target genes. Under iron excess, DtxR represses the expression of *ripA*. Under iron limiation, DtxR repression is relieved; RipA protein is synthesized and partially represses expression of its target genes, which encode iron-containing proteins, except for *narK*, *pta* and *ackA*. In this way, intracellular iron usage is modulated and supplements mechanisms for iron uptake that are directly regulated by DtxR.

6.2 Supplemental Material – DtxR

Table S1. Oligonucleotides used in this study.

Oligonucleotide	Sequence (5´→ 3´) and properties[a]
Delta-dtxR-1	ATATATGAATTCAGAGCGCGCATCACGTCTTCG(EcoRI)
Delta-dtxR-2	*CCCATCCACTAAACTTAAACA*TTGTTTTTCCAAACTCAATTTATGCC
Delta-dtxR-3	*TGTTTAAGTTTAGTGGATGGG*GCACATGCAGTCCGCCTAGAA
Delta-dtxR-4	ATATATGGATCCGGGCATGTCCTCGGTGATGGG(BamHI)
Delta-dtxR-for	GCGTGAAGTCATGAGTAAGCTC
Delta-dtxR-rev	GACAGCTTFCGTTGCGCCATATG
dtxR-for-1	ATATATCATATGGTGAAGGATCTGGTCGATACC (NdeI)
dtxR-rev-1	ATATATCTCGAGGTGGTGGTGGTGGCCCTCAACCTTTTCTACGCG (XhoI)
0329-for	ACTTCAGACAGTCACGTGTCGG
0329-rev	GGCCAGAGGCAGGAGACAAAAATGC
0123-for	TCTTGTCTTCAGCCACATCTATTCG
0123-rev	TTCGGTGCTAACCATGTCAGAG
1646-for	CGCTCGACCTTGTACGAATATCTC
1646-rev	CTTGATCCATGTCAGACTTCGTTTG
0430-for	GAAAGCTCAGAAGAAGGTCCAGAG
0430-rev	GCTGGATGGGATAACGGAGGTC
0381-for	GGAAAATATGTTCGAGTGGAGCCG
0381-rev	GCTTGTTCATTTTTGTTCTCCTGTTC
0358-1-for	ACTGTACGTCCCAGATCGGGGC
0358-1-rev	TCCCTGGATCGGAAGGTTGGGC
0358-2-for	TCCGAACAGTTTCTAACCCCGTTTG
0358-2-rev	GGACCCCACATATGTCTTTCCC
2027-for	AGCTTCAGAGGAGCCTGAAGCGG
2027-rev	CGGAGTGGGTTGATTCTGGGATG
1955-for	GTTCGCTACGTCCGAGTGATCACC
1955-rev	GTCCCCCACGATTGTTTAAAAGTC
2766-for	CCCTTTTAAATACTTTGAAAATTACTC
2766-rev	CATTACTTTAAGCCTTTGGGGCAG
0465-for	GTCACTTCCTGTTGTGGCTGCCTG
0465-rev	GGTATTAAGTTTTTTATTCATAACCCC
2718-for	ACCGCTTGGTCTGTAAACGTAGC
2718-rev	CATGGGGAGTTAATCCTTAAAGAGC
2450-for	GGCACACATTTCCAACCCTCGAC
2450-rev	TTGAGTTTGGCAGCTTCCACGAATGC
2146-for	GCGGAAAATTGTTCCAACTAAGGG
2146-rev	CCTCCGATAGGTCGCTGTTGCTTGC
2752-for	GAGCTTTCCGCCAGTAGGCCAAGC
2752-rev	GCAGCGGTCAGTACTGCGAAAGC
0377-for	CTGCATTTTGAAAAGTCATGATGGCG
0377-rev	CATGAACAGCAGTGTCCTTTTCCGC
0484-for	GCGCTAAAAATTCATACGTTTAGC
0484-rev	CCGCCGTCATATCGCGTGACTCC
0618-for	AGGACCTGCTTCCAGATTTGAGG
0618-rev	GCGGGATTGCACGACAAATCTCCG
0914-for	CCAGAGTTCAGGATTCATTGATCC
0914-rv	CGCCAAACGCAACCTTGCCCCGC

0639-for	TTTCCAGATTCGTGCATGTAAGCAC
0639-rev	GCCGGCTAGAACGCGAGACGTACGC
0774-for	TCTAGGCATTTAAGGCTTTCAGGCC
0774-rev	GCTGCGAGAAGCACGATCAGTGCG
1200-for	CGATCGTCTCTACCGCGTCGGCG
1200-rev	GCGCTGGAGTGTTCATGGAAAACC
2970-for	GTGTTGTGAGTGATTGCGCGCATGG
2970-rev	CGATAACTGCGCTGCGTGAAAGCG
1209-for	GTGGTTTGCGTTTTAGGAGGCGACTTC
1209-rev	GCTGACTTAAATAAACTGACACGC
1395-for	GCGCACAATCTCGTCGGGAAGCTTG
1395-rev	CGCCCATGACGGTCAAAATAGCG
1959-for	CACTCTAGCAGCATTACATTAAGGC
1959-rev	TACAGCAAGGGTGGTGGCGCCGAGC
0775-for	AGCAACAGTTGCGATTGAAACTAGC
0775-rev	CACGGGGAGACCTCCGGGTGGG
0776-for	CAAGCCAAGTTGGGGCCTTGGGTG
0776-rev	AGCAACAGTTGCGATTGAAACTAGC
0777-for	TCCGACAATGAAGCACTGGCAAACG
0777-rev	GTTGCCATCAGTGCCGATCCCC
1875-for	CCTGCCCCTCTGCGGTTTCTGGG
1875-rev	CTGTGGTCTGCGTCATAAGGGTAGC
1915-for	CCGACGCCTGGCGTGTCTTCTGC
1915-rev	TGACCTCCGTTGTTATGAATATTCC
2108-for	CTAGCCTTCTCAGGGTTCTAGGG
2108-rev	CACTGATGAAACTCCAAATTCTTCC
1504-for	GGGGACGAGGTGCCCGAGGAAACC
1504-rev	TCCCACTGGTGTCACCTCCTGC
2170-for	CCACGTCTTGGTAAGTATCTAGATCG
2170-rev	AAAGTGTTATTTTCAAAAAGGGGCAG
2971-for	GCACAACGGTGCGGGGGAATTGGC
2971-rev	CGCATGGTGGTGTTCCTCTCATCGC
0376-for	TTGCGGAACGATTGCCTAAATCCC
0376-rev	GATGGCGTCTCGGGCTCTGTGAAAGG
0155-for	GTAACTGAGTTGCGGGTGGTGG
0155-rev	CATGTGGCGATGCAACCCTTCACTC
0154-for	ACCCTCACGATCGCATGTCATGAC
0154-rev	CATGATGTCTCCTTTCGTTGCCCACC
1110-for	AAGGATCCGTGCGATTTCGTGGTC
1110-rev	TTGTTCGCGTTTTTGTGCACGGCG
1120-for	AGAAGTCGAGGTGGGGAAGTGGAC
1120-rev	ATGATTTCATGAATACGCATGTC
1127-for	AGCGGTACCGACTCGAATCCAATTC
1127-rev	GTAAGCGGTGACCTGGACATCGC
1145-for	TCATTCATGTGCGAGACACCCTTGG
1145-rev	AAAGCTGGCGCTGGGGCCACGAAC
0120-for	TTCAGCTCGGCAGTTCGAAACGC
0120-rev	GTGCATGCACTTTGCAGCCGGGG
1339-for	GCAAAGAATACGGCTTCCTTGGCTG
1339-rev	GGTCGAAGAAGAGGTGGTTGAGG
1355-for	TGTCGGGTGGTCCTGGTTTGATTGC
1355-rev	TATTCCGTGATTACACTCATAGACC
1444-for	ACGGGAGCAGCTGGAATTCTTCG
1444-rev	TGCGGAGCTACCACGAACACTCC

1500-for	GCTTCGCGAGTGGGTTAAGG
1500-rev	GGACATGTTACTTGATGAACTGG
1571-for	TTCGTGGTAGCTGCAACCAAGGCC
1571-rev	CCCGCTTACCTTTCCATTGTTTAGTG
1594-for	TATCGTGCGTGTGCTGTCCAAGGC
1594-rev	AACCACGCTTGTCGACGCCCACC
1645-for	TGACTTTGAGTCAGCAAAAAGCG
1645-rev	CGGGTGACAGTGGGGTAGTGGTTG
1677-for	CATATCGAGCTCAGTATCAATGTC
1677-rev	AATTCCTTTAATTGACACTTAATTGACC
1669-for	TACTACCTACGACCACATAAGCG
1669-rev	GCACGCCGACTGATAGGTTTAGTC
1930-for	CCGGCTTCTCAGCACTTTCTTCC
1930-rev	GGTCTCGGTCTCTGCTGCAGGAGG
2006-for	CAATCCCCAATGCACTGTTTGCC
2006-rev	ACCAGCGCAGATTATGCGCCAGC
2037-for	GTTCCCGGCGCGCCAATTACTGC
2037-rev	GGACGTGCCATGATGAAACACCC
2159-for	GGCATGCGAGATTTGCTGATCCG
2159-rev	CATACGAAAACAATTTCCACAGGTAGC
2282-for	CGTTTGGCCAGTTGATGTACGCGG
2282-rev	AACTCGAGTGGCTCCAGCGAGGAC
2374-for	CAAAGCTTTCTCCCAACGCGAAGG
2374-rev	TAGTGACGTGCCGCAGCATCTCCC
2414-for	ACTGCGATGTTCTGCAAGCTGACG
2414-rev	GATGCAAGAAGAAGTTTCATCCGG
0027-for	CCGGTTGGGAAGCGTGCCGTGATG
0027-rev	CAGGCCAATGCTGACGTCTTGGG
2750-for	TCCCCTGCGGAGACTCCGTATGG
2750-rev	CGCAGCCTCCGCATAATCAGTAGTG
2819-for	AACTCTCTAAAGGAACACGAGCGCG
2819-rev	ATTCTATCAATGGTCACTGTTTGG
2834-for	ACCTACGAAGACACAGAAGTACG
2834-rev	CGCGAATCATTGTTTGAACTAGG
2877-for	CACCGTGGTGGCCCGATCGATACC
2877-rev	TGATGTCCATGTCCGTGCCCTTC
0486-for	GCGGGGCAGTGAAAGTAAAAACG
0486-rev	TTGTCCGGGCTTGGGGCTCGGGC
0594-for	ATATTTGATAACCTCATGGTTTGG
0594-rev	CCCTCGACGCCGCCTTTGCGGGG
0802-for	AGTATTAATCCCACCAGTAACAGTG
0802-rev	TGCGGTGATGTGGTCTTCGCTGG
0891-for	GCGCGATTGAGCCTCTATAACGG
0891-rev	ACGTGTGTGGTGATGCTCATGGTG

[a] In some cases oligonucleotides were designed to introduce recognition sites for restriction endonucleases (recognition sites underlined, restriction endonucleases indicated in parentheses) or complementary 21mer sequences for generating cross-over PCR products (printed in italics).

Table S2. Overview on genes whose average mRNA ratio (Δ*dtxR* mutant/wild type) was altered ≥2-fold or ≤0.5-fold (p-value ≤0.05) under iron excess or under iron limitation in at least two independent experiments. The mRNA ratios represent average values obtained from four (iron excess) or three (iron limitation) DNA microarray experiments performed with RNA isolated from four or three independent cultures in CGXII minimal medium containing either 100 µM $FeSO_4$ or 1 µM $FeSO_4$. Ratios labelled with an asterisk could be analyzed in only a single experiment.

NCgl	Annotation	Ratio Fe	Ratio Fe
	Genes with an increased mRNA ratio (mutant/wild type)		
NCgl0122	hypothetical protein	31.33	21.49*
NCgl0123	hypothetical protein	20.93	10.76
NCgl0138	hypothetical protein	2.14	1.35
NCgl0376	hypothetical membrane protein	3.66	2.99
NCgl0377	put. secreted heme transport associated protein, C-term TMH	16.82	5
NCgl0378	heme ABC transporter, secreted lipoprotein, *hmuT*	2.97	2.64*
NCgl0379	heme ABC transporter, permease, *hmuU*	9.33	3.98
NCgl0381	put. secreted heme transport assosiated protein, C-term. TMH	17.66	5.99
NCgl0382	put. secreted heme transport assosiated protein, C-term. TMH	13.99	6.51*
NCgl0430	transcriptional regulator, ArsR family	6.68	7.39
NCgl0481	hypothetical protein	3.89	1.18*
NCgl0482	put siderophore ABC transporter, ATPase	5.72	1.73
NCgl0483	put siderophore ABC transporter, permease, FecCD family	6.43	1.55*
NCgl0516	ribosomal protein L6	1.66	2.82
NCgl0565	putative membrane protein	2.07	1.68
NCgl0590	hypothetical exported protein	3.17	n.d.
NCgl0627	2-methylcitrate dehydratase, *prpD2*	0.94*	6.34
NCgl0630	2-methylcitrate synthase, *prpC2*	0.7*	5.95
NCgl0631	put. malate/L-lactate dehydrogenase	1.24*	3.73
NCgl0635	put. soluble, cytoplasmic siderophore-interacting protein	6.53	1.7
NCgl0636	put. siderophore ABC transporter, ATPase	6.78	1.62
NCgl0637	put. siderophore ABC transporter, permease, FecCD family	5.7	1.74
NCgl0638	put. siderophore ABC transporter, permease, FecCD family	2.35	1.42
NCgl0639	put. siderophore ABC transporter, secreted lipoprotein	7.85	1.72
NCgl0649	hypothetical membrane protein	2.11	1.24
NCgl0666	2-methylcitrate synthase, *prpC1*	0.78*	2.34
NCgl0700	put. ATP-dependent helicase	2.76	0.99*
NCgl0701	hypothetical protein	2.81	0.83*
NCgl0773	put. soluble, cytoplasmic siderophore-interacting protein	11.63	2.38
NCgl0774	put. siderophore ABC transporter, secreted lipoprotein	8.43	2.51
NCgl0776	put. siderophore ABC transporter, secreted lipoprotein	4.16	1.17*
NCgl0779	put. siderophore ABC transporter, ATPase	4.21	1.27*
NCgl0858	putative helicase	2.42	n.d.
NCgl0891	hypothetical protein	6.38	5.91
NCgl0943	transcriptional regulator, AraC family, *ripA*	12.16	4.13
NCgl1091	hypothetical protein	8.27	2.5
NCgl1119	put. DNA repair exonuclease	3.44	2.13
NCgl1120	ATPase involved in DNA repair	2.95	1.36
NCgl1200	put. soluble, cytoplasmic siderophore-interacting protein	4.76	2.42*
NCgl1209	put. siderophore ABC transporter, secreted lipoprotein	3.31	1.94*
NCgl1217	hypothetical protein	2.09	1.16*
NCgl1251	hypothetical protein	1.3*	2.71
NCgl1253	put. thiamine biosynthesis protein	1.56	3.13
NCgl1254	hypothetical protein	1.04*	2.58
NCgl1289	hypothetical protein	3.85	1.58
NCgl1490	hypothetical protein	2.05	2.47
NCgl1616	hypothetical membrane protein	1.75	2.8
NCgl1617	hypothetical protein	2.66	2.81*
NCgl1618	hypothetical protein	5.88	17.48
NCgl1633	hypothetical protein	2.37	2.3

NCgl1635	hypothetical protein	24	20.55
NCgl1636	hypothetical membrane protein	3.46	4.74*
NCgl1637	hypothetical protein	5.86	3.13*
NCgl1642	hypothetical protein	2.38	1.84
NCgl1644	hypothetical protein	2.73	1.88
NCgl1645	putative resolvase, *res*	6.59	5.17
NCgl1646	secretory serine protease	33.09	11.92
NCgl1647	hypothetical protein	8.72	7.01
NCgl1648	predicted protein-tyrosine phosphatase	3.76	1.5*
NCgl1649	hypothetical protein	5.12	2.63
NCgl1651	hypothetical exported protein	13.72	11.53
NCgl1652	hypothetical protein	7.42	5.8
NCgl1654	hypothetical protein	4.23	2.91*
NCgl1661	hypothetical protein	2.46	1.29*
NCgl1666	hypothetical protein	6.13*	4.6
NCgl1668	hypothetical protein	2.58*	2.31
NCgl1669	DNA primase	6.57	6.88*
NCgl1671	hypothetical protein	4.25	2.84*
NCgl1673	hypothetical helicase	3.81	2.71*
NCgl1677	hypothetical protein	7.47	14.78
NCgl1678	hypothetical protein	23.04	10.11
NCgl1679	hypothetical protein	16	9.27*
NCgl1680	hypothetical protein	14.99	9.97
NCgl1682	hypothetical protein	10.4	8.04
NCgl1684	hypothetical protein	7.47	6.26*
NCgl1685	hypothetical membrane protein	12.54	9.1
NCgl1687	put. (AAA) ATPase	7.22	4.78
NCgl1688	hypothetical protein	8.58	3.73*
NCgl1690	hypothetical protein	5.18	2.46*
NCgl1692	hypothetical helicase	3.88	2.17*
NCgl1693	hypothetical protein	4.18	1.99*
NCgl1696	hypothetical protein	5.39	1.83*
NCgl1700	hypothetical protein	6.55	3.56
NCgl1702	hypothetical protein	7.87	7.98
NCgl1703	type II restriction-modification system, methylation subunit, *cglIM*	5.75	1.81*
NCgl1704	type II restriction-modification system restriction subunit, *cglIR*	2.41	1.57*
NCgl1706	hypothetical protein	5.01	4.09
NCgl1707	hypothetical membrane protein	2.56	1.9*
NCgl1711	hypothetical protein	3	2.66*
NCgl1712	hypothetical membrane associated protein	3.3	2.52
NCgl1714	hypothetical membrane protein	3.87	3.42
NCgl1716	ATP-dependent Clp protease, *clpA*	5.76	4.16
NCgl1718	hypothetical membrane protein	3.56	3.27
NCgl1720	hypothetical protein	2.27	8.85*
NCgl1721	hypothetical protein	4.06	3.01
NCgl1726	hypothetical protein	7.63	3.82*
NCgl1727	hypothetical membrane protein	9.76	7.78
NCgl1730	hypothetical protein	3.75	1.5
NCgl1736	hypothetical protein	2.54	1.56*
NCgl1770	superfamily I DNA and RNA helicases	2.48	2.29*
NCgl1816	putative phage integrase	2.05	1.72
NCgl1959	put. secreted siderophore binding lipoprotein	8.48	3.26
NCgl2089	hypothetical protein	6.08	2.84
NCgl2145	hypothetical protein	2.89	2.4
NCgl2146	heme oxygenase, *hmuO*	4.02	3.17
NCgl2149	hypothetical protein	6.77	4.54
NCgl2201	transposase	4.87	5.44
NCgl2356	transposase	5.81	5.36
NCgl2434	hypothetical membrane protein	2.42	0.98*
NCgl2439	ferritin, *ftn*	1.07*	2.54
NCgl2450	put. 2-methylcitrate dehydratase	10.1	11.52

NCgl2705	hypothetical protein	2.15	1.2*
NCgl2706	hypothetical ATP/GTP binding protein	2.39	1.34
NCgl2864	hypothetical protein	4.71	4.22
NCgl2897	starvation-inducible DNA-binding protein, *dps*	1.28	6.39*
NCgl2969	putative membrane transport protein	4.35	1.43
NCgl2970	put secreted siderophore binding lipoprotein	4.94	1.37
NCgl2972	hypothetical membrane protein	2.35	1.28*
	Genes with an decreased mRNA ratio (mutant/wild type)		
NCgl0155	sugar kinase	0.37	0.33*
NCgl0156	hypothetical cytosolic protein	0.42	0.35*
NCgl0161	put. myo-inositol 2-dehydrogenase	0.48	0.51*
NCgl0162	sugar phosphate isomerase/epimerase	0.47	0.67
NCgl0180	put.sensor protein with PAS domain, *fixL*	0.37	0.3*
NCgl0251	catalase, *katA*	0.27	3.06
NCgl0358	transcriptional regulator, *ramB*,	0.39	0.67*
NCgl0359	succinate dehydrogenase, *sdhC*	0.16	0.46*
NCgl0360	succinate dehydrogenase, *sdhA*	0.08	0.28*
NCgl0361	succinate dehydrogenase, *sdhB*	0.18	0.46
NCgl0362	hypothetical membrane protein	0.36	0.75
NCgl0670	propionyl-CoA carboxylase, biotin-containing subunit	0.36	0.34*
NCgl0694	ABC transporter, permease component	0.29	0.38
NCgl0696	hypothetical protein	0.35	0.43*
NCgl0697	ABC transporter, periplasmic binding protein	0.28	0.48
NCgl0785	RPF protein precursor, *rpf*	0.37	0.49
NCgl1021	transposase	0.55*	0.43
NCgl1114	hypothetical membrane protein	0.27	0.67*
NCgl1141	nitrate reductase, β subunit, *narH*	0.21	0.24*
NCgl1142	nitrate reductase, α subunit, *narG*	0.1	0.41
NCgl1143	nitrate/nitrite transporter, *narK*	0.34	0.6*
NCgl1262	3-isopropylmalate dehydratase, large subunit, *leuC*	0.28	0.5*
NCgl1263	3-isopropylmalate dehydratase small subunit, *leuD*	0.28	0.59*
NCgl1368	put. acetyltransferase	0.22	0.44
NCgl1384	preprotein translocase subunit, *secA*	0.47	0.86*
NCgl1409	NADH dehydrogenase, *ndh*	0.41	0.52
NCgl1482	aconitase, *acn*	0.29	0.63*
NCgl1502	Fe-S cluster assembly, *sufD*	0.47	0.43
NCgl1503	Fe-S cluster assembly, *sufB*	0.48	0.43
NCgl1876	glutamate ABC transporter, periplasmic binding protein, *gluB*	0.41	0.74
NCgl1877	glutamate ABC transporter, permease, *gluC*	0.49	0.64*
NCgl1915	oligopeptide ABC transporter, periplasmic binding protein, *oppA*	0.15	0.38
NCgl1917	put. oligopeptide ABC transporter, permease	0.25	0.3*
NCgl1918	put. oligopeptide ABC transporter, duplicated ATPase	0.35	0.28*
NCgl2001	hypothetical protein	1.04*	0.52
NCgl2108	cell wall-associated peptidase, *nlpC*	0.5	0.66
NCgl2127	lipoate-protein ligase B	0.4	0.53*
NCgl2170	ABC transporter, periplasmic binding protein	0.49	0.81*
NCgl2319	catechol 1,2-dioxygenase, *katA*	0.05	0.14
NCgl2376	hypothetical protein	0.5	0.84*
NCgl2377	sugar ABC transporter, ATPase	0.46	0.77*
NCgl2477	succinyl-CoA synthetase, β subunit, *sucC*	0.45*	0.47
NCgl2657	phosphotransacetylase, *pta*	0.26	1.1*
NCgl2698	NAD-dependent aldehyde dehydrogenase	0.38	0.7
NCgl2748	putative transposase	0.42	0.51*

Table S3. Putative DtxR binding sites in the genome of *C. glutamicum* genome as identified by a motif search of the *C. glutamicum* genome using the consensus sequence TWAGGTWAGSCTWACCTWA from *C. diphtheriae* and allowing up to five mismatches, but no insertions or deletions. The position of the center of the binding sites relative to the predicted translation start site of the neighbouring gene is given by the numbers in the column "Location". The column labelled "Bandshift" indicates whether DtxR bound to the predicted DtxR box (+), did not bind (-), or was even not tested in bandshift assays (n.d.).

NCgl	Putative DtxR box	Annotated function	Location	Bandshift
NCgl0027	TTTGCGCAGGCTAACCTTT	ABC transporter, permease component	+125.5	+
NCgl0051	TTCTGGAAGGCCAACCTGA	Zn-dependent hydrolase	+712.5	n.d.
NCgl0120	TTGGCTATGGTTTACCTAT	put. transcriptional regulator	+13.5	+
NCgl0123	AATGGTTAGGCTAACCTTA	hypothetical protein	+10.5	+
NCgl0167	TAGGTTTACGCGTACCTGA	transcriptional repressor	+775.5	-
NCgl0177	TTTGGAAAGCTTAATTTTA	hypothetical membrane spanning protein	+120.5	n.d.
NCgl0310	GAAGGTCACGCCAACCTTC	pseudouridylate synthase, 23S rRNA-specific	-120.5	n.d.
NCgl0323	CTTGGAAAGCCTTACAAAA	hypothetical protein	+289.5	n.d.
NCgl0329	AGAGTTAAGGATAACCTTG	secreted siderophore binding lipoprotein	-42.5	+
NCgl0352	TTGGATAGGTTTAACCTTA	hypothetical membrane protein	+1109.5	n.d.
NCgl0353	TGACGAAAGCCTTAGCTCA	glycosyltransferase involved in cell wall biogenesis	+596.5	n.d.
NCgl0358	TTAGGATAGCCTTACTTTA	transcriptional regulator RamB	-390.5	+
NCgl0377	TTAAGTTAGCATAGCCTTA	put. secreted heme transport associated protein	-150.5	+
NCgl0381	TAAGGTTACCCTACCCTCT	put. secreted heme transport associated protein, C-term. TMH	-90.5	+
NCgl0381	CCAGGTTAGGTTAAGCTAA	put. secreted heme transport associated protein, C-term. TMH	-45.5	+
NCgl0430	TTCACTTAGGCTTGCCATA	transcriptional regulator, ArsR family	-25.5	+
NCgl0465	TAGGGAAAGCCCATCCTTA	copper-transporting P-type ATPase	-31.5	+
NCgl0469	AAAGGTCACCCTTAAGTAA	ribosomal protein L7/L12	+377.5	n.d.
NCgl0484	TTAGTAAAGGCTCACCTAA	put. siderophore ABC transporter, permease	-100.5	+
NCgl0486	GTTGGTAAGGCAAACATGA	ribosomal protein S10	-378.5	+
NCgl0552	TGAGGTTCGGCGCACCTAT	DNA segregation ATPase FtsK/SpoIIIE and related proteins	+326.5	n.d.
NCgl0594	TTTGGTCTGGCCTACCTAT	lycopene elongase, CrtEb	+78.5	+
NCgl0603	GATGTTTTGCATTACCTAA	putative nucleoside-diphosphate-sugar epimerase	+708.5	n.d.
NCgl0618	ATAGGATAGGTTAACCTGA	secreted siderophore binding lipoprotein	-34.5	+
NCgl0639	GTCGGGCAGCCTAACCTAA	put. siderophore ABC transporter, secreted lipoprotein	-49.5	+
NCgl0752	TAAGGAAAACTCAACCTTC	putative integral membrane protein	+731.5	n.d.
NCgl0774	TAAGGTTTGCCTAATCTTT	put. siderophore ABC transporter, secreted lipoprotein	-39.5	+
NCgl0776	AAAGGTTTGGCTTGGTTAA	put. siderophore ABC transporter, secreted lipoprotein	-113.5	+
NCgl0776	TTTAGGTAACCTAACCTCA	put. siderophore ABC transporter, secreted lipoprotein	-73.5	+
NCgl0777	TTAGGTTAGGCTCTAATAT	put. siderophore ABC transporter, permease	-182.5	+
NCgl0802	TTCGGCTACGCTCACGTAA	fatty acid synthase, FasA	-73.5	+
NCgl0891	TGAGGTACGCGTTACCTGT	hypothetical protein	-186.5	+
NCgl0900	ATAGGTTATCCAAGCCTAA	glyceraldehyde 3-phosphate dehydrogenase	+1448.5	n.d.
NCgl0914	TTAAGTCAGTGTTACCTAA	put. siderophore export ABC transporter, permease	-92.5	+
NCgl0926	AAAGGTAAGCACTTCCAAA	ABC transporter ATP-binding and permease protein	-786.5	n.d.
NCgl0943	TGAGGTTAGCGTAACCTAC	AraC-type transcriptional regulator, RipA	-42.5	+
NCgl0945	TGAGGTGAAGCTTTCCTTC	hypothetical protein	+374.5	n.d.
NCgl0989	GAAGGTAAGGACTACGTGA	virulence-associated protein I	-375.5	-
NCgl1005	CAAGGAAAGCCTGACCGCA	putative nucleoside-diphosphate-sugar epimerase	+624.5	n.d.
NCgl1042	TAAGGAAAGGAGTGCCCAA	hypothetical protein	-8.5	-
NCgl1110	TCAGCTAAGGTTTTCCCTA	transcriptional regulator, TetR-family	-8.5	-
NCgl1120	GTAGAAAAGGAATACCTAA	ATPase involved in DNA repair	+536.5	-
NCgl1127	TAAGGGAATTGTAATCTAA	transcriptional regulator, Crp-family	-353.5	+

NCgl1137	TAAGGTTACCGTCACGGTA	homoserine kinase	+35.5	(+)
NCgl1145	CGTGGGAAGCCTAACTTAA	put. secreted serine protease	-51.5	+
NCgl1200	TTTTGTTAGGCTTGCCTAG	put. soluble, cytoplasmic siderophore interacting protein	-42.5	+
NCgl1209	TTAGGTAAGGTTTGCATAC	put. siderophore ABC transporter, secreted lipoprotein	-40.5	+
NCgl1251	TTCGGTAAAGATTTCCTTT	endo-1,4-beta-xylanase	+723.5	n.d.
NCgl1279	GAAGGAATGGCCAACCCTA	hypothetical protein	+126.5	n.d.
NCgl1339	TTAGGGAAGGAAAACATAT	hypothetical protein	+7.5	+
NCgl1355	TTGGATCAGGATAACCTGA	haloacid dehalogenase-like hydrolase	-286.5	-
NCgl1379	TTAGGTTGGGCGACCCTCT	zinc uptake transporter	+567.5	n.d.
NCgl1395	TTAGGTTAGGCAAGCCATA	cytoplasmic siderophore-interacting protein	-48.5	+
NCgl1444	TTAGGGACGCTTTACCTGC	put. transcriptional regulator, HTH-motif	-130.5	+
NCgl1453	TTCGGTATGACAAAACTAA	arsenical-resistance protein	+292.5	n.d.
NCgl1482	TAAGGATCTGCCAACCTAC	aconitase Acn	+1184.5	n.d.
NCgl1501	TACGTTAAGCCTGACTTCA	Fe-S cluster assembly SufC	+654.5	-
NCgl1504	TAAGCATAGCCGTACGGAA	DeoR-type transcriptional regulator SufR	-141.5	+
NCgl1594	TATGGGAAGGCAAAACTAC	protein translocase subunit SecD	-160.5	+
NCgl1645	TAACTTAAGCCTCACATAC	putative resolvase Res	-759.5	+
NCgl1646	TTAGGTAAAGCTTGCCTAT	secretory serine protease	-183.5	+
NCgl1669	TGATGTAACGCTTATATTA	DNA primase	-601.5	n.d.
NCgl1677	TTAGGTTATGTCAAAGTTA	hypothetical protein	-563.5	+
NCgl1692	TTCCGTTCTGCTAACCCTA	hypothetical helicase	+705.5	n.d.
NCgl1739	TTACGTTCGCGTTACCGAT	hypothetical protein	-165.5	-
NCgl1756	TATGGTGATGTTAACCTTG	hypothetical protein	+582.5	n.d.
Ncgl1757	TCAGCTGCGCCTTACCTTT	hypothetical protein	+232.5	n.d.
NCgl1769	TGATGTAACGCTTATATTA	DNA topoisomerase I	-379.5	-
NCgl1776	TAAGTCAAGCATTACGTTG	hypothetical membrane spanning protein	+635.5	n.d.
NCgl1897	TTTGATAAGCCGAACCCTC	thymidylate synthase ThyX	+147.5	n.d.
NCgl1915	TTTTTTAAGCCTAACCCTC	put. oligopeptide ABC transporter, binding protein OppA	-396.5	-
NCgl1919	CAAGGTTAGCCCTGGCGTA	prolyl-tRNA synthetase	+1589.5	n.d.
NCgl1930	ATAGCTTAGCTTTACTGAA	hypothetical protein	-21.5	-
NCgl1950	GTTGGTATGCCTTACGTGA	ribosomal protein S2P	+276.5	n.d.
NCgl1952	TGAGGCAAGCCTAAGTAAA	DNA integration/recombination/inversion protein	-97.5	n.d.
NCgl1955	TTAGATAAGCCTGACATCA	predicted endonuclease	-342.5	+
NCgl1959	TACATTAAGGCTGACCTGA	put. secreted siderophore binding lipoprotein	-153.5	+
NCgl1959	TTAGGCAAGGCTACCTTTT	put. secreted siderophore binding lipoprotein	-19.5	+
NCgl1970	CATGCTTTGGATAACCTTA	hypothetical cytosolic protein	-75.5	(+)
NCgl2006	CAATCTTAGGCTTAGTTTA	glycogen phosphorylase GlgP2	-14.5	+
NCgl2027	TCAAGTAAGGTTTACCTTA	SAM-dependent methyltransferase	-8.5	+
NCgl2037	ATAGGCACGGCTTTCCTTG	(1→4)-α-D-glucan 1-α-D-glucosylmutase	-131.5	-
NCgl2146	GTAGGTGTGGGTAACCTAA	heme oxygenase HmuO	-129.5	+
NCgl2159	TTGGGTTGGACGAACCAAA	protein tyrosine phosphatase	-194.5	-
NCgl2197	TTCGCTAAGGCGAATGTAA	hypothetical protein	-59.5	-
NCgl2198	ATCGGTAAGTCTTTCCGTA	glycyl-tRNA synthetase	+576.5	n.d.
NCgl2233	TACGGTTTGCATTATCTTG	glycerol-3-phosphate dehydrogenase	+666.5	n.d.
NCgl2278	TTCGGCAGGGCTTGCCGAA	hypothetical protein	+134.5	n.d.
NCgl2282	TTAGGTCAAGCTTGCATTT	hypothetical membrane spanning protein	-29.5	+
NCgl2325	CTAGTTTCAGCTTTCCTTA	benzoate transport protein	-85.5	-
NCgl2333	TTAGGTTGTAAAAACCTTA	hypothetical protein	-55.5	-
NCgl2374	TTCTTTATGCCGAACCTTA	sugar ABC transporter, permease protein	+324.5	n.d.
NCgl2414	TAATGTATGCCTTGACTTG	xanthosine triphosphate pyrophosphatase	-227.5	+
NCgl2439	TTATGCTGCGCTAACCTAT	ferritin Ftn	-46.5	+
NCgl2450	GAAGGCAAGCCAAACTTAA	put. 2-methylcitrate dehydratase	-27.5	+
NCgl2480	TACGGTTACGCAGACCTTC	succinyl-CoA:coenzyme A transferase	+1308.5	n.d.

NCgl2495	CTACGTTGGCCGAACCTTC	amidophosphoribosyltransferase	+1061.5	n.d.
NCgl2508	TCCGGTTAGCTTTACGCTA	phosphoribosylaminoimidazole-succinocarboxamide synthase	-272.5	-
NCgl2581	CGAGGTAAGCCCTGCCGAA	hypothetical protein	+752.5	n.d.
NCgl2605	TAGGGTAAGCCCTAATTTC	tRNA(Ile)-lysidine synthetase TilS	+41.5	-
NCgl2620	GTTGGTGAGCCTGACCCTA	polyphosphate kinase	+873.5	n.d.
NCgl2659	TTGGGTGAGGAATACCTTG	acetyltransferase, GNAT family	+465.5	n.d.
NCgl2686	TTAGGTAAAGCCCACGGAA	dimethylaniline monooxygenase	+174.5	n.d.
NCgl2713	TCAGGTAGGTGAAACCTAA	hypothetical membrane spanning protein	+991.5	n.d.
NCgl2719	TTAGGTTAGGTTCACCGTG	put. sulfite reductase CysI	-213.5	+
NCgl2720	TCTGGTTCGGCTAAGCTTT	hypothetical cytosolic protein	+897.5	n.d.
NCgl2750	ATTGGTACGGGTTACCTTG	putative UDP-glucose 6-dehydrogenase	+24.5	+
NCgl2752	TAAGGCAAGCCTAAATTAG	hypothetical exported protein, heme transport	-106.5	+
NCgl2766	TTAACTTTGCCCTACCTAA	permease	-199.5	+
NCgl2803	TTATGAAACCCTGACCGAA	hypothetical protein	+506.5	n.d.
NCgl2819	TAGGATTAGACATACCGTA	transcriptional regulator	-245.5	-
NCgl2834	ATGAGTAAGGCTAGACTAA	response regulator CgtR11	-95.5	+
NCgl2877	TTTGGCAAGACTTACCGAC	transcriptional regulator PadR-like family	-110.5	+
NCgl2897	TCAGGATAGGACAACCTAA	starvation-inducible DNA-binding protein Dps	-70.5	+
NCgl2947	TAAGGTATCGCTAGACTTG	putative short chain dehydrogenase	-752.5	n.d.
NCgl2970	TTGCGTTAGGATAGCCTAA	put. secreted siderophore binding lipoprotein	-8.5	+
NCgl2981	TTGGATAACCCTAAGCCAA	hypothetical protein	+1308.5	n.d.

Molecular Microbiology (2007) in press.

Coordinated regulation of gluconate catabolism and glucose uptake in *Corynebacterium glutamicum* by two functionally equivalent transcriptional regulators, GntR1 and GntR2

Julia Frunzke, Verena Engels, Sonja Hasenbein, Cornelia Gätgens and Michael Bott*

Institute of Biotechnology 1, Research Centre Jülich, D-52425 Jülich, Germany.

Summary

Corynebacterium glutamicum **is a Gram-positive soil bacterium that prefers the simultaneous catabolism of different carbon sources rather than their sequential utilization. This type of metabolism requires an adaptation of the utilization rates to the overall metabolic capacity. Here we show how two functionally redundant GntR-type transcriptional regulators, designated GntR1 and GntR2, coordinately regulate gluconate catabolism and glucose uptake. GntR1 and GntR2 strongly repress the genes encoding gluconate permease (*gntP*), gluconate kinase (*gntK*), and 6-phosphogluconate dehydrogenase (*gnd*) and weakly the pentose phosphate pathway genes organized in the *tkt-tal-zwf-opcA-devB* cluster. In contrast, *ptsG* encoding the EII^{Glc} permease of the glucose phosphotransferase system (PTS) is activated by GnR1 and GntR2. Gluconate and glucono-δ-lactone interfere with binding of GntR1 and GntR2 to their target promoters, leading to a derepression of the genes involved in gluconate catabolism and reduced *ptsG* expression. To our knowledge, this is the first example for gluconate-dependent transcriptional control of PTS genes. A mutant lacking both *gntR1* and *gntR2* shows a 60% lower glucose uptake rate and growth rate than the wild type when cultivated on glucose as sole carbon source. This growth defect can be complemented by plasmid-encoded GntR1 or GntR2.**

Introduction

Corynebacterium glutamicum is a predominantly aerobic, biotin-auxotrophic Gram-positive soil bacterium that was isolated in Japan due to its ability to excrete L-glutamate under biotin-limiting growth conditions (Kinoshita *et al.*, 1957). It is used today for the industrial production of more than two million tons of amino acids per year, mainly L-glutamate and L-lysine. Additionally, this species has become a model organism of the *Corynebacterineae*, a suborder of the *Actinomycetales* which also comprises the genus *Mycobacterium*. An overview on the current knowledge on *C. glutamicum* can be found in a recent monograph (Eggeling and Bott, 2005).

C. glutamicum is able to grow on a variety of sugars, sugar alcohols and organic acids (e.g. acetate, lactate, or citrate) as carbon and energy sources. The use of gluconate as an additional carbon source besides glucose was previously shown to have a positive effect on L-lysine production (Bianchi *et al.*, 2001; Lee *et al.*, 1998). In order to be metabolized, gluconate is first transported into the bacterial cytoplasm *via* a specific gluconate permease (GntP). Subsequently, it is phosphorylated to 6-phosphogluconate by gluconate kinase (GntK). In *C. glutamicum*, 6-phosphogluconate is further metabolized in the pentose phosphate pathway, as the alternative Entner-Doudoroff pathway is absent in this organism. Although in recent studies several transcriptional regulators involved in the regulation of central metabolic pathways in *C. glutamicum* were identified and characterized knowledge about transcriptional regulation of genes involved in gluconate metabolism and pentose phosphate pathway is

*For correspondence. E-mail m.bott@fz-juelich.de; Tel. (+49) 2461 615515; Fax (+49) 2461 612710.

scarce (Bott, 2007; Cramer *et al.*, 2006; Engels and Wendisch, 2007; Gerstmeir *et al.*, 2004; Kim *et al.*, 2004; Krug *et al.*, 2005; Wennerhold *et al.*, 2005). In many bacteria genes involved in gluconate utilization are subject to negative control by GntR-like transcriptional regulators. In the case of GntR of *Bacillus subtilis* and *Escherichia coli*, it was shown that gluconate itself interferes with the binding of these regulators to their target promoters (Fujita and Fujita, 1987; Peekhaus and Conway, 1998). In several *Bacillus* species the genes encoding GntR, GntP, GntK, as well as a putative 6-phosphogluconate dehydrogenase (*gntZ*) are clustered in one operon. Expression of these genes is derepressed in the presence of gluconate and also subject to carbon catabolite repression by the catabolite control protein CcpA and the phosphocarrier protein HPr (Reizer *et al.*, 1996). In *E. coli* the *gnt* genes are also repressed by the gluconate repressor GntR and activated by CRP (cAMP receptor protein) in complex with cAMP (Peekhaus and Conway, 1998). These data demonstrate that expression of the *gnt* genes is controlled in dependency of gluconate availability and the presence of a catabolite repressive carbohydrate like glucose.

Recently, it was reported that the genes encoding gluconate permease and gluconate kinase (*gntP* and *gntK*) in *C. glutamicum* are also subject to carbon catabolite repression, presumably *via* the cAMP-dependent regulator GlxR which binds to the promoter regions of *gntP* and *gntK* (Letek *et al.*, 2006). *C. glutamicum* GlxR contains a cAMP binding motif and shows 27% sequence identity with the CRP protein of *E. coli*. GlxR was first identified as a repressor of *aceA* and *aceB* encoding the key enzymes of the glyoxylate cycle, isocitrate lyase and malate synthase, respectively (Kim *et al.*, 2004). Letek *et al.* (2006) reported that expression of *gntP* and *gntK* are not induced (or derepressed) by gluconate.

In this study, we have identified two paralogous GntR-type regulators in *C. glutamicum*, designated GntR1 and GntR2, which repress the expression of genes involved in gluconate metabolism (e. g. *gntK*, *gntP* and *gnd*) in the absence of gluconate. Surprisingly, these regulators function at the same time as activators of *ptsG* and *ptsS* encoding the permeases EII^{Glc} and EII^{Suc} of the PEP-dependent phosphotransferase system (PTS) for glucose and sucrose uptake in *C. glutamicum* (Kotrba *et al.*, 2001; Lengeler *et al.*, 1994; Moon *et al.*, 2005; Parche *et al.*, 2001). To our knowledge, this is the first example for a gluconate-dependent transcriptional control of PTS genes.

Results

Identification of putative gluconate-dependent transcriptional regulators in C. glutamicum

In *C. glutamicum* genes involved in gluconate metabolism (*gntP*, *gntK*, *gnd*) are not clustered in an operon, like in *E. coli* or *B. subtilis*, but are scattered on the genome of this organism. In their close vicinity, no genes for transcriptional regulators belonging to the GntR-family, which might act as gluconate-dependent regulators of these genes, could be detected. The genome of *C. glutamicum* ATCC 13032 contains 11 genes which encode GntR-type transcriptional regulators (Brune *et al.*, 2005); two of them (*cg1935* and *cg2783*) show 78% sequence identity on the level of amino acid sequence and may have arisen by gene duplication. Interestingly, orthologs of *cg1935* and *cg2783* could also be found in *Mycobacterium flavescens* (Mflv_0501) and *Mycobacterium smegmatis* (MSMEG_0454) where they are located divergently to *gntK* and *gntP* (Fig. 1). This finding indicated a possible function of *cg1935* and *cg2783* in the regulation of gluconate metabolism in *C. glutamicum*. In *Corynebacterium efficiens*, an orthologous gene (CE2422) was located in a similar genomic context as *cg2783* in *C. glutamicum* (Fig. 1). Due to their proposed function in gluconate catabolism, the *C. glutamicum* genes were designated as *gntR1* (*cg2783*) and *gntR2* (*cg1935*). The sequence identity of GntR1 and GntR2 to GntR of *B. subtilis* and *E. coli*, which are known to control the expression of genes involved in gluconate metabolism, is below 30%.

GntR1 and GntR2 of *C. glutamicum* consist of an N-terminal GntR-type helix-turn-helix motif (PFAM: PF00392) responsible for DNA-binding and a C-terminal putative ligand binding domain (PFAM: PF07729) typical for many GntR-type regulators. GntR-type regulators constitute to a large family of transcriptional regulators which typically share a highly conserved N-terminal

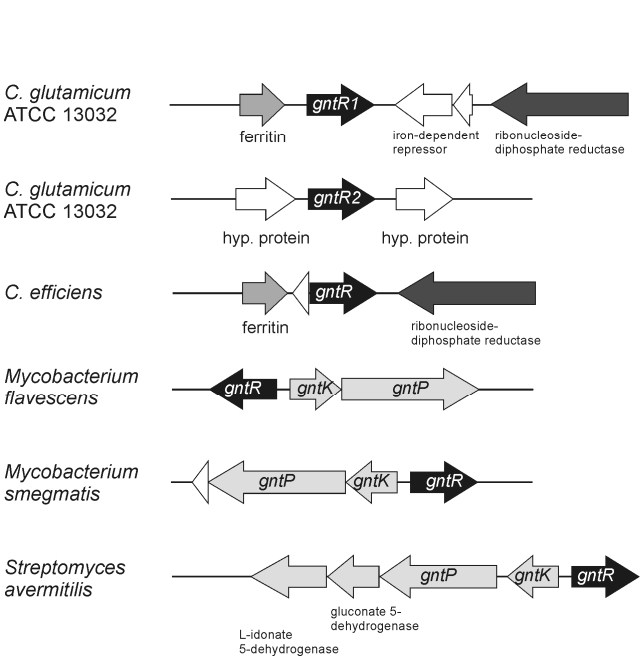

Fig. 1. Genomic organization of GntR-type regulators with high sequence identity to GntR1. Genes for GntR-type regulators with high sequence identity to GntR1 from *C. glutamicum* are shown in black. In several *Mycobacterium* species and *Streptomyces avermitilis* genes encoding gluconate kinase (*gntK*) and gluconate permease (*gntP*) are located divergently to *gntR*. Data were taken from the bioinformatics software ERGO (Integrated Genomics).
[a] Identity of the amino acid sequence to GntR1 (encoded by *cg2783*) of *C. glutamicum*.

DNA-binding motif, whereas the C-terminal parts show large divergence. Therefore GntR members were classified into four subfamilies designated as FadR, HutC, MocR and YtrA (Rigali *et al.*, 2002). Due to the presence of an FCD domain (FCD stands for FadR C-terminal domain) in GntR1 and GntR2 of *C. glutamicum*, these regulators most probably belong to the FadR family, which also includes GntR of *B. subtilis*. The coding region of *gntR2* (*cg1935*) lies within the prophage region CGP3 of the *C. glutamicum* genome (Kalinowski, 2005a) which spans more than 180 kb covering approximately 200 coding regions for proteins most of which lack any significant similarities to known bacterial genes. In *C. glutamicum* strain R (Yukawa *et al.*, 2007) and *C. efficiens* (Nishio *et al.*, 2003), only orthologs of *gntR1* are present and located in the same genomic environment as *gntR1* of *C. glutamicum*.

The genes gntR1 *and* gntR2 *are functionally redundant*

In order to explore the regulatory function of GntR1 and GntR2 in *C. glutamicum* ATCC 13032, in-frame deletion mutants of the genes *cg2783* (Δ*gntR1*) and *cg1935* (Δ*gntR2*) as well as a double deletion mutant (Δ*gntR1*Δ*gntR2*) were constructed. Subsequently, growth of the different mutant strains was compared with that of the wild type using CGXII minimal medium containing either 4% (w/v) glucose or 2% (w/v) gluconate as carbon and energy source. When cultivated in minimal medium with 2% (w/v) gluconate, all four strains showed the same growth rate (0.46 ± 0.02 h^{-1}) and the same final cell density (OD_{600} = 25 ± 1.5). In minimal medium with 4% (w/v) glucose, the mutant strains Δ*gntR1* and Δ*gntR2* displayed the same growth behaviour (μ = 0.41 ± 0.02 h^{-1}, final OD_{600} = 60 ± 1.2) as the wild type (Fig. 2A). In contrast, the double mutant Δ*gntR1*Δ*gntR2* showed a strongly reduced growth rate of only 0.16 ± 0.01 h^{-1}, but reached the same final cell density as the other strains after 24 h (Fig. 2B). As shown in Fig. 2C and 2D, the growth defect of mutant Δ*gntR1*Δ*gntR2* on glucose could be reversed by transformation with a plasmid carrying either the *gntR1* or the *gntR2* gene under control of the non-induced *tac* promoter. This result confirms that the simultaneous absence of GntR1 and GntR2 is responsible for the reduced growth rate in glucose minimal medium and indicates that GntR1 and GntR2 can replace each other. Complementation of the growth defect of strain Δ*gntR1*Δ*gntR2* on glucose was only possible when *gntR1* or *gntR2* were expressed at low levels due to a basal activity of the *tac* promoter. Strong overexpression of either *gntR1* or *gntR2* in strain Δ*gntR1*Δ*gntR2* by addition of 1 mM isopropylthiogalactoside (IPTG) to the medium resulted in a growth defect in glucose and gluconate minimal medium, but not in acetate minimal (data not shown). Thus, high cellular

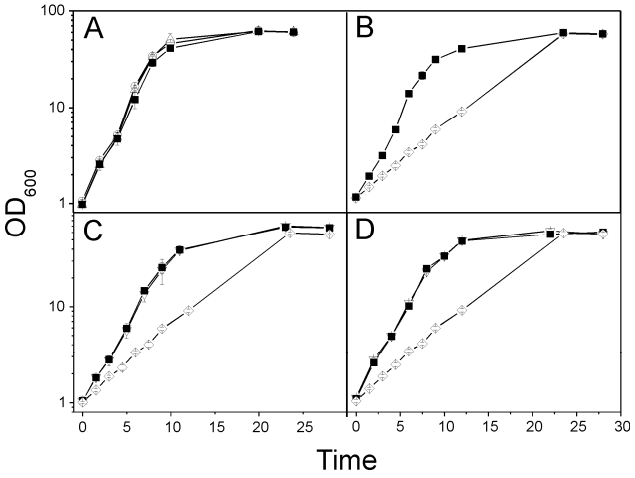

Fig. 2. Growth of *C. glutamicum* wild type and different deletion mutants in CGXII minimal medium with 4% (w/v) glucose. In experiments C and D, the medium contained in addition 50 µg/ml kanaymycin. A, wild type (■), Δ*gntR1* (□) and Δ*gntR2* (○); B, wild type (■) and Δ*gntR1*Δ*gntR2* (◊). C, wild type/pAN6 (■), Δ*gntR1*Δ*gntR2*/pAN6 (◊) and Δ*gntR1*Δ*gntR2*/ pAN6-*gntR2* (□); D, wild type/pAN6 (■), Δ*gntR1*-Δ*gntR2*/pAN6 (◊) and Δ*gntR1*Δ*gntR2*/pAN6-*gntR1* (□).

levels of either GntR1 or GntR2 are inhibitory if glucose or gluconate are used as carbon source.

Transcriptome analyses of the ΔgntR1*,* ΔgntR2 *and* ΔgntR1ΔgntR2 *mutant strains*

The growth experiments described above revealed that the single deletion mutants Δ*gntR1* and Δ*gntR2* grow like wild type under all tested conditions, whereas the Δ*gntR1*Δ*gntR2* deletion mutant shows a strongly reduced growth rate when cultivated on glucose, but not on gluconate. In order to elucidate the molecular basis of this phenotype, expression profiles of the different deletion mutants were compared with that of the *C. glutamicum* wild type using DNA microarray analysis. For this purpose, strains were cultivated in CGXII minimal medium with either 100 mM glucose (Glu) or 100 mM gluconate (Gnt). Additionally, expression profiles of wild type and the mutant Δ*gntR1*Δ*gntR2* were also compared after cultivation in CGXII minimal medium with 50 mM glucose and 50 mM gluconate (Glu_Gnt). For each comparison, a set of two to three experiments starting from independent cultures was performed. RNA was isolated from cells harvested in the early exponential phase (OD_{600} 4 - 6) and always the expression levels of wild type and a deletion mutant were compared. No remarkable differences were observed between the expression levels of the single mutants Δ*gntR1* and Δ*gntR2* and the wild type, both for glucose- and gluconate-grown cells. A similar result was obtained in the comparison of wild type and the double mutant Δ*gntR1*Δ*gntR2* when the strains were cultivated either on gluconate alone or on glucose plus gluconate. In contrast, a variety of significant differences in gene expression was detected between wild type and strain Δ*gntR1*Δ*gntR2* when cells were cultivated with glucose as sole carbon source (Table 2).

Fig. 3 shows a hierarchical cluster of all genes which showed a ≥4-fold altered mRNA level in the Δ*gntR1*Δ*gntR2* mutant cultivated on glucose. Under the chosen criteria, 26 genes showed a decreased and 19 genes an increased mRNA level in the Δ*gntR1*Δ*gntR2* mutant. Interestingly, one of the genes with the most significantly decreased mRNA level (factor 25) is *ptsG*, encoding the permease EII^{Glc} of the phospho*enol*pyruvate-dependent sugar phosphotransferase system (PTS) responsible for glucose uptake in *C. glutamicum* (Lee *et al.*, 1994; Moon *et al.*, 2005). Additionally, also the mRNA level of the *ptsS* gene encoding the EII^{Suc} permease involved in sucrose uptake was lower by a factor of four in the double mutant. On the other hand, the genes involved in gluconate uptake and metabolism showed a strongly increased mRNA level in the Δ*gntR1*Δ*gntR2* mutant (*gntP* 25-fold, *gntK* 2700-fold, *gnd* 12-fold). Besides the mRNA level of 6-phosphogluconate dehydrogenase (*gnd*), also the mRNA levels of other pentose phosphate pathway genes (*tkt-tal-zwf-opcA-devB*) showed a 1.6- to 3-fold increased mRNA level. Although the mRNA ratio of these genes did not exceed a factor of four, the ratios obtained for these genes were also included in the hierarchical cluster analysis shown in Fig. 3. The microarray data indicate an important function of GntR1 and GntR2 in gluconate metabolism and sugar uptake in *C. glutamicum.*

Table 1. Genome-wide comparison of mRNA levels in *C. glutamicum* wild type with the mutant strains Δ*gntR1*, Δ*gntR1* or Δ*gntR1*Δ*gntR2* using DNA microarrays. The mRNA ratios shown represent mean values from 2 or 3 independent microarray experiments starting from independent cultures (see Experimental procedures). In total, 17 microarray experiments were performed for the three comparisons Δ*gntR1 vs.* wild type, Δ*gntR1*Δ*gntR2 vs.* wild type, and Δ*gntR2 vs*. wild type. The strains were cultivated in CGXII minimal medium with either 100 mM glucose (Glu), or 100 mM gluconate (Gnt), or 50 mM glucose and 50 mM gluconate (Glu + Gnt) and mRNA was prepared from cells in the exponential growth phase. The table includes those genes which showed a ≥4-fold changed mRNA level (increased or decreased) in at least two of the three experiments comparing the double mutant Δ*gntR1*Δ*gntR2 vs.* wild type on glucose minimal medium and which had a *p*-value of ≤0.05. The genes are ordered according to the mRNA ratio of this comparison. In addition, the gene cluster encoding enzymes of the pentose phosphate pathway have been included, although their mRNA ratio was changed less than 4-fold.

Gene	Annotation	mRNA ratio						
		Δ*gntR1*Δ*gntR2* / wild type			Δ*gntR1* / wild type		Δ*gntR2* / wild type	
		Glu	Glu + Gnt	Gnt	Glu	Gnt	Gnt	Glu
cg1935	transcriptional regulator of GntR family, *gntR2*	<0.01	0.05	<0.01	2.09	1.00	0.05	<0.01
cg2783	transcriptional regulator of GntR family, *gntR1*	<0.01	0.03	<0.01	<0.01	0.02	1.00	1.23
cg2940	dipeptide transport ATP-binding protein, *dppF*	0.01	0.73	1.17	1.05	1.11	0.99	0.93
cg0211	myo-inositol 2-dehydrogenase	0.02	1.12	2.66	1.18	1.32	1.13	0.93
cg2691	hypothetical protein	0.02	0.92	0.77	0.99	1.02	0.90	0.84
cg0751	hypothetical protein	0.03	1.08	3.23	1.10	1.09	0.87	0.85
cg0082	chloride channel protein	0.03	1.36	1.69	1.04	1.06	1.10	0.95
cg1493	D-alanine--D-alanine ligase	0.03	1.28	0.90	1.25	1.19	1.00	1.16
cg1369	F_1F_0 ATP synthase ε subunit, *atpC*	0.03	1.05	5.36	1.44	1.14	0.84	0.97
cg1537	PTS system, glucose-specific IIABC component,*ptsG*	0.04	0.57	1.11	1.31	1.37	0.81	1.13
cg0993	transcriptional regulator of ArsR family	0.05	0.74	7.14	0.93	0.98	0.93	0.95
cg2725	transposase	0.08	0.69	0.45	0.37	0.65	1.34	2.83
cg0658	hypothetical membrane spanning protein	0.08	0.89	0.91	1.13	1.06	0.99	0.90
cg1488	3-isopropylmalate dehydratase small subunit, *leuD*	0.10	1.23	1.09	1.27	1.15	0.98	0.98
cg1451	D-3-phosphoglycerate dehydrogenase, *serA*	0.12	1.10	0.86	1.00	1.09	0.67	1.14
cg2125	uracil permease, *uraA*	0.14	1.11	1.22	0.86	1.10	1.03	0.98
cg0564	LSU ribosomal protein L1P	0.19	0.75	0.97	0.80	1.43	0.86	0.85
cg0770	ABC-type siderophore transport system, permease	0.19	1.03	0.71	0.71	0.72	0.81	0.70
cg0687	O-sialoglycoprotein endopeptidase, *gcp*	0.19	1.24	0.67	0.80	1.13	0.88	1.03
cg1002	hypothetical protein	0.19	0.91	0.99	0.81	0.86	0.93	1.22
cg0286	transporter	0.21	0.67	1.20	0.90	1.16	0.99	1.10
cg1487	3-isopropylmalate dehydratase large subunit, *leuC*	0.21	1.76	1.31	1.05	1.24	1.34	0.92
cg2399	glucose kinase, *glk*	0.22	0.93	0.82	0.66	1.09	0.91	0.81
cg2925	PTS system, sucrose-specific IIABC component,*ptsS*	0.26	1.05	1.37	1.17	1.47	1.14	1.28
cg2178	N utilization substance protein A	0.26	1.03	0.68	1.09	1.26	0.93	0.85
cg3398	superfamily II DNA and RNA helicase	0.27	1.14	1.10	1.13	1.19	1.04	1.10
cg1778	glucose-6-phosphate dehydrogenase, *zwf*	1.60	1.16	0.89	0.97	1.02	1.14	0.87
cg1779	glucose-6-phosphate dehydrogenase, *opcA*	1.77	1.03	0.88	0.89	1.09	1.15	0.74
cg1776	transaldolase, *tal*	2.01	1.21	0.81	1.06	1.02	1.12	0.97
cg1780	6-phosphogluconolactonase, *devB*	2.51	1.28	0.89	1.14	1.02	0.91	1.08
cg1774	transketolase, *tkt*	2.87	1.13	0.83	1.07	1.09	1.03	1.12
cg2836	succinyl-CoA synthetase α chain, *sucD*	4.48	0.93	0.52	1.41	0.75	0.81	0.97
cg3399	hypothetical protein	4.50	1.85	0.76	0.83	1.01	1.22	0.97
cg0143	mannitol 2-dehydrogenase	4.52	1.19	2.11	1.27	0.98	1.13	1.76
cg0291	protocatechuate 3,4-dioxygenase β chain	4.64	0.75	0.72	0.91	1.14	1.19	1.11
cg1454	taurine-binding protein	5.03	0.97	0.89	0.83	0.90	1.01	1.13
cg1642	cytoplasmic siderophore-interacting protein	5.03	1.15	1.12	n.d.	1.11	1.15	1.55
cg2616	vanillate O-demethylase oxygenase subunit	5.87	1.21	0.79	0.61	1.24	1.04	1.36
cg0797	methylisocitrate lyase, *prpB1*	5.91	1.01	0.90	1.51	0.86	0.85	0.89
cg0796	2-methylcitrate dehydratase, *prpD1*	6.34	1.08	0.78	0.93	0.73	0.89	0.81
cg0798	2-methylcitrate synthase, *prpC1*	6.69	1.14	0.68	1.24	0.88	1.09	1.29
cg0144	transporter	8.11	1.03	1.87	1.01	0.98	1.17	1.29
cg1589	hypothetical protein	9.33	1.06	1.21	0.98	1.08	1.15	1.11
cg1643	6-phosphogluconate dehydrogenase, *gnd*	12.40	1.12	1.76	1.36	1.28	0.97	1.19
cg3216	gluconate permease, *gntP*	25.08	0.79	0.83	1.38	0.91	1.33	1.07
cg2810	Na^+/H^+-dicarboxylate symport protein	65.46	1.04	1.29	1.20	1.04	1.01	2.41
cg1255	HNH endonuclease family protein	129.02	1.01	1.60	1.33	0.94	1.01	1.44
cg2733	HNH endonuclease family protein	155.10	1.05	1.46	1.01	0.95	1.05	11.53
cg0385	periplasmic β-glucosidase/β-xylosidase, *bglS*	935.79	1.36	0.01	n.d.	1.27	1.77	21.08
cg2732	gluconate kinase, *gntK*	2716.50	1.05	1.06	1.11	1.10	1.19	4.69

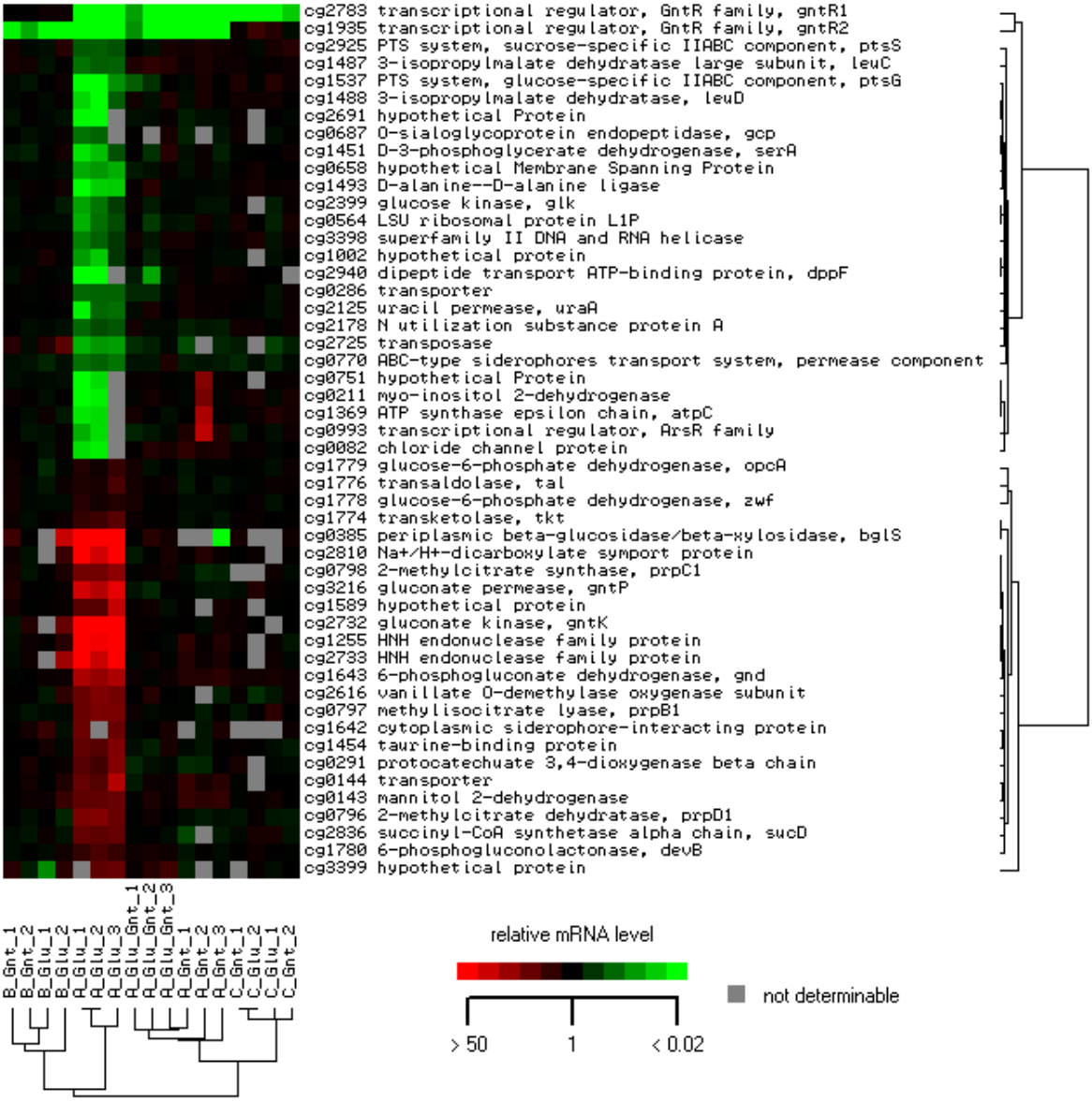

Fig. 3. Hierarchical cluster analysis of gene expression changes in three series of DNA microarray experiments. The expression profiles of three different deletion mutants were compared with *C. glutamicum* wild type in totally 17 microarray experiments: A, Δ*gntR1*Δ*gntR2 vs.* wild type; B**,** Δ*gntR2 vs.* wild type; C, Δ*gntR1 vs***.** wild type. The strains were cultivated in CGXII minimal medium with either 100 mM glucose (Glu), or 100 mM gluconate (Gnt), or 50 mM glucose and 50 mM gluconate (Glu_Gnt). The cluster includes those genes which showed a ≥4-fold changed mRNA level (increased or decreased) in at least two of the experiments A_Glu and had a *p*-value of ≤0.05).

Additionally, they support the assumption that GntR1 and GntR2 are able to complement each other, because no significant gene expression differences were detected between the single deletion mutants Δ*gntR1* and Δ*gntR2* and the wild type.

Influence of GntR1 and GntR2 on the activity of gluconate kinase, 6-phosphogluconate dehydrogenase and glucose-6-phosphate dehydrogenase

The microarray data indicated that GntR1 and GntR2 act as repressors of the genes required for gluconate catabolism, *i.e. gntP*, *gntK*, *gnd* and other pentose phosphate pathway genes. To test whether the differences observed at the mRNA level are also present at the protein level, we determined the specific activities of

gluconate kinase, 6-phosphogluconate dehydrogenase and glucose-6-phosphate dehydrogenase in cell-free extracts of wild type and the deletion mutant Δ*gntR1*Δ*gntR2*. For this purpose, the strains were cultivated in CGXII minimal medium with either 4% glucose or 2% gluconate or 1% of glucose and gluconate or 2% acetate and harvested in the early exponential phase (OD_{600} 4 - 6). As shown in Table 3, the activities of all three enzymes were significantly increased in the Δ*gntR1*Δ*gntR2* mutant when the cells were grown with glucose or acetate as carbon source. As expected from the transcriptome analysis, gluconate kinase showed the strongest increase, as its activity was below the detection limit (0.01 U/mg) in wild type cells cultivated on glucose or acetate. The activities of 6-phosphogluconate dehydrogenase and glucose-6-phosphate dehydrogenase were increased ~10-fold and ~3-fold, respectively, in the Δ*gntR1*Δ*gntR2* mutant grown on glucose, which is in very good agreement with the increase in the mRNA levels. When extracts of cells grown on gluconate or glucose plus gluconate were tested, the enzyme activities were also increased in strain Δ*gntR1*Δ*gntR2*, but to a much lower extent (≤2-fold). These data support the assumption that GntR1 and GntR2 act as gluconate-responsive repressors of genes involved in gluconate catabolism and pentose phosphate pathway.

The activity of all three enzymes measured in the derepressed background of a Δ*gntR1*Δ*gntR2* mutant was higher (~25-60%) in glucose-grown cells compared to gluconate-grown cells. This difference could be due to a regulatory effect on the transcriptional level elicited by the influence of GntR1 and GntR2 on glucose uptake (see below).

Activation of PTS dependent sugar uptake via GntR1 and GntR2

In contrast to genes involved in gluconate metabolism and the pentose phosphate pathway, the genes *ptsG* and *ptsS* encoding the permeases EII^{Glc} and EII^{Suc} of the PTS system showed 25-fold or 4-fold decreased mRNA levels in the Δ*gntR1*Δ*gntR2* mutant, respectively. In order to investigate a potential activation of *ptsG* expression by GntR1 and GntR2, reporter gene fusion analyses were performed. The plasmid pET2-*ptsG* containing the *ptsG* promoter region in front of a promoterless chloramphenicol acetyltransferase gene (Engels and Wendisch, 2007) was transferred into *C. glutamicum* wild type and the Δ*gntR1*Δ*gntR2* mutant. Subsequently, the two strains were grown in CGXII minimal medium with either a single carbon source (100 mM glucose or 100 mM gluconate) or mixed carbon sources (50 mM glucose + 50 mM gluconate). When cultivated on glucose, expression of the *ptsG-cat* fusion was 9-fold lower in the Δ*gntR1*Δ*gntR2* mutant in comparison to the wild type (Table 4); showing that the reduced *ptsG* mRNA level observed in the microarray experiments is caused by reduced transcription. When cultivated on gluconate or glucose plus gluconate, the CAT activity of the mutant was only 1.5- to 1.8-fold lower than the activity of the wild type. These results can be explained by the assumption that *ptsG* expression is strongly activated by GntR1 and GntR2 in the absence of gluconate.

Table 2. Specific activity of gluconate kinase, 6-phosphogluconate dehydrogenase and glucose-6-phosphate dehydrogenase in *C. glutamicum* wild type and the Δ*gntR1*Δ*gntR2* mutant. The two strains were grown in CGXII minimal medium containing either 4% (w/v) glucose or 2% (w/v) gluconate or 1% glucose plus 1% gluconate or 2% acetate. Cells were harvested in the early exponential growth phase (OD_{600} ~5). Enzyme activities were determined in cell-free extracts. The values for the specific activities represent means ± standard deviations from at least three independent cultivations.

Strain	Carbon source	Specific activity (U/mg)		
		gluconate kinase	6-phospho-gluconate DH	glucose-6-phosphate DH
Wild type	Glucose	n.d.[a]	0.19 ± 0.02	0.15 ± 0.02
Δ*gntR1*Δ*gntR2*		2.37 ± 0.3	2.62 ± 0.18	0.49 ± 0.08
Wild type	Gluconate	0.92 ± 0.1	0.84 ± 0.01	0.35 ± 0.02
Δ*gntR1*Δ*gntR2*		1.50 ± 0.2	1.69 ± 0.03	0.40 ± 0.03
Wild type	Glucose +	0.60 ± 0.1	0.69 ± 0.03	0.11 ± 0.01
Δ*gntR1*Δ*gntR2*	Gluconate	1.20 ± 0.1	1.13 ± 0.10	0.16 ± 0.03
Wild type	Acetate	n.d.[a]	0.12 ± 0.01	0.03 ± 0.01
Δ*gntR1*Δ*gntR2*		1.27 ± 0.3	1.79 ± 0.08	0.16 ± 0.04

Table 3. Specific chloramphenicol acetyltransferase (CAT) activities of *C. glutamicum* wild type and the mutant Δ*gntR1*Δ*gntR2*, both carrying the promoter-probe plasmid pET2-*ptsG*. The cells were grown in CGXII minimal medium with either 100 mM glucose or 100 mM gluconate or with 50 mM of both carbon sources. Enzyme activities were determined in cell-free extracts. The values for the specific activities represent means ± standard deviations from three independent cultivations.

Carbon source(s)	Specific CAT activities (U/mg)	
	Wild type/ pET2-*ptsG*	Δ*gntR1*Δ*gntR2*/ pET2-*ptsG*
Glucose	1.84 ± 0.30	0.21 ± 0.05
Gluconate	0.61 ± 0.13	0.41 ± 0.05
Glucose + Gluconate	0.77 ± 0.03	0.43 ± 0.05

Binding of purified GntR1 and GntR2 to the promoter regions of putative target genes

The microarray experiments reported above identified *gntP*, *gntK*, *ptsG*, *ptsS* and the gene cluster *tkt-tal-zwf-opcA-devB* as putative target genes of GntR1 and GntR2. In order to test for a direct interaction of GntR1 and GntR2 with the promoter regions of these genes, the binding of the purified proteins was tested *in vitro*. For this purpose, GntR1 and GntR2 were overproduced in *E. coli* BL21(DE3)/pLysS and purified to homogeneity by means of an amino-terminal decahistidine tag (see Experimental procedures). The histidine tag does not interfere with the functionality of the proteins, as His-tagged GntR1 and GntR2 were able to complement the growth defect of the Δ*gntR1*Δ*gntR2* mutant on glucose (data not shown). In gel shift assays, DNA fragments covering the corresponding promoter regions were incubated with increasing concentrations of purified GntR1 or GntR2 and subsequently separated on a 10% native polyacrylamide gel. As shown in Fig. 4, all six promoter regions were shifted by GntR1 as well as by GntR2. A complete shift was observed at a 5- to 10-fold molar excess of protein. Interestingly, at a 10- to 20-fold molar excess of protein, the formation of multiple GntR/DNA complexes was observed with all tested promoter regions. This observation could indicate the presence of several GntR1/2 binding motifs within the target promoter regions and/or the oligomerization of the protein once it is bound to DNA. Different DNA fragments covering for example the promoter regions of *acn* (aconitase) or *sdhCAB* (succinate dehydrogenase) served as negative controls and were incubated with the same protein concentrations as the putative target genes. The GntR2 protein also bound to these control DNA fragments, but with much lower affinity compared to the promoter regions of the identified target genes (Fig. 4B), indicating that this binding is unspecific.

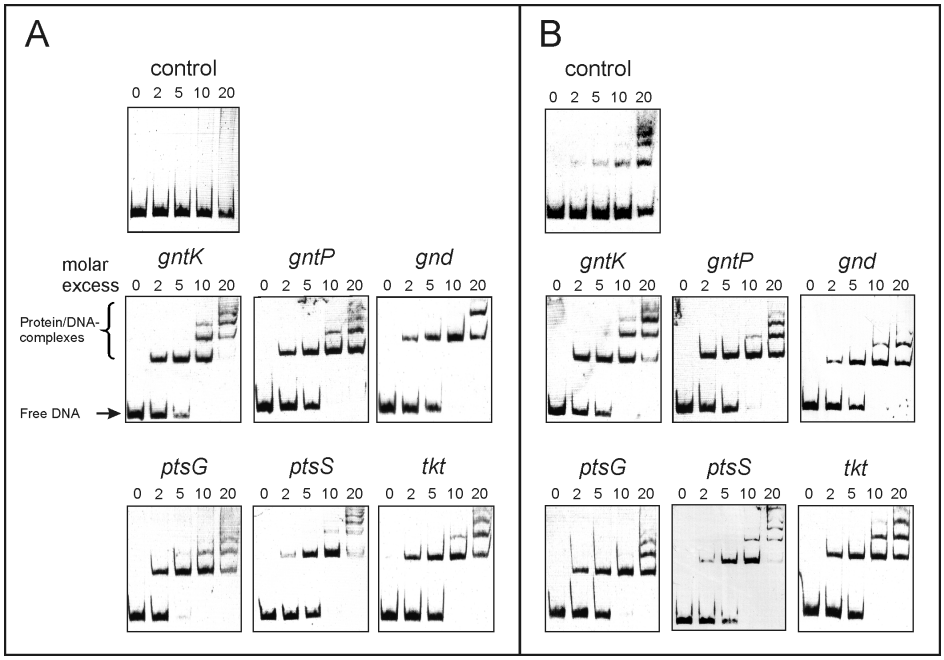

Fig. 4. Binding of GntR1 (A) and GntR2 (B) to the promoter regions of the predicted target genes. DNA fragments (550 bp, 14 nM) covering the promoter regions of the putative target genes *gntP*, *gntK*, *gnd*, *ptsG*, *ptsS* and *tkt* were incubated for 20 min at room temperature either without protein or with a 2-, 5-, 10-, or 20-fold molar excess of either purified GntR1 (A) or GntR2 protein (B). A DNA fragment containing the *acn* (aconitase) promoter region was used as a negative control. The samples were separated by native PAGE (10%) and stained with SybrGreen I.

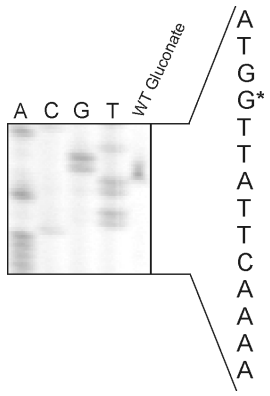

Fig. 5: Identification of the transcriptional start site of the *gntK* gene by primer extension analysis using the oligonucleotide PE-gntK-1 (Table S1). 10 µg of total RNA isolated from *C. glutamicum* wild type grown on CGXII minimal medium with 100 mM gluconate was used as template. The transcriptional start site is indicated by an asterisk. The Sanger sequencing reactions (lanes A, C, G, and T) were generated with a PCR product covering the corresponding DNA region as template and oligonucleotide PE-gntK-1.

In subsequent experiments the exact location of the binding sites of GntR1 and GntR2 was determined for four of the target genes (see below). In the case of *gntK*, the binding site was found to extend from position -45 to -59 with respect to the transcriptional start site reported by Letek *et al.* (2006), which is located 17 bp upstream of the ATG start codon. As the position of the binding site is unusual for a regulator acting as a repressor, we determined the transcriptional start site of *gntK* by primer extension analysis. A single primer extension product was detected using two independent oligonucleotides (PE-gntK-1 and PE-gntK-2, Table S1) and total RNA isolated from *C. glutamicum* wild type cultivated on minimal medium with 100 mM gluconate as carbon source. The transcriptional start site identified by these experiments is located 65 bp upstream of the start codon of *gntK* (Fig. 5). The extended "-10" region derived from this start site (agagtTATGATag) shows a good agreement with the corresponding consensus sequence (tgngnTA(c/t)aaTgg) (Patek *et al.*, 2003). No evidence for the previously reported transcriptional start site 17 bp upstream of the start codon was obtained in the primer extension experiments.

In order to identify the binding sites of GntR1 and GntR2 in the promoter region of *gntK*, the originally used DNA fragment was divided into several subfragments which were then also tested in gel shift assays with purified GntR1 and GntR2. As shown in Fig. 6A, GntR2 bound to fragments 4 and 6 which cover an overlapping region of approximately 100 bp. A further refinement using fragments 7-9 showed that an essential part of GntR2 binding site is located between position -5 and -23 with respect to the transcription start site identified in this work. Further inspection of this region revealed a potential binding motif of GntR2 extending from position +4 to -11. Subsequently, the relevance of this motif was tested by mutational analysis. To this end, seven mutated DNA fragments were synthesized by PCR, each of which contained three nucleotide exchanges. All mutations within the postulated motif (fragments M1-M5) abolished binding of GntR2 (data not shown) and also of GntR1 (Fig. 6B) nearly completely, whereas the mutations outside the motif (fragments M6 and M7) had no effect on binding. These data confirm the relevance of the identified motif and show that GntR1 and GntR2 share the same binding site.

In an independent approach, the binding site of GntR1 and GntR2 within the *gntK* promoter was searched by DNase I footprinting. A protected region could be detected on the template strand extending from position +3 to -10 relative to the transcription start site, which completely overlaps with the binding motif previously identified by gel shift assays (Fig. 6C). This site was also confirmed by DNase I footprinting analysis with GntR1 and GntR2 and the non-template strand (data not shown). Interestingly, an additional protected region was present on the template strand between -38 and -48 (Fig. 6C). This indicates the existence of at least one additional GntR1/2 binding site, whose sequence shows no obvious similarity to those of the other identified GntR1/2 binding sites. Repression of *gntK* by GntR1 and GntR2 might involve formation of a DNA loop between the two binding sites.

Analysis of the promoter regions of *gntP*, *gnd* and *ptsG* by gel shift analyses with subfragments of the promoter regions also led to the identification of distinct sites involved in GntR1/2 binding (Fig. 7). The relevance of these sites was again confirmed by mutation studies which showed that an exchange of three bp within these sites prevented binding (data not shown). The binding sites were centred at

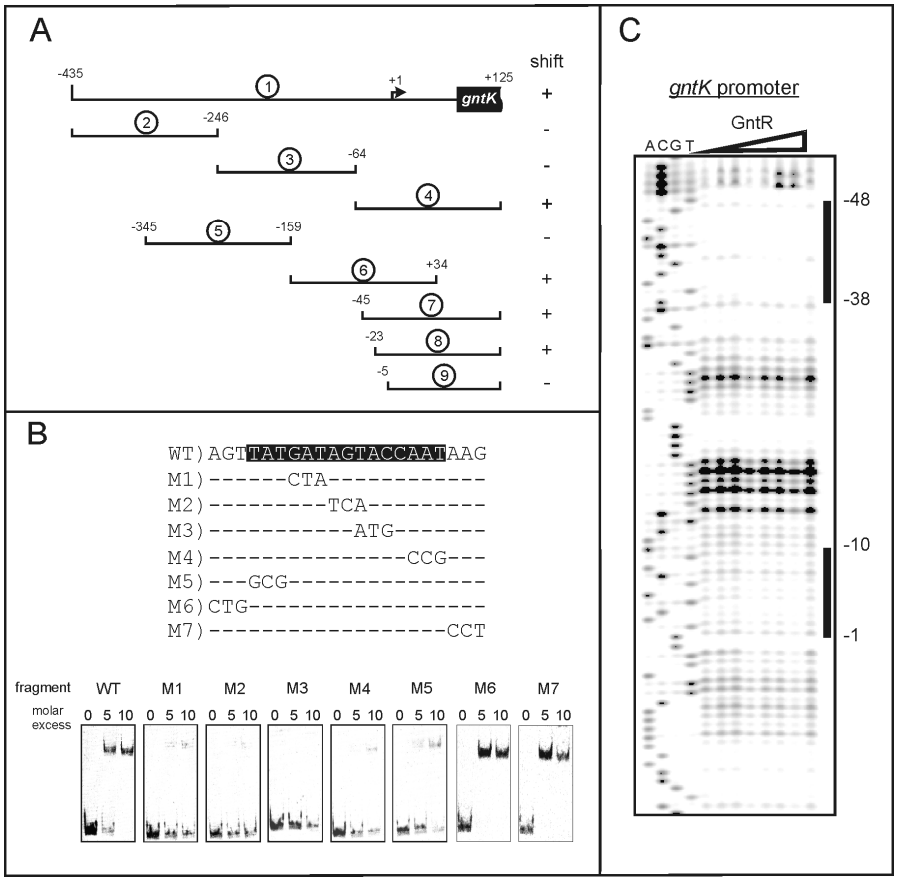

Fig. 6. Identification of the GntR1/2 binding site in the promoter region of *gntK*. A, DNA fragments used to determine the location of the GntR1/2 binding site in the *gntK* promoter. The numbers indicate the position of the fragments relative to the transcription start site (+1) determined in this work (see Fig. 5). Oligonucleotides used for amplification by PCR are listed in Table S1. At the right, it is indicated whether the fragment, when tested in bandshift assays with purified GntR2, was shifted (+) or not (-). B, Mutational analysis of the putative GntR1/2 binding site within the *gntK* promoter region. Mutations introduced are listed below the wild type sequence. Oligonucleotides used for amplification of the corresponding fragments are listed in Table S1. The fragments were incubated with purified GntR1 and the samples were separated on a 10% nondenaturating polyacrylamide gel and stained with SybrGreen I. C, DNase I footprinting analysis with GntR2 and the *gntK* promoter region. 2 nM IRD-800-labelled *gntK* template strand was incubated with increasing concentrations of GntR2 (0 - 2 µM). The first and the last lane were loaded with samples containing no protein. Regions protected from digestion by DNase I are indicated by the black bars. The DNA sequencing reactions were set up using the same IRD-800-labelled oligonucleotide as for generating labelled footprinting probes as well as suitable PCR template.

position +2 with respect to the recently reported transcriptional start site of *gntP* (Letek *et al.*, 2006) and at position -11 with respect to the start codon of *gnd*. In the case of *ptsG*, the binding site was centred at position -60 with respect to the transcriptional start site determined previously by primer extension experiments (Engels and Wendisch, 2007). These positions fit with a repressor function for *gntP* and *gnd* and an activator function for *ptsG* of GntR1/2. All GntR1/2 binding sites identified in this work are in reasonable agreement (1-2 mismatches) with a consensus operator site deduced for GntR-type regulators of the FadR subfamily (TNGTNNNACNA) (Rigali *et al.*, 2002).

Promoter	Sequence	Location	Orientation
gntK	TATGATAGTACCAAT	- 3	+
gntP	TTTGATCATACTAAT	+ 2	+
gnd	ATTGATCGTACTTGA	-11	-
ptsG	AAAAGTATTACCTTT	-60	+
Consensus	WWtgaTMNTACYWNt		

Fig. 7. Experimentally identified GntR1/2 binding sites in the promoter regions of *gntK*, *gntP*, *gnd* and *ptsG*. The location of the central nucleotide of the 15-bp binding sites is indicated with respect to the transcriptional start site for *gntK, gntP*, and *ptsG*, but with respect to the start codon for *gnd*. The orientation of the binding sites is indicated by plus and minus signs. The relevance of each binding site was confirmed by mutational analysis using gel shift assays with purified GntR1 and GntR2. Nucleotides shaded in black are conserved in all binding sites, those shaded in grey are identical in three of four binding sites.

Gluconate interferes with the binding of GntR1 and GntR2 to their target promoters

The transcriptome comparisons as well as the measurement of enzyme activities (gluconate kinase, 6-phosphogluconate dehydrogenase and glucose-6-phosphate dehydrogenase) indicated that the activity of GntR1 and GntR2 is dependent on the carbon source available. In order to identify putative effector molecules, the binding of GntR1 and GntR2 to the *gntK* promoter was assayed in the presence of glucose, gluconate, glucono-δ-lactone, 6-phosphogluconate, glucose-6-phosphate, fructose, sucrose, mannitol, sorbitol and glucuronate. For this purpose, purified GntR1 or GntR2 was incubated with the potential effector substances (50 mM) for 5–10 min before addition of a DNA fragment covering the *gntK* promoter and another 20 min of incubation. Subsequently, the samples were separated on a 10% native polyacrylamide gel. Of the 10 compounds tested only gluconate and, to a lower extent, glucono-δ-lactone inhibited binding of GntR1 and GntR2 to its target DNA (Fig. 8). In further studies it was shown that already a concentration of 1 mM gluconate led to a partial inhibition of binding. However, as even a concentration of 50 mM gluconate led only to a partial inhibition of binding, the possibility that a contaminating compound rather than gluconate or glucono-δ-lactone itself is responsible for the effect cannot be completely excluded. Similar results as described above for the *gntK* promoter were also obtained with the promoter regions of *gntP*, *gnd*, *tkt*, *ptsG* and *ptsS* (data not shown).

Co-utilization of glucose and gluconate by C. glutamicum

It has previously been reported that *C. glutamicum*, like several other bacteria, is able to consume glucose and gluconate simultaneously (Lee *et al.*, 1998). The results described above have uncovered that the genes involved in gluconate catabolism, including the pentose phosphate pathway, and the *ptsG* gene encoding the permease EII^{Glc} of the glucose PTS are coordinately regulated by GntR1 and GntR2. We therefore investigated whether the deletion of both transcriptional regulators has an effect on the co-consumption of glucose and gluconate. *C. glutamicum* wild type and the Δ*gntR1*Δ*gntR2* mutant were cultivated in CGXII minimal medium containing either 100 mM glucose, or 100 mM gluconate, or 50 mM glucose plus 50 mM gluconate and growth as well as glucose and gluconate uptake rates were monitored (Fig. 9). As described before, the Δ*gntR1*Δ*gntR2* mutant showed a drastically reduced growth rate when cultivated in minimal medium with 100 mM glucose ($\mu = 0.15 \pm 0.01$ h^{-1}) in comparison to the wild type ($\mu = 0.43 \pm 0.02$ h^{-1}). As expected from this observation, the glucose uptake rate of the *ΔgntR1ΔgntR2* mutant (33 nmol mg^{-1} min^{-1}) was only one third of that of the wild type (90 nmol mg^{-1} min^{-1}) (Table 4). In contrast, cultivation on gluconate as carbon source resulted in almost identical growth rates of both strains ($\mu = 0.46 \pm 0.02$ h^{-1}) and nearly identical gluconate uptake rates (99 nmol mg^{-1} min^{-1}). The final cell density reached in gluconate medium ($OD_{600} = 25.3 \pm 0.5$) was somewhat lower than the one reached in

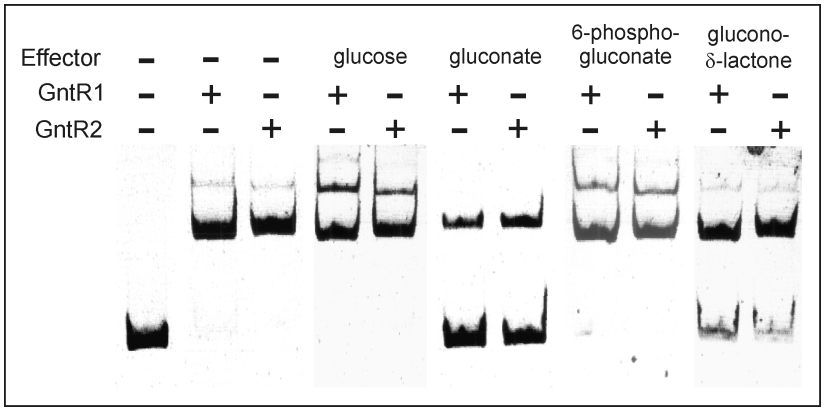

Fig. 8. Search for putative effector molecules of GntR1 and GntR2. Various carbohydrates were tested for their influence on GntR1/2 binding to a DNA fragment containing the promoter region of *gntK*. 0.28 pmol of the 550 bp gntK fragment was incubated with either 2.8 pmol purified GntR1 or GntR2 protein in the presence of the following carbohydrates (50 mM each): glucose, gluconate, 6-phospho-gluconate, glucono-δ-lactone. Not shown are the experiments with glucuronic acid, glucose-6-phosphate, fructose, sucrose, mannitol and sorbitol, which had no influence on DNA binding.

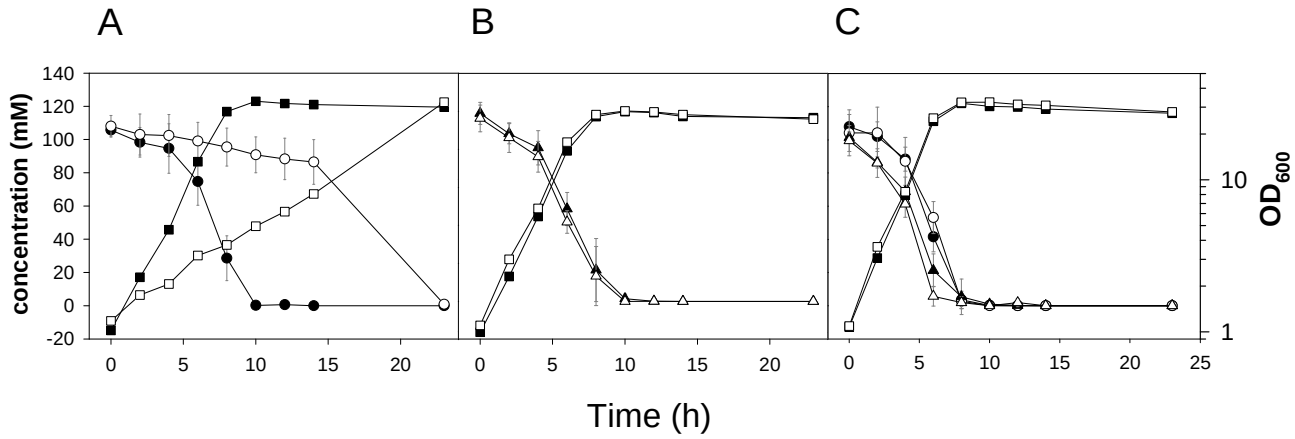

Fig. 9. Growth (squares) and carbon source consumption of *C. glutamicum* wild type (filled symbols) and the mutant Δ*gntR1*Δ*gntR2* (open symbols). The two strains were cultivated in CGXII minimal medium containing as carbon source either 100 mM glucose (A), or 100 mM gluconate (B), or 50 mM glucose + 50 mM gluconate (C). The values are means obtained from three independent cultivations.

glucose medium (OD_{600} = 30.1 ± 1.1), which might be caused by an increased loss of substrate carbon as CO_2 in the 6-phosphogluconate dehydrogenase reaction. In contrast to glucose, gluconate has to be metabolized completely via the oxidative pentose phospate pathway. Interestingly, when cells were cultivated with glucose plus gluconate, both *C. glutamicum* wild type and the Δ*gntR1*Δ*gntR2* mutant showed a significantly increased growth rate (μ = 0.52 ± 0.02 h^{-1}). In this case, the final cell density (OD_{600} = 27.5 ± 0.3) was in between that obtained for glucose and gluconate as single carbon sources. Determination of the uptake rates confirmed that both strains consumed glucose and gluconate simultaneously. In the wild type, comparable uptake rates between 50 and 60 nmol mg^{-1} min^{-1} were determined (Table 4). Whereas the reduced glucose uptake in the wild type during cultivation in the presence of gluconate is presumably a consequence of the missing *ptsG* activation by GntR1 and GntR2, the reduced gluconate uptake in the presence of glucose might be caused by repression of *gntP* and *gntK* by the GlxR-cAMP complex, as suggested previously (Letek *et al.*, 2006). In the Δ*gntR1*Δ*gntR2* mutant glucose uptake was slightly decreased compared to the wild type (52 *vs*. 56 nmol mg^{-1} min^{-1}), whereas gluconate uptake was slightly increased (65 *vs*. 52 nmol mg^{-1} min^{-1}). These minor differences might be explained by the assumption that in the wild type, but not in the Δ*gntR1*Δ*gntR2* mutant, there is some weak residual activation of *ptsG* and repression of *gntP*, *gntK* and *gnd* by GntR1 and GntR2 even in the presence of gluconate. Such a behavior fits with the observation that even high gluconate concentrations did not completely prevent binding of GntR1/2 to its target promoters (see above). The finding that the glucose uptake rate of the Δ*gntR1*Δ*gntR2* mutant during growth on glucose plus gluconate was 50% higher than during growth on glucose alone indicates that gluconate has not only a negative effect on glucose uptake via GntR1/2, but also a positive effect via another transcriptional regulator or another regulatory mechanism.

Discussion

In this study we have identified two functionally redundant GntR-type regulators in *C. glutamicum*, GntR1 and GntR2, which co-ordinately control gluconate catabolism and glucose uptake, presumably in dependency of the intracellular concentration of gluconate and glucono-δ-lactone. Whereas the negative control of genes involved in gluconate metabolism by GntR-type regulators has previously been demonstrated e.g. in *E. coli* (Izu *et al.*, 1997; Peekhaus and Conway, 1998; Porco *et al.*, 1997) or *B. subtilis* (Fujita and Miwa, 1989; Miwa and Fujita, 1988; Reizer *et al.*, 1991), the simultaneous positive control by these regulators of the *ptsG* gene encoding the key protein for glucose uptake via the PTS is a novel and surprising aspect. If the activation of *ptsG* expression is abolished by deletion of

Table 4. Carbon consumption rates of *C. glutamicum* wild type and the Δ*gntR1*Δ*gntR2* mutant during growth in CGXII minimal medium with either 100 mM glucose or gluconate or with 50 mM of both carbon sources. The represent means ± standard deviations for at least three independent cultivations.

	Carbon source consumption rates (nmol min^{-1} mg^{-1})			
Strain	Glucose	Gluconate	Glucose + Gluconate	
Wild type	90 ± 8	98 ± 9	56 ± 8	52 ± 4
Δ*gntR1*Δ*gntR2*	33 ± 6	99 ± 8	52 ± 7	65 ± 3

gntR1 and *gntR2*, the growth rate and the glucose uptake rate of the corresponding strain in glucose minimal medium is reduced by about 60%. The question arises why this type of opposite co-regulation of glucose and gluconate metabolism has been established in *C. glutamicum*. One reason might be the fact that this species, in contrast to e.g. *E. coli* or *B. subtilis*, usually prefers the simultaneous consumption of different carbon sources rather than their sequential utilization. Examples are the co-utilization of glucose with acetate (Wendisch *et al.*, 2000), lactate (Stansen *et al.*, 2005), propionate (Claes *et al.*, 2002), fructose (Dominguez *et al.*, 1997) or citrate (von der Osten *et al.*, 1989). In the case of glucose-acetate co-metabolism it was shown that both the acetate consumption rate (270 nmol min^{-1} (mg protein)$^{-1}$) and the glucose consumption rate (72 nmol min^{-1} (mg protein)$^{-1}$) were two-fold decreased compared to growth on acetate or glucose as sole carbon source, resulting in a comparable rate of total carbon uptake of about 1000 nmol C min^{-1} (mg protein)$^{-1}$ under all three growth conditions (Wendisch *et al.*, 2000). The carbon uptake rates (nmol C min^{-1} (mg protein)$^{-1}$, based on the assumption that protein constitutes 50% of the cell dry weight) determined in this work for the wild type were in the same order of magnitude (Table 4): 1080 for growth on glucose, 1180 for growth on gluconate, and 1290 for growth on glucose (670) plus gluconate (620). These two examples show that *C. glutamicum* is able to adjust the uptake rates for different carbon sources in such a way that they match its metabolic capacities. The co-metabolism of glucose and gluconate is advantageous for *C. glutamicum* as its growth rate (0.52 h^{-1}) is increased by 20% compared to growth on glucose alone (0.43 h^{-1}) and by 13% compared to growth on gluconate alone (0.46 h^{-1}). Thus, activation of *ptsG* expression by GntR1 and GntR2 can be interpreted as one of the mechanisms that allow *C. glutamicum* the simultaneous consumption of carbon sources and thereby a maximization of its growth rate and a selective advantage in the competition with other microorganisms. Gluconate is likely to be a frequent substrate in nature, since (i) many bacteria, such as pseudomonads, acetic acid bacteria, or enterobacteria (Anthony, 2004; Neijssel *et al.*, 1989), possess membrane-bound glucose dehydrogenases that catalyse the extracytoplasmic oxidation of glucose to gluconic acid and (ii) a high number of bacteria possess gluconate permeases and are able to utilize gluconate either via the Entner-Doudoroff pathway or via the pentose phosphate pathway.

Besides its negative influence on *ptsG* expression mediated by GntR1 and GntR2, gluconate appears to have also a positive effect on *ptsG* expression: in the *ptsG'-'cat* fusion assays, expression of *ptsG* in the Δ*gntR1*Δ*gntR2* mutant was two-fold higher on gluconate or glucose plus gluconate than on glucose alone (Table 3). Similarly, the glucose consumption rate of the double mutant was ~60% higher during growth on glucose and gluconate than during growth on glucose alone (Table 4). These differences might be caused by the SugR protein, which was recently identified as a repressor of *ptsG* and other PTS genes during growth on gluconeogenic carbon sources (Engels and Wendisch, 2007). The activity of SugR is controlled by fructose-6-phosphate, which was shown to abolish binding of SugR to the *ptsG* promoter region *in vitro*. When gluconate is catabolized via the pentose phosphate pathway, it enters glycolysis at the level of fructose-6-phosphate and glyceraldehyde-3-phosphate. Therefore, it seems possible that the intracellular fructose-6-phosphate concentration is increased in the presence of gluconate and repression of *ptsG* by SugR is diminished. Analysis of *ptsG* expression in a Δ*gntR1*Δ*gntR2*Δ*sugR* triple mutant and measurement of the intracellular fructose-6-phosphate concentration might allow confirming or disproving this explanation.

The genomes of the closely related organisms *C. glutamicum* strain R (Yukawa *et al.*, 2007) and *C. efficiens* contain just one *gntR* orthologous gene. Thus, the presence of *gntR2*,

which most likely resulted from of a gene duplication event of *gntR1*, seems to be a characteristic of the *C. glutamicum* type strain ATCC 13032. As all results obtained in this work show that GntR1 and GntR2 can fully replace each other, the question arises why both *gntR* genes are retained in the chromosome. A convincing answer to this question is not yet available. The possibility exists that differences in the expression of the two genes or not yet uncovered individual functions of the regulators allow the cell a better adaptation to certain growth conditions.

In this work ten direct target genes of GntR1 and GntR2 have been identified. Those involved in gluconate transport and metabolism (*gntP*, *gntK*, *gnd*, *tkt-tal-zwf-opcA-devB*) are repressed by GntR1 and GntR2, whereas *ptsG* and *ptsS* encoding the permeases EII^{Glc} and EII^{Suc} of the PTS system are activated. Activation of gene expression by GntR-type regulators has also been demonstrated for other members of this family, e.g. MatR, an activator of genes involved in malonate metabolism of *Rhizobium leguminosarum* (Rigali *et al*., 2002). Binding of GntR1 and GntR2 to all of its target promoters was inhibited by gluconate and glucono-δ-lactone (Fig. 8), which fits with their function in gluconate metabolism. The same metabolites were previously shown to interfere with binding of the *B. subtilis* GntR protein to its target promoters (Miwa and Fujita, 1988). Binding of *E. coli* GntR to the *gntT* promoter was likewise inhibited by gluconate, but at higher concentrations also by 6-phosphogluconate (Peekhaus and Conway, 1998). 1 mM and 20 mM gluconate were sufficient to completely inhibit binding of *E. coli* GntR and *B. subtilis* GntR to target promoters, respectively. In the case of *C. glutamicum* GntR1 and GntR2, only a partial inhibition of DNA binding was achieved with 50 mM gluconate, indicating a lower affinity for gluconate. Although the possibility exists that a contaminant present in the source of gluconate or glucono-δ-lactone could be responsible for inhibition of binding, this seems not very likely.

Besides being induced by gluconate, genes involved in the catabolism of this sugar acid are often subject to catabolite repression, e.g. in *E. coli* or *B. subtilis* (Peekhaus and Conway, 1998; Reizer *et al.*, 1996; Titgemeyer and Hillen, 2002; Tong *et al.*, 1996; Warner and Lolkema, 2003). Recently, it was reported that *gntK* and *gntP* of *C. glutamicum* are also subject to catabolite repression, mediated by the transcriptional regulator GlxR in complex with cAMP (Letek *et al.*, 2006). Kim *et al.* (2004) reported that in *C. glutamicum* the cAMP concentration is 10-fold higher during growth on glucose than during growth on acetate, indicating that GlxR is active in the presence of glucose. Our finding that the gluconate consumption rate of *C. glutamicum* wild type is about two-fold lower during growth on glucose plus gluconate compared with growth on gluconate alone (Table 4) could be due to catabolite repression of *gntP* and *gntK* by the GlxR-cAMP complex. A prerequisite for this explanation is that cells cultivated in the presence of glucose plus gluconate have a higher cAMP level than cells grown on gluconate alone.

In a previous study on gluconate metabolism in *C. glutamicum* it was reported that *gntP* and *gntK* are not induced by gluconate (Letek *et al.*, 2006). Our results clearly show that *gntP* and *gntK* together with pentose phosphate pathway genes are induced by gluconate via GntR1 and GntR2. Simultaneously these regulators control glucose uptake by activation of *ptsG* expression in the absence of gluconate. In conclusion, these transcriptional regulators are important players in a complex regulatory network that controls uptake and metabolism of carbon sources in *C. glutamicum* in order to allow the most favourable combination of the available substrates.

Experimental procedures

Bacterial strains, media and growth conditions

All strains and plasmids used in this work are listed in Table 5. The *C. glutamicum* type strain ATCC 13032 (Kinoshita *et al.*, 1957) was used as wild type. Strain Δ*gntR1* and strain Δ*gntR2* are derivatives containing an in-frame deletion of the genes *gntR1* (*cg2783*) and *gntR2* (*cg1935*), respectively. In strain Δ*gntR1*Δ*gntR2* both genes were deleted. For growth experiments, 5 ml of brain heart infusion (BHI) medium (Difco Laboratories, Detroit, USA) was inoculated with colonies from a fresh LB agar plate (Sambrook, 1989) and incubated for 6 hours at 30℃ and 170 rpm. After washing with

Table 5. Bacterial strains and plasmids used in this study.

Strains or plasmids	Relevant characteristics	Source or reference
Strains		
C. glutamicum		
ATCC 13032	Biotin-auxotrophic wild type	(Kinoshita *et al.*, 1957)
Δ*gntR1*	In-frame deletion of the *gntR1* (*cg2783*) gene	This work
Δ*gntR2*	In-frame deletion of the *gntR2* (*cg1935*) gene	This work
Δ*gntR1*Δ*gntR2*	In-frame deletion of the genes *gntR1* and *gntR2*	This work
E. coli		
DH5α	*supE44* Δ*lacU169* (ϕ80*lacZ*DM15) *hsdR17 recA1 endA1 gyrA96 thi-1 relA1*	Invitrogen
BL21(DE3)/pLysS	F^- *ompT hsdS*$_B$($r_B^-m_B^-$) *gal dcm* (DE3) ; contains plasmid pLysS (Cam^R)	(Studier and Moffatt, 1986)
Plasmids		
pK19*mobsacB*	Kan^R; vector for allelic exchange in *C. glutamicum*; (pK18 *oriV*$_{E.c.}$, *sacB*, *lacZ*α)	(Schäfer *et al.*, 1994)
pK19*mobsacB*-Δ*cg1935*	Kan^R; pK19*mobsacB* derivative containing a crossover PCR product covering the up- and downstream regions of *cg1935* (*gntR2*)	This work
pK19*mobsacB*-Δ*cg2783*	Kan^R; pK19*mobsacB* derivative containing a crossover PCR product covering the up- and downstream regions of *cg2783* (*gntR1*)	This work
pAN6	Kan^R; *C. glutamicum*/*E. coli* shuttle vector for regulated gene expression; derivative of pEKEx2 (P_{tac}, $lacI^q$, pBL1 *oriV*$_{C.g.}$, pUC18 *oriV*$_{E.c.}$) ; for details see Experimental procedures	This work
pAN6-*gntR1*	Kan^R; pAN6 derivative containing the *gntR1* gene (*cg2783*) under control of the *tac* promoter	This work
pAN6-*gntR2*	Kan^R; pAN6 derivative containing the *gntR2* gene (*cg1935*) under control of the *tac* promoter	This work
pEKEx2	Kan^R; *C. glutamicum*/*E. coli* shuttle vector for regulated gene expression (P_{tac}, $lacI^Q$, pBL1 *oriV*$_{C.g.}$, pUC18 *oriV*$_{E.c.}$)	(Eikmanns *et al.*, 1991)
pEKEx2-*gntR1*-His	Kan^R; pEKEx2 derivative encoding GntR1 with an aminoterminal decahistidine tag	This work
pEKEx2-*gntR2*-His	Kan^R; pEKEx2 derivative encoding GntR2 with an aminoterminal decahistidine tag	This work
pET16b	Amp^R; vector for overexpression of genes in *E. coli*, adding a C-terminal hexahistidine affinity tag to the synthesized protein (pBR322 *oriV*$_{E.c.}$, P_{T7}, *lacI*)	Novagen
pET16b-*gntR1*	Kan^R; pET16b derivative for overproduction of GntR1 with an N-terminal decahistidine tag.	This work
pET16b-*gntR2*	Kan^R; pET16b derivative for over-production of GntR2 with an N-terminal decahistidine tag.	This work
pET2-*ptsG*	KanR; *C. glutamicum* promoter-probe plasmid with a 707-bp fragment covering the *C. glutamicum ptsG* promoter	(Engels and Wendisch, 2007)

5 ml 0.9% (w/v) NaCl, the cells of this first preculture were used to inoculate a 500-ml shake flask containing 50 ml CGXII minimal medium (Keilhauer *et al.*, 1993) with either glucose, or gluconate, or glucose plus gluconate in the indicated concentrations as carbon source(s). Additionally, the medium was supplemented with 30 mg/l 3,4-dihydroxybenzoate as iron chelator. This second preculture was cultivated overnight at 30℃ and then used to inoculate the main culture to an optical density at 600 nm (OD_{600}) of ~1. The trace element solution was always added after autoclaving. For all cloning purposes, *E. coli* DH5α (Invitrogen, Karlsruhe, Germany) was used as host, for overproduction of the proteins Cg2783 (= GntR1) and Cg1935 (= GntR2) *E. coli* BL21(DE3)/pLysS. The *E. coli*

strains were cultivated aerobically in LB medium at 37℃ (strain DH5 α) or at 30℃ (strain BL21 (DE3)/pLysS). When appropriate, the media contained chloramphenicol (34 µg/ml for cultivation of *E. coli* BL21 (DE3)/pLysS), ampicillin (100 µg/ml for *E. coli*), or kanamycin (25 µg/ml for *C. glutamicum*, 50 µg/ml for *E. coli*).

Recombinant DNA work

The enzymes for recombinant DNA work were obtained from Roche Diagnostics (Mannheim, Germany) or New England Biolabs (Frankfurt, Germany). The oligonucleotides used in this study are listed in Table S1 and were obtained from Operon (Cologne, Germany), except for the IRD800-labelled oligonucleotides, which were purchased from MWG Biotech (Ebersberg, Germany). Routine methods like PCR, restriction or ligation were carried out according to standard protocols (Sambrook, 1989). Chromosomal DNA from *C. glutamicum* was prepared as described (Eikmanns *et al.*, 1994). Plasmids from *E. coli* were isolated with the QIAprep spin miniprep Kit (Qiagen, Hilden, Germany). *E. coli* was transformed by the RbCl method (Hanahan, 1985), *C. glutamicum* by electroporation (van der Rest *et al.*, 1999). DNA sequencing was performed with a Genetic Analyzer 3100-Avant (Applied Biosystems, Darmstadt, Germany). Sequencing reactions were carried out with the BigDye Terminator v3.1 Cycle Sequencing Kit (Applied Biosystems, Darmstadt, Germany).

In-frame deletion mutants of C. glutamicum were constructed via a two-step homologous recombination procedure as described previously (Niebisch and Bott, 2001). The primers used for this purpose are listed in Table S1. The chromosomal deletions were confirmed by PCR with oligonucleotides annealing outside the deleted regions.

In order to complement the ΔgntR1ΔgntR2 mutant, the gntR1 (cg2783) and gntR2 (cg1935) coding region were amplified using oligonucleotides (2783NdeN, 2783Ex1, 1935NdeN and1935Ex1) introducing an NdeI restriction site that included the start codon and a NheI restriction site behind the stop codon. The resulting PCR products were cloned into the expression vector pAN6, resulting in plasmids pAN6-*gntR1* and pAN6-*gntR2*. These plasmids and as a control pAN6 were used to transform C. glutamicum wild type and the ΔgntR1ΔgntR2 strain. The vector pAN6 is a derivative of pEKEx2 (Eikmanns *et al.*, 1991b) that contains a 56-bp insertion between the PstI and EcoRI restriction sites. This insertion harbours a ribosome-binding site (GGAGATA) in an optimal distance to a unique NdeI cloning site. Downstream of the NdeI site, there is a unique NheI cloning site which is followed by a *Strep*Tag-II-coding sequence and a stop codon before the EcoRI site. For the construction of pAN6, the original NdeI restriction site of pEKEx2 was first removed by Klenow fill-in and religation and subsequently a DNA fragment of the sequence 5'-GACCTGCAGAAGGAGAT-ATACATATGACCTGAGCTAGCTGGTCCCAC CCACAGTTCGAGAAGTAAGAATTCGTC-3' was cut with PstI and EcoRI and ligated with the modified pEXEx2 vector cut with the same enzymes.

For overproduction and purification of GntR1 and GntR2 with an N-terminal decahistidine tag, the corresponding coding regions were amplified using oligonucleotides that introduce an NdeI restriction site including the start codon and an XhoI restriction site after the stop codon. The purified PCR products were cloned into the expression vector pET16b (Novagen, Darmstadt, Germany), resulting in plasmids pET16b-gntR1 and pET16b-gntR2. The GntR proteins encoded by these plasmids contain 21 additional amino acids (MGHHHHHHHHHH-SSGHIEGRH) at the amino terminus. The PCR-derived portion of the constructed plasmids were analyzed by DNA sequence analysis and found to contain no spurious mutations. For overproduction of the GntR proteins, the plasmids were transferred into E. coli BL21 (DE3)/pLysS.

Global gene expression analysis

Preparation of RNA and synthesis of fluorescently labelled cDNA were carried out as described (Möker *et al.*, 2004b). Custom-made DNA microarrays for *C. glutamicum* ATCC 13032 printed with 70mer oligonucleotides were obtained from Operon (Cologne, Germany) and are based on the genome sequence entry NC_006958 (Kalinowski *et al.*, 2003).

Hybridisation and stringent washing of the microarrays were performed according to the instructions of the supplier. Hybridisation was carried out for 16-18 h at 42℃ using a MAUI hybridization system (BioMicro Systems, Salt Lake City, USA). After washing the microarrays were dried by centrifugation (5 min, 1600 x *g*) and fluorescence was determined at 532 nm (Cy3-dUTP) and 635 nm (Cy5-dUTP) with 10 µm resolution using an Axon GenePix 6000 laser scanner (Axon Instruments, Sunnyvale, U.S.A. Quantitative image analysis was carried out using GenePix image analysis software and results were saved as GPR-file (GenePix Pro 6.0, Axon Instruments). For data normalization, GPR-files were processed using the BioConductor/R-packages limma and marray (www.bioconductor.org). Processed and normalized data as well as experimental details (MIAME (Brazma *et al.*, 2001)) were stored in the in-house microarray database for further analysis (Polen and Wendisch, 2004).

Using the DNA microarray technology, the genome-wide mRNA concentrations of *C. glutamicum* wild type was compared with those of the mutant strains Δ*gntR1*Δ*gntR2* (A), Δ*gntR2* (B), and Δ*gntR1* (C). The strains were cultivated in CGXII minimal medium with either 100 mM glucose (Glu), or 100 mM gluconate (Gnt), or 50 mM glucose plus 50 mM gluconate (only for comparison A). RNA used for the synthesis of labelled cDNA was prepared from cells in the exponential growth phase. For each of the seven comparisons, two or three independent DNA microarray experiments were performed, each starting from an independent culture. To filter for differentially expressed genes and reliable signal detection in each of the seven comparisons, the following quality filter was applied: (i) flags ≤0 (GenePix Pro 6.0), (ii) signal/noise ≥3 for Cy5 (F635Median /B635Median, GenePix Pro 6.0) or Cy3 (F532Median/B532Median, GenePix Pro 6.0), (iii) ≥4-fold change in the comparison Δ*gntR1*Δ*gntR2* mutant *vs*. wild type in glucose minimal medium, (iv) significant change ($p < 0.05$) in a Student's *t*-test (EXCEL, Microsoft).

Primer extension analysis

For non-radioactive primer extension analysis of the *gntK* gene total RNA was isolated from exponentially growing *C. glutamicum* wild type cultivated in CGXII minimal medium with 100 mM gluconate as carbon source. Primer extension analysis with 10 to 13 µg of total RNA was performed using IRD800-labeled oligonucleotides (PE-gntK-1 and PE-gntK-2, Table S1) (MWG Biotech, Ebersberg, Germany) as described previously (Engels *et al.*, 2004). The template for the DNA sequence analysis used to localize the 3'-end of the primer extension product was amplified in a standard PCR reaction using the unlabelled oligonucleotides gntK-seq-for and gntK-seq-rev (Table S1). The oligonucleotides PE-gntK-1 or PE-gntK-2 served as primers for the sequencing reactions.

Measurement of enzyme activities

For the measurement of enzyme activities, cells of *C. glutamicum* wild type and the double deletion mutant Δ*gntR1*Δ*gntR2* were cultivated in CGXII minimal medium with either 4% (w/v) glucose or 2% (w/v) gluconate up to the exponential growth phase (OD_{600} ~5). Then cells of 20 ml culture were harvested with ≈25 g of crushed ice (precooled to -20 ℃) by centrifugation at 4,000 x *g* for 5 min. The cell pellet was resuspended in 900 µl of Tris/HCl (50 mM; pH 7.5) and the cells were mechanically disrupted by 3 x 20 s bead beating with 1 g of zirconia-silica beads (diameter 0.1 mm; Roth, Karlsruhe, Germany) using a Silamat S5 (Vivadent, Ellwangen, Germany). After centrifugation (5 min; 18,320 x *g*; 4 ℃), the supernatant was used immediately for the enzyme assay.

For the determination of glucose-6-phosphate dehydrogenase and 6-phosphogluconate dehydrogenase activity, the assay mixtures (1 ml total volume) contained 50 mM Tris/HCl pH 7.5, 10 mM $MgCl_2$, 1 mM $NADP^+$, 200 mM potassium glutamate and 3-20 µl cell-free extract (1-5 mg protein/ml). The reaction was initiated by the addition of 4 mM glucose-6-phosphate or 1 mM 6-phosphogluconate, and the increase in absorption at 340 nm was monitored at 30 ℃ using a Jasco V560 spectrophotometer (Jasco, Gross-Umstadt, Germany).

Gluconate kinase activity was determined in a coupled assay with 6-phosphogluconate

dehydrogenase. The assay mixture (1 ml total volume) contained 50 mM Tris/HCl pH 8.0, 0.25 mM NADP, 1 mM ATP, 1.2 U 6-phosphogluconate dehydrogenase, and 5-50 µl cell-free extract (1-5 mg protein/ml). After preincubation for 5 min at 30 °C, the reaction was started by the addition of 50 µl of a 200 mM gluconic acid solution (pH 6.8) and the increase in absorption at 340 nm was measured at 30°C.

Chloramphenicol acetyltransferase assay

For analysing the expression of the *ptsG* gene, *C. glutamicum* wild type and the double mutant Δ*gntR1*Δ*gntR2* were transformed with plasmid pET2-*ptsG* (Engels and Wendisch, 2007), which is based on the corynebacterial promoter-probe vector pET2 (Vasicova *et al.*, 1998) and contains the *ptsG* promoter region (-399 to +309) in front of a promoter-less *cat* (chloramphenicol acetyltransferase) gene. The promoter activity was tested by measuring chloramphenicol acetyltransferase activity in cell extracts. For this purpose, 5 ml Luria-Bertani (LB) medium was inoculated with colonies from a fresh LB agar plate and incubated for 6 hours at 30 °C and 170 rpm. After washing the cells in CGXII medium without carbon source, the second preculture and subsequently the main culture (both 60 ml CGXII minimal medium with 50 µg/ml kanamycin) were inoculated to an OD_{600} of 0.5. As carbon and energy source either 100 mM glucose, or 100 mM gluconate, or 50 mM glucose plus 50 mM gluconate were used. Precultures and main cultures were incubated at 30 °C and 120 rpm on a rotary shaker in 500-ml baffled shake flasks. The preparation of the crude extract and the measurement of its chloramphenicol acetyltransferase activity were performed as described by Engels and Wendisch (2007).

Overproduction and purification of GntR1 and GntR2

The *C. glutamicum* proteins GntR1 and GntR2 containing 21 additional amino acids at the N-terminus (MGHHHHHHHHHHSSGHIEGRH) were overproduced in *E. coli* BL21(DE3)/pLysS using the expression plasmids pET16b-*gntR1* and pET16b-*gntR2*, respectively. Expression was induced at an A_{600} of 0.3 with 1 mM isopropyl β-D-thiogalactoside. Four hours after induction, cells were harvested by centrifugation and stored at -20 °C. For cell extract preparation, thawed cells were washed once and resuspended in 10 ml of TNGI5 buffer (20 mM Tris/HCl, pH 7.9, 300 mM NaCl, 5% (v/v) glycerol, and 5 mM imidazol). After the addition of 1 mM diisopropylfluorophosphate and 1 mM phenylmethylsulfonyl fluoride, the cell suspension was passed three times through a French pressure cell (SLM Aminco, Spectronic Instruments, Rochester, NY) at 207 MPa. Intact cells and cell debris were removed by centrifugation (15 min, 5,000 x *g*, 4 °C), and the cell-free extract was subjected to ultracentrifugation (1 h, 150,000 x *g*, 4 °C). GntR1 or GntR2 present in the supernatant of the ultracentrifugation step was purified by nickel chelate affinity chromatography using nickel-activated nitrilotriacetic acid-agarose (Novagen, Darmstadt, Germany). After washing the column with TNGI50 buffer (which contains 50 mM imidazol), specifically bound protein was eluted with TNGI100 buffer (which contains 100 mM imidazol). Fractions containing GntR1 or GntR2 were pooled, and the elution buffer was exchanged against TG buffer (30 mM Tris/HCl, pH 7.5, 10% (v/v) glycerol).

Gel shift assays

For testing the binding of GntR1 and GntR2 to putative target promoters, purified protein was mixed with DNA fragments (100 – 700 bp, final concentration 8 – 20 nM) in a total volume of 20 µl. The binding buffer contained 20 mM Tris/HCl (pH 7.5), 50 mM KCl, 10 mM $MgCl_2$, 5% (v/v) glycerol, and 0.5 mM EDTA. Approximately 13 nM promoter fragments of putative non-target genes of GntR1/2 (*acn*, *sucCD* and *sdh*) were used as negative controls. The reaction mixtures were incubated at room temperature for 20 min and then loaded onto a 10% native polyacrylamide gel. Electrophoresis was performed at room temperature and 170 V using 1x TBE (89 mM Tris base, 89 mM boric acid, 2 mM EDTA) as electrophoresis buffer. The gels were subsequently stained with SybrGreen I according to the instructions of the supplier (Sigma-Aldrich, Taufkirchen, Germany) and photographed. All PCR products used in the gel

shift assays were purified with the PCR purification kit (Qiagen, Hilden, Germany) and eluted in EB buffer (10 mM Tris/HCl pH 8.5).

DNase I footprinting

Labelled DNA fragments were obtained by amplification with 5´-IRD800-labelled oligonucleotides (MWG Biotech, Ebersberg, Germany). The *gntK* promoter region was amplified using the oligonucleotides gntK-2-for-M* and gntK-prom-rev-M (labelled template strand). Binding reactions, DNase I digestion and DNA precipitation were performed as described previously (Engels *et al.*, 2004). A sample of 1.4 µl was then loaded onto a denaturating 4.6% (w/v) Long Ranger (Biozym, Hamburg, Germany) sequencing gel (separation length 61 cm) and separated in a Long Read IR DNA sequencer (Licor, Bad Homburg, Germany). The DNA sequencing reactions were set up using one of the IRD-800-labelled oligonucleotides and a suitable unlabelled PCR product of the promoter region as template.

Determination of glucose and gluconate

To determine the concentration of glucose or gluconate in culture supernatants, a 1-ml sample of the culture was centrifuged for 2 min at 16,060 x *g* and aliquots of the supernatant were used directly for the assay or stored at -20 °C. D-glucose and D-gluconate were quantified enzymatically using a D-Glucose/D-Fructose or a D-Gluconic acid/Glucono-δ-lactone Kit, respectively (R-Biopharm, Darmstadt, Germany) as described by the manufacturer. Concentrations were calculated based on calibration curves with standards of glucose or gluconate. Uptake rates (nmol min^{-1} (mg dry $weight)^{-1}$) for glucose and gluconate (Table 4) were calculated according to the following equation:

$$\left(\frac{S}{M}\right)\times\mu\left[\left(\frac{mmol\times l^{-1}\times OD^{-1}}{gDW\times l^{-1}\times OD^{-1}}\right)\times h^{-1}\right]=\left[\frac{mmol}{gDW\times h}\right]$$

Where S is the slope of a plot of the substrate concentration in the medium *versus* the OD_{600} (mmol x l^{-1} x OD_{600}^{-1}), M the correlation between dry weight and OD (g dry weight x l^{-1} x OD^{-1}) and µ the growth rate (h^{-1}). An OD_{600} of 1 corresponds to 0.25 g dry weight l^{-1} (Kabus *et al.*, 2007).

Acknowledgements

The authors thank Degussa AG, Division Feed Additives (Halle-Künsebeck, Germany), and the Federal Ministry for Education and Research (BMBF) for financial support of this work, and our colleagues Axel Niebisch and Lena Gebel for construction of plasmid pAN6.

References

Anthony, C. (2004) The quinoprotein dehydrogenases for methanol and glucose. *Arch Biochem Biophys* **428**: 2-9.

Bianchi, D., Bertrand, O., Haupt, K., and Coello, N. (2001) Effect of gluconic acid as a secondary carbon source on non-growing L-lysine producers cells of *Corynebacterium glutamicum*. Purification and properties of 6-phosphogluconate dehydrogenase. *Enzyme Microb Technol* **28**: 754-759.

Bott, M. (2007) Offering surprises: TCA cycle regulation in *Corynebacterium*. *Trends Microbiol* **15**: 417-425.

Brazma, A., Hingamp, P., Quackenbush, J., Sherlock, G., Spellman, P., Stoeckert, C., Aach, J., Ansorge, W., Ball, C.A., Causton, H.C., Gaasterland, T., Glenisson, P., Holstege, F.C., Kim, I.F., Markowitz, V., Matese, J.C., Parkinson, H., Robinson, A., Sarkans, U., Schulze-Kremer, S., Stewart, J., Taylor, R., Vilo, J., and Vingron, M. (2001) Minimum information about a microarray experiment (MIAME)-toward standards for microarray data. *Nat Genet* **29**: 365-371.

Brune, I., Brinkrolf, K., Kalinowski, J., Pühler, A., and Tauch, A. (2005) The individual and common repertoire of DNA-binding transcriptional regulators of *Corynebacterium glutamicum*, C*orynebacterium efficiens*, *Corynebacterium diphtheriae* and *Corynebacterium jeikeium* deduced from the complete genome sequences. *BMC Genomics* **6**: 86.

Claes, W.A., Pühler, A., and Kalinowski, J. (2002) Identification of two *prpDBC* gene clusters in *Corynebacterium glutamicum* and their involvement in propionate degradation via the 2-methylcitrate cycle. *J Bacteriol* **184**: 2728-2739.

Cramer, A., Gerstmeir, R., Schaffer, S., Bott, M., and Eikmanns, B.J. (2006) Identification of RamA, a novel LuxR-type transcriptional regulator of genes involved in acetate

metabolism of *Corynebacterium glutamicum*. *J Bacteriol* **188**: 2554-2567.

Dominguez, H., Cocaign-Bousquet, M., and Lindley, N.D. (1997) Simultaneous consumption of glucose and fructose from sugar mixtures during batch growth of *Corynebacterium glutamicum*. *Appl Microbiol Biotechnol* **47**: 600-603.

Eggeling, L., and Bott, M. (2005) *Handbook of Corynebacterium glutamicum.* Inc., Boca Raton, FL: Academic Press.

Eikmanns, B.J., Kleinertz, E., Liebl, W., and Sahm, H. (1991) A family of *Corynebacterium glutamicum*/*Escherichia coli* shuttle vectors for cloning, controlled gene expression, and promoter probing. *Gene* **102**: 93-98.

Eikmanns, B.J., Thum-Schmitz, N., Eggeling, L., Lüdtke, K.U., and Sahm, H. (1994) Nucleotide sequence, expression and transcriptional analysis of the *Corynebacterium glutamicum gltA* gene encoding citrate synthase. *Microbiology* **140**: 1817-1828.

Engels, S., Schweitzer, J.E., Ludwig, C., Bott, M., and Schaffer, S. (2004) *clpC* and *clpP1P2* gene expression in *Corynebacterium glutamicum* is controlled by a regulatory network involving the transcriptional regulators ClgR and HspR as well as the ECF sigma factor sigmaH. *Mol Microbiol* **52**: 285-302.

Engels, V., and Wendisch, V.F. (2007) The DeoR-type regulator SugR represses expression of *ptsG* in *Corynebacterium glutamicum*. *J Bacteriol* **189**: 2955-2966.

Fujita, Y., and Fujita, T. (1987) The gluconate operon *gnt* of *Bacillus subtilis* encodes its own transcriptional negative regulator. *Proc Natl Acad Sci U S A* **84**: 4524-4528.

Fujita, Y., and Miwa, Y. (1989) Identification of an operator sequence for the *Bacillus subtilis gnt* operon. *J Biol Chem* **264**: 4201-4206.

Gerstmeir, R., Cramer, A., Dangel, P., Schaffer, S., and Eikmanns, B.J. (2004) RamB, a novel transcriptional regulator of genes involved in acetate metabolism of *Corynebacterium glutamicum*. *J Bacteriol* **186**: 2798-2809.

Hanahan (1985) Techniques for transformation of *E. coli*. In *DNA-cloning*. Vol. 1. M., G.D. (ed). Oxford/Washington DC: IRL-Press, pp. 109-135.

Izu, H., Adachi, O., and Yamada, M. (1997) Gene organization and transcriptional regulation of the *gntRKU* operon involved in gluconate uptake and catabolism of *Escherichia coli*. *J Mol Biol* **267**: 778-793.

Kabus, A., Georgi, T., Wendisch, V.F., and Bott, M. (2007) Expression of the *Escherichia coli pntAB* genes encoding a membrane-bound transhydrogenase in *Corynebacterium glutamicum* improves L-lysine formation. *Appl Microbiol Biotechnol* **75**: 47-53.

Kalinowski, J., Bathe, B., Bartels, D., Bischoff, N., Bott, M., Burkovski, A., Dusch, N., Eggeling, L., Eikmanns, B.J., Gaigalat, L., Goesmann, A., Hartmann, M., Huthmacher, K., Krämer, R., Linke, B., McHardy, A.C., Meyer, F., Möckel, B., Pfefferle, W., Pühler, A., Rey, D.A., Rückert, C., Rupp, O., Sahm, H., Wendisch, V.F., Wiegräbe, I., and Tauch, A. (2003) The complete *Corynebacterium glutamicum* ATCC 13032 genome sequence and its impact on the production of L-aspartate-derived amino acids and vitamins. *J Biotechnol* **104**: 5-25.

Kalinowski, J. (2005) The genomes of amino acid-producing corynebacteria. In *Handbook of Corynebacterium glutamicum*. Eggeling, L. and Bott, M. (eds). Boca Raton, Florida, USA: CRC Press, pp. 37-56.

Keilhauer, C., Eggeling, L., and Sahm, H. (1993) Isoleucine synthesis in *Corynebacterium glutamicum*: molecular analysis of the *ilvB-ilvN-ilvC* operon. *J Bacteriol* **175**: 5595-5603.

Kim, H.J., Kim, T.H., Kim, Y., and Lee, H.S. (2004) Identification and characterization of *glxR*, a gene involved in regulation of glyoxylate bypass in *Corynebacterium glutamicum*. *J Bacteriol* **186**: 3453-3460.

Kinoshita, S., Udaka, S., and Shimono, M. (1957) Studies on the amino acid fermentation: I. Production of L-glutamic acid by various microorganisms. *J Gen Appl Microbiol* **3**: 193-205.

Kotrba, P., Inui, M., and Yukawa, H. (2001) The *ptsI* gene encoding enzyme I of the phosphotransferase system of *Corynebacterium glutamicum*. *Biochem Biophys Res Commun* **289**: 1307-1313.

Krug, A., Wendisch, V.F., and Bott, M. (2005) Identification of AcnR, a TetR-type repressor of the aconitase gene *acn* in *Corynebacterium glutamicum*. *J Biol Chem* **280**: 585-595.

Lee, H.W., Pan, J.G., and Lebeault, J.M. (1998) Enhanced L-lysine production in threonine-limited continuous culture of *Corynebacterium glutamicum* by using gluconate as a secondary carbon source with glucose. *Appl Microbiol Biotechnol* **49**: 9-15.

Lee, J.K., Sung, M.H., Yoon, K.H., Yu, J.H., and Oh, T.K. (1994) Nucleotide sequence of the gene encoding the Corynebacterium glutamicum mannose enzyme-II and

analyses of the deduced protein sequence. *FEMS Microbiol Lett* **119**: 137-145.

Lengeler, J.W., Jahreis, K., and Wehmeier, U.F. (1994) Enzymes II of the phospho enol pyruvate-dependent phosphotransferase systems: their structure and function in carbohydrate transport. *Biochim Biophys Acta* **1188**: 1-28.

Letek, M., Valbuena, N., Ramos, A., Ordonez, E., Gil, J.A., and Mateos, L.M. (2006) Characterization and use of catabolite-repressed promoters from gluconate genes in *Corynebacterium glutamicum*. *J Bacteriol* **188**: 409-423.

Miwa, Y., and Fujita, Y. (1988) Purification and characterization of a repressor for the *Bacillus subtilis gnt* operon. *J Biol Chem* **263**: 13252-13257.

Möker, N., Brocker, M., Schaffer, S., Krämer, R., Morbach, S., and Bott, M. (2004) Deletion of the genes encoding the MtrA-MtrB two-component system of *Corynebacterium glutamicum* has a strong influence on cell morphology, antibiotics susceptibility and expression of genes involved in osmoprotection. *Mol Microbiol* **54**: 420-438.

Moon, M.W., Kim, H.J., Oh, T.K., Shin, C.S., Lee, J.S., Kim, S.J., and Lee, J.K. (2005) Analyses of enzyme II gene mutants for sugar transport and heterologous expression of fructokinase gene in *Corynebacterium glutamicum* ATCC 13032. *FEMS Microbiol Lett* **244**: 259-266.

Neijssel, O.M., Hommes, R.W.J., Postma, P.W., and Tempest, D.W. (1989) Physiological significance and bioenergetic aspects of glucose dehydrogenase. *A. van Leeuwenhoek* **56**: 51-61.

Niebisch, A., and Bott, M. (2001) Molecular analysis of the cytochrome bc_1-aa_3 branch of the *Corynebacterium glutamicum* respiratory chain containing an unusual diheme cytochrome c_1. *Arch Microbiol* **175**: 282-294.

Nishio, Y., Nakamura, Y., Kawarabayasi, Y., Usuda, Y., Kimura, E., Sugimoto, S., Matsui, K., Yamagishi, A., Kikuchi, H., Ikeo, K., and Gojobori, T. (2003) Comparative complete genome sequence analysis of the amino acid replacements responsible for the thermostability of *Corynebacterium efficiens*. *Genome Res* **13**: 1572-1579.

Parche, S., Burkovski, A., Sprenger, G.A., Weil, B., Krämer, R., and Titgemeyer, F. (2001) *Corynebacterium glutamicum*: a dissection of the PTS. *J Mol Microbiol Biotechnol* **3**: 423-428.

Patek, M., Nesvera, J., Guyonvarch, A., Reyes, O., and Leblon, G. (2003) Promoters of *Corynebacterium glutamicum*. *J Biotechnol* **104**: 311-323.

Peekhaus, N., and Conway, T. (1998) Positive and negative transcriptional regulation of the *Escherichia coli* gluconate regulon gene *gntT* by GntR and the cyclic AMP (cAMP)-cAMP receptor protein complex. *J Bacteriol* **180**: 1777-1785.

Polen, T., and Wendisch, V.F. (2004) Genomewide expression analysis in amino acid-producing bacteria using DNA microarrays. *Appl Biochem Biotechnol* **118**: 215-232.

Porco, A., Peekhaus, N., Bausch, C., Tong, S., Isturiz, T., and Conway, T. (1997) Molecular genetic characterization of the *Escherichia coli gntT* gene of GntI, the main system for gluconate metabolism. *J Bacteriol* **179**: 1584-1590.

Reizer, A., Deutscher, J., Saier, M.H., Jr., and Reizer, J. (1991) Analysis of the gluconate (*gnt*) operon of *Bacillus subtilis*. *Mol Microbiol* **5**: 1081-1089.

Reizer, J., Bergstedt, U., Galinier, A., Küster, E., Saier, M.H., Jr., Hillen, W., Steinmetz, M., and Deutscher, J. (1996) Catabolite repression resistance of *gnt* operon expression in *Bacillus subtilis* conferred by mutation of His-15, the site of phosphoenolpyruvate-dependent phosphorylation of the phosphocarrier protein HPr. *J Bacteriol* **178**: 5480-5486.

Rigali, S., Derouaux, A., Giannotta, F., and Dusart, J. (2002) Subdivision of the helix-turn-helix GntR family of bacterial regulators in the FadR, HutC, MocR, and YtrA subfamilies. *J Biol Chem* **277**: 12507-12515.

Sambrook, J., Fritsch, E.F., and Maniatis, T. (1989) Molecular Cloning. A Laboratory Manual. *Cold Spring Harbor, NY: Cold Spring Harbor Laboratoy Press.*

Schäfer, A., Tauch, A., Jäger, W., Kalinowski, J., Thierbach, G., and Pühler, A. (1994) Small mobilizable multi-purpose cloning vectors derived from the *Escherichia coli* plasmids pK18 and pK19: selection of defined deletions in the chromosome of *Corynebacterium glutamicum*. *Gene* **145**: 69-73.

Stansen, C., Uy, D., Delaunay, S., Eggeling, L., Goergen, J.L., and Wendisch, V.F. (2005) Characterization of a *Corynebacterium glutamicum* lactate utilization operon induced during temperature-triggered glutamate production. *Appl Environ Microbiol* **71**: 5920-5928.

Studier, F.W., and Moffatt, B.A. (1986) Use of bacteriophage T7 RNA polymerase to direct

selective high-level expression of cloned genes. *J Mol Biol* **189**: 113-130.

Titgemeyer, F., and Hillen, W. (2002) Global control of sugar metabolism: a gram-positive solution. *Antonie Van Leeuwenhoek* **82**: 59-71.

Tong, S., Porco, A., Isturiz, T., and Conway, T. (1996) Cloning and molecular genetic characterization of the *Escherichia coli gntR*, *gntK*, and *gntU* genes of GntI, the main system for gluconate metabolism. *J Bacteriol* **178**: 3260-3269.

van der Rest, M.E., Lange, C., and Molenaar, D. (1999) A heat shock following electroporation induces highly efficient transformation of *Corynebacterium glutamicum* with xenogeneic plasmid DNA. *Appl Microbiol Biotechnol* **52**: 541-545.

von der Osten, C.H., Gioannetti, C., and Sinskey, A.J. (1989) Design of a defined medium for growth of *Corynebacterium glutamicum* in which citrate facilitates iron uptake. *Biotechnol Lett* **11**: 11-16.

Warner, J.B., and Lolkema, J.S. (2003) CcpA-dependent carbon catabolite repression in bacteria. *Microbiol Mol Biol Rev* **67**: 475-490.

Wendisch, V.F., de Graaf, A.A., Sahm, H., and Eikmanns, B.J. (2000) Quantitative determination of metabolic fluxes during coutilization of two carbon sources: comparative analyses with *Corynebacterium glutamicum* during growth on acetate and/or glucose. *J Bacteriol* **182**: 3088-3096.

Wennerhold, J., Krug, A., and Bott, M. (2005) The AraC-type regulator RipA represses aconitase and other iron proteins from *Corynebacterium* under iron limitation and is itself repressed by DtxR. *J Biol Chem* **280**: 40500-40508.

Yukawa, H., Omumasaba, C.A., Nonaka, H., Kos, P., Okai, N., Suzuki, N., Suda, M., Tsuge, Y., Watanabe, J., Ikeda, Y., Vertes, A.A., and Inui, M. (2007) Comparative analysis of the *Corynebacterium glutamicum* group and complete genome sequence of strain R. *Microbiology* **153**: 1042-1058.

Curriculum vitae

Julia Frunzke, née Wennerhold

Date of birth:	15.02.1980
Place of birth:	Lich, Germany
Nationality:	German

Education:

08/1986-05/1990	Primary School, Münzenberg
08/1990-06/1999	Weidig-Gymnasium Butzbach
10/1999-09/2004	Studies of Biology at the Philipps-Universiät Marburg
09/2003-12/2003	EU scholarship within the ERASMUS/SOKRATES programme at the University of Oxford, practical course in the group of Prof. A. Watts, Department of Biochemistry.
01/2004-09/2004	Diploma thesis at the Max Planck Institute for Terrestrial Microbiology in the group of PD Dr. R. Hedderich at the Department of Biochemistry. Title: "Investigations on the role of the H_2:heterodisulfide oxidoreductase complex in energy conservation in *Methanothermobacter marburgensis*."
11/2004-11/2007	Experimental PhD thesis in the group of Prof. Dr. M. Bott at the Institute of Biotechnology 1, Research Centre Jülich. Oral examination: November 29, 2007.

Danksagung

Ein ganz besonderer Dank gilt Prof. Michael Bott für die Überlassung des interessanten und abwechslungsreichen Themas, für die hervorragende Betreuung und das große Interesse, das er meiner Arbeit entgegengebracht hat.

Des Weiteren möchte ich mich bei Herrn Prof. Dr. Wagner für die Übernahme des Zweigutachtens bedanken.

Bei Herr Prof. Dr. Sahm bedanke ich mich für die freundliche Unterstützung und die wertvollen Ratschläge.

Der Evonik (ehemals Degussa) danke ich für die finanzielle Unterstützung und das stete Interesse am Fortschritt dieser Arbeit.

Weiterhin möchte ich mich bei allen Mitgliedern meiner Arbeitsgruppe für die angenehme Atmosphäre und ständige Hilfsbereitschaft während der gemeinsamen Zeit in Büro und Labor bedanken. Ein besonderer Dank gilt hierbei meinen Bürokollegen Sarah und Christian und ehemals Melanie und Jens für die Gewährung (Erduldung) eines angenehm muffelig-warmen Pumakäfigs und natürlich meiner Laborkollegin Brita, für Zellen von brillianter Kompetenz und die Bereitstellung der ein oder anderen Platte.

Bei Melanie, Tino, Tobias und Verena bedanke ich mich für die Einarbeitung und die Hilfe bei den DNA-Microarrays.

Ein großer Dank gilt Conny und Verena für Ihre Unterstützung bei den Arbeiten zu unserem Gluconat-Projekt.

Allen Mitarbeitern des IBT1 danke ich für die gute Arbeitsatmosphäre und die stete Hilfsbereitschaft. Besonders danke ich Ramon für die Einführung in die Untiefen des Lightcyclers und bei Jan für die vertrauensvolle Überlassung von geheimen Schriften.

Bei Sonja Vogt und Julia Eckardt-Michel bedanke ich mich für viele erfrischende Gespräche zu Themen innerhalb und außerhalb der Biologie, für die netten Feiern, die schon waren und natürlich die, die bald kommen.

Meiner Familie danke ich von ganzem Herzen: Meiner Mutter für die dauerhafte moralische Unterstützung, meiner Schwester für die nötige Prise Chaos, meinem Bruder und Cheflektor für das kritische Durchsehen diverser Schriften und bei meinem Schwager für die unglaublich gute Verköstigung.

Ein ganz lieber Dank gilt Jan für die wunderschöne Zeit, die entgegengebrachte Geduld und besonders dafür, dass er mich bei allem was ich tue unterstützt und für mich da ist.

Erklärung

Die hier vorgelegte Dissertation habe ich eigenständig und ohne unerlaubte Hilfe angefertigt. Die Dissertation wurde in der vorgelegten oder in ähnlicher Form noch bei keiner anderen Institution eingereicht. Ich habe bisher keine erfolglosen Promotionsversuche unternommen.

Bergheim, den 10.12.2007